

PREPARATION AND REACTIVITY OF TANTALUM(V) ALKYLIDENE  
AND METALLACYCLOBUTANE COMPLEXES

by

KEVIN C. WALLACE

B.S. Furman University  
(1983)

M.S. Furman University  
(1984)

Submitted to the Department of Chemistry  
in Partial Fulfillment of the Requirements  
for the degree of

DOCTOR OF PHILOSOPHY

at the

MASSACHUSETTS INSTITUTE OF TECHNOLOGY

June 1988

© Massachusetts Institute of Technology 1988

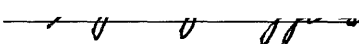
Signature of Author \_\_\_\_\_  
Department of Chemistry, May 11, 1988

Certified by \_\_\_\_\_  
Richard R. Schrock, Thesis Supervisor


Accepted by \_\_\_\_\_  
Glenn A. Berchtold, Chairman  
Departmental Committee on Graduate Students

MASSACHUSETTS INSTITUTE  
OF TECHNOLOGY  
JUN 10 1988  
ARCHIVES

This doctoral thesis has been examined by a Committee of the Department of Chemistry  
as follows:

Professor Stephen J. Lippard  \_\_\_\_\_ Chairman

Professor Richard R. Schrock \_\_\_\_\_ Thesis Supervisor

Professor Stephen L. Buchwald  \_\_\_\_\_

To Susie and Sugar

PREPARATION AND REACTIVITY OF TANTALUM(V) ALKYLIDENE  
AND METALLACYCLOBUTANE COMPLEXES

by

KEVIN C. WALLACE

Submitted to the Department of Chemistry June 1988  
in partial fulfillment of the requirements  
for the Degree of Doctor of Philosophy in Chemistry

ABSTRACT

Chapter 1

$\text{Ta}(\text{CHCMe}_3)(\text{THF})_2\text{Cl}_3$  reacts with three equivalents of  $\text{LiX}$  ( $\text{X} = \text{DIPP}$ ,  $\text{DMP}$ , and  $\text{TIPT}$ ;  $\text{DIPP} = 2,6$ -diisopropylphenoxide,  $\text{DMP} = 2,6$ -dimethylphenoxide,  $\text{TIPT} = 2,4,6$ -triisopropylbenzenethiolate) to give alkylidene complexes of the type  $\text{Ta}(\text{CHCMe}_3)\text{X}_3(\text{THF})$ . Other base adducts are straightforwardly prepared by displacement of  $\text{THF}$ . Both phenoxide ( $\text{DIPP}$ ) and arylthiolate ( $\text{TIPT}$ ) complexes display Wittig-like reactivity with organic carbonyls (e.g.  $\text{PhCHO}$ ), but only phenoxide complexes react with acyclic olefins.  $\text{Ta}(\text{CHCMe}_3)(\text{DIPP})_3(\text{THF})$  reacts with acyclic olefins (ethylene, styrene, and bistrimethylsilylethylene) to give a variety of base adduct alkylidene complexes and base-free metallacyclobutane complexes.  $\text{Ta}(\text{CHCMe}_3)(\text{DMP})_3(\text{THF})$  reacts with acyclic olefins but no stable products have been isolated. The reactivity differences are discussed in terms of steric and electronic properties associated with  $\text{DIPP}$ ,  $\text{DMP}$ , and  $\text{TIPT}$  ligation.  $\text{DIPP}$  ligation provides much more steric protection in alkylidene and metallacyclobutane complexes than does analogous  $\text{DMP}$  ligation. Solid state structures, determined by X-ray crystallography, of representative  $\text{DIPP}$  and  $\text{TIPT}$  alkylidene complexes also reveal fundamental differences in complex geometry for phenoxide and thiolate compounds and suggest the observed reactivity (or lack of reactivity) is related to these structural differences.

The metallacyclobutane complexes prepared represent the first examples of such complexes for tantalum; X-ray analysis of the tantalacycle  $\text{Ta}[\text{CH}(\text{Ph})\text{CH}(\text{CMe}_3)\text{CH}_2](\text{DIPP})_3$  showed a distorted square pyramidal geometry for the complex, with the  $\text{MC}_3$  ring occupying two basal sites. Tantalacyclobutanes are isolated base-free and react with base ( $\text{THF}$ , pyridine) to give base adduct alkylidene complexes  $\text{Ta}(\text{CHR})(\text{DIPP})_3(\text{Base})$  (with olefin loss). Tantalacyclobutanes react with organic carbonyls (formaldehyde, pivaldehyde, benzaldehyde, acetone, and benzophenone) to give Wittig-like products or insertion products (i.e. oxytantalacyclohexane complexes), depending on reaction conditions employed.

Chapter 2

$\text{Ta}(\text{CHCMe}_3)(\text{DIPP})_3(\text{THF})$  reacts with one equivalent of norbornene ( $\text{NBE}$ ) to give the trisubstituted tantalacyclobutane  $\text{Ta}[\text{CH}(\text{C}_5\text{H}_8)\text{CHCH}(\text{CMe}_3)](\text{DIPP})_3$ . An X-ray study of this tantalacycle revealed a trigonal bipyramidal geometry, with the  $\text{MC}_3$  ring in the equatorial plane.  $\text{Ta}[\text{CH}(\text{C}_5\text{H}_8)\text{CHCH}(\text{CMe}_3)](\text{DIPP})_3$  polymerizes  $\text{NBE}$  at elevated temperatures in a reaction that is first order in catalyst complex and zero order in  $\text{NBE}$ . The rate limiting step is ring-opening of tantalacyclobutane complexes  $\text{Ta}[\text{CH}(\text{C}_5\text{H}_8)\text{CHCH}(\text{P})](\text{DIPP})_3$  ( $\text{P} = \text{polynorbornene}$ ), and alkylidene intermediates formed are then rapidly trapped with  $\text{NBE}$ . Polynorbornene is readily cleaved from  $\text{Ta}[\text{CH}(\text{C}_5\text{H}_8)\text{CHCH}(\text{P})](\text{DIPP})_3$  on reaction with organic carbonyls; polymer samples were analyzed by gel permeation chromatography. Initiation is slightly slower than propagation but does not significantly affect the molecular weight distributions of resulting polynorbornenes. Secondary metathesis occurs after all  $\text{NBE}$  has been consumed and causes a broadening of the polymer molecular weight distributions



(i.e. an increase in polydispersity), but if the reaction is terminated before complete consumption of NBE, monodisperse polymers ( $d < 1.05$ ) can be obtained. Intermediate complexes have also been isolated and studied. On the basis of these results, the reaction of  $\text{Ta}[\text{CH}(\text{C}_5\text{H}_8)\text{CHCH}(\text{CMe}_3)](\text{DIPP})_3$  with excess NBE is considered a living polymerization.  $\text{Ta}[\text{CH}(\text{C}_5\text{H}_8)\text{CHCH}(\text{CMe}_3)](\text{DMP})_3$  also polymerizes NBE, but the reaction is ill-defined; more than one polymerization mechanism appears to be operative. Direct interaction of the tantalacycle with NBE and olefins of the polymer chain is considered likely, considering the sterically less demanding DMP ligation.

$\text{Ta}(\text{CHCMe}_3)(\text{TIPT})_3(\text{B})$  ( $\text{B} = \text{THF}, \text{py}$ ) complexes also polymerize NBE. The reaction is first order in both catalyst complex and NBE; the rate-limiting step is addition of NBE to alkylidene complexes, and formed intermediate tantalacyclobutanes then rapidly ring-open. The active species is base-free, so manipulation of base ( $\text{B}$ ) dramatically affects the reaction rate. Monodisperse polynorbornenes are obtained in all cases (after capping with benzaldehyde); secondary metathesis does not occur. Reactions with other cyclic olefins have also been investigated.

### Chapter 3

$\text{Ta}(\text{CHCMe}_3)(\text{DIPP})_3(\text{THF})$  reacts with one equivalent of the acetylenes 2-butyne, diphenylacetylene, and bistrimethylsilylacetylene to give base-free tantalacyclobutene complexes  $\text{Ta}[\text{C}(\text{R})\text{C}(\text{R})\text{CH}(\text{CMe}_3)](\text{DIPP})_3$  ( $\text{R} = \text{Me}, \text{Ph}, \text{TMS}$ ). Reaction of  $\text{Ta}(\text{CHCMe}_3)(\text{DIPP})_3(\text{THF})$  with the ene-yne 2-methyl-but-1-ene-3-yne also gives a tantalacyclobutene,  $\text{Ta}[\text{CH}_2\text{C}(\text{Me})\text{C}(\text{CHCHCMe}_3)](\text{DIPP})_3$ , formed on rearrangement of the initially formed tantalacycle. For  $\text{R} = \text{Me}$  or  $\text{Ph}$ , pyridine addition to  $\text{Ta}[\text{C}(\text{R})\text{C}(\text{R})\text{CH}(\text{CMe}_3)](\text{DIPP})_3$  results in vinyl alkylidene formation,  $\text{Ta}(\text{C}(\text{R})\text{C}(\text{R})\text{CHCMe}_3)(\text{DIPP})_3(\text{py})$ ; other metallacyclobutene complexes react with pyridine to form base adducts. While the metallacyclobutene  $\text{Ta}[\text{C}(\text{Me})\text{C}(\text{Me})\text{CH}(\text{CMe}_3)](\text{DIPP})_3$  only reacts with excess 2-butyne to give intractable polymer (and recovery of most starting catalyst), the alkylidene  $\text{Ta}(\text{CMeCMeCHCMe}_3)(\text{DIPP})_3(\text{py})$  (structure determined by X-ray crystallography) affects the living polymerization of 2-butyne. Monodisperse polymers ( $d < 1.05$ ) of controlled molecular weights are obtained after capping the living polymer,  $\text{Ta}(\text{CMeCMeCMeP})(\text{DIPP})_3$  ( $\text{P} = \text{poly-2-butyne}$ ), by reaction with an organic carbonyl. The successful reaction is largely the result of effective initiation - trisubstituted metallacyclobutene complexes, such as  $\text{Ta}[\text{C}(\text{Me})\text{C}(\text{Me})\text{CH}(\text{CMe}_3)](\text{DIPP})_3$ , do not ring-open in the absence of a base, but tetrasubstituted metallacyclobutenes, such as the one formed on addition of 2-butyne to the disubstituted alkylidene  $\text{Ta}(\text{CMeCMeCHCMe}_3)(\text{DIPP})_3(\text{py})$ , are unstable and readily ring-open, even in the absence of a base. The preparation of block copolymers, of 2-butyne and NBE, has also been investigated.

Addition of one equivalent of 2-butyne to  $\text{Ta}(\text{CMeCMeCHCMe}_3)(\text{DIPP})_3(\text{py})$  gives a base-free complex that does not polymerize 2-butyne efficiently. X-ray analysis of this complex showed it to be an unusual tantalacyclopentene complex, formed by activation of a methyl group in an intermediate species. Thus a potential deactivation process has been identified. This complex and/or similar species do not form when excess 2-butyne is polymerized by  $\text{Ta}(\text{CMeCMeCHCMe}_3)(\text{DIPP})_3(\text{py})$ , suggesting the trisubstituted end olefin group of the polymer chain,  $-\text{C}(\text{Me})=\text{CH}(\text{CMe}_3)$ , must be accessible to the metal center for such a reaction to occur. (Attempts to polymerize other acetylenes, such as 1-pentyne, and attempts to employ other catalysts, such as the arylthiolate complex  $\text{Ta}(\text{CHCMe}_3)(\text{TIPT})_3(\text{THF})$ , did not lead to the isolation of monodisperse polymers.)

Thesis Supervisor: Richard R. Schrock  
 Title: Professor of Chemistry

## TABLE OF CONTENTS

	<u>page</u>
Title Page .....	1
Signature Page .....	2
Dedication .....	3
Abstracts .....	4
Table of Contents .....	6
List of Figures .....	9
List of Tables .....	11
List of Abbreviations used in Text .....	12
 CHAPTER 1: Preparation of Tantalum(V) Alkylidene Complexes Supported with Bulky Ligation and their Reactivity with Ordinary Olefins and Organic Carbonyls .....	14
INTRODUCTION .....	15
RESULTS .....	17
Preparation of Ta(CHCMe <sub>3</sub> )X <sub>3</sub> (B) Complexes .....	17
Attempted Preparation of Ta(CHCMe <sub>3</sub> )(DIPP) <sub>3</sub> (B) from Ta(CH <sub>2</sub> CMe <sub>3</sub> ) <sub>2</sub> (DIPP) <sub>3</sub> ...	30
Wittig Reactivity of Ta(CHCMe <sub>3</sub> )X <sub>3</sub> (THF) Complexes .....	32
Lack of Reactivity of Ta(CHCMe <sub>3</sub> )(TIPT) <sub>3</sub> (THF) with Acyclic Olefins .....	34
Reactivity of Ta(CHCMe <sub>3</sub> )(OAr) <sub>3</sub> (THF) Complexes with Acyclic Olefins .....	35
Reactivity of Tantalacyclobutane Complexes with Organic Carbonyls .....	52
DISCUSSION .....	56
Experimental Section .....	62
General Details .....	62
Preparation of Compounds .....	62

CHAPTER 2:	Ring-Opening Polymerization of Norbornene and Related Cyclic Olefins with Tantalum Alkylidene and Metallacyclobutane Complexes .....	76
INTRODUCTION .....		77
RESULTS .....		78
Preparation and Crystal Structure of Ta[CH(C <sub>5</sub> H <sub>8</sub> )CHCH(CMe <sub>3</sub> )](DIPP) <sub>3</sub> .....		78
Polymerization of NBE with Ta[CH(C <sub>5</sub> H <sub>8</sub> )CHCH(CMe <sub>3</sub> )](DIPP) <sub>3</sub> .....		85
Wittig Reactivity of Ta[CH(C <sub>5</sub> H <sub>8</sub> )CHCH(R)](DIPP) <sub>3</sub> Complexes, and GPC analysis of resulting Polynorbornenes .....		94
Polymerization of NBE with Ta[CH(C <sub>5</sub> H <sub>8</sub> )CHCH(CMe <sub>3</sub> )](DMP) <sub>3</sub> .....		99
Polymerization of NBE with Ta(CHCMe <sub>3</sub> )(TIPT) <sub>3</sub> (B) Complexes .....		102
Reactions of Other Cyclic Olefins with DIPP and TIPT Catalysts .....		106
DISCUSSION .....		110
Experimental Section .....		113
Preparation of Compounds .....		113
CHAPTER 3:	The Living Polymerization of 2-Butyne by a Tantalum Alkylidene Catalyst and Related Reactions .....	120
INTRODUCTION .....		121
RESULTS .....		124
Formation of Metallacyclobutene Complexes and their Reactivity with Bases .....		124
Polymerization of 2-Butyne by Ta(CMeCMeCHCMe <sub>3</sub> )(DIPP) <sub>3</sub> (py) .....		139
Preparation of 2-Butyne/NBE Block Copolymers .....		147
Reaction of Ta(CMeCMeCHCMe <sub>3</sub> )(DIPP) <sub>3</sub> (py) with One Equivalent of 2-Butyne ..		152
Deactivation Reactions of Tantalum Catalysts in Acetylene Polymerization .....		158
Polymerization of Acetylenes with Ta(CHCMe <sub>3</sub> )(TIPT) <sub>3</sub> (THF) .....		160
DISCUSSION .....		161
Experimental Section .....		166

Preparation of Compounds .....	166
APPENDIX 1: X-Ray Analysis of Ta(CHCMe <sub>3</sub> )(TIPT) <sub>3</sub> (Et <sub>2</sub> S) .....	178
APPENDIX 2: Preparation and Reactivity of Tantalum Imido and Dinitrogen Compounds .....	185
APPENDIX 3: Organization of Notebooks, Spectra, and Other Data .....	191
REFERENCES .....	193
ACKNOWLEDGEMENTS .....	203

## List of Figures

	<u>page</u>
<u>Chapter 1</u>	
Figure 1. The $^1\text{H}$ NMR spectrum of $\text{Ta}(\text{CHCMe}_3)(\text{DIPP})_3(\text{THF})$ ( <b>2</b> ) in $\text{C}_6\text{D}_6$ at $25^\circ$ .....	21
Figure 2. The $^1\text{H}$ NMR spectrum of $\text{Ta}(\text{CHCMe}_3)(\text{TIPT})_3(\text{THF})$ ( <b>6</b> ) in $\text{C}_6\text{D}_6$ at $25^\circ$ (* = mesitylene) .....	27
Figure 3. A view of $\text{Ta}[\text{CH}(\text{Ph})\text{CH}(\text{CMe}_3)\text{CH}_2](\text{DIPP})_3$ ( <b>15</b> ) (molecule 1) .....	38
Figure 4. A comparison of metallacyclobutane rings in <b>15</b> , $\text{Ta}[\text{CH}(\text{C}_5\text{H}_8)\text{CHCH}(\text{CMe}_3)](\text{DIPP})_3$ , and $\text{W}[\text{CH}(\text{SiMe}_3)\text{CH}(\text{SiMe}_3)\text{CH}_2](\text{N}-2,6-\text{C}_6\text{H}_3\text{iPr}_2)[\text{OCMe}(\text{CF}_3)_2]_2$ .....	41
Figure 5. The $^1\text{H}$ NMR spectrum of $\text{Ta}(\text{CH}_2\text{CH}_2\text{CH}_2)(\text{DIPP})_3$ ( <b>17</b> ) in $\text{C}_6\text{D}_6$ at $25^\circ$ (* = mesitylene) .....	44
Figure 6. The $^1\text{H}$ NMR spectrum of $\text{Ta}[\text{OCH}(\text{CMe}_3)\text{CH}_2\text{CH}_2\text{CH}_2](\text{DIPP})_3$ ( <b>25</b> ) in $\text{C}_6\text{D}_6$ at $25^\circ$ .....	55
<u>Chapter 2</u>	
Figure 1a. The $^1\text{H}$ NMR spectrum of $\text{Ta}[\text{CH}(\text{C}_5\text{H}_8)\text{CHCH}(\text{CMe}_3)](\text{DIPP})_3$ ( <b>26</b> ) in $\text{C}_6\text{D}_6$ .....	80
Figure 1b. The $^1\text{H}$ NMR spectrum of $\text{Ta}[\text{CH}(\text{C}_5\text{H}_8)\text{CHCH}(\text{CMe}_3)](\text{DMP})_3$ ( <b>30</b> ) in $\text{C}_6\text{D}_6$ (* = diethyl ether) .....	81
Figure 2. A view of $\text{Ta}[\text{CH}(\text{C}_5\text{H}_8)\text{CHCH}(\text{CMe}_3)](\text{DIPP})_3$ ( <b>26</b> ) .....	83
Figure 3. The $^1\text{H}$ NMR spectrum of $\text{Ta}[\text{CH}(\text{C}_5\text{H}_8)\text{CHCH}(\text{P})](\text{DIPP})_3$ ( <b>27</b> ) in $\text{C}_6\text{D}_6$ at $50^\circ$ (* = mesitylene) .....	86
Figure 4. A plot of the consumption of 20 equivalents of NBE by <b>26</b> (and <b>27</b> ) at $50^\circ$ in $\text{C}_6\text{D}_6$ .....	89
Figure 5. GPC traces for the benzylidene-capped polynorbornene produced by adding 100 eq of NBE to <b>26</b> (a) ( $d = 1.63$ ) and <b>6</b> (b) ( $d = 1.09$ ) .....	98
Figure 6. The $^1\text{H}$ NMR spectrum of $\text{Ta}(\text{CHC}_5\text{H}_8\text{CHCHP})(\text{TIPT})_3(\text{py})$ ( <b>34</b> ) in $\text{C}_6\text{D}_6$ at $50^\circ$ (* = NBE; some mesitylene also present) .....	104
Figure 7. (a) Calculated spectrum for the protons of the <i>trans</i> phenyl-substituted olefin cap in the Wittig product produced on treating $\text{Ta}[\text{CH}(\text{C}_5\text{H}_8)\text{CHCH}(\text{P})](\text{DIPP})_3$ ( <b>27</b> ) with benzaldehyde. (b) Observed spectrum for the protons of the phenyl-substituted olefin cap in the Wittig product produced on treating <b>27</b> with benzaldehyde .....	117

Chapter 3

Figure 1.	The $^1\text{H}$ NMR spectrum of $\text{Ta}[\text{C}(\text{Me})\text{C}(\text{Me})\text{CH}(\text{CMe}_3)](\text{DIPP})_3$ ( <b>35</b> ) in $\text{C}_6\text{D}_6$ .....	127
Figure 2a.	A view of $\text{Ta}(\text{CMeCMeCHCMe}_3)(\text{DIPP})_3(\text{py})$ ( <b>42</b> ) .....	132
Figure 2b.	The core geometry of $\text{Ta}(\text{CMeCMeCHCMe}_3)(\text{DIPP})_3(\text{py})$ ( <b>42</b> ) .....	133
Figure 3.	The $^1\text{H}$ NMR spectrum of <b>42</b> in $\text{C}_6\text{D}_6$ after standing at $40^\circ$ for 2 days .....	138
Figure 4.	The $^1\text{H}$ NMR spectrum of <b>42</b> after reaction with 10 equivalents of 2-butyne in $\text{C}_6\text{D}_6$ (i.e. complex <b>44</b> ) .....	140
Figure 5.	GPC traces for the benzylidene-capped poly-2-butyne formed by reaction of <b>42</b> with (a) 50 equivalents, (b) 100 equivalents, and (c) 150 equivalents of 2-butyne, and GPC traces for a benzylidene capped block copolymer formed by reaction of <b>42</b> with 50 equivalents of 2-butyne and 50 equivalents of NBE ((d) UV/VIS detection (e) refractive index detection). x axis = minutes; * = highest molecular weight solvent peak (i.e. all peaks of a lower molecular weight, or a higher retention time, are also solvent peaks) .....	146
Figure 6.	The $^1\text{H}$ NMR spectrum of <b>47</b> in $\text{C}_6\text{D}_6$ .....	153
Figure 7.	A view of $\text{Ta}[\text{C}(\text{Me})\text{C}(\text{Me})\text{C}(\text{CMeCH}_2\text{CMe}_3)\text{CH}_2](\text{DIPP})_3$ ( <b>47</b> ) .....	155
<u>Appendix 1</u>		
Figure 1.	A view of $\text{Ta}(\text{CHCMe}_3)(\text{TIPT})_3(\text{Et}_2\text{S})$ ( <b>9</b> ) .....	180
Figure 2.	A comparison of the core geometries in $\text{Ta}(\text{CHCMe}_3)(\text{TIPT})_3(\text{Et}_2\text{S})$ ( <b>9</b> ) and $\text{Ta}(\text{CMeCMeCHCMe}_3)(\text{DIPP})_3(\text{py})$ ( <b>42</b> ) .....	182

## List of Tables

	<u>page</u>
<u>Chapter 1</u>	
Table I. NMR Data for the Alkylidene Ligands in Tantalum Alkylidene Complexes of the Type Ta(CHR)X <sub>3</sub> (B) .....	20
Table II. Products of the Reactions of Tantalum Alkylidene Complexes with Organic Carbonyls .....	33
Table III. Proton and Carbon NMR Data for the TaC <sub>3</sub> Ring in Tantalacyclobutane Complexes .....	37
Table IV. Selected Bond Distances (Å) and Angles (°) in Ta[CH(Ph)CH(CMe <sub>3</sub> )CH <sub>2</sub> ](DIPP) <sub>3</sub> ( <b>15</b> ) .....	39
Table V. Products of the Reactions of Tantalacycles with Organic Carbonyls .....	54
<u>Chapter 2</u>	
Table I. Proton and Carbon NMR Data for the TaC <sub>3</sub> Ring in Tantalacycles .....	79
Table II. Selected Bond Distances (Å) and Angles (°) in Ta[CH(C <sub>5</sub> H <sub>8</sub> )CHCH(CMe <sub>3</sub> )](DIPP) <sub>3</sub> ( <b>26</b> ) .....	84
Table III. Kinetic Data for the Polymerization of NBE by <b>26</b> and Ta(CHCMe <sub>3</sub> )(TIPT) <sub>3</sub> (py) ( <b>7</b> ) .....	90
Table IV. The Results of GPC Analysis of Polynorbornenes .....	97
<u>Chapter 3</u>	
Table I. NMR Data for the MC <sub>3</sub> Ring in Metallacyclobutene Complexes .....	126
Table II. NMR Data for the Alkylidene Ligand in Tantalum Vinyl Alkylidene Complexes .....	130
Table III. Selected Bond Distances (Å) and Angles (°) in Ta(CMeCMeCHCMe <sub>3</sub> )(DIPP) <sub>3</sub> (py) ( <b>42</b> ) .....	134
Table IV. The Results of GPC Analysis of Polyacetylenes .....	144
Table V. Selected Bond Distances (Å) and Angles (°) in Ta[C(Me)C(Me)C(CMeCH <sub>2</sub> CMe <sub>3</sub> )CH <sub>2</sub> ](DIPP) <sub>3</sub> ( <b>47</b> ) .....	156
<u>Appendix 1</u>	
Table I. Selected Bond Distances (Å) and Angles (°) in Ta(CHCMe <sub>3</sub> )(TIPT) <sub>3</sub> (Et <sub>2</sub> S) ( <b>9</b> ) .....	181

## Abbreviations Used in Text

B	base
br	broad
<sup>t</sup> Bu	CMe <sub>3</sub>
C <sub>α</sub>	carbon bound to the metal
C <sub>β</sub>	carbon bound to C <sub>α</sub>
C <sub>m</sub>	carbon in meta position of DIPP, DMP, or TIPT
C <sub>o</sub>	carbon in ortho position of DIPP, DMP, or TIPT
C <sub>p</sub>	carbon in para position of DIPP, DMP, or TIPT
COT	cyclooctatetraene
d	polydispersity, M <sub>w</sub> /M <sub>n</sub>
DIPP	2,6-diisopropylphenoxide
DIPT	2,6-diisopropylbenzenethiolate
DMP	2,6-dimethylphenoxide
Et	ethyl
Et <sub>2</sub> S	diethylsulfide
GC	gas chromatography
GPC	gel permeation chromatography
H <sub>α</sub>	hydrogen bound to C <sub>α</sub>
H <sub>β</sub>	hydrogen bound to C <sub>β</sub>
H <sub>m</sub>	hydrogen in meta position of DIPP, DMP, or TIPT
H <sub>o</sub>	hydrogen in ortho position of DIPP, DMP, or TIPT
H <sub>p</sub>	hydrogen in para position of DIPP, DMP, or TIPT
HFF	hexafluoro Feast monomer
Hz	Hertz
L	ligand
M	metal
m	minutes (used in preparation of compounds)
m	multiplet (used in NMR data)
M <sub>n</sub>	number average molecular weight
M <sub>w</sub>	weight average molecular weight
Me	methyl
NBE	norbornene
NMR	nuclear magnetic resonance



## Abbreviations Used in Text (continued)

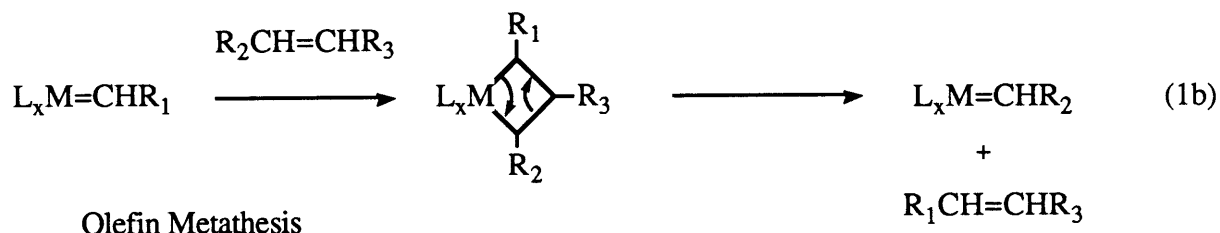
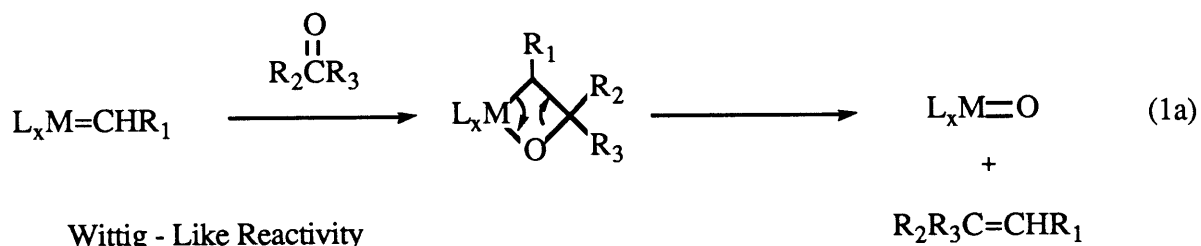
OAr	phenoxide
P	polymer
Ph	phenyl
ppm	parts per million
<sup>i</sup> Pr	isopropyl
py	pyridine
quin	quinuclidine
R	alkyl
SAr	arylthiolate
THF	tetrahydrofuran
TIPT	2,4,6-triisopropylbenzenethiolate
δ	chemical shift in ppm upfield from tetramethylsilane

## CHAPTER 1

### Preparation of Ta(V) Alkylidene Complexes Supported with Bulky Ligations and their Reactivity with Ordinary Olefins and Organic Carbonyls

## INTRODUCTION

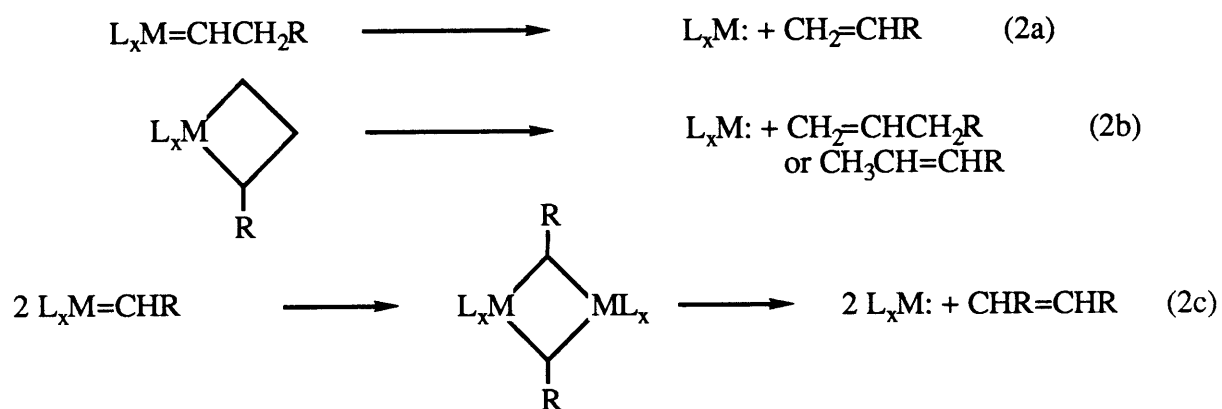
High oxidation state transition metal alkylidene compounds display a variety of interesting behavior, centering around the reactivity of the metal carbon double bond in these complexes ( $M^{\delta+}C^{\delta-}$ ).<sup>1-4</sup> Two characteristic reactions of these complexes, Wittig-like behavior with organic carbonyls (equation 1a) and olefin metathesis (equation 1b) are shown below.



A great deal of research has centered around the reactivity of transition metal alkylidene compounds (and related metallacyclobutane complexes), resulting in a thorough understanding of the mechanisms involved in the above reactions and some novel applications of the chemistry (such as ring-opening polymerization of cyclic olefins).

Tantalum complexes were among the first to be reported in this area. A tantalum alkylidene complex ( $\text{Ta}(\text{CHCMe}_3)(\text{CH}_2\text{CMe}_3)_3$ ) was reported by Schrock in 1974,<sup>5</sup> and the subsequent report of Wittig-like reactivity for  $\text{Ta}(\text{CHCMe}_3)(\text{CH}_2\text{CMe}_3)_3$  with organic carbonyls, such as acetone, benzaldehyde, and DMF, demonstrated the potential utility of these compounds in organic synthesis.<sup>6</sup> Studies of olefin metathesis with tantalum alkylidene complexes<sup>7,8</sup> (such as  $\text{Ta}(\text{CHR})\text{X}_3\text{B}_2$ ; X = halide, B = base) demonstrated many key features,

including the importance of metallacyclobutane species as intermediates in these reactions. Although no tantalacyclobutane complexes were observed, the experiments in olefin metathesis and experiments in related areas<sup>9,10</sup> revealed conclusive evidence for their existence as transient intermediates in these processes. Metathesis of olefins using these tantalum alkylidene complexes, however, was limited by deactivation reactions of the catalyst species (alkylidenes and metallacyclobutanes). Rearrangement reactions of alkylidene ligands to olefins (2a) and of metallacyclobutane rings to olefins (2b), and bimolecular coupling reactions of alkylidenes to olefins (2c), were thought to be probable deactivation processes. Rearrangements



of the type shown in equations 2a and 2b are generally considered as potential deactivation pathways for complexes with  $\beta$  hydrogens on an alkylidene ligand or metallacyclobutane ring ( $\beta$ -hydride elimination); coupling deactivation reactions (equation 2c) are thought to occur most often for complexes with less substitution on the alkylidene ligand (i.e. most often for methylidenes).<sup>1,7,8</sup>

More recently, the preparation of tungsten<sup>11-14</sup> and molybdenum<sup>15</sup> alkylidyne compounds containing bulky alkoxide ligands has demonstrated the utility of bulky ligation in stabilizing the metal center from decomposition reactions similar to those described above, as evidenced by the efficient catalytic activity shown by these complexes for acetylene metathesis. Building on this work, which utilized bulky ligation as a means of catalyst stabilization, and on

that previously outlined in tantalum alkylidene chemistry in the areas of Wittig-like reactivity and olefin metathesis, the preparation and reactivity of a variety of tantalum alkylidene complexes supported with bulky ligation has been investigated.

The purpose of this study has been to obtain useful catalyst systems by systematically varying the electronic and steric properties imposed in the complexes (by varying the ligation within them). In this chapter the synthesis of tantalum alkylidene complexes containing bulky phenoxide and arylthiolate ligands is reported, along with their reactivity toward a variety of acyclic olefins. Previous to this report, no complexes of the type  $\text{Ta}(\text{CHR})(\text{SR})_3$  had been reported, and only one complex of the type  $\text{Ta}(\text{CHR})(\text{OR})_3$  had been reported.<sup>7</sup> This complex,  $\text{Ta}(\text{CHCMe}_3)(\text{OCMe}_3)_3$ , was not isolated in crystalline form and showed limited use as an olefin metathesis catalyst, much like related complexes of the general formula  $\text{Ta}(\text{CHR})\text{X}_3\text{B}_2$ . However, the reaction chemistry of the current compounds has proven to be more useful, and in many cases DIPP alkylidene complexes react with olefins to form stable tantalacyclobutane compounds. The Wittig-like reactivity of these alkylidene and metallacyclobutane complexes with organic carbonyls is also reported, as these reactions represent an important method for selectively cleaving polymer chains from tantalum catalysts. Some of this work has been published.<sup>16,17</sup> In chapter 2, the activity of tantalum alkylidene and tantalacyclobutane complexes as catalysts for the ring-opening polymerization of cyclic olefins is described, and in chapter 3 the polymerization of substituted acetylenes by tantalum alkylidene complexes is discussed.

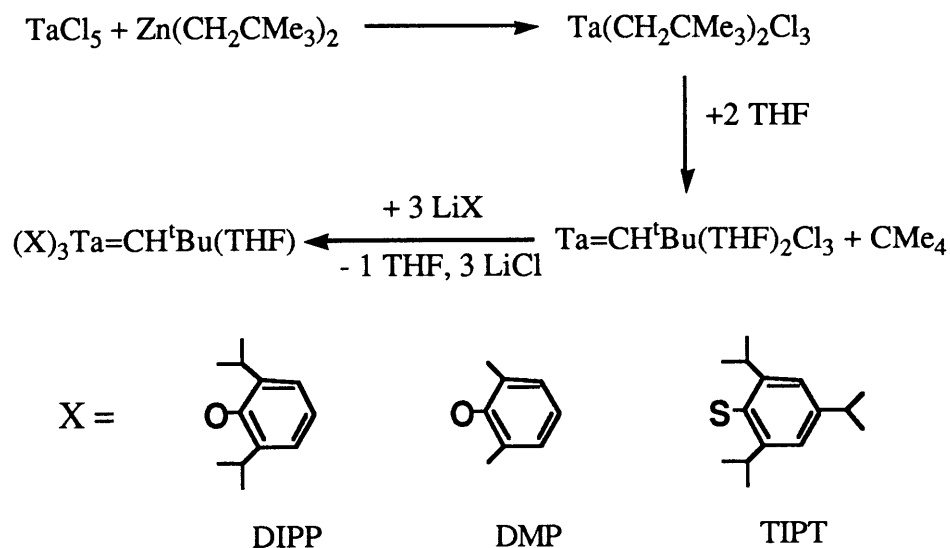
## RESULTS

### Preparation of $\text{Ta}(\text{CHCMe}_3)\text{X}_3(\text{B})$ Complexes ( $\text{X} = \text{DIPP}, \text{DMP}, \text{and TIPT}$ ; $\text{B} = \text{base}$ ).

The alkylidene  $\text{Ta}(\text{CHCMe}_3)(\text{THF})_2\text{Cl}_3$ <sup>18</sup> serves as an excellent starting material for the preparation of other alkylidene complexes, as its preparation is straightforward and can be performed on a large scale.  $\text{Ta}(\text{CHCMe}_3)(\text{THF})_2\text{Cl}_3$  is formed in two steps from  $\text{TaCl}_5$  (Scheme I): addition of  $\text{ZnNp}_2$  to  $\text{TaCl}_5$  in pentane results in the formation of  $\text{TaNp}_2\text{Cl}_3$ , and

this complex can be reacted with 2 equivalents of THF to give  $\text{Ta}(\text{CHCMe}_3)(\text{THF})_2\text{Cl}_3$ .

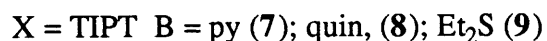
Scheme I: General Preparative Route to  $\text{Ta}(\text{CHR})\text{X}_3(\text{THF})$  Complexes.



$\text{Ta}(\text{CHCMe}_3)(\text{THF})_2\text{Cl}_3$  can be isolated from ether as dark purple crystals, and the overall yield from  $\text{TaCl}_5$  is excellent. A side product sometimes observed in this reaction (when performed on a large scale) in trace amounts is  $\text{Ta}(\text{CH}_2\text{CMe}_3)\text{Cl}_4(\text{THF})$  (1), formed as a result of incomplete alkylation of  $\text{TaCl}_5$  in the first step of the reaction. This complex can be isolated as large orange-red crystals from the ether filtrate after several crops of  $\text{Ta}(\text{CHCMe}_3)(\text{THF})_2\text{Cl}_3$  have been collected.

Addition of 3 equivalents of solid  $\text{LiDIPP}\cdot\text{Et}_2\text{O}$  ( $\text{DIPP} = 2,6$ -diisopropylphenoxide) to  $\text{Ta}(\text{CHCMe}_3)(\text{THF})_2\text{Cl}_3$  in ether results in the formation of  $\text{Ta}(\text{CHCMe}_3)(\text{DIPP})_3(\text{THF})$  (2; Scheme I). This reaction can be performed on a large scale ( $\sim 20$  g), with isolation of complex 2 as yellow crystals from ether in  $\sim 85\%$  yield. On a smaller scale ( $< 5$  g)  $\text{Ta}(\text{CHCMe}_3)(\text{DIPP})_3(\text{THF})$  forms in 90% yield from addition of solid  $\text{LiDIPP}\cdot\text{Et}_2\text{O}$  to  $\text{Ta}(\text{CHCMe}_3)(\text{THF})_2\text{Cl}_3$  generated *in situ*. Complex 2 is stable as a solid at  $25^\circ$  for at least several days, and when stored at  $-30^\circ$  appears to be stable over a period of months; in solution

(C<sub>6</sub>D<sub>6</sub>) some decomposition, to unidentified products, does occur over a period of days at 25°. Ta(CHCMe<sub>3</sub>)(DIPP)<sub>3</sub>(THF) reacts readily with pyridine to give an analogous pyridine adduct of the alkylidene, Ta(CHCMe<sub>3</sub>)(DIPP)<sub>3</sub>(py) (**3**; equation 3). <sup>1</sup>H and <sup>13</sup>C NMR data



for these alkylidene complexes (and others) are listed in Table I. In the <sup>1</sup>H NMR spectra of **2** and **3** (C<sub>6</sub>D<sub>6</sub>, 25°) the neopentylidene H<sub>α</sub> resonances are observed at 5.73 and 6.29 ppm, respectively (the spectrum for **2** is shown in Figure 1), and the <sup>13</sup>C NMR spectra (C<sub>6</sub>D<sub>6</sub>, 25°) show resonances for the alpha carbons at 227.1 (J<sub>CH</sub> = 95 Hz) and 231.2 (J<sub>CH</sub> = 96 Hz). These values are somewhat typical of tantalum alkylidene complexes, and the observed values for J<sub>CαH</sub> are consistent with a distorted alkylidene ligand in a complex with a highly electrophilic metal center.<sup>1,8</sup>

The spectra of both complexes display resonances for only a *single* type of DIPP ligand at 25°, with those in the pyridine complex **3** being broadened. Upon cooling solutions of Ta(CHCMe<sub>3</sub>)(DIPP)<sub>3</sub>(THF) (**2**) in toluene-d<sub>8</sub>, several broad DIPP resonances are observed, but unfortunately even at very low temperatures (~-80°) a distinct complex cannot be identified, suggesting that at these low temperatures some fluxionality in the compound persists. If the structures of these complexes can be described as trigonal bipyramidal, and the DIPP ligands occupy equatorial positions (shown as A), then a rapid rotation of the phenyl groups about the C-O bonds in the DIPP ligands at 25°, with this process slowed at lower temperatures, could account for the observed spectrum of **2** at 25° and at lower temperatures (i.e. resonances only observed for a single type of DIPP ligand at 25°, broader resonances observed at lower temperatures). In complex **3** (pyridine adduct) this process would be slowed even at 25°.

**Table I.** NMR Data for the Alkylidene Ligands in Tantalum Alkylidene Complexes of the Type Ta(CHR)X<sub>3</sub>(B).<sup>a</sup>

Cmpd	CHR	X	B	$\delta H_{\alpha}$	$\delta C_{\alpha}$	$J_{CH}$
2	CHCMe <sub>3</sub>	DIPP	THF	5.73	227.1	95
3	CHCMe <sub>3</sub>	DIPP	py	6.29	231.2	96
4	CHCMe <sub>3</sub>	DMP	THF	6.93	237.4	107
5	CHCMe <sub>3</sub>	DMP	py	7.51	241.9	107
6	CHCMe <sub>3</sub>	TIPT	THF	c	251.9 <sup>b</sup>	76
7	CHCMe <sub>3</sub>	TIPT	py	4.09	252.4	94
8	CHCMe <sub>3</sub>	TIPT	quin	c	c	
9	CHCMe <sub>3</sub>	TIPT	Et <sub>2</sub> S	c	262	d
10	CHCMe <sub>3</sub>	TIPT	none	1.80	c	
16	CHPh	DIPP	THF	8.49	221.1	114
19	CH <sub>2</sub>	DIPP	py	e	217.4	135
20	CHSiMe <sub>3</sub>	DIPP	THF	7.73	210.6	102

<sup>a</sup> Solvent = C<sub>6</sub>D<sub>6</sub> and T = 25° unless otherwise noted.

<sup>b</sup> THF-d<sub>8</sub>

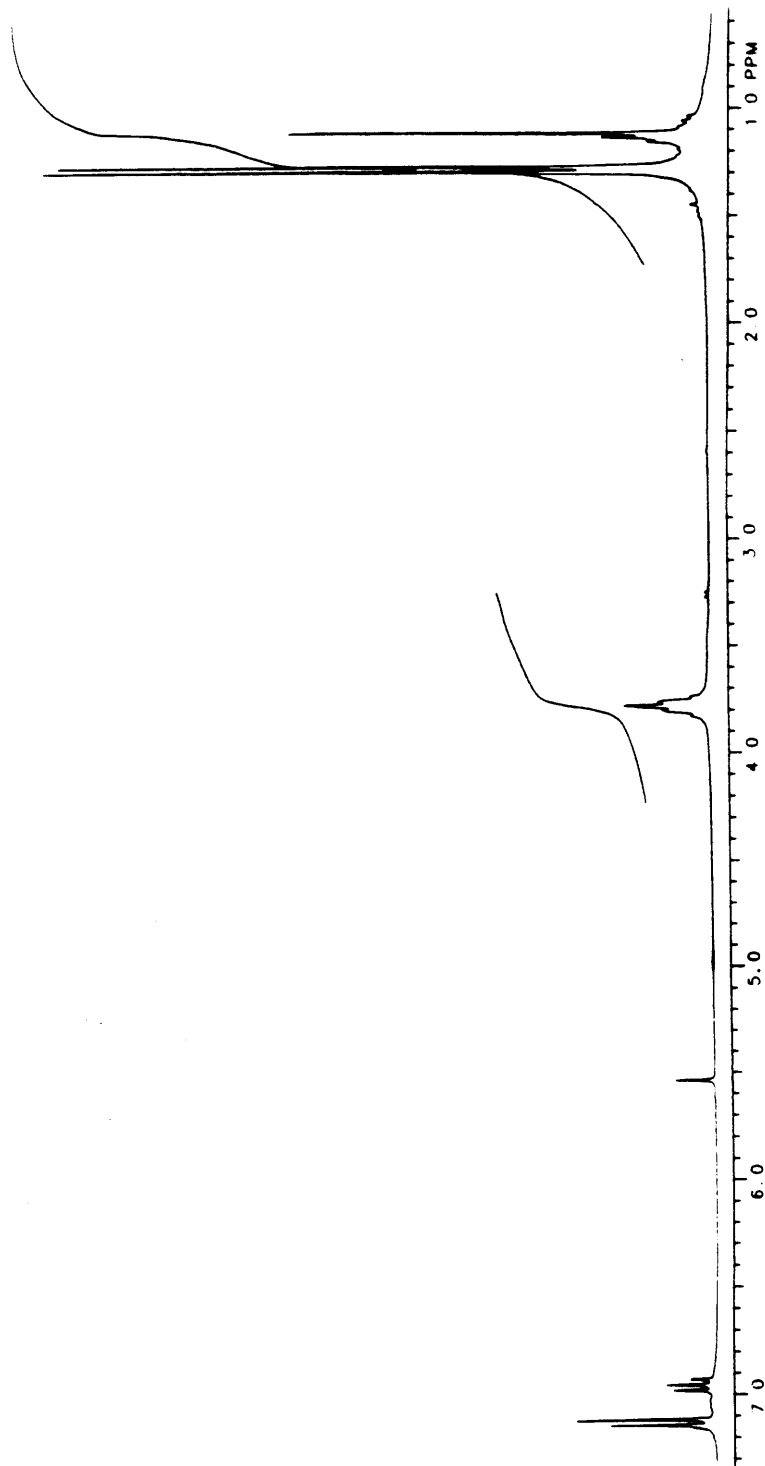
<sup>c</sup> Not observed.

<sup>d</sup> The C<sub>α</sub> resonance was broad, and J<sub>CH</sub> could not be determined.

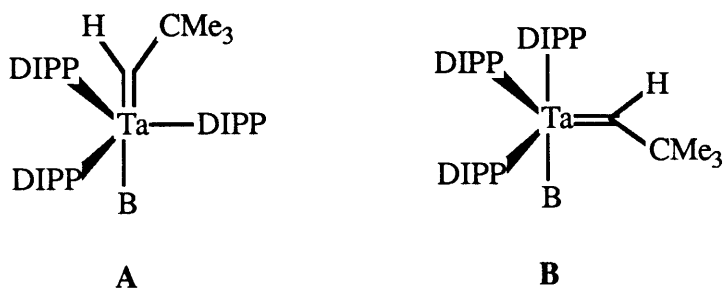
<sup>e</sup> The methyldene was only observed by <sup>13</sup>C NMR spectroscopy.



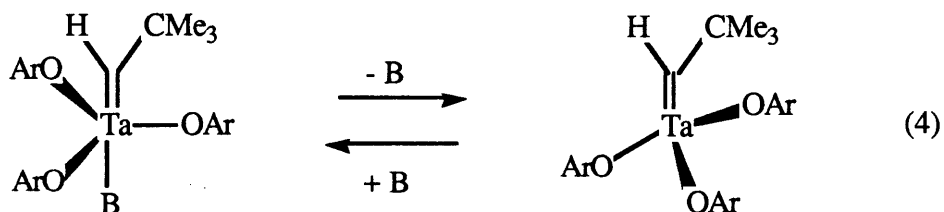
**Figure 1.** The  $^1\text{H}$  NMR spectrum of  $\text{Ta}(\text{CHCMe}_3)(\text{DIPP})_3(\text{THF})$  (**2**) in  $\text{C}_6\text{D}_6$  at  $25^\circ$ .



However, based on the observed geometries of the analogous alkylidene complex  $\text{Ta}(\text{CMe}_2\text{CHCMe}_3)(\text{DIPP})_3(\text{py})$  (described in chapter 3) and the related dinitrogen complex  $(\text{THF})(\text{DIPP})_3\text{Ta}=\text{N}=\text{N}=\text{Ta}(\text{DIPP})_3(\text{THF})$ ,<sup>19</sup> the structures for complexes **2** and **3** are more likely to be approximately trigonal bipyramidal in geometry with the alkylidene ligands occupying equatorial sites and the base (THF or pyridine) occupying an axial site (i.e. **B**).



For a complex such as **B**, in the absence of any ligand exchange process, resonances for at least two types of DIPP ligands should be observed in the  $^1\text{H}$  and  $^{13}\text{C}$  NMR spectra, but an interchange of **B** with a base-free complex, in which all DIPP ligands equilibrate, could result in only one type of DIPP ligand observed in spectra at  $25^\circ$  (equation 4). At lower temperatures



the base should be bound more strongly to the metal, resulting in inequivalent DIPP ligands. The broadened resonances seen for  $\text{Ta}(\text{CHCMe}_3)(\text{DIPP})_3(\text{py})$  (**3**), as opposed to the sharp resonances seen for  $\text{Ta}(\text{CHCMe}_3)(\text{DIPP})_3(\text{THF})$  (**2**), in spectra at  $25^\circ$  are consistent with such an equilibrium, since pyridine is a stronger base than THF and consequently should bind more strongly to the metal center. As would be expected from the above discussion, when additional

equivalents of THF are added to a sample of **2** in C<sub>6</sub>D<sub>6</sub>, rapid exchange of coordinated THF with free THF is evident in the <sup>1</sup>H NMR spectrum at 25°.

Interestingly, THF cannot be removed from complex **2** even when left *in vacuo* (as a solid) at 25° for several days, and heating this sample leads to decomposition (in complex **3** pyridine also is bound strongly in the solid state; the previously reported t-butoxide complex, Ta(CHCMe<sub>3</sub>)(OCMe<sub>3</sub>)<sub>3</sub>, is base-free<sup>7</sup>). Other attempts to remove the base, such as reacting complex **2** with NEt<sub>3</sub> or methyl-THF (bulkier bases) in solution, followed by removal of the solvent *in vacuo*, were not successful.<sup>20</sup> The inability to remove THF and pyridine from these complexes *without decomposition* suggests the presence of a highly electrophilic metal center.

A dimethylphenoxide complex, Ta(CHCMe<sub>3</sub>)(DMP)<sub>3</sub>(THF) (**4**; DMP = 2,6-dimethylphenoxide), is prepared by addition of 3 equivalents of LiDMP to Ta(CHCMe<sub>3</sub>)(THF)<sub>2</sub>Cl<sub>3</sub> in ether/THF (~10/1) (Scheme I). This complex is isolated as an orange-yellow precipitate from ether or pentane in lower yield (~60%) than that seen for the related DIPP complex **2**. Complex **4** is more soluble than complex **2** in common hydrocarbon solvents, a result not expected based on the larger number of hydrocarbon substituents in a DIPP ligand. However, because the DMP ligands are smaller, rotation of the phenyl groups about the C-O bonds in these ligands should be less hindered, making this complex perhaps more fluxional than the related DIPP complex **2** in solution, and leading to an unexpected increased solubility.

Ta(CHCMe<sub>3</sub>)(DMP)<sub>3</sub>(THF) is less stable than the analogous DIPP complex, as evidenced by an accelerated rate of decomposition in room temperature solution. Additionally, the preparation reaction of **4** is extremely sensitive to concentration effects, such that a large volume of solvent is required for the reaction in order to attain the moderate yields. The absence of high yields may be the result of decomposition during the required workup steps in this reaction, which involve removal of the solvent *in vacuo* (to remove any excess THF and residual LiCl) before redissolution for crystallization. These observations suggest the presence of increased intermolecular decomposition for Ta(CHCMe<sub>3</sub>)(DMP)<sub>3</sub>(THF) (versus

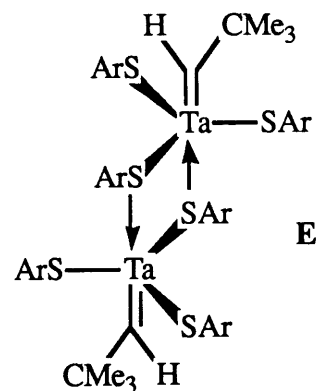
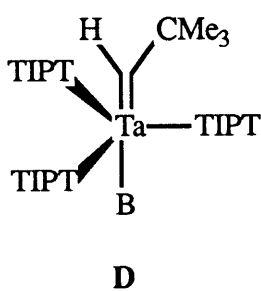
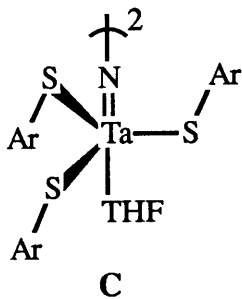
Ta(CHCMe<sub>3</sub>)(DIPP)<sub>3</sub>(THF)) when in solution, consistent with a reduction of steric protection in this complex (the phenoxide ligands are substituted with ortho methyl groups instead of ortho isopropyl groups). Rothwell has recently reported similar findings.<sup>21</sup> Clean formation of methyldene complexes of the type Ta(OAr)<sub>2</sub>(CH<sub>2</sub>)(CH<sub>3</sub>) (OAr = phenoxide ligand) was observed on irradiation of Ta(OC<sub>6</sub>H<sub>3</sub>Bu<sup>t</sup><sub>2</sub>-2,6)<sub>2</sub>(CH<sub>3</sub>)<sub>3</sub> and Ta(OC<sub>6</sub>H<sub>2</sub>Bu<sup>t</sup><sub>2</sub>-2,6-OMe-4)<sub>2</sub>(CH<sub>3</sub>)<sub>3</sub>. Irradiation of the DMP complex Ta(OC<sub>6</sub>H<sub>3</sub>Me<sub>2</sub>-2,6)<sub>2</sub>(CH<sub>3</sub>)<sub>3</sub> resulted in the formation of methane (indicative of an α-hydrogen atom abstraction leading to an alkylidene), but no alkylidene species were detected. These results were attributed to the smaller size of the DMP ligand, which is more likely to form a complex that is susceptible to intermolecular decomposition.

Ta(CHCMe<sub>3</sub>)(DMP)<sub>3</sub>(THF) reacts with pyridine to give the pyridine adduct Ta(CHCMe<sub>3</sub>)(DMP)<sub>3</sub>(py) (**5**; equation 3). The <sup>1</sup>H and <sup>13</sup>C NMR spectra (C<sub>6</sub>D<sub>6</sub>, 25°) of complexes **4** and **5** displayed expected resonances for H<sub>α</sub> at 6.93 and 7.51 ppm and for C<sub>α</sub> at 237.4 and 241.9 ppm (J<sub>CH</sub> = 107 Hz for each), respectively (Table I). As was noted for the DIPP compounds, resonances for only a single type of phenoxide ligand were observed in the spectra at 25°. Although no X-ray studies have been performed on a Ta(CHR)(DMP)<sub>3</sub>(B) compound, the structures of these complexes are thought likely to be analogous to those of the related DIPP alkylidene complexes.

Reaction of Ta(CHCMe<sub>3</sub>)(THF)<sub>2</sub>Cl<sub>3</sub> with 3 equivalents of LiTIPT (TIPT = 2,4,6-triisopropylbenzenethiolate) in ether or pentane results in the formation of Ta(CHCMe<sub>3</sub>)(TIPT)<sub>3</sub>(THF) (**6**; Scheme I). This compound can be isolated from pentane as a yellow precipitate in ~60% yield. Complex **6** reacts rapidly with pyridine, quinuclidine, and Et<sub>2</sub>S in ether at room temperature to form the corresponding base adduct complexes Ta(CHCMe<sub>3</sub>)(TIPT)<sub>3</sub>(py) (**7**), Ta(CHCMe<sub>3</sub>)(TIPT)<sub>3</sub>(quin) (**8**; quin = quinuclidine), and Ta(CHCMe<sub>3</sub>)(TIPT)<sub>3</sub>(Et<sub>2</sub>S) (**9**) in good yield (equation 3). Complexes **7** and **8** are isolated as yellow precipitates, and complex **9** alone can be isolated in crystalline form. All of these complexes are reasonably stable as solids at 25° and for extended periods of time when stored

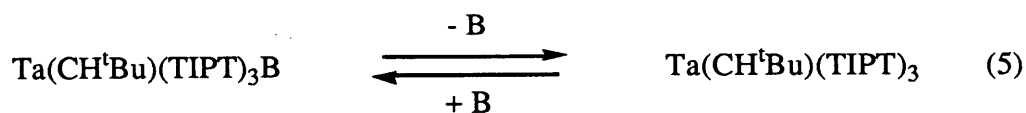
at  $-30^{\circ}$ . In solution, no noticeable decomposition is observed for these compounds over a period of a few hours, but studies with  $\text{Ta}(\text{CHCMe}_3)(\text{TIPT})_3(\text{THF})$  (**6**) show this complex to be unstable in solution over a period of days at  $25^{\circ}$ .

Very recently, the solid state structure of  $\text{Ta}(\text{CHCMe}_3)(\text{TIPT})_3(\text{Et}_2\text{S})$  (**9**) was determined by X-ray crystallography; because this study was conducted only recently, a full description of the structure is given in Appendix 1. While the structure of this complex is neither an ideal trigonal bipyramid or square pyramid, the large interligand angle of  $\sim 162^{\circ}$  between the alkylidene ligand and the base  $\text{Et}_2\text{S}$  (i.e.  $\angle \text{C-Ta-S}$ ) suggests a distorted trigonal bipyramidal description is reasonable. From this description, the three arylthiolate ligands occupy approximately equatorial positions (as shown in **D**), with one of these ligands bent (i.e. the aromatic ring of the thiolate ligand) in the direction of the axial  $\text{Et}_2\text{S}$  ligand and two bent in the direction of the axial alkylidene ligand. The related dinitrogen complex  $(\text{THF})(\text{DIPT})_3\text{Ta}=\text{N}=\text{N}=\text{Ta}(\text{DIPT})_3(\text{THF})$ <sup>19</sup> ( $\text{DIPT} = 2,6\text{-diisopropylbenzenethiolate}$ ) was shown by X-ray crystallography to be a trigonal bipyramidal complex in which the three arylthiolate ligands occupy equatorial positions, with two bent in the direction of the axial THF ligand and one bent in the direction of the axial "imido" ligand, on each end of the complex (as shown in **C**; average  $\angle \text{Ta-S-C} = 117^{\circ}$ ). A similar arrangement is observed



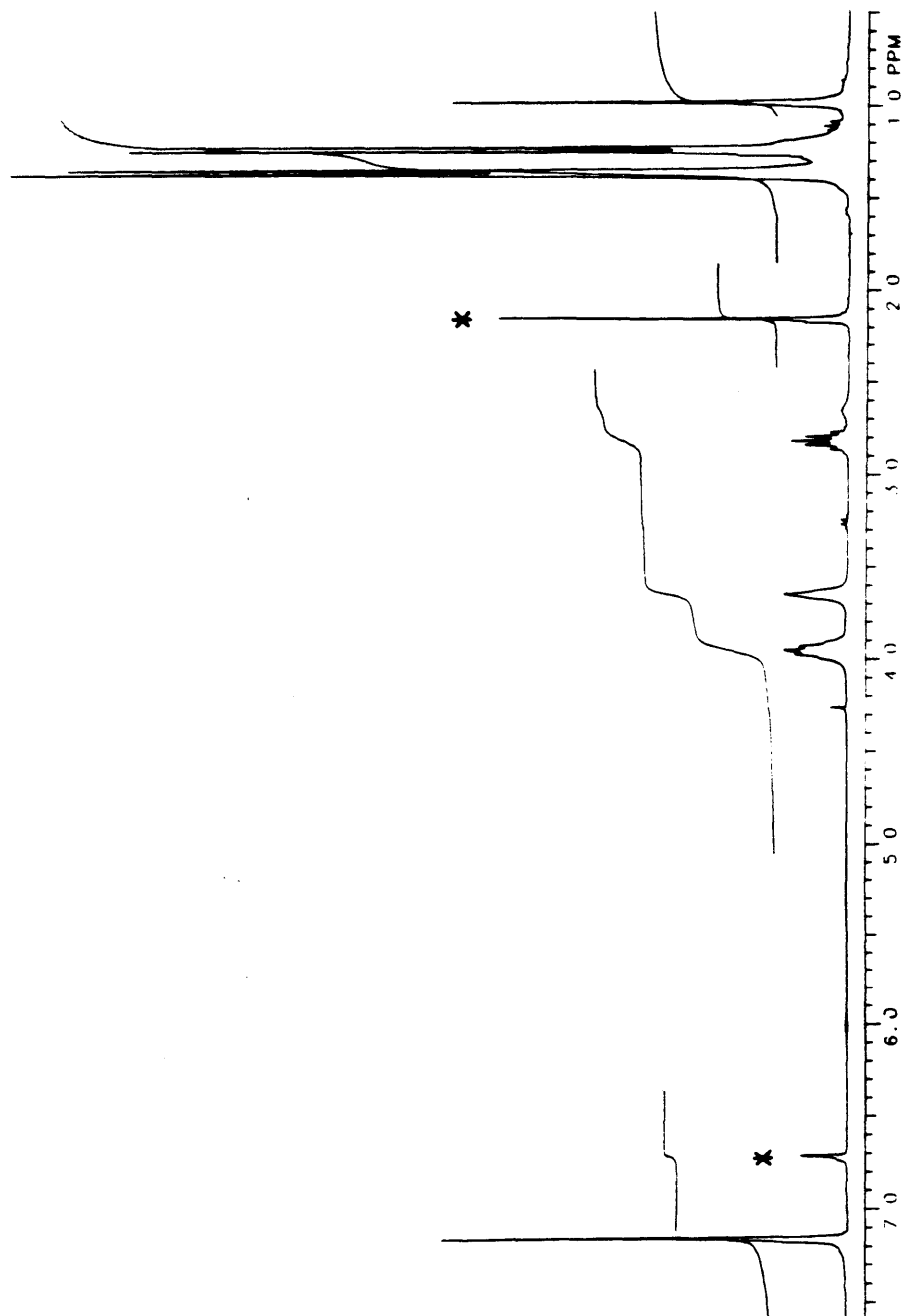
for all other structurally characterized transition metal complexes that contain three bulky arylthiolate ligands and display a trigonal bipyramidal geometry.<sup>22-26</sup> Additionally, from an NMR study on related five-coordinate arylthiolate alkylidyne complexes of molybdenum and tungsten, the authors concluded this type of structural arrangement was most reasonable.<sup>27</sup> Based on all this information, the structures of the tantalum arylthiolate alkylidene complexes **6-8** are thought to be somewhat analogous to that of the Et<sub>2</sub>S adduct **9** and the related tantalum dinitrogen complex.

The <sup>1</sup>H NMR spectra of complexes **6** (THF adduct), **8** (quin adduct), and **9** (Et<sub>2</sub>S adduct) (Table I) display relatively sharp signals for all observed resonances except those arising from the base (the <sup>1</sup>H NMR spectrum of complex **6** is shown in Figure 2). Resonances for only one type of TIPT ligand are observed in these spectra, and resonances for the neopentylidene H<sub>α</sub>'s are noticeably absent. When 7 equivalents of THF are added to a solution of the THF adduct **6** in C<sub>6</sub>D<sub>6</sub> at 25°, facile exchange of the coordinated THF with free THF is evident in the <sup>1</sup>H NMR spectrum. Considering this facile exchange, these base adduct complexes could be (and are thought to be) in rapid equilibrium with the base-free alkylidene Ta(CHCMe<sub>3</sub>)(TIPT)<sub>3</sub> in solution at 25°, causing a broadening of the neopentylidene H<sub>α</sub> resonances such that they cannot be distinguished from the baseline (equation 5); alternatively these resonances might be obstructed by other resonances arising in the complexes.



Interestingly, a sharp resonance for H<sub>α</sub> (4.09 ppm) can be seen in the <sup>1</sup>H NMR spectrum of the pyridine adduct **7** in C<sub>6</sub>D<sub>6</sub> at 25°, along with broad resonances for the TIPT ligands. Apparently pyridine is bound more strongly to the metal than are THF, quinuclidine, and Et<sub>2</sub>S in **6**, **8**, and **9**, respectively, with the equilibrium between the base-free alkylidene and the base adduct complex **7** largely favoring the latter. In complex **7** rotation of the Ta-S bonds

**Figure 2.** The  $^1\text{H}$  NMR spectrum of  $\text{Ta}(\text{CHCMe}_3)(\text{TIPT})_3(\text{THF})$  (**6**) in  $\text{C}_6\text{D}_6$  at  $25^\circ$  (\* = mesitylene).



in the TIPT ligands must be sterically restricted by the bound pyridine, causing broad resonances for these ligands (in the static structure **D**, since two TIPT ligands are pointed toward one axial ligand and one TIPT ligand is pointed toward the other axial ligand, in the absence of rotation these TIPT ligands should not all be equivalent). In the other complexes **6**, **8**, and **9** the ready equilibrium with base-free Ta(CHCMe<sub>3</sub>)(TIPT)<sub>3</sub> allows a more free rotation of the Ta-S bonds in the TIPT ligands, resulting in resonances observed for only a single type of TIPT ligand. The <sup>13</sup>C NMR spectra of complexes **6-9** further support the equilibrium hypothesis. In C<sub>6</sub>D<sub>6</sub> at 25°, a resonance for C<sub>α</sub> is clearly seen in the spectrum of the pyridine adduct **7** (252.4 ppm, J<sub>CH</sub> = 94 Hz), while this resonance is very broad in the spectrum of the ethylsulfide adduct **9** (centered around 262 ppm) and not observable in the spectrum of the quinuclidine adduct **8**. The <sup>13</sup>C NMR spectrum (25°) of the THF adduct **6** was acquired employing the solvent THF-d<sub>8</sub>, and the C<sub>α</sub> resonance was clearly seen at 251.9 ppm (J<sub>CH</sub> = 76 Hz), consistent with an equilibrium of this complex with the base-free complex (equation 5) shifted largely toward the base adduct as a result of the large excess of THF in solution (in the <sup>1</sup>H NMR spectrum of **6** in THF-d<sub>8</sub>, a broad singlet was observed at ~1.68 that might arise from H<sub>α</sub>, although this could not be determined unequivocally due to near solvent resonances).

An interesting side product in the preparation of Ta(CHCMe<sub>3</sub>)(TIPT)<sub>3</sub>(THF) (**6**) turns out to be the base-free complex Ta(CHCMe<sub>3</sub>)(TIPT)<sub>3</sub> (**10**). Fortunately, complex **10** is very soluble in common organic solvents, resulting in minimal contamination of the THF adduct **6** in the preparation reaction. Complex **10** can be isolated from pentane as deep red crystals, after the majority of complex **6** has precipitated. The formation of **10** is most evident when the preparation reaction (of **6**) is initiated at a low temperature (-30°) and when the concentration of the reactants is high. Complex **10** is thought to be dimeric, and reaction of **10** with pyridine supports a dimeric assignment. Reaction of Ta(CHCMe<sub>3</sub>)(TIPT)<sub>3</sub> (**10**) with ~50 equivalents of pyridine in C<sub>6</sub>D<sub>6</sub> results in only trace formation of the pyridine adduct **7** after 24 hours at 25°. However, when this same sample is heated to 50°, after ~15 minutes ~15% of the pyridine adduct **7** is seen. A monomeric base-free complex would be expected to react rapidly with



pyridine at 25° (since the THF adduct does), but a dimeric complex could show limited reactivity with pyridine at 25°, if the dimer was not in equilibrium with a significant amount of the monomer at this temperature; higher temperatures would increase the probability of monomer formation, resulting in increased reactivity (as was observed).

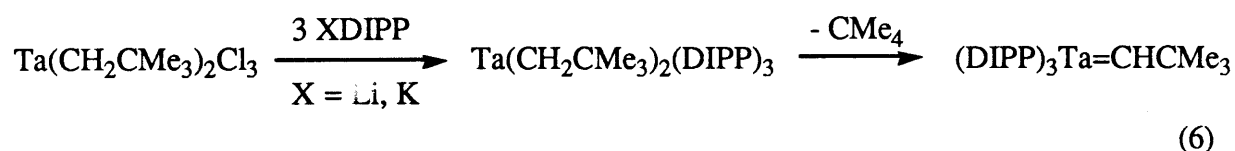
The proposed structure for complex **10** is **E** (shown earlier with **C** and **D**), which is analogous to structure **D** (Ta(CHCMe<sub>3</sub>)(TIPT)<sub>3</sub>(Et<sub>2</sub>S), **9**) except that bridging arylthiolate ligands occupy the axial sites previously occupied by the base ligands. Thiolate ligands are known to form many bridging complexes with transition metals,<sup>28,29</sup> and analogous dimers have been reported for related arylthiolate alkylidyne complexes of molybdenum and tungsten.<sup>27</sup> The <sup>1</sup>H NMR spectrum of complex **10** in C<sub>6</sub>D<sub>6</sub> at 25° shows a neopentylidene H<sub>α</sub> resonance at 1.80 ppm as a broad singlet, and resonances are seen for only a single type of TIPT ligand. The <sup>13</sup>C NMR spectrum also displays resonances for a single type of TIPT ligand, and a resonance for C<sub>α</sub> could not be identified. In the structure of **E**, even when allowing for facile rotation of the Ta-S bonds in the TIPT ligands, two distinct types of TIPT ligands are present (bridging and non-bridging). Thus complex **10** must be in ready equilibrium with at least a *very small* amount of the monomeric complex, allowing for the TIPT resonances to be averaged in the observed spectra. The broadening of the neopentylidene H<sub>α</sub> resonance and the absence of an observable C<sub>α</sub> resonance are also consistent with such an equilibrium, as is the formation of a *very small* amount of the pyridine adduct **7** from reaction of complex **10** with pyridine at 25°.

If some dimer complex forms during the synthesis of the THF adduct **6**, and the base adducts **6**, **8**, and **9** are in equilibrium with the base-free complex Ta(CHCMe<sub>3</sub>)(TIPT)<sub>3</sub> in solution at 25°, then one must ask why similar dimer formation is not observed in the spectra of these adducts at 25°. Dimer formation (a bimolecular reaction) was reported to be greatest when the preparation reaction for **6** was initiated at a low temperature (where the equilibrium between dimer and monomer should largely favor the former) and when the reactants were present in high concentrations. Additionally, in any preparation of complex **6**, workup of the

reaction mixture requires removal of the solvent *in vacuo* before redissolution in pentane for precipitation, thereby systematically increasing the concentration of the solution. These conditions are more conducive to dimer formation than are conditions under which NMR spectra were obtained for the base adduct complexes. These spectra were obtained at 25°, and if the equilibrium shown in equation 5 largely favors the base adduct complexes (this was not determined since only averaged resonances were observed), then the base-free complex may be present in only very low concentrations. (Attempts to limit the amount of dimer formation in the preparation of **6**, such as adding THF to the reaction mixture or to the pentane solution before cooling, did not result in a significant depression of dimer formation.)

#### Attempted Preparation of Ta(CHCMe<sub>3</sub>)(DIPP)<sub>3</sub>(B) from Ta(CH<sub>2</sub>CMe<sub>3</sub>)<sub>2</sub>(DIPP)<sub>3</sub>.

In the synthetic route to Ta(CHCMe<sub>3</sub>)(DIPP)<sub>3</sub>(THF) (**2**) shown in Scheme I, an alkylidene complex (Ta(CHCMe<sub>3</sub>)(THF)<sub>2</sub>Cl<sub>3</sub>) is first prepared via a base induced  $\alpha$ -hydrogen atom abstraction in Ta(CH<sub>2</sub>CMe<sub>3</sub>)<sub>2</sub>Cl<sub>3</sub>. The chloride ligands in this alkylidene are then replaced with DIPP ligands, leading to the formation of complex **2**. The alternative synthetic strategy shown in equation 6 was also investigated. In this strategy, replacement

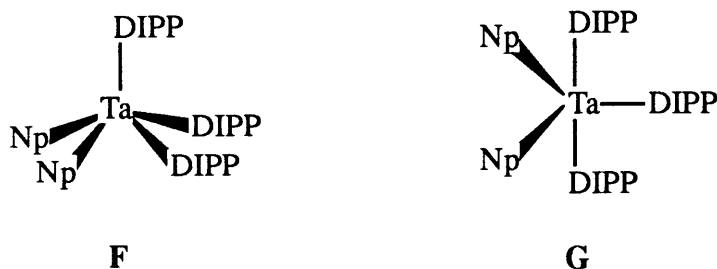


of the chloride ligands in Ta(CH<sub>2</sub>CMe<sub>3</sub>)<sub>2</sub>Cl<sub>3</sub> with DIPP ligands would give the new dialkyl complex Ta(CH<sub>2</sub>CMe<sub>3</sub>)<sub>2</sub>(DIPP)<sub>3</sub>, and an  $\alpha$ -hydrogen abstraction in this complex would lead to the formation of the alkylidene complex Ta(CHCMe<sub>3</sub>)(DIPP)<sub>3</sub> (there are many examples of  $\alpha$ -hydrogen atom abstraction reactions<sup>1,21,30-35</sup> and related  $\alpha$ -hydride elimination reactions<sup>36,37</sup> reported in the literature).

Ta(CH<sub>2</sub>CMe<sub>3</sub>)<sub>2</sub>Cl<sub>3</sub> does react readily with LiDIPP in ether at 25°, but in the product obtained only two chloride ligands have been replaced to give Ta(CH<sub>2</sub>CMe<sub>3</sub>)<sub>2</sub>(DIPP)<sub>2</sub>Cl (**11**), isolated as a white precipitate from pentane. Further reaction of this complex with KDIPP, a

stronger source of the DIPP anion, results in the formation of the tris DIPP complex  $\text{Ta}(\text{CH}_2\text{CMe}_3)_2(\text{DIPP})_3$  (**12**), isolated as a white precipitate from pentane or as colorless crystals from ether. Complex **12** can be prepared directly from  $\text{Ta}(\text{CH}_2\text{CMe}_3)_2\text{Cl}_3$ , without isolation of the intermediate complex **11**, by reaction of  $\text{Ta}(\text{CH}_2\text{CMe}_3)_2\text{Cl}_3$  with two equivalents of LiDIPP followed by reaction with KDIPP.

$^1\text{H}$  and  $^{13}\text{C}$  NMR spectra of complex **12** ( $\text{C}_6\text{D}_6$ ,  $25^\circ$ ) display resonances for two inequivalent DIPP ligands (2:1 ratio) and equivalent neopentyl ligands. Two likely structures for **12** are shown as **F** (square pyramidal geometry) and **G** (trigonal bipyramidal geometry).



In either structure the two neopentyl ligands are *cis* to one another, a condition thought conducive for  $\alpha$ -hydrogen atom abstraction involving two alkyl groups.<sup>31</sup> Obviously, though, an  $\alpha$ -hydrogen atom abstraction does not occur in complex **12** under normal conditions (or at elevated temperatures), contrasting earlier reports of spontaneous  $\alpha$ -hydrogen atom abstractions such as those seen in the decomposition of  $\text{Ta}(\text{CH}_2\text{Ph})_5$ <sup>30</sup> and the formation of  $\text{Ta}(\text{CHCMe}_3)(\text{CH}_2\text{CMe}_3)_3$  from  $\text{Ta}(\text{CH}_2\text{CMe}_3)_3\text{Cl}_2$  and 2 equivalents of  $\text{LiCH}_2\text{CMe}_3$ .<sup>5</sup>

Several attempts were made to induce an  $\alpha$ -hydrogen atom abstraction in  $\text{Ta}(\text{CH}_2\text{CMe}_3)_2(\text{DIPP})_3$  (**12**). In some cases this type of reaction has been induced by the presence of a base,<sup>18</sup> so complex **12** was reacted with a variety of bases (THF, pyridine, and triethylamine) both at  $25^\circ$  and at elevated temperatures. However, in none of these cases was alkylidene formation observed, and in most cases very little reaction was observed at all. Other alkylidene forming  $\alpha$ -hydrogen atom abstractions have been shown to be induced

photochemically,<sup>21,31-35</sup> but exposure of **12** to light for extended periods of time, both in the absence and presence of a base, led to no such formation.

The absence of an  $\alpha$ -hydrogen atom abstraction in  $\text{Ta}(\text{CH}_2\text{CMe}_3)_2(\text{DIPP})_3$  (**12**) is noteworthy. In such reactions, as mentioned above, a *cis* configuration of the two participating alkyl groups is thought most conducive, and this condition is met in complex **12**. Furthermore, an initial interaction between the metal center and an  $\alpha$ -hydrogen is thought likely to be involved, allowing the  $\alpha$ -hydrogen to be more easily removed as a "proton" by the other participating alkyl group.<sup>8</sup> This also might be the case in **12**, considering the low  $J_{\text{CH}}$  value (average) of 113 Hz for the  $\alpha$  methylene groups. Why an  $\alpha$  hydrogen atom abstraction reaction cannot be efficiently induced in complex **12**, then, is not known. Perhaps in  $\text{Ta}(\text{CH}_2\text{CMe}_3)_2(\text{DIPP})_3$  the presence of the bulky DIPP ligands sterically hinders any further interaction that would lead to an  $\alpha$ -hydrogen atom abstraction; strong  $\pi$  donation by these ligands may also prevent further  $\text{M}\cdots\text{H}$  interaction. Fortunately, the earlier described preparation of  $\text{Ta}(\text{CHCMe}_3)(\text{DIPP})_3(\text{THF})$  (**2**) from  $\text{Ta}(\text{CHCMe}_3)(\text{THF})_2\text{Cl}_3$  is a convenient and high yield reaction, making the lack of formation of  $\text{Ta}(\text{CHCMe}_3)(\text{DIPP})_3$  from complex **12** curious, but not limiting.

#### **Wittig Reactivity of $\text{Ta}(\text{CHCMe}_3)\text{X}_3(\text{THF})$ Complexes.**

The Wittig-like behavior of early transition metal alkylidene complexes<sup>6,38-40</sup> (equation 1a) and of related complexes such as Tebbe's reagent  $(\text{Ti}(\text{CH}_2\text{AlMe}_2\text{Cl})\text{Cp}_2)$ <sup>41,42</sup> and metallacyclobutane complexes<sup>43,44</sup> is well documented in the literature. These reactions are thought to proceed by formation of a metallaoxacyclobutane complex from addition of an organic carbonyl across an alkylidene ligand, followed by subsequent ring-opening to yield a metal oxo complex and a new olefin. (Grubbs has reported the isolation of stable titanaoxacyclobutane complexes,<sup>45</sup> and related intermediates have also been observed in solution.<sup>38</sup>)

The phenoxide and thiolate alkylidene complexes **2** and **6** have also been found to display Wittig-like reactivity when reacted with organic carbonyls. The results of these

**Table II.** Products of the Reactions of Tantalum Alkylidene Complexes with Organic Carbonyls.<sup>a</sup>

Compound	Carbonyl	Temp.	Rn Time	Wittig Product	% Yield
2	Me <sub>2</sub> CO	25°	1 hr	Me <sub>2</sub> C=CHCMe <sub>3</sub>	95 (GLC)
2	PhCHO	40°	4 hr	PhHC=CHCMe <sub>3</sub> <sup>b</sup>	96 (GCMS)
2	Ph <sub>2</sub> CO	40°	8 hr	Ph <sub>2</sub> C=CHCMe <sub>3</sub>	88 (NMR)
2	MeCO <sub>2</sub> Et	40°	5 hr	(Me)(EtO)C=CHCMe <sub>3</sub>	65 (GCMS)
2	Me <sub>2</sub> NCHO	40°	10 hr	Me <sub>2</sub> NHC=CHCMe <sub>3</sub>	95 (NMR)
6	PhCHO	25°	< 1 hr	PhHC=CHCMe <sub>3</sub> <sup>c</sup>	82 (GLC)

<sup>a</sup> All reactions were performed in a hydrocarbon solvent (usually ether), with [Ta] = ~20 mM and 1-2 equivalents of organic carbonyl.

<sup>b</sup> *trans:cis* ratio = 1.9:1.0.

<sup>c</sup> *trans:cis* ratio = 1.0:1.0.

reactions are given in Table II.  $\text{Ta}(\text{CHCMe}_3)(\text{DIPP})_3(\text{THF})$  (**2**) reacts with acetone at  $25^\circ$  to give the expected Wittig product 2,4,4-trimethyl-2-pentene in high yield, and an analogous reaction with benzaldehyde at  $40^\circ$  gives a mixture of *cis* and *trans* 1-phenyl-3,3-dimethyl-1-butene, also in high yield (*trans*:*cis* = 1.9:1.0). The reaction with benzophenone and N,N-dimethylformamide is slower (as was previously reported for  $\text{Ta}(\text{CHCMe}_3)(\text{CH}_2\text{CMe}_3)_3$ )<sup>6</sup>, but the expected Wittig products are still obtained in high yield. Complex **2** also reacts with ethyl acetate to give Wittig products, but in lower yields (65%), as was observed previously with  $\text{Ta}(\text{CH}_2\text{CMe}_3)(\text{CH}_2\text{CMe}_3)_3$ .<sup>6</sup> The metal product in these reactions is  $\text{Ta}(\text{O})(\text{DIPP})_3$  (**13**), a white precipitate that appears to be completely insoluble in common organic solvents. Based on the insolubility of this complex and its similarity to  $[\text{Ta}(\text{O})(\text{CH}_2\text{CMe}_3)_3]_x$ <sup>6</sup>, complex **13** is thought to be polymeric, with bridging oxo ligands connecting the tantalum atoms in a polymer chain.

The arylthiolate alkylidene complex **6** reacts with benzaldehyde at  $25^\circ$  to give a mixture of *cis* and *trans* 1-phenyl-3,3-dimethyl-1-butene in good yield (*trans*:*cis* = 1.0:1.0), and the metal product in this case is an orange oil, soluble in common organic solvents. The  $^1\text{H}$  NMR spectrum of this oil in  $\text{C}_6\text{D}_6$  at  $25^\circ$  displayed many broad resonances, hindering analysis, but based on the observed Wittig products the oil is thought to be  $\text{Ta}(\text{O})(\text{TIPT})_3$  (**14**).

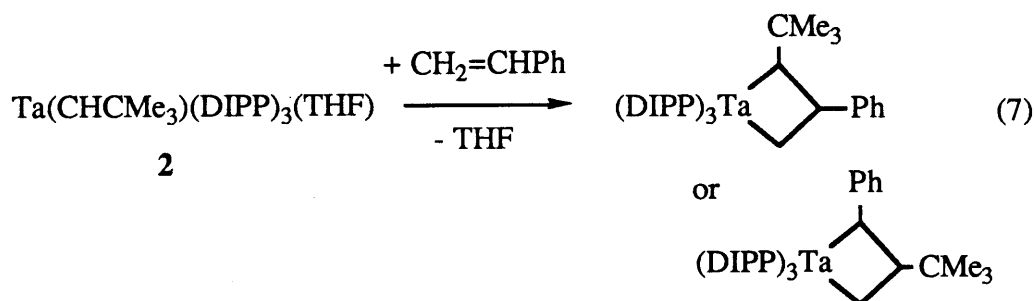
#### **Lack of Reactivity of $\text{Ta}(\text{CHCMe}_3)(\text{TIPT})_3(\text{THF})$ (**6**) with Acyclic Olefins.**

While both phenoxide and arylthiolate alkylidene complexes react readily with organic carbonyls, their behavior with ordinary olefins differs dramatically.  $\text{Ta}(\text{CHCMe}_3)(\text{TIPT})_3(\text{THF})$  (**6**) shows no reactivity with acyclic olefins. When combined with *cis*-3-hexene in ether at  $25^\circ$ , no sign of a reaction is observed even after several hours. Likewise, complex **6** does not metathesize 2-pentenes at  $25^\circ$  or  $50^\circ$ . A similar lack of reactivity (relative to corresponding phenoxide complexes) has been documented for arylthiolate alkylidyne complexes of molybdenum and tungsten.<sup>27</sup> Although the lack of reactivity with acyclic olefins limits the accessibility of other alkylidene complexes from the parent arylthiolate complex **6**, it also makes these arylthiolate compounds potentially attractive catalysts for the

polymerization of strained cyclic olefins and acetylenes, since secondary metathesis of the polymer chain would not occur. ( $\text{Ta}(\text{CHCMe}_3)(\text{TIPT})_3(\text{THF})$  *does* show reactivity towards strained cyclic olefins and acetylenes, and these reactions are described in chapters 2 and 3, respectively.)

### Reactivity of $\text{Ta}(\text{CHCMe}_3)(\text{OAr})_3(\text{THF})$ Complexes (OAr = DIPP, DMP) with Acyclic Olefins.

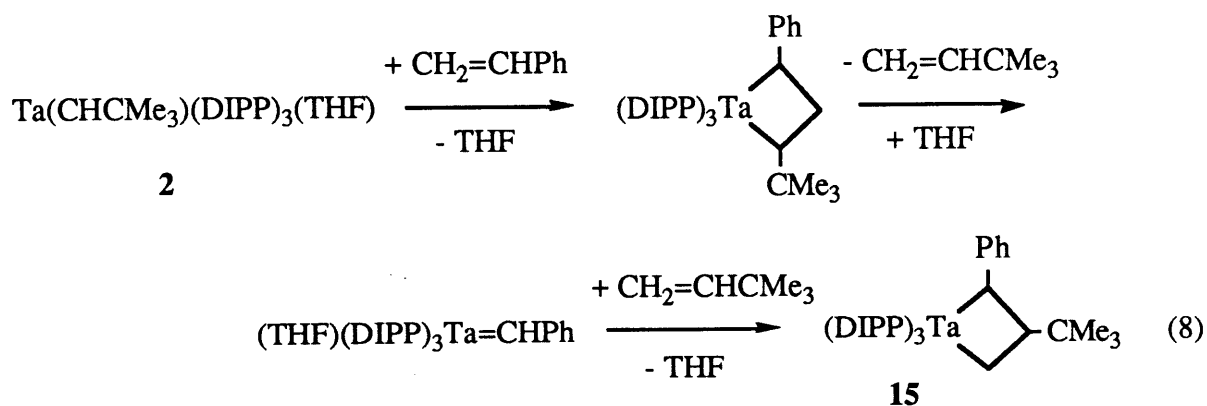
The phenoxide complex  $\text{Ta}(\text{CHCMe}_3)(\text{DIPP})_3(\text{THF})$  (**2**) displays a variety of reactivity with acyclic olefins, depending on the olefin and the reaction conditions employed. Reaction of one equivalent of styrene with  $\text{Ta}(\text{CHCMe}_3)(\text{DIPP})_3(\text{THF})$  (**2**) in ether at  $25^\circ$  results in the formation of a new base-free compound (**15**) which can be isolated as orange crystals from pentane. In the  $^1\text{H}$  NMR spectrum of these crystals ( $\text{C}_6\text{D}_6$ ,  $25^\circ$ ) resonances for a t-butyl group, a phenyl group, and one type of DIPP ligand (3 present, with diastereotopic DIPP methyl groups) were observed, along with several new resonances between 1 and 4 ppm, and no resonances indicative of an alkylidene complex were noted. These data are consistent with the formation of a tantalacyclobutane complex in which the two ring substituents (the phenyl and t-butyl groups) reside on  $\alpha$  and  $\beta$  carbons (equation 7; the NMR data does not distinguish between the two possible products shown).



The  $^{13}\text{C}$  NMR spectrum ( $\text{C}_6\text{D}_6$ ,  $25^\circ$ ) supported the metallacyclobutane assignment, displaying resonances for the ring carbons at 81.9 ( $\text{C}_\alpha$ ;  $J_{\text{CH}} = 133$  Hz), 63.8 ( $\text{C}_\alpha$ ;  $J_{\text{CH}} = 129$  Hz), and 42.9 ppm ( $\text{C}_\beta$ ;  $J_{\text{CH}} = 125$  Hz), and displaying resonances for a single type of DIPP

ligand with diastereotopic methyl groups (NMR data for metallacyclobutane complexes are listed in Table III). Metallacyclobutane complexes have been postulated as *intermediates* in the reactions of tantalum alkylidenes for some time,<sup>7,8</sup> but the formation of stable tantalacyclobutane complexes here (others are presented later) represents the first time tantalacyclobutanes have actually been observed.

The structure of complex **15** was determined by X-ray crystallography and found to be the tantalacyclobutane complex shown in equation 7 in which the phenyl group is substituted on an  $\alpha$  carbon and the t-butyl group is substituted on the  $\beta$  carbon of the ring (i.e. Ta[CH(Ph)CH(CMe<sub>3</sub>)CH<sub>2</sub>](DIPP)<sub>3</sub>; a drawing of **15** is shown in Figure 3). The formation of complex **15** follows initial formation of a metallacyclobutane complex in which the t-butyl group occupies an  $\alpha$  site on the ring; the presence of THF in the reaction mixture probably accelerates this rearrangement process by aiding in intermediate alkylidene formation and/or stabilization (equation 8, shown for an initial  $\alpha,\alpha$  substituted metallacycle; an initial  $\alpha$ (t-butyl), $\beta$ (phenyl) substituted metallacycle is also possible).



Relevant bond distances and angles for **15** are given in Table IV. Although the structure is neither clearly a trigonal bipyramid nor a square pyramid, the structure is thought best described as a distorted square pyramid with O(21) occupying the apical site. (the largest interligand angle in the complex is 151°). Many of the observed interligand angles in complex



**Table III.** Proton and Carbon NMR Data for the TaC<sub>3</sub> Ring in Tantalacyclobutane Complexes.<sup>a,f</sup>

Compound	H <sub>α</sub>	H <sub>β</sub>	C <sub>α</sub> (J <sub>CH</sub> )	C <sub>β</sub> (J <sub>CH</sub> )
<b>15<sup>c</sup></b>	3.10-2.85(2) 2.17(1)	1.57	81.9(d, 133) 63.8(t, 129)	42.9(d, 125)
<b>17</b>	3.86	0.48	96.1(t, 147)	-0.68(t, 150)
<b>18</b>	2.95	2.00	78.0(t, 120)	36.3(t, 129)
<b>21</b>	4.98(t) 3.64(t) 2.95(d)	-0.33	108.1(t, 145) 99.3(d, 128)	6.41(d, 131)
<b>26<sup>b</sup></b>	5.32(d) 3.88(br)	0.88		
W[CH <sub>2</sub> CHRCH <sub>2</sub> ](NAr)(OR') <sub>2</sub> <sup>b,d</sup>	5.71(dd) 4.36(dd) 4.04(m)	-0.77	110.8(t, 155) 105.7(d, 134)	5.2(d, 141)
W[CH <sub>2</sub> CH <sub>2</sub> CH <sub>2</sub> ](NAr)(OR) <sub>2</sub> <sup>b,e</sup>	4.87 4.58	-1.65	103.5(t, 158)	-6.79(t, 158)

<sup>a</sup> Solvent = C<sub>6</sub>D<sub>6</sub> and T = 25° unless otherwise noted.

<sup>b</sup> Approximately trigonal bipyramidal in geometry by X-ray crystallography.

<sup>c</sup> Approximately square pyramidal in geometry by X-ray crystallography.

<sup>d</sup> Reference 50; NAr = N-2,6-C<sub>6</sub>H<sub>3</sub><sup>i</sup>Pr<sub>2</sub>, R = SiMe<sub>3</sub>, OR' = OMe(CF<sub>3</sub>)<sub>2</sub>.

<sup>e</sup> Reference 50; NAr = N-2,6-C<sub>6</sub>H<sub>3</sub><sup>i</sup>Pr<sub>2</sub>, OR = OC(CF<sub>3</sub>)<sub>2</sub>(CF<sub>2</sub>CF<sub>2</sub>CF<sub>3</sub>).

<sup>f</sup> Compounds: Ta[CH(Ph)CH(<sup>t</sup>Bu)CH<sub>2</sub>](DIPP)<sub>3</sub> (**15**); Ta(CH<sub>2</sub>CH<sub>2</sub>CH<sub>2</sub>)(DIPP)<sub>3</sub> (**17**); Ta(CH<sub>2</sub>CH<sub>2</sub>CH<sub>2</sub>)(DIPP)<sub>3</sub>(py) (**18**); Ta[CH(SiMe<sub>3</sub>)CH(SiMe<sub>3</sub>)CH<sub>2</sub>](DIPP)<sub>3</sub> (**21**); Ta[CH(C<sub>5</sub>H<sub>8</sub>)CHCH(CMe<sub>3</sub>)](DIPP)<sub>3</sub> (**26**, chapter 2).

**Figure 3.** A view of Ta[CH(Ph)CH(<sup>t</sup>Bu)CH<sub>2</sub>](DIPP)<sub>3</sub> (**15**) (molecule 1).

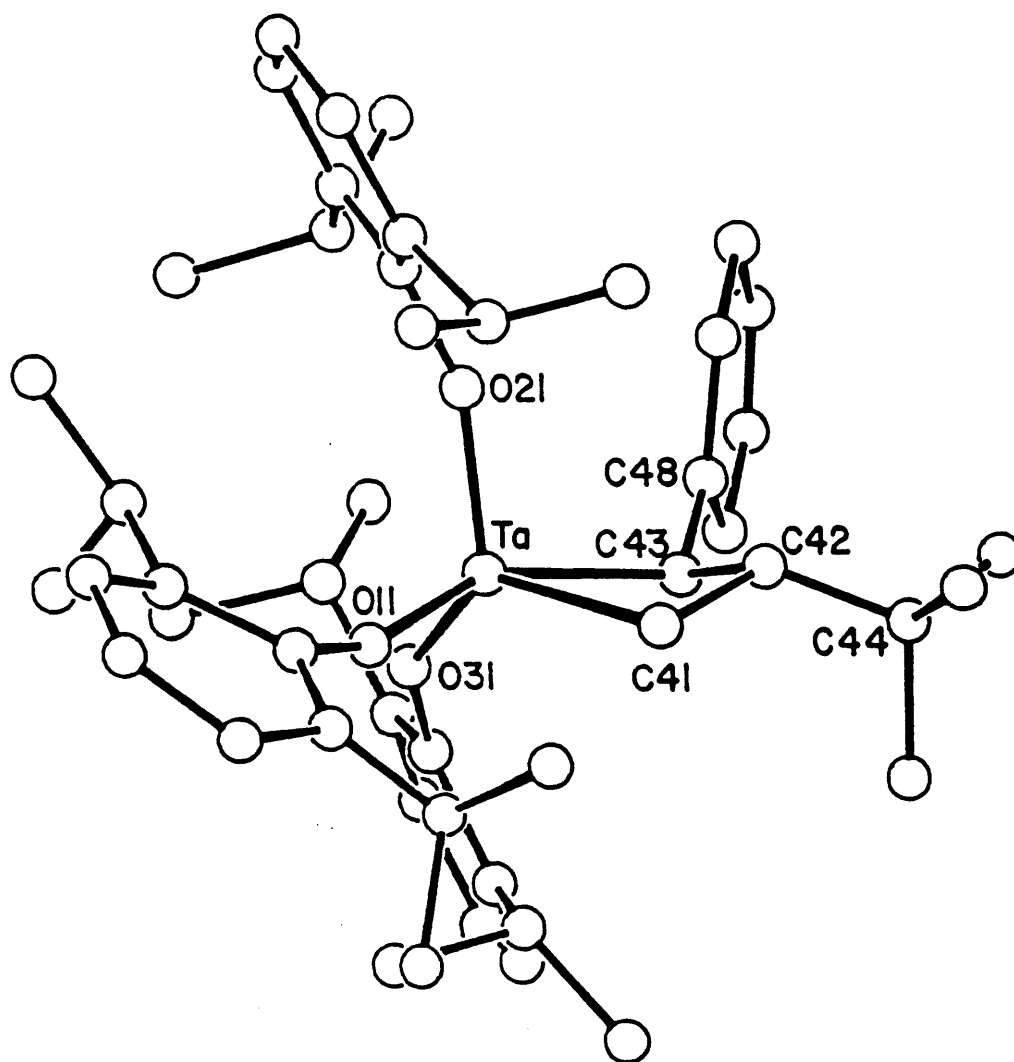


**Table IV.** Selected Bond distances (Å) and Angles (°) in Ta[CH(Ph)CH(CMe<sub>3</sub>)CH<sub>2</sub>](DIPP)<sub>3</sub> (15).

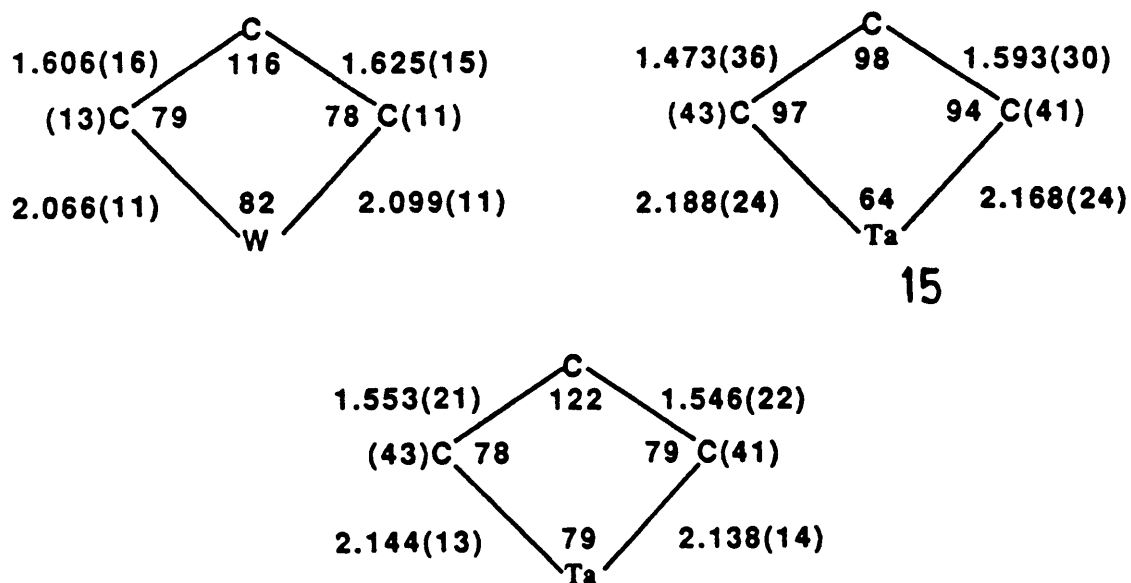
Ta-O(11)	1.893(13)	O(21)-Ta-O(31)	120.2(7)
Ta-O(21)	1.820(14)	C(41)-Ta-O(11)	90.3(7)
Ta-O(31)	1.864(15)	C(41)-Ta-O(21)	106.7(7)
Ta-C(41)	2.168(24)	C(41)-Ta-O(31)	128.8(7)
Ta···C(42)	2.782(24)	C(43)-Ta-O(11)	150.9(8)
Ta-C(43)	2.188(24)	C(43)-Ta-O(21)	96.7(7)
C(41)-C(42)	1.593(30)	C(43)-Ta-O(31)	89.3(8)
C(42)-C(43)	1.473(36)	C(43)-Ta-C(41)	64.4(9)
Ta-C(41)-C(42)	94.2(1.4)	C(41)-C(42)-C(43)	98.4(18)
Ta-C(43)-C(42)	97.0(1.5)	Ta-O(11)-C(11)	157.0(13)
O(11)-Ta-O(21)	104.7(6)	Ta-O(21)-C(21)	154.5(13)
O(11)-Ta-O(31)	96.6(6)	Ta-O(31)-C(31)	146.3(15)

**15** appear to result from steric demands within the complex; in related tantalum phenoxide complexes both square pyramidal and trigonal bipyramidal geometries have been observed.<sup>21</sup>

The large Ta-O-C angles of the DIPP ligands (average  $\approx 153^\circ$ ) indicate a significant amount of  $\pi$  (O  $p\pi$  to metal  $d\pi$ ) bonding from these ligands, as is usually the case in high-valent early transition metal complexes containing phenoxide ligands.<sup>12,21,46-49</sup> Within the known examples of structurally characterized tantalum(V) complexes containing terminal phenoxide ligands (i.e. those reported here and in reference 21), little variation is seen in the Ta-O bond lengths ( $\sim 1.82$ - $1.95$  Å). The Ta-O bond lengths in **15** fall into the short side of this range, with Ta-O(21) being the shortest bond reported to date for this class of compounds (1.820(14) Å). The Ta-C bond lengths are also quite normal for tantalum carbon single bonds in a Ta(V) complex.<sup>1</sup>

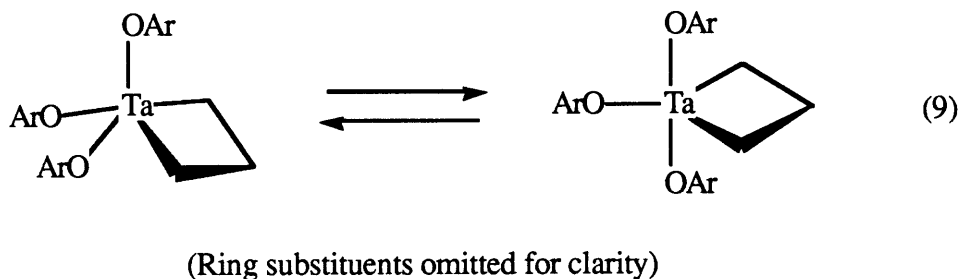
The ring in complex **15** is bent, with a dihedral angle of  $25.2^\circ$  between the planes defined by C(41)/C(42)/C(43) and Ta/C(41)/C(43), and the t-butyl and phenyl ring substituents are *trans* to one another. The Ta $\cdots$ C $\beta$  distance of 2.782(24) Å is longer than that observed in the trigonal bipyramidal tantalacyclobutane complex Ta[CH(C<sub>5</sub>H<sub>8</sub>)CHCH(CMe<sub>3</sub>)](DIPP)<sub>3</sub> (Ta $\cdots$ C $\beta$  = 2.382(16) Å; described in chapter 2) and in the related trigonal bipyramidal tungstanacyclobutane complex W[CH(SiMe<sub>3</sub>)CH(SiMe<sub>3</sub>)CH<sub>2</sub>](NAr)[OCMe(CF<sub>3</sub>)<sub>2</sub>]<sub>2</sub> (W $\cdots$ C $\beta$  = 2.372(11) Å),<sup>50</sup> but similar in length to those observed in related square pyramidal tungstenacyclobutane complexes.<sup>51</sup> The metallacyclobutane rings for some of these complexes are compared in Figure 4. The differences in the M $\cdots$ C $\beta$  bond lengths are thought to result from the different interligand angles associated with a square pyramidal complex versus a trigonal bipyramidal complex (in the trigonal bipyramidal complexes cited above, the metallacyclobutane ring resides in the equatorial plane; in complex **15** and square pyramidal tungsten complexes, the metallacyclobutane ring occupies two basal positions). In the trigonal bipyramidal metallacycles, the C $\alpha$ -Ta-C $\alpha$  angle is larger ( $\sim 80^\circ$  in Ta[CH(C<sub>5</sub>H<sub>8</sub>)CHCH(CMe<sub>3</sub>)](DIPP)<sub>3</sub> and W[CH(SiMe<sub>3</sub>)CH(SiMe<sub>3</sub>)CH<sub>2</sub>](NAr)[OCMe(CF<sub>3</sub>)<sub>2</sub>]<sub>2</sub>) than it is for the square pyramidal

**Figure 4.** A comparison of metallacyclobutane rings in complex **15**, Ta[CH(C<sub>5</sub>H<sub>8</sub>)CHCH(CMe<sub>3</sub>)](DIPP)<sub>3</sub>, and W[CH(SiMe<sub>3</sub>)CH(SiMe<sub>3</sub>)CH<sub>2</sub>](N-2,6-C<sub>6</sub>H<sub>3</sub><sup>i</sup>Pr<sub>2</sub>)[OCMe(CF<sub>3</sub>)<sub>2</sub>]<sub>2</sub>.

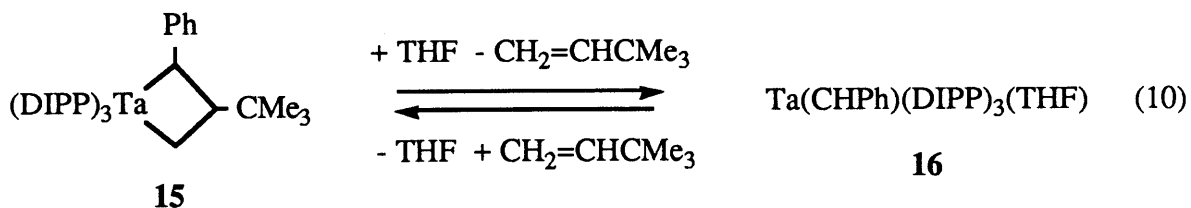


complex **15** ( $64^\circ$ ), resulting in a more "compressed" ring in the former complexes and consequently a shorter distance between the metal center and  $C_\beta$ .

In the crystal structure of **15** each DIPP ligand can certainly be described as unique. In spectra of **15** ( $C_6D_6$ ,  $25^\circ$ ), however, the DIPP ligands appear to be equivalent. This result is expected for an unsymmetric disubstituted metallacyclobutane complex such as **15** only if a fluxional process readily interconverts the DIPP ligands. An equilibrium process between the observed complex and a trigonal bipyramidal complex, in which all DIPP ligands interconvert, could account for such a result (equation 9) *without* breaking C-C bonds in the  $MC_3$  ring core, which appears to be stable and intact in solution at  $25^\circ$  in the absence of a base (an equilibrium with some other geometric isomer is also possible).



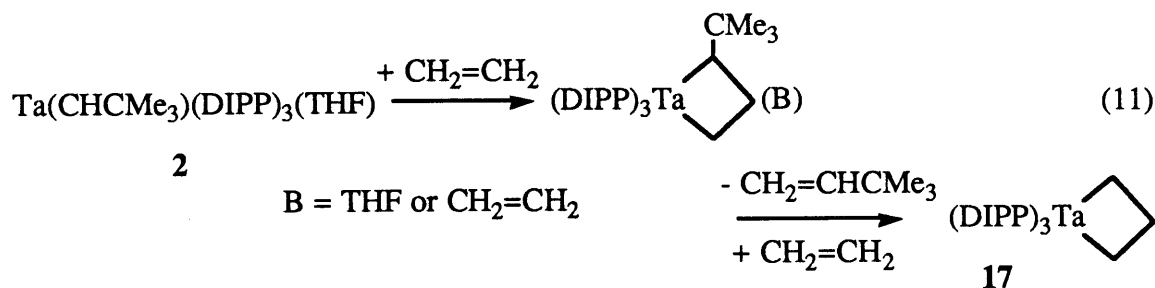
In the presence of several equivalents of THF at  $25^\circ$ , complex **15** shows an equilibrium with the benzylidene complex  $Ta(CHPh)(DIPP)_3(THF)$  (**16**) and *t*-butylethylene (equation 10). Thus both tantalacyclobutane and alkylidene complexes can be prepared by reaction of the



parent complex **2** with olefins. This new alkylidene complex can be isolated by reaction of  $Ta[CH(Ph)CH(CMe_3)CH_2](DIPP)_3$  (**15**) with excess THF in ether, followed by removal of

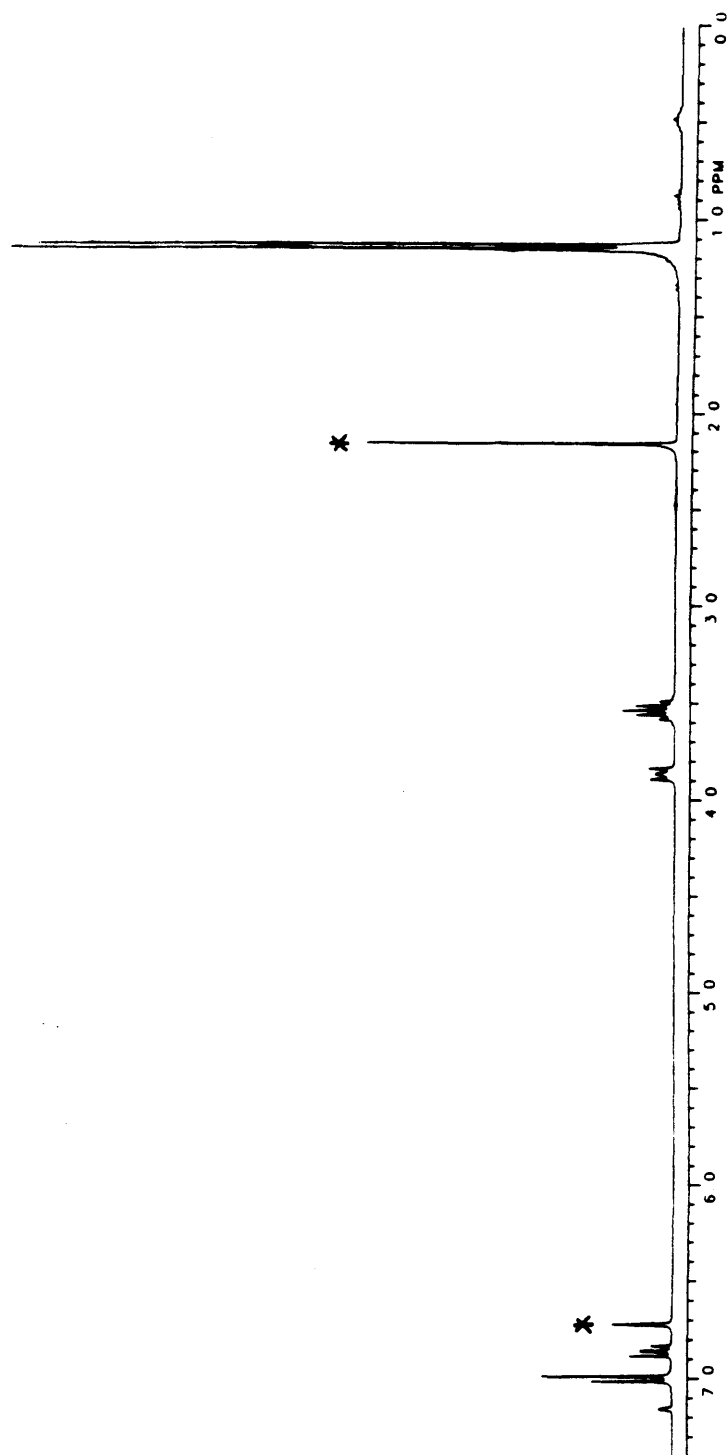
the solvent *in vacuo*, or by reaction of the parent complex  $\text{Ta}(\text{CHCMe}_3)(\text{DIPP})_3(\text{THF})$  (**2**) with styrene in the presence of a large excess of THF. The formation of complex **16** (shown in equation 10) is probably base-assisted (i.e. THF coordinates to the metallacyclobutane and enhances the rate of ring-opening), since addition of THF to solutions of  $\text{Ta}[\text{CH}(\text{Ph})\text{CH}(\text{CMe}_3)\text{CH}_2](\text{DIPP})_3$  gives equilibrium mixtures of **15** and **16** quickly.  $^1\text{H}$  and  $^{13}\text{C}$  NMR spectra ( $\text{C}_6\text{D}_6$ ,  $25^\circ$ ; Table I) support the alkylidene assignment for **16**, with  $\text{H}_\alpha$  seen at 8.49 ppm and  $\text{C}_\alpha$  at 221.1 ppm ( $J_{\text{CH}} = 114$  Hz). The benzylidene complex is noticeably less stable than the corresponding neopentylidene complex **2**, both in solution and in the solid state. A similar lack of stability has been observed for other benzylidene complexes.<sup>1,21</sup>

$\text{Ta}(\text{CHCMe}_3)(\text{DIPP})_3(\text{THF})$  (**2**) reacts with 30 psi of ethylene at  $25^\circ$  virtually instantaneously to give the base-free unsubstituted tantalacyclobutane complex  $\text{Ta}(\text{CH}_2\text{CH}_2\text{CH}_2)(\text{DIPP})_3$  (**17**), releasing (by GLC) 0.90 equivalents of t-butylethylene (equation 11). Complex **17** can be isolated from pentane as colorless crystals in good yield.



The initial tantalacycle containing an  $\alpha$  t-butyl group is not observed; apparently this monosubstituted tantalacycle ring-opens readily in a reaction that is likely to be accelerated by coordination of THF or ethylene to the initial metallacyclobutane (judging from the virtually instantaneous formation of **17** from **2**, and the notably slow ring-opening of related trisubstituted tantalacyclobutane complexes (discussed in chapter 2) in solution at  $25^\circ$ ). In the  $^1\text{H}$  NMR spectrum of **17** in  $\text{C}_6\text{D}_6$  at  $25^\circ$  (Figure 5), the  $\alpha$  proton resonances are seen as an overlapping doublet of doublets at 3.86 ppm, and the  $\beta$  proton resonances occur at 0.48 ppm

**Figure 5.** The  $^1\text{H}$  NMR spectrum of  $\text{Ta}(\text{CH}_2\text{CH}_2\text{CH}_2)(\text{DIPP})_3$  (**17**) in  $\text{C}_6\text{D}_6$  at  $25^\circ$  (\* = mesitylene).





as a multiplet (~broad pentet). A  $^{13}\text{C}$  NMR spectrum shows the ring carbons at 96.1 ( $J_{\text{CH}} = 147$  Hz) and -0.68 ( $J_{\text{CH}} = 150$  Hz). In both the  $^1\text{H}$  and  $^{13}\text{C}$  NMR spectra, resonances for a single type of DIPP ligand are observed. A similar conversion of the DIPP ligands as described earlier for **15** (i.e. equation 9) could account for this.

The ring resonances in **17** occur at chemical shifts markedly different from those seen for **15** (a distorted square pyramidal complex) - the  $\alpha$  methylene resonances occur downfield of those seen in  $\text{Ta}[\text{CH}(\text{Ph})\text{CH}(\text{CMe}_3)\text{CH}_2](\text{DIPP})_3$  (**15**), and the  $\beta$  methylene resonances occur upfield of those seen in **15**, resulting in a larger field separation for the ring resonances of **17**. Resonances similar to those in **15** were observed in the trigonal bipyramidal tantalacyclobutane complex  $\text{Ta}[\text{CH}(\text{C}_5\text{H}_8)\text{CHCH}(\text{CMe}_3)](\text{DIPP})_3$  (by X-ray crystallography, chapter 2), suggesting that the structure of **17** might also be trigonal bipyramidal. In fact, in a related area of tungsten chemistry, by determining the structures of several tungstenacyclobutane complexes, the geometry of the complexes was correlated with the NMR chemical shifts of the ring resonances in these complexes.<sup>51</sup> In that study, trigonal bipyramidal complexes (which contain a "compressed" ring, or a shorter  $\text{M}\cdots\text{C}_\beta$  distance) were found to display  $\alpha$  and  $\beta$  ring resonances downfield and upfield, respectively, of  $\alpha$  and  $\beta$  ring resonances in the corresponding square pyramidal complexes (which display a longer  $\text{M}\cdots\text{C}_\beta$  distance). Furthermore, ring resonances of square pyramidal tungstenacyclobutane complexes are very similar to those in  $\text{Ta}[\text{CH}(\text{Ph})\text{CH}(\text{CMe}_3)\text{CH}_2](\text{DIPP})_3$  (a distorted square pyramidal complex by X-ray crystallography), and ring resonances of trigonal bipyramidal tungstenacyclobutane complexes are very similar to those in  $\text{Ta}[\text{CH}(\text{C}_5\text{H}_8)\text{CHCH}(\text{CMe}_3)](\text{DIPP})_3$  (a trigonal bipyramidal complex by X-ray crystallography; see Table III for examples). These observations strongly suggest that chemical shifts in tantalacyclobutane complexes can be correlated with complex geometry, just as they can for tungstenacyclobutane complexes.<sup>51</sup>

The unsubstituted metallacycle **17** will react with pyridine readily to give an apparent adduct,  $\text{Ta}(\text{CH}_2\text{CH}_2\text{CH}_2)(\text{DIPP})_3(\text{py})$  (**18**); no reaction is observed between **17** and THF.  $\text{Ta}(\text{CH}_2\text{CH}_2\text{CH}_2)(\text{DIPP})_3(\text{py})$  is less soluble than **17** in common organic solvents and is

isolated as a white precipitate from ether or pentane. Complex **18** is the only example of a tantalacyclobutane base adduct that has actually been *isolated*. However, considering the mode of formation of  $\text{Ta}[\text{CH}(\text{Ph})\text{CH}(\text{CMe}_3)\text{CH}_2](\text{DIPP})_3$  (described earlier) and of other tantalacyclobutane complexes (discussed later in this section and in chapter 2), it is clear the possibility exists that other adducts might also be formed as transient intermediates during reactions of **2** with olefins.

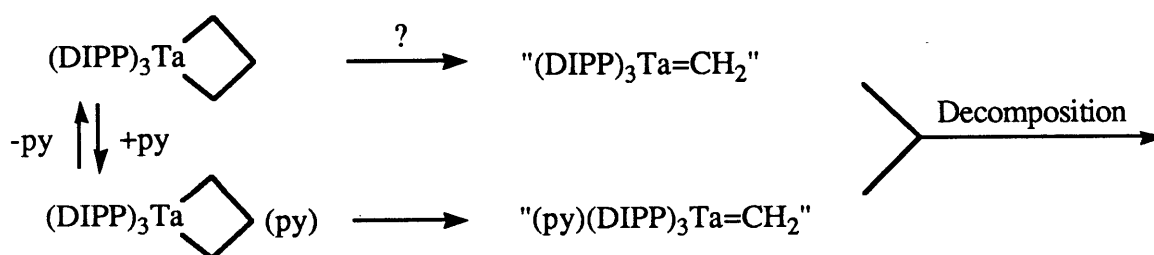
A  $^1\text{H}$  NMR spectrum of complex **18** at  $25^\circ$  ( $\text{C}_6\text{D}_6$ ) displays resonances for the  $\alpha$  and  $\beta$  protons at 2.95 and 2.00 ppm, respectively (the resonances are broader than those observed for **17**). On heating, the  $\alpha$  proton resonance shifts downfield while the  $\beta$  proton resonance shifts upfield, indicating an approach to the base-free metallacycle **17**, and suggesting that **18** is in equilibrium with **17** in solution. In the  $^{13}\text{C}$  NMR spectrum ( $\text{C}_6\text{D}_6$ ,  $25^\circ$ ) of **18** the  $\alpha$  and  $\beta$  carbons are seen at 78.0 ( $J_{\text{CH}} = 120$  Hz) and 36.3 ( $J_{\text{CH}} = 129$  Hz), respectively. Overall then, at  $25^\circ$  complex **18** displays ring resonances indicative of complex containing a "compressed" ring, in which the  $\text{C}_\alpha\text{-Ta-C}_\alpha$  angle is perhaps  $\sim 65^\circ$ , based on that angle in  $\text{Ta}[\text{CH}(\text{Ph})\text{CH}(\text{CMe}_3)\text{CH}_2](\text{DIPP})_3$  (**15**). A smaller  $\text{C}_\alpha\text{-Ta-C}_\alpha$  angle in **18**, versus base-free **17**, is to be expected, since **18** is a six-coordinate complex (presumably approximately octahedral in geometry), while **17** is only five-coordinate and thought to be trigonal bipyramidal with the ring in equatorial positions.

In addition to the differences cited above, complexes **17** and **18** also display markedly different  $J_{\text{CH}}$  values for the  $\alpha$  and  $\beta$  ring carbons. In general, large CH coupling constants are observed in high oxidation state metallacyclobutane complexes,<sup>50,52</sup> consistent with what is observed for strained cycloalkanes (e.g.  $J_{\text{CH}} = 161$  Hz in cyclopropane, 134 Hz in cyclobutane, but 123 Hz in cyclohexane).<sup>53</sup> In the pyridine adduct **18** the CH coupling constants are somewhat reduced (relative to those in **17**). With the additional coordination of pyridine, it seems plausible that the metal center in **18** would be less electrophilic than that in **17**. This, combined with the increased coordination in **18**, could possibly result in an elongation of the metal carbon bonds for **18**. Such an elongation should relieve some of the

ring strain in the metallacyclobutane complex and result in a decrease of  $J_{\text{CH}}$  values for the  $\alpha$  and  $\beta$  carbons. Consequently in the pyridine adduct **16**, where such a decrease is observed, the metal carbon bonds are thought to be elongated.

The pyridine adduct **18** is not especially stable in solution. **18** slowly decomposes to give dark red solutions at 25°; base-free **17** also decomposes in solution at 25°, but the rate is qualitatively less than that seen for **18**. The  $^1\text{H}$  NMR spectra of these darkened solutions ( $\text{C}_6\text{D}_6$ , 25°) display multiple resonances; no products have been isolated from these decomposition reactions. In one instance, however, in the process of collecting  $^{13}\text{C}$  NMR data ( $\text{C}_6\text{D}_6$ , 25°) on complex **18**, a triplet resonance at 217.4 ppm with  $J_{\text{CH}} = 135$  Hz was observed that is thought to have arisen from a methylene complex (**19**), perhaps  $\text{Ta}(\text{CH}_2)(\text{DIPP})_3(\text{py})$  (Scheme II) (cf.  $\text{W}(\text{CH}_2)(\text{N}-2,6-\text{C}_6\text{H}_3^i\text{Pr}_2)[\text{OCMe}(\text{CF}_3)_2]_2(\text{PMe}_3)$ ,<sup>50</sup> with  $\text{C}_\alpha$  at 252.2 ppm,  $J_{\text{CH}} = 145$  Hz). Stable tantalum(V) methyldene complexes are rare.<sup>1,54</sup> Based on the observation (by  $^{13}\text{C}$  NMR spectroscopy) of the metastable methyldene

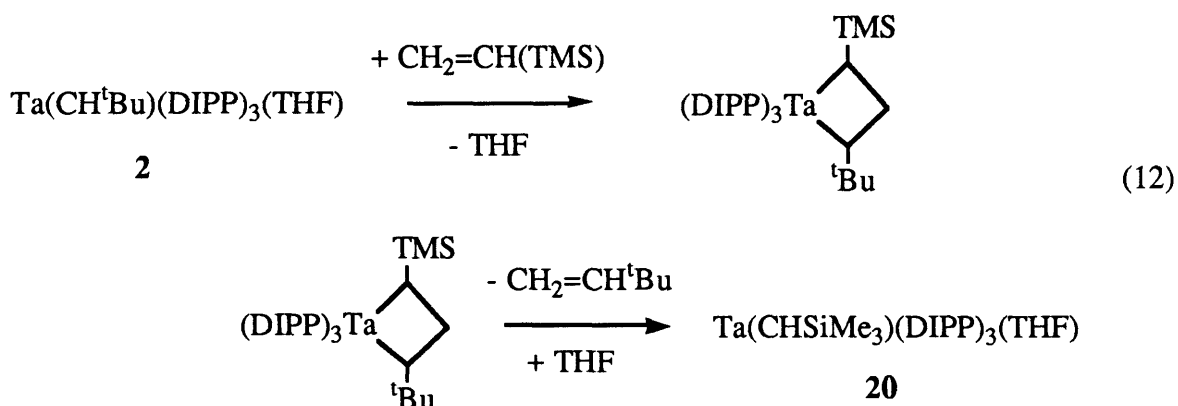
Scheme II: Formation (and Decomposition) of tris DIPP Methyldene Complexes.



complex **19**, methyldene complexes are thought likely to be involved at least in part in the decomposition reactions of the unsubstituted tantalacyclobutanes **17** and **18**, with an enhanced rate of decomposition in the presence of pyridine (i.e. in **18**). Direct decomposition of the intact metallacycles must also be considered as possible, since the rings in these complexes are

unsubstituted and not as sterically demanding as substituted rings in other tantalacyclobutane complexes reported here (all of which do *not* form observable base adducts).

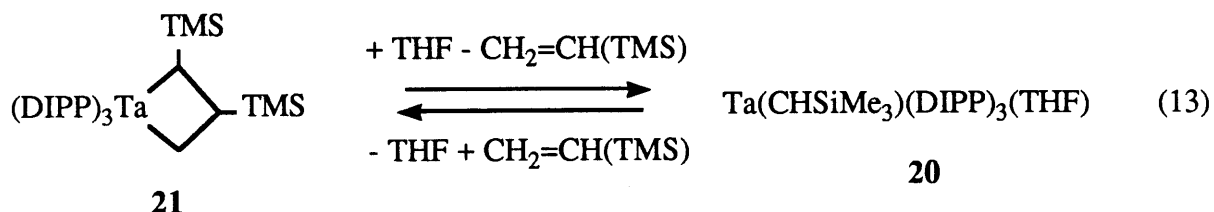
The new alkylidene complex  $\text{Ta}(\text{CHSiMe}_3)(\text{DIPP})_3(\text{THF})$  (**20**) is formed after several hours reaction of  $\text{Ta}(\text{CHCMe}_3)(\text{DIPP})_3(\text{THF})$  (**2**) with one equivalent of vinyltrimethylsilane; an initial metallacyclobutane intermediate is not observed (equation 12). The formation of



complex **20** is significantly accelerated when the reaction is performed in the presence of excess THF, suggesting again a base assisted reaction in which THF binds to the initially formed tantalacyclobutane complex and enhances the rate of ring-opening for this complex.  $\text{Ta}(\text{CHSiMe}_3)(\text{DIPP})_3(\text{THF})$  can be isolated as yellow crystals from pentane in good yield (for reactions performed in the presence of excess THF). The  $^1\text{H}$  and  $^{13}\text{C}$  NMR spectra ( $\text{C}_6\text{D}_6$ ,  $25^\circ$ ) of complex **20** are not unusual and display expected resonances for  $\text{H}_\alpha$ ,  $\text{C}_\alpha$ , and a single type of DIPP ligand (Table I).

When complex **20** is treated with one or more additional equivalents of vinyltrimethylsilane, or when **2** is reacted with several equivalents of vinyltrimethylsilane over several hours, colorless  $\text{Ta}[\text{CH}(\text{SiMe}_3)\text{CH}(\text{SiMe}_3)\text{CH}_2](\text{DIPP})_3$  (**21**) can be isolated in good yield. Addition of THF to this disubstituted metallacyclobutane complex (**21**) yields solutions that contain both **20** and **21** in equilibrium (equation 13; a solution of **21** (~50 mM) and THF

(~200 mM) in  $C_6D_6$  resulted in an equilibrium mixture with  $K_{eq} = 7.9 \times 10^{-3}$  at  $25^\circ$  and  $2.7 \times 10^{-2}$  at  $50^\circ$ ).



$^1\text{H}$  and  $^{13}\text{C}$  NMR data suggest that complex **21** contains a "compressed" ring (i.e. probably a trigonal bipyramidal complex) and that the substituents are located on  $\alpha$  and  $\beta$  ring carbon atoms (Table III). Interestingly, the  $^1\text{H}$  NMR spectrum of **21** displays broad resonances for the DIPP ligands, indicating fluxionality in this complex is limited, but the ring protons give rise to sharp resonances at 4.98 (t, 1,  $\alpha$   $\text{CH}_2$ ), 3.64 (t, 1,  $\alpha$   $\text{CH}_2$ ), 2.95 (d, 1,  $\alpha$   $\text{CH}(\text{TMS})$ ), and -0.33 ppm (m, 1,  $\beta$   $\text{CH}(\text{TMS})$ ); the ring assignments were made with the aid of decoupling experiments. The  $\alpha$  and  $\beta$  substituents are thought to be *trans* to one another ( $J_{\text{H}\alpha\text{H}\beta} = 14.5 \text{ Hz}$ ), as is found in the structure of  $\text{W}[\text{CH}(\text{SiMe}_3)\text{CH}(\text{SiMe}_3)\text{CH}_2](\text{N}-2,6\text{-C}_6\text{H}_3\text{iPr}_2)[\text{OCMe}(\text{CF}_3)_2]_2$ .<sup>50</sup> The  $^{13}\text{C}$  NMR spectrum ( $C_6D_6$ ,  $25^\circ$ ) displayed resonances for the ring carbons at 108.1 (t,  $J_{\text{CH}} = 145 \text{ Hz}$ ,  $\alpha$   $\text{CH}_2$ ), 99.3 (d,  $J_{\text{CH}} = 128 \text{ Hz}$ ,  $\alpha$   $\text{CH}(\text{TMS})$ ), and 6.41 (d,  $J_{\text{CH}} = 131 \text{ Hz}$ ,  $\beta$   $\text{CH}(\text{TMS})$ ) ppm. Evidence for the presence of a small amount of the  $\alpha,\alpha'$  substituted isomer (~15%) is also observed in the  $^1\text{H}$  and  $^{13}\text{C}$  NMR spectra of **21** ( $^1\text{H}$  NMR:  $\delta$  3.93 (m,  $\alpha$   $\text{CHSiMe}_3$ );  $^{13}\text{C}$  NMR:  $\delta$  106.2 (d,  $J_{\text{CH}} = 122 \text{ Hz}$ ,  $\alpha$   $\text{CHSiMe}_3$ )). In the related tungsten complex described above, the  $\alpha,\beta$  isomer is formed exclusively; a crystal structure of this tungsten complex suggests the  $\alpha,\alpha'$  isomer would be sterically unfavorable. The overall ligand environment in this complex apparently limits the number of possible stable orientations of the ring substituents about the  $\text{MC}_3$  ring core. The tris DIPP configuration found in the present compounds, however, is more tolerant of sterically demanding orientations: a trisubstituted

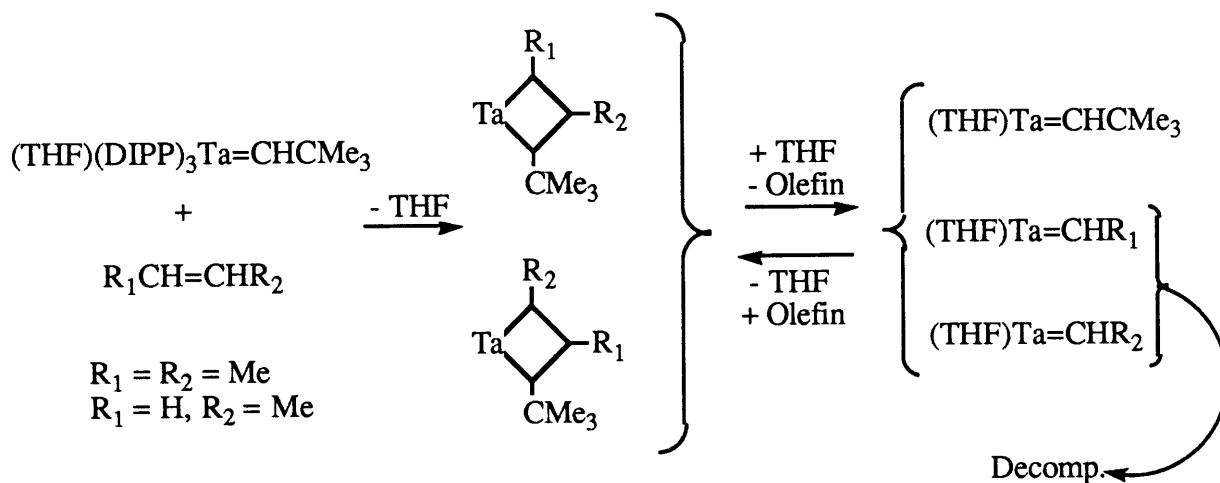
tantalacyclobutane complex readily forms from the parent alkylidene complex **2** and remains intact in solution at 25° (chapter 2).

While reaction of the parent DIPP alkylidene complex  $\text{Ta}(\text{CHCMe}_3)(\text{DIPP})_3(\text{THF})$  (**2**) with styrene, ethylene, and vinyltrimethylsilane leads to the formation of new stable metallacyclobutane and alkylidene complexes, the attempted synthesis of alkylidene complexes with  $\beta$  hydrogens on the alkylidene ligand or of new metallacyclobutane complexes containing linear alkyl substituents on the ring was not as straightforward. When solutions of complex **2** were placed under propylene or *cis*-2-butene gas (~30 psi), quick reactions, evidenced by a lightening of the solution's color, were observed to take place. This loss of color qualitatively appeared to be consistent with initial tantalacyclobutane formation, since these metallacycles are always less colored than analogous alkylidene complexes (and most often colorless). On workup of these reaction mixtures, however, and especially during removal of the solvent *in vacuo*, these solutions darkened rapidly, resulting in dark oils that displayed multiple and broad resonances in subsequent NMR spectra.

No products were isolated from the reaction between complex **2** and *cis*-2-butene, but an off white powder was obtained in small amounts from the reaction between **2** and propylene. This powder is extremely pentane soluble and not very stable in solution (when left in common organic solvents, such as ether or pentane at 25°, within one hour significant darkening of the solution is seen to take place). A  $^{13}\text{C}$  NMR spectrum of this powder was not totally definitive but did reveal characteristic tantalacyclobutane resonances, specifically for one in which the *t*-butyl group from **2** was still present, along with at least one methyl substituent on the ring. In Scheme III the results with propylene and butene are summarized. Initial formation of tantalacyclobutane complexes appears likely, and these complexes show at least a limited stability when under pressure of olefin (propylene or butene). When excess olefin is removed from the system, the metallacycles decompose rapidly, probably initially to give alkylidene complexes containing  $\beta$  hydrogens on the alkylidene ligand. These alkylidene complexes, which have not been observed at all here, must then rapidly decompose (as shown

in equations 2a and 2c) as have previously reported tantalum alkylidene complexes that contain  $\beta$  hydrogens on the alkylidene ligand.<sup>7,8</sup> Direct decomposition of the tantalacyclobutane

Scheme III: A Possible Decomposition Pathway in Reactions of **2** with Propene and *cis*-2-Butene.



complexes cannot be ruled out (i.e. equation 2b), but is thought to be less likely considering the number of stable tantalacyclobutane complexes isolated in the DIPP system, all of which contain at least one  $\beta$  hydrogen.

Similar results are obtained on reacting complex **2** with methylenecyclohexane or 3-hexene. Complex **2** will metathesize *cis*-2-pentene rapidly in room temperature solution (100 equivalents within 15 minutes), giving rise to colorless solutions. These solutions, though, show no further activity with additional aliquots of *cis*-2-pentene (at 25° or at elevated temperatures). Here as well decomposition of intermediate alkylidene species containing  $\beta$  hydrogens on the alkylidene ligand is thought most likely. These types of decomposition reactions for alkylidene complexes containing  $\beta$  hydrogens are more the rule than the exception with tantalum.<sup>1,7</sup> The isolation of several stable tantalacyclobutane complexes reported here, however, reveals that tantalacycles can exhibit an enhanced stability over the corresponding

alkylidenes (i.e. the unsubstituted tantalacycle **17** versus the transient methyldiene Ta(CH<sub>2</sub>)(DIPP)<sub>3</sub>(py), **19**). In chapter 2, where the application of tantalacycles as alkylidene precursors in NBE polymerization is discussed, this enhanced stability is used to an advantage.

In contrast to **2**, Ta(CHCMe<sub>3</sub>)(DMP)<sub>3</sub>(THF) (**4**) generally does not react cleanly with olefins. For example, when placed under ethylene pressure in ether at 25°, the solution was seen to darken significantly, but no products could be isolated from the reaction; a <sup>1</sup>H NMR spectrum of the crude reaction mixture (C<sub>6</sub>D<sub>6</sub>, 25°) showed broad and multiple resonances. As mentioned earlier, complexes containing the sterically less encumbering DMP ligands, including metallacyclobutane complexes, are thought to be more prone to decomposition reactions, both intramolecular (less steric protection within the complex) and intermolecular (less steric constraints from interaction with other species in solution). An exception is the observation of a stable trisubstituted metallacyclobutane complex formed upon reaction of complex **4** with NBE (described in chapter 2). Apparently the steric bulk gained through trisubstitution leads to a more sterically saturated metallacycle.

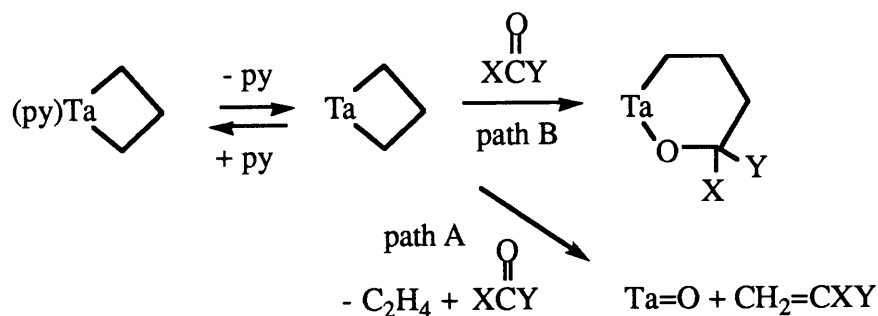
#### **Reactivity of Tantalacyclobutane Complexes with Organic Carbonyls.**

Earlier the Wittig-like reactivity of the alkylidene complexes **2** and **6** was described. Tantalacyclobutane complexes (all of which are supported by DIPP ligation) also react with organic carbonyls in a Wittig-like fashion under certain conditions, thus acting as precursors to alkylidenes in these reactions. This is illustrated in path A of Scheme IV for the unsubstituted tantalacyclobutanes **17** and **18** (pyridine adduct). Under conditions in which metallacyclobutanes do *not* readily lose olefin to yield intermediate alkylidene species, insertion reactions, of an organic carbonyl into the tantalum carbon single bond of a metallacyclobutane complex, lead to the formation of stable oxytantalacyclohexane complexes (Scheme IV, path B). Insertion reactions of the type shown in path B of Scheme IV have been reported in the literature. Petersen<sup>55</sup> has observed insertions of organic carbonyls into 1-sila-3-zirconacyclobutane complexes (here the β silicon substitution inhibits ring-opening of



the metallacycle), and Erker<sup>56</sup> has reported the formation of an oxyhafnacyclohexane complex

Scheme IV: Wittig and Insertion Reactions of Complexes **17** and **18** with Organic Carbonyls.



from the reaction of  $Cp_2Hf(CH_2CH_2CH_2)$  with equimolar amounts of benzaldehyde. Interestingly, Bickelhaupt<sup>57,58</sup> reported earlier the products of *double* insertion (i.e. each of the metal-carbon bonds reacted) when  $Cp_2Hf(CH_2CH_2CH_2)$  was reacted with cyclohexanone. In the present reactions, insertion of only one equivalent of the organic carbonyl is observed, even when excess organic carbonyl is employed and the reaction is performed at elevated temperatures.

The results of these reactions are given in Table V. Complexes **17** and **18** react with formaldehyde, acetone, benzaldehyde, and pivaldehyde at lower temperatures (generally 25° and below) to give largely products derived from an insertion reaction (i.e. path B, oxytantalacyclohexane complexes **22-25**). The compounds obtained from the pyridine adduct **18** are initially isolated as pyridine adducts, but most of these readily lose pyridine under vacuum. Besides base loss, though, the oxytantalacyclohexane complexes derived from formaldehyde, acetone, benzaldehyde, and pivaldehyde are robust compounds, showing very little decomposition after heating at 70° overnight in  $C_6D_6$ . The  $^1H$  and  $^{13}C$  NMR spectra ( $C_6D_6$ , 25°) of these complexes are straightforward, showing resonances for a single type of DIPP ligand (with a pair of diastereotopic resonances noted for the DIPP isopropyl methyl groups in **24** and **25**; in **22** and **23** these resonances must be coincident) and showing ring

Table V. Products of the Reactions of Tantalacycles with Organic Carbonyls.

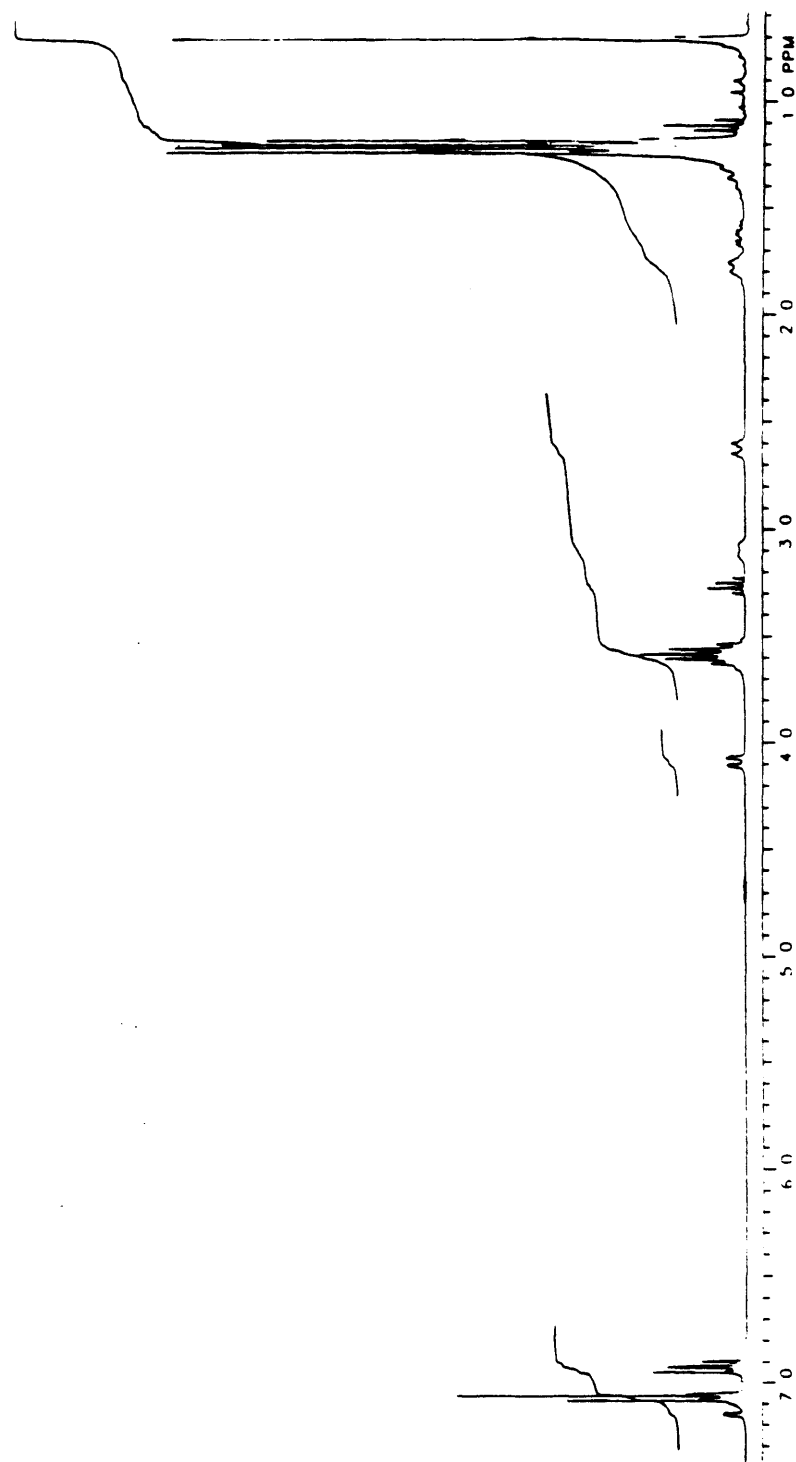
Compound	Carbonyl	Conditions	Insertion (%)	Wittig (% by NMR)
15	1.5 Me <sub>2</sub> CO	C <sub>6</sub> D <sub>6</sub> , 25°, 60 m	a	86 (Me <sub>2</sub> C=CCHPh) 91 ( <sup>t</sup> BuCH=CH <sub>2</sub> )
17	1.5 Me <sub>2</sub> CO	C <sub>6</sub> D <sub>6</sub> , 25°, 60 m	100 (NMR)	b
17	1.5 Me <sub>2</sub> CO	C <sub>6</sub> D <sub>6</sub> , 60°, 30 m	75 (NMR)	19 (Me <sub>2</sub> C=CH <sub>2</sub> )
17	1.0 <sup>t</sup> BuCHO	ether, 25°, 12 h <sup>c</sup>	100 (NMR)	b
17	1.5 Ph <sub>2</sub> CO	C <sub>6</sub> D <sub>6</sub> , 25°, 60 m	45 (NMR)	46 (Ph <sub>2</sub> C=CH <sub>2</sub> )
17	1.5 Ph <sub>2</sub> CO	C <sub>6</sub> D <sub>6</sub> , 60°, 30 m	24 (NMR)	71 (Ph <sub>2</sub> C=CH <sub>2</sub> )
18	1.5 Me <sub>2</sub> CO	ether, 25°, 45 m <sup>c</sup>	100(NMR)	b
18	1.0 PhCHO	ether, 25°, 60 m <sup>c</sup>	80 (isolated)	b
18	1.2 <sup>t</sup> BuCHO	C <sub>6</sub> D <sub>6</sub> , 25°, 30 m	100 (NMR)	b
18	1.5 Ph <sub>2</sub> CO	C <sub>6</sub> D <sub>6</sub> , 70°, 35 m	< 6 (NMR)	86 (Ph <sub>2</sub> C=CH <sub>2</sub> )

a No insertion products observed by NMR.

b No Wittig products observed.

c Reaction was initiated at -30°.

Figure 6. The  $^1\text{H}$  NMR spectrum of  $\text{Ta}[\text{OCH}(\text{CMe}_3)\text{CH}_2\text{CH}_2\text{CH}_2](\text{DIPP})_3$  (**25**) in  $\text{C}_6\text{D}_6$  at  $25^\circ$ .



resonances similar to those reported earlier for other oxymetallacyclohexane complexes;<sup>55-58</sup> the  $^1\text{H}$  NMR spectrum for one of these complexes, **25**, is shown in Figure 6.

At higher temperatures (up to  $70^\circ$ ), reactions with organic carbonyls result in both insertion and Wittig-like products, consistent with an increased ring-opening of metallacyclobutane complexes at elevated temperatures. Reaction of complexes **17** and **18** with benzophenone even at  $25^\circ$  results in formation of both Wittig and insertion products, with the latter slowly decomposing to give mostly Wittig products over a period of days (when heated this decomposition is significantly accelerated). Therefore, the course of the reaction is also highly dependent on the organic carbonyl employed. As expected then, more substituted tantalacyclobutane complexes also give largely Wittig products when reacted with organic carbonyls: the disubstituted metallacycle  $\text{Ta}[\text{CH}(\text{Ph})\text{CH}(\text{CMe}_3)\text{CH}_2](\text{DIPP})_3$  (**15**) reacts with acetone at  $25^\circ$  to give at least 90% Wittig products (by  $^1\text{H}$  NMR), with no evidence for oxytantalacyclohexane formation.

The study of these reactions has been largely pragmatic, with an emphasis on developing methods for effectively inducing Wittig-like reactions in tantalacyclobutane complexes (for capping reactions, discussed in chapter 2). Qualitatively, the base-free and base bound complexes **17** and **18** show similar trends in reactivity (concerning reaction rates and products formed), suggesting the base-free complex may be the reactive species in both reactions, with the pyridine adduct **18** reacting after dissociation of pyridine (as is shown in Scheme IV). This seems reasonable for at least the insertion reactions, where in the absence of pyridine dissociation a seven-coordinate intermediate would be required. As in earlier olefin reactions involving alkylidenes and metallacyclobutanes, the organic carbonyls may accelerate the rate of these reactions by initially coordinating to the metallacyclobutane complex.

## DISCUSSION

Reaction of the DIPP complex  $\text{Ta}(\text{CHCMe}_3)(\text{DIPP})_3(\text{THF})$  (**2**) with olefins in the presence of excess THF demonstrates a convenient route to new alkylidene complexes. The preparation of a class of alkylidenes which contain varying substituents on the alkylidene

ligand has been one of the goals of this investigation, since the substituents on the alkylidene ligand can affect the reactivity and properties of the complex as much as other supporting ligation present (i.e. here DIPP, DMP, or TIPT). The most important example of such a reactivity difference in the present investigations is described at length in chapter 3, where the use of a disubstituted alkylidene (prepared by the analogous reaction of **2** with an acetylene) was found to affect the efficient polymerization of 2-butyne, while the monosubstituted alkylidene **2** only reacted with 2-butyne to form a stable metallacyclobutene complex. Alkylidene complexes can also be used as Wittig reagents with a variety of organic carbonyls, as was demonstrated in this chapter for complexes **2** and **6**. Although this has not been the main objective in the present research, with the added choice of substituents on the alkylidene ligand in complexes derived from **2** (e.g. a phenyl group versus a TMS group), Wittig-like reactions could be used to prepare very specific olefins.

Complex **2** also reacts with olefins to give stable tantalacyclobutane complexes as the first examples of such complexes for tantalum. The substituents in these complexes are varied, and their behavior is directly related to the nature of those substituents. While the unsubstituted tantalacycles **17** and **18** react largely with organic carbonyls to give insertion products at 25°, the disubstituted tantalacycle **15** reacts to give largely Wittig products. Fortunately, by simply elevating the reaction temperature complexes **17** and **18** also become effective Wittig reagents. This demonstrates that tantalacyclobutane complexes can be used as alkylidene precursors for reaction with organic carbonyls, and in chapter 2 tantalacyclobutanes are shown to act as efficient precursors to alkylidenes for reaction with *strained cyclic olefins* as well.

Apparently in the DIPP class of compounds tantalacyclobutane complexes and base adducts of alkylidenes are of about equal energy, since either can be prepared from **2** depending on the reaction conditions, or transformed to the other. Why stable tantalacyclobutane complexes are observed *here* and have not been observed in *earlier* tantalum studies may not be so much dependent upon these complexes being more thermodynamically or kinetically favored, but on the stability of such complexes when favored (i.e. stability from

reactions such as that shown in equation 2b). The presence of the bulky DIPP ligands in complexes **15**, **17**, **18**, and **21** prevents deleterious intramolecular interactions between the metal center and the metallacyclic ring substituents (including the  $\beta$  hydrogens), as well as intermolecular decomposition.

Several other metallacyclobutane complexes of the early transition metals have been reported, such as bis(cyclopentadienyl) titanium,<sup>52,59</sup> zirconium,<sup>55</sup> hafnium,<sup>56</sup> and thorium<sup>60</sup> complexes. Tungstenacyclobutane complexes have also more recently been reported,<sup>50,61,62</sup> and at least one example of a molybdenacyclobutane complex is now known.<sup>63</sup> As described earlier in the text, from the trends that have been observed for tungstenacyclobutane complexes regarding metallacycle structure,<sup>51</sup> and considering the similar results that have been observed here for tantalacyclobutane complexes, some correlations can probably be made between the NMR data seen for a particular complex and the most likely ring structure in that complex.

The DIPP, DMP, and TIPT alkylidene complexes prepared from  $\text{Ta}(\text{CHCMe}_3)(\text{THF})_2\text{Cl}_3$  display strikingly different reactivities with ordinary olefins, due to the differing steric and electronic properties of the supporting ligation within them. The calculated  $\text{pK}_a$ <sup>64</sup> of TIPTH (~8) is significantly lower than that of DIPPH (~11) or DMPH (~11), suggesting qualitatively the conjugate base of TIPTH might be weaker. The lower electronegativity of sulfur (versus oxygen), however, makes arylthiolate anions more polarizable. Consequently, thiolate anions form many stable complexes with the transition metals,<sup>28</sup> and in fact have been described as "strongly electron-releasing" in some cases.<sup>23</sup> While phenoxide ligands display strong  $\pi$  donation in high-valent early transition metal complexes, as evidenced by the large M-O-C angles ( $\angle \text{M-O-C} \approx 130\text{-}170^\circ$ ) noted in the structures of these complexes (see also those reported in this dissertation),<sup>12,21,46-49</sup> the extent of  $\pi$  donation from arylthiolate ligands is not entirely clear. The smaller M-S-C angles ( $\angle \text{M-S-C} \approx 110\text{-}115^\circ$ ) observed in the structures of these complexes.<sup>19,22-26,65</sup> (see also  $\text{Ta}(\text{CHCMe}_3)(\text{TIPT})_3(\text{Et}_2\text{S})$  (**9**) in appendix 1) are not necessarily indicative of a lack of  $\pi$  donation from the thiolate ligands, since the sulfur atom orbital used for  $\sigma$  bonding with the

metal is likely to contain more p character than the related oxygen orbital (e.g. in  $\text{H}_2\text{O}$   $\angle$  H-O-H =  $104.5^\circ$ , but in  $\text{H}_2\text{S}$   $\angle$  H-S-H =  $92.1^\circ$ <sup>70</sup>). X-ray analysis of the complex  $\text{Mo}(\text{Cp})(\text{NO})(\text{SPh})_2$  and related molecular orbital calculations suggest the presence of significant  $\pi$  donation from the arylthiolate ligands in this case, and the M-S-C angles are still only  $\sim 110^\circ$ .<sup>66</sup> Several other structurally characterized arylthiolate complexes have been described as containing *weak*  $\pi$  donor arylthiolate ligands, but the orientation of the arylthiolate ligands in these complexes was thought to maximize any possible  $\pi$  donation.<sup>23,24</sup> The solid state structure of the tantalum arylthiolate complex **9** is considered in appendix 1.

While it is difficult to say which ligand environment creates a more electrophilic metal center, the different bonding modes of phenoxide and arylthiolate ligands *are* manifested in the structures of such complexes. In the only known structure of a  $\text{Ta}(\text{CHR})(\text{DIPP})_3(\text{B})$  complex (chapter 3), the phenoxide ligands occupy two equatorial sites and one axial site in a distorted trigonal bipyramidal complex, leaving the alkylidene ligand (in an equatorial site) and the base (in an axial site) effectively *cis* to one another; an analogous situation is observed in  $(\text{THF})(\text{DIPP})_3\text{Ta}=\text{N}-\text{N}=\text{Ta}(\text{DIPP})_3(\text{THF})$  for the "imido" and THF ligands. However, in the structure of  $\text{Ta}(\text{CHCMe}_3)(\text{TIPT})_3(\text{Et}_2\text{S})$  (**9**) the geometry can be described as distorted trigonal bipyramidal with the arylthiolate ligands occupying equatorial sites. An equatorial preference is observed in all structurally characterized trigonal bipyramidal complexes containing three bulky arylthiolate ligands.<sup>19,22,22-26,65</sup> Consequently, the two other ligands in such complexes, here the alkylidene and the base, occupy axial sites and are *trans* to one another. Knowing that  $\text{Ta}(\text{CHR})(\text{TIPT})_3(\text{B})$  complexes react with strained cyclic olefins via a base-free intermediate complex (this is shown in chapter 2), it seems reasonable to assume that an olefin would initially bind *trans* to the alkylidene ligand in these arylthiolate complexes (at the coordination site made vacant by dissociation of the base). This *trans*-olefin complex would then have to rearrange to a form in which the alkylidene ligand and the olefin are *cis* to one another before a metathesis reaction could take place (certainly in a stable or intermediate metallacyclobutane complex the two sites occupied must be *cis* to one another). With ordinary olefins, apparently

the initial interaction between olefin and metal is not strong enough to allow such a rearrangement *before* dissociation of the olefin from the complex (with benzaldehyde and strained cyclic olefins the interaction is strong enough). In the analogous phenoxide alkylidene complexes the olefin should bind *cis* to the alkylidene ligand if base dissociation precedes olefin coordination. If the olefin coordinates to the metal *before* base dissociation, subsequent base loss should place the olefin *cis* to the alkylidene ligand (if this is not initially the case), considering the preferred orientations of the phenoxide ligands. In either situation, a facile reaction is allowed to take place for phenoxide complexes. Therefore, one *can* say electronic differences between phenoxide and arylthiolate complexes are very important here, but not necessarily because one creates a more electrophilic metal center than the other.

Steric properties within these complexes are also important in accessing reactivity differences. Several new stable alkylidene and metallacyclobutane complexes are obtained from reaction of the DIPP complex **2** with ordinary olefins, but reaction of the DMP complex **4** with ordinary olefins (such as ethylene and styrene) results in no identifiable products. Clearly the isopropyl groups of the DIPP ligands are very important in stabilizing these alkylidene and metallacyclobutane complexes, while the methyl groups of the DMP ligands lack enough steric bulk to stabilize such complexes from various decomposition reactions (such as a bimolecular coupling reaction between the alkylidene ligands of two molecules, or a rearrangement of the alkylidene ligand or metallacyclobutane ring to an olefin within one molecule). If steric protection lacking in the DMP ligands is provided in the other ligation within the complex, however, stable products can be obtained. This is the case for the DMP trisubstituted metallacyclobutane complex  $\text{Ta}[\text{CH}(\text{C}_5\text{H}_8)\text{CHCH}(\text{CMe}_3)](\text{DMP})_3$ , formed by reaction of complex **4** with NBE (described in chapter 2).

In addition to a lack of steric saturation, *excessive* steric saturation in a complex also leads to complicating reactions. In several tantalum complexes reported by Rothwell, the presence of 2,6-di-*t*-butylphenoxide ligands led to cyclometalation reactions involving the *t*-butyl groups of these ligands and the metal center.<sup>32,46,47,67-69</sup> Overall, the steric properties



of all ligation within a particular complex must be considered to achieve a balance of protection and reactivity regarding some specific application. Increasingly in the literature the benefits of such an approach are being demonstrated for a variety of systems.<sup>11-15,21,50,61,71-79</sup>

## Experimental Section

**General Details.** All experiments were performed under a nitrogen atmosphere in a Vacuum Atmospheres drybox or by using standard Schlenk techniques. Reagent grade ether, tetrahydrofuran, and toluene were distilled from sodium benzophenone ketyl under nitrogen. Pentane was washed with 5% nitric acid in sulfuric acid, stored over calcium chloride, and then distilled from sodium benzophenone ketyl under nitrogen. Dichloromethane was distilled from calcium hydride under nitrogen.

$\text{Ta}(\text{CH}_2\text{CMe}_3)_2\text{Cl}_3$ ,<sup>35</sup>  $\text{Ta}(\text{CHCMe}_3)(\text{THF})_2\text{Cl}_3$ ,<sup>18</sup> and 2,4,6- $\text{C}_6\text{H}_2^i\text{Pr}_3\text{SH}$  (HTIPT)<sup>23,80,81</sup> were prepared as described in the literature.  $\text{LiDIPP}\cdot\text{Et}_2\text{O}$ ,  $\text{LiDMP}$ , and  $\text{LiTIPT}$  were prepared from the appropriate phenol or thiol and n-butyllithium in ether (for  $\text{LiDIPP}\cdot\text{Et}_2\text{O}$ ) or pentane (for  $\text{LiDMP}$  and  $\text{LiTIPT}$ ). All other reagents were purchased from commercial sources. Removal of oxygen and water, and purification, was performed by standard techniques.

All deuterated NMR solvents were passed through a column of activated alumina prior to use. Chemical shifts are listed in ppm downfield from TMS, and coupling constants are given in Hertz. In most cases, the NMR solvent is  $\text{C}_6\text{D}_6$ , and the temperature is 25°, unless otherwise noted. NMR spectra were recorded on a Bruker WM-250, a Bruker WM-270, a Varian XL-300, and a Varian XL-400 nuclear magnetic resonance spectrometer. Each of the Varian instruments was equipped with a Nicolet Zeta plotter and an automated variable temperature accessory. GLC analyses were performed using a Shimadzu gas chromatograph GC-9A installed with a 50 meter fused glass capillary column (type: methyl phenyl 5). GCMS analyses were performed using a Hewlett Packard 59990A, 5992 GC/MS System. Elemental analyses were performed by Schwarzkopf Microanalytical Laboratory (Woodside, N.Y.) or Spang Microanalytical Laboratory (Eagle Harbor, Michigan).

**Preparation of Compounds.**  $\text{Ta}(\text{CH}_2\text{CMe}_3)\text{Cl}_4(\text{THF})$  (1). Complex 1 is isolated as a side product from the preparation reaction of  $\text{Ta}(\text{CHCMe}_3)(\text{THF})_2\text{Cl}_3$ . This complex can be isolated as large orange-red crystals from the ether filtrate after several crops of

Ta(CHCMe<sub>3</sub>)(THF)<sub>2</sub>Cl<sub>3</sub> have been collected; no attempts were made to formulate a preparative route for complex **1**: <sup>1</sup>H NMR (250 Mz) δ 3.91 (s, 2, CH<sub>2</sub>CMe<sub>3</sub>), 3.65 (t, 4, THF), 1.22 (s, 9, CH<sub>2</sub>CMe<sub>3</sub>), 1.03 (m, 4, THF); <sup>13</sup>C NMR (75.4 MHz) δ 140.8 (t, J<sub>CH</sub> = 114, CH<sub>2</sub>CMe<sub>3</sub>), 73.3 (t, THF), 41.6 (s, CH<sub>2</sub>CMe<sub>3</sub>), 33.6 (q, CH<sub>2</sub>CMe<sub>3</sub>), 25.2 (t, THF). Anal. Calcd for TaC<sub>9</sub>H<sub>19</sub>Cl<sub>4</sub>O: C, 23.20; H, 4.11; Cl, 30.43. Found: C, 23.22; H, 4.01; Cl, 29.94.

Ta(CHCMe<sub>3</sub>)(DIPP)<sub>3</sub>(THF) (DIPP = O-2,6-C<sub>6</sub>H<sub>3</sub><sup>i</sup>Pr<sub>2</sub>) (**2**). Ta(CH<sub>2</sub>CMe<sub>3</sub>)<sub>2</sub>Cl<sub>3</sub> (2.00 g, 4.66 mmol) was dissolved in ether (50 mL) and the solution was cooled to -30°. THF (12 g) was added dropwise. As this solution was allowed to warm to room temperature the color changed from yellow to violet. After 2 h the solution was again cooled to -30° and stirred while solid LiDIPP·Et<sub>2</sub>O (3.62 g, 14.0 mmol) was added. As the solution warmed to room temperature the color changed from violet to yellow-orange. The total reaction time (including the time of addition) was 20 m. The mixture was then filtered through Celite, and the solvent was removed *in vacuo*. The resulting yellow-orange solid was dissolved in pentane (or ether for larger scale preparations), and the solution was filtered through Celite to remove any remaining LiCl. The solvent was removed *in vacuo* and the residue dissolved in ether. Orange-yellow crystals were obtained by cooling the solution to -30° (3.58 g, 90%): <sup>1</sup>H NMR (250 MHz) δ 7.32 (d, 6, H<sub>m</sub>), 7.15 (t, 3, H<sub>p</sub>), 5.73 (s, 1, CHCMe<sub>3</sub>), 3.99 (m, 10, CHMe<sub>2</sub> and THF), 1.48 (d, 36, CHMe<sub>2</sub>), 1.31 (s plus m, 13, CHCMe<sub>3</sub> and THF); <sup>13</sup>C NMR (67.9 MHz) δ 227.1 (d, J<sub>CH</sub> = 95, CHCMe<sub>3</sub>), 159.0 (s, C<sub>ipso</sub>), 137.4 (s, C<sub>o</sub>), 123.6 (d, J<sub>CH</sub> = 150, C<sub>m</sub>), 121.7 (d, J<sub>CH</sub> = 134, C<sub>p</sub>), 73.8 (t, J<sub>CH</sub> = 148, THF), 45.0 (s, CHCMe<sub>3</sub>), 35.7 (q, J<sub>CH</sub> = 124, CHCMe<sub>3</sub>), 27.1 (d, J<sub>CH</sub> = 127, CHMe<sub>2</sub>), 25.6 (unresolved, THF), 24.5 (q, J<sub>CH</sub> = 125, CHMe<sub>2</sub>). Anal. Calcd for TaC<sub>45</sub>H<sub>69</sub>O<sub>4</sub>: C, 63.20; H, 8.15; Cl, 0.00. Found: C, 63.13; H, 8.09; Cl, < 0.5. On a larger scale best yields are obtained if Ta(CHCMe<sub>3</sub>)(THF)<sub>2</sub>Cl<sub>3</sub> is isolated before being treated with LiDIPP·Et<sub>2</sub>O. **2** has been isolated in 85% yield on a 20 g scale.

Ta(CHCMe<sub>3</sub>)(DIPP)<sub>3</sub>(py) (**3**). Ta(CHCMe<sub>3</sub>)(DIPP)<sub>3</sub>(THF) (0.50 g, 0.58 mmol) was dissolved in ether (10 mL) and the solution was cooled to -30°. While this solution was

stirred, pyridine (280  $\mu$ L, excess) was added. After 10 m at 25° the solution had changed color from orange-yellow to orange. The solvent was removed *in vacuo* and the residue recrystallized from ether at -30° to give 0.38 g of orange crystals (75%):  $^1\text{H}$  NMR (250 MHz)  $\delta$  8.70 (d, 2, py H<sub>O</sub>), 7.06 (unresolved, 6, H<sub>m</sub>), 6.92 (unresolved, 3, H<sub>p</sub>), 6.51 (t, 1, py H<sub>p</sub>), 6.29 (s, 1, CHCMe<sub>3</sub>), 6.22 (t, 2, py H<sub>m</sub>), 3.83 (unresolved, 6, CHMe<sub>2</sub>), 1.22 (unresolved, 45, CHCMe<sub>3</sub> and CHMe<sub>2</sub>);  $^{13}\text{C}$  NMR (67.9 MHz)  $\delta$  231.2 (d, J<sub>CH</sub> = 96, CHCMe<sub>3</sub>), 157.0 (s, C<sub>ipso</sub>), 151.0 (d, py C<sub>O</sub>), 137.8 (d, py C<sub>p</sub>), 137.6 (s, C<sub>O</sub>), 124.4 (d, py C<sub>m</sub>), 123.7 (d, C<sub>m</sub>), 121.7 (unresolved, C<sub>p</sub>), 45.2 (s, CHCMe<sub>3</sub>), 35.4 (q, CHCMe<sub>3</sub>), 27.1 (d, CHMe<sub>2</sub>), 24.4 (q, CHMe<sub>2</sub>). Anal. Calcd for TaC<sub>46</sub>H<sub>66</sub>NO<sub>3</sub>: C, 64.08; H, 7.73. Found: C, 64.27; H, 7.78.

**Ta(CHCMe<sub>3</sub>)(DMP)<sub>3</sub>(THF) (DMP = O-2,6-C<sub>6</sub>H<sub>3</sub>Me<sub>2</sub>) (4).** Ta(CHCMe<sub>3</sub>)(THF)<sub>2</sub>Cl<sub>3</sub> (2.00 g, 3.99 mmol) was dissolved in a mixture of ether (110 mL) and THF (10 mL), and the solution was cooled to -30°. This solution was stirred while solid LiDMP (1.53 g, 11.9 mmol) was added. While this mixture was stirred at room temperature for 20 m, LiCl precipitated and the color changed from purple to orange-yellow. The reaction mixture was then filtered through Celite, and the solvent removed *in vacuo*. The resulting yellow-orange oil was dissolved in ether and the solution filtered again through Celite. Partial removal of the solvent *in vacuo* yielded an orange-yellow precipitate (1.25 g). An additional 0.32 g was obtained by cooling the filtrate to -30° (total yield 57%):  $^1\text{H}$  NMR (300 MHz)  $\delta$  7.01 (d, 6, H<sub>m</sub>), 6.93 (s, 1, CHCMe<sub>3</sub>), 6.77 (t, 3, H<sub>p</sub>), 3.58 (t, 4, THF), 2.46 (s, 18, DMP Me), 1.15 (s, 9, CHCMe<sub>3</sub>), 1.01 (m, 4, THF);  $^{13}\text{C}$  (67.9 MHz)  $\delta$  237.4 (d, J<sub>CH</sub> = 107, CHCMe<sub>3</sub>), 161.7 (s, C<sub>ipso</sub>), 128.8 (d, J<sub>CH</sub> = 158, C<sub>m</sub>), 126.7 (s, C<sub>O</sub>), 120.7 (d, J<sub>CH</sub> = 160, C<sub>p</sub>), 74.5 (t, J<sub>CH</sub> = 149, THF), 43.1 (s, CHCMe<sub>3</sub>), 36.0 (q, J<sub>CH</sub> = 127, CHCMe<sub>3</sub>), 25.3 (t, J<sub>CH</sub> = 134, THF), 18.2 (q, J<sub>CH</sub> = 126, DMP Me). Anal. Calcd for TaC<sub>33</sub>H<sub>45</sub>O<sub>4</sub>: C, 57.71; H, 6.62. Found: C, 57.02; H, 6.38. The %C and %H found appear to demonstrate a significant loss of THF while sealed under a vacuum during the analysis period (Calcd for Ta(CHCMe<sub>3</sub>)(DMP)<sub>3</sub>, TaC<sub>29</sub>H<sub>37</sub>O<sub>3</sub>: C, 56.67; H, 6.08); decomposition in the solid state is also possible.

**Ta(CHCMe<sub>3</sub>)(DMP)<sub>3</sub>(py) (5).** Pyridine (280  $\mu$ L, 3.48 mmol), was added via syringe to a stirred solution of Ta(CHCMe<sub>3</sub>)(DMP)<sub>3</sub>(THF) (0.80 g, 1.16 mmol) in ether (150 mL) at -30°. The solution was stirred at room temperature for 10 m, during which time the color changed from orange to orange-red. The solvent was removed *in vacuo* from the filtrate, and the resulting oil was dissolved in a minimal amount of a 1:1 mixture of ether and pentane. Dark yellow crystals were isolated from this solution at -30° (0.49 g, 61%): <sup>1</sup>H NMR (300 MHz)  $\delta$  8.54 (d, 2, py H<sub>O</sub>), 7.51 (s, 1, CHCMe<sub>3</sub>), 7.1-6.1 (broad m, 12, py and DMP ring protons), 2.45 (s, 18, DMP Me), 1.25 (s, 9, CHCMe<sub>3</sub>); <sup>13</sup>C NMR (75.4 MHz)  $\delta$  241.9 (d, J<sub>CH</sub> = 107, CHCMe<sub>3</sub>), 160.0, 128.8, 126.9, and 120.8 (DMP ring carbons), 150.9 (d, py C<sub>O</sub>), 137.9 (d, py C<sub>p</sub>), 124.5 (d, py C<sub>m</sub>), 43.4 (s, CHCMe<sub>3</sub>), 35.7 (q, CHCMe<sub>3</sub>), 18.3 (q, DMP Me). Anal. Calcd for TaC<sub>34</sub>H<sub>42</sub>NO<sub>3</sub>: C, 58.86; H, 6.11. Found: C, 57.70; H, 5.93. The %C and %H found appear to demonstrate some loss of pyridine while sealed under a vacuum during the analysis period (Calcd for Ta(CHCMe<sub>3</sub>)(DMP)<sub>3</sub>, TaC<sub>29</sub>H<sub>37</sub>O<sub>3</sub>: C, 56.67; H, 6.08); decomposition in the solid state is also possible.

**Ta(CHCMe<sub>3</sub>)(TIPT)<sub>3</sub>(THF) (TIPT = S-2,4,6-C<sub>6</sub>H<sub>2</sub><sup>i</sup>Pr<sub>3</sub>) (6).** A solution of LiTIPT (1.45 g, 5.98 mmol; NaTIPT can also be employed<sup>82</sup>) in ether (25 mL) was added dropwise to a solution of Ta(CHCMe<sub>3</sub>)(THF)<sub>2</sub>Cl<sub>3</sub> (1.00 g, 1.99 mmol) in ether (50 mL) at room temperature. As the solution was stirred at room temperature, the color changed from purple to orange-red. After 20 m the mixture was filtered through Celite, and the solvent was removed from the filtrate *in vacuo*. The resulting oil was dissolved in pentane, and the solution was cooled to -30° to give a yellow powder (1.25 g, 61%): <sup>1</sup>H NMR (300 MHz)  $\delta$  7.15 (s, H<sub>m</sub>), 3.95 (broad septet, 6, ortho CHMe<sub>2</sub>), 3.65 (broad, 4, THF), 2.82 (septet, 3, para CHMe<sub>2</sub>), 1.36 (d, 36, ortho CHMe<sub>2</sub>), 1.23 (d plus m, 22, para CHMe<sub>2</sub> and THF), 0.98 (s, 9, CHCMe<sub>3</sub>); <sup>13</sup>C NMR (THF-d<sub>8</sub>, 75.4 MHz)  $\delta$  251.9 (d, J<sub>CH</sub> = 76, CHCMe<sub>3</sub>), 149.6, 148.9, and 148.0 (s's, C<sub>ipso</sub>, C<sub>O</sub> and C<sub>p</sub>), 121.1 (d, J<sub>CH</sub> = 144, C<sub>m</sub>), 48.3 (s, CHCMe<sub>3</sub>), 35.2 (d, J<sub>CH</sub> = 127, para CHMe<sub>2</sub>), 33.0 (d, J<sub>CH</sub> = 127, ortho CHMe<sub>2</sub>), 31.9 (q, J<sub>CH</sub> = 126, CHCMe<sub>3</sub>), 24.8 and 24.3 (q's, J<sub>CH</sub> = 125 and 123, ortho and para CHMe<sub>2</sub>). Coordinated

THF resonances were assumed to be coincident with the solvent resonances. Anal. Calcd for  $\text{TaC}_{54}\text{H}_{87}\text{OS}_3$ : C, 62.99; H, 8.53. Found: C, 62.94; H, 8.70.

**Ta(CHCMe<sub>3</sub>)(TIPT)<sub>3</sub>(py) (7).** Pyridine (70  $\mu\text{L}$ , 0.87 mmol) was added to a stirred solution of Ta(CHCMe<sub>3</sub>)(TIPT)<sub>3</sub>(THF) (0.30 g, 0.29 mmol) in ether (10 mL) at room temperature. After 20 m the solution was filtered through Celite, and the solvent was removed *in vacuo*, leaving the product as an orange-yellow powder (0.21 g, 70%): <sup>1</sup>H NMR (60°, 300 MHz)  $\delta$  6.84 (broad, 6, H<sub>m</sub>), 4.2–4.0 (broad, 6, ortho CHMe<sub>2</sub>), 4.09 (s, 1, CHCMe<sub>3</sub>), 2.72 (m, 3, para CHMe<sub>2</sub>), 1.38 (d, 36, ortho CHMe<sub>2</sub>), 1.24 (s, 9, CHCMe<sub>3</sub>), 1.13 (d, 18, para CHMe<sub>2</sub>); <sup>13</sup>C NMR (75.4 MHz)  $\delta$  252.4 (d, J<sub>CH</sub> = 94.2, CHCMe<sub>3</sub>), 150.3 (d, py C<sub>o</sub>), 135.2 (d, py C<sub>p</sub>), 123.5 (d, py C<sub>m</sub>), 150–118 (broad resonances, TIPT ring carbons), 47.1 (s, CHCMe<sub>3</sub>), 34.5 (d, para CHMe<sub>2</sub>), 32.4 (broad, ortho CHMe<sub>2</sub>), 31.4 (q, CHCMe<sub>3</sub>), 24.7 (q, para CHMe<sub>2</sub>), 24.5 (broad, ortho CHMe<sub>2</sub>). Anal. Calcd for  $\text{TaC}_{55}\text{H}_{84}\text{NS}_3$ : C, 63.73; H, 8.19. Found: C, 64.10; H, 8.30.

**Ta(CHCMe<sub>3</sub>)(TIPT)<sub>3</sub>(quin) (8).** Quinuclidine (0.066 g, 0.59 mmol) was added as a solid to a stirring solution of Ta(CHCMe<sub>3</sub>)(TIPT)<sub>3</sub>(THF) (0.200 g, 0.19 mmol) in ether (5 mL) at room temperature. The color of the solution quickly turned orange-yellow, and some yellow precipitate was observed. After 15 minutes the solvent was removed *in vacuo*, and the resulting solid was dissolved in ether. After filtration of this solution through Celite, cooling to -30° resulted in a yellow precipitate (0.145 g, 70%): <sup>1</sup>H NMR (300 MHz)  $\delta$  7.13 (s, H<sub>m</sub>), 3.91 (broad septet, 6, ortho CHMe<sub>2</sub>), 3.11 (broad, 6, N(CH<sub>2</sub>CH<sub>2</sub>)<sub>3</sub>CH), 2.80 (septet, 3, para CHMe<sub>2</sub>), 1.35 (d, 36, ortho CHMe<sub>2</sub>), 1.22 (d, 18, para CHMe<sub>2</sub>), 0.80 (broad, 6, N(CH<sub>2</sub>CH<sub>2</sub>)<sub>3</sub>CH); <sup>13</sup>C NMR (75.4 MHz; decoupled only)  $\delta$  151.2, 149.2, and 148.9 (C<sub>ipso</sub>, C<sub>o</sub>, and C<sub>p</sub>), 121.7 (C<sub>m</sub>), 48.5 (N(CH<sub>2</sub>CH<sub>2</sub>)<sub>3</sub>CH), 47.8 (CHCMe<sub>3</sub>), 34.6 and 33.0 (ortho and para CHMe<sub>2</sub>), 32.6 (CHCMe<sub>3</sub>), 26.8 (N(CH<sub>2</sub>CH<sub>2</sub>)<sub>3</sub>CH), 24.5 and 23.9 (ortho and para CHMe<sub>2</sub>), 20.8 (N(CH<sub>2</sub>CH<sub>2</sub>)<sub>3</sub>CH). The compound did not analyze well.

**Ta(CHCMe<sub>3</sub>)(TIPT)<sub>3</sub>(Et<sub>2</sub>S) (9).** Ethylsulfide (Et<sub>2</sub>S; 94  $\mu\text{L}$ , 0.87 mmol) was added via syringe to a stirring solution of Ta(CHCMe<sub>3</sub>)(TIPT)<sub>3</sub>(THF) (0.300 g, 0.29 mmol) in ether (10

mL) at room temperature. The color of the solution remained ~orange, and after 15 minutes the solution was filtered through Celite, followed by removal of the solvent *in vacuo*. The resulting orange-red solid was dissolved in pentane; cooling this solution to  $-30^{\circ}$  gave large orange crystals (0.203 g, 66%):  $^1\text{H}$  NMR (300 MHz)  $\delta$  7.15 (s,  $\text{C}_m$ ), 3.93 (septet, 6, ortho  $\text{CHMe}_2$ ), 2.83 (para  $\text{CHMe}_2$ ), 2.47 (q, 4,  $(\text{CH}_3\text{CH}_2)_2\text{S}$ ), 1.36 (d, 36, ortho  $\text{CHMe}_2$ ), 1.25 (d, 18, para  $\text{CHMe}_2$ ), 1.02 (t, 6,  $(\text{CH}_3\text{CH}_2)_2\text{S}$ ), 0.83 (s, 9,  $\text{CHCMe}_3$ );  $^{13}\text{C}$  NMR (75.4 MHz)  $\delta$  262 (broad,  $\text{J}_{\text{CH}}$  unresolved,  $\text{CHCMe}_3$ ), 151.1, 149.1, and 134.2 (s's,  $\text{C}_{\text{ipso}}$ ,  $\text{C}_o$ , and  $\text{C}_p$ ), 121.7 (d,  $\text{C}_m$ ), , 48.0 (s,  $\text{CHCMe}_3$ ), 34.6 (d, para  $\text{CHMe}_2$ ), 33.0 (d, ortho  $\text{CHMe}_2$ ), 32.4 (q,  $\text{CHCMe}_3$ ), 27.6 (broad t,  $(\text{CH}_3\text{CH}_2)_2\text{S}$ ), 24.5 (q, para  $\text{CHMe}_2$ ), 24.0 (q,  $\text{CHMe}_2$ ), 15.1 (q,  $(\text{CH}_3\text{CH}_2)_2\text{S}$ ). The compound did not analyze well.

**[Ta(CHCMe<sub>3</sub>)(TIPT)<sub>3</sub>]<sub>2</sub> (10)**. During the isolation of complex **6** from cooled solutions of pentane (see preparation of **6** given above), after most of **6** has precipitated small amounts of deep red microcrystalline **10** can be isolated. This complex has been prepared exclusively under alternative reaction conditions, but the preparation is not always repeatable; a typical example is given here. THF (5 mL, excess) was added to a stirring solution of  $\text{Ta}(\text{CH}_2\text{CMe}_3)_2\text{Cl}_3$  (0.400 g, 0.93 mmol) in ether (10 mL) at  $-30^{\circ}$ . After 2 hours of stirring at room temperature (during which time the color turned violet), the solvent was removed *in vacuo*. The resulting oil was redissolved in ether (10 mL) and the solution cooled to  $-30^{\circ}$ , and a solution of LiTIPT (1.008 g, 4.16 mmol) in ether (10 mL), also cooled to  $-30^{\circ}$ , was added dropwise. The mixture was stirred at room temperature for 20 hours (the color changed to deep red over the first hour as LiCl precipitated), followed by filtration of the mixture through Celite and removal of the solvent *in vacuo* to give a deep red oil. On dissolution of this oil in pentane and subsequent cooling of the solution to  $-30^{\circ}$ , some yellow precipitate was observed to form (i.e. the THF adduct **6**), so the solvent was again removed *in vacuo* and the oil/solid redissolved in ether (10 mL). This solution was stirred for an additional 12 hours at room temperature, followed by removal of the solvent *in vacuo* to give a deep red oil. Dissolution of the oil in pentane followed by cooling the solution to  $-30^{\circ}$  resulted in the formation of a deep

red microcrystalline precipitate (0.706 g, 79%):  $^1\text{H}$  NMR (300 MHz)  $\delta$  7.15 (s,  $\text{H}_m$ ), 3.80 (septet, 6, ortho  $\text{CHMe}_2$ ), 2.82 (septet, 3, para  $\text{CHMe}_2$ ), 1.80 (s, 1,  $\text{CHCMe}_3$ ), 1.26 (d, 18, para  $\text{CHMe}_2$ ), 1.22 (d, 36, ortho  $\text{CHMe}_2$ ), 1.08 (s, 9,  $\text{CHCMe}_3$ );  $^{13}\text{C}$  NMR (75.4 MHz)  $\delta$  149.4, 148.7, and 140.8 (s's,  $\text{C}_{\text{ipso}}$ ,  $\text{C}_o$ , and  $\text{C}_p$ ), 121.5 (d,  $\text{C}_m$ ), 37.5 (s,  $\text{CHCMe}_3$ ), 34.6 (d, para  $\text{CHMe}_2$ ), 33.8 (q,  $\text{CHCMe}_3$ ), 33.0 (d, ortho  $\text{CHMe}_2$ ), 24.5 and 24.2 (q's, ortho and para  $\text{CHMe}_2$ ). Anal. Calcd for  $\text{TaC}_{50}\text{H}_{79}\text{S}_3$ : C, 62.73; H, 8.32; S, 10.05. Found: C, 63.12; H, 8.29; S, 10.09.

**$\text{Ta}(\text{CH}_2\text{CMe}_3)_2(\text{DIPP})_2\text{Cl}$  (11).** A solution of LiDIPP (0.641 g, 3.48 mmol) in ether (10 mL), cooled to  $-30^\circ$ , was added to a stirring solution of  $\text{Ta}(\text{CH}_2\text{CMe}_3)_2\text{Cl}_3$  (0.500 g, 1.16 mmol) in ether (15 mL) at  $-30^\circ$ . The solution was then allowed to stir at room temperature overnight, resulting in the formation of a white precipitate (LiCl) and significant loss of color from the solution. Filtration of this mixture through Celite, followed by removal of the solvent *in vacuo*, gave an off-white solid. The solid was dissolved in pentane, and the solution was filtered through Celite to remove any remaining LiCl. Concentration of this pentane solution, by partial removal of solvent *in vacuo*, and subsequent cooling to  $-30^\circ$  yielded a white precipitate (0.360 g, 43%):  $^1\text{H}$  NMR (250 MHz)  $\delta$  7.18 (d, 4,  $\text{H}_m$ ), 7.02 (t, 2,  $\text{H}_p$ ), 4.01 (septet, 4,  $\text{CHMe}_2$ ), 2.01 (s, 4,  $\text{CH}_2\text{CMe}_3$ ), 1.35 (d, 24,  $\text{CHMe}_2$ ), 1.03 (s, 18,  $\text{CH}_2\text{CMe}_3$ );  $^{13}\text{C}$  NMR (75.4 MHz)  $\delta$  156.5 (s,  $\text{C}_{\text{ipso}}$ ), 140.2 (s,  $\text{C}_o$ ), 124.7 and 124.1 (d's,  $\text{C}_m$  and  $\text{C}_p$ ), 97.3 (t,  $J_{\text{CH}} = 118$ ,  $\text{CH}_2\text{CMe}_3$ ), 36.7 (s,  $\text{CH}_2\text{CMe}_3$ ), 34.5 (q,  $\text{CH}_2\text{CMe}_3$ ), 27.5 (d,  $\text{CHMe}_2$ ), 24.6 (q,  $\text{CHMe}_2$ ). Anal. Calcd for  $\text{TaC}_{34}\text{H}_{56}\text{ClO}_2$ : C, 57.26; H, 7.91; Cl, 4.97. Found: C, 56.87; H, 7.90; Cl, 4.87.

**$\text{Ta}(\text{CH}_2\text{CMe}_3)_2(\text{DIPP})_3$  (12).** LiDIPP·Et<sub>2</sub>O (0.902 g, 3.50 mmol) was added as a solid to a stirring solution of  $\text{Ta}(\text{CH}_2\text{CMe}_3)_2\text{Cl}_3$  (0.750 g, 1.75 mmol) in ether (20 mL) at room temperature, resulting in the formation of a white precipitate (LiCl) and loss of color in the solution. After 60 m, solid KDIPP (0.378 g, 1.75 mmol) was added, and the mixture was allowed to stir at room temperature for an additional 6 hours. Filtration of this mixture followed by removal of the solvent *in vacuo* yielded a white powder. This powder was then



dissolved in pentane and filtered through Celite, followed by removal of the solvent *in vacuo* to again give a white powder. Crystallization of this powder from ether at  $-30^{\circ}$  gave large colorless crystals (0.665 g, 45%):  $^1\text{H}$  NMR (250 MHz)  $\delta$  7.06 (d, 4,  $\text{H}_m$ ), 6.92 (d, 2,  $\text{H}_m$ ), 6.90 (t, 2,  $\text{H}_p$ ), 6.81 (t, 1,  $\text{H}_p$ ), 3.85 (septet, 4,  $\text{CHMe}_2$ ), 3.23 (septet, 2,  $\text{CHMe}_2$ ), 2.32 (s, 4,  $\text{CH}_2\text{CMe}_3$ ), 1.22 (s, 18,  $\text{CH}_2\text{CMe}_3$ ), 1.15 (d, 24,  $\text{CHMe}_2$ ), 1.00 (d, 12,  $\text{CHMe}_2$ );  $^{13}\text{C}$  NMR (75.4 MHz)  $\delta$  158.8 and 156.8 (s's,  $\text{C}_{\text{ipso}}$ ), 139.4 and 136.4 (s's,  $\text{C}_o$ ), 124.6, 123.9, 123.3, and 122.4 (d's,  $\text{C}_m$  and  $\text{C}_p$ ), 103.2 (t,  $J_{\text{CH}} = 113$ ,  $\text{CH}_2\text{CMe}_3$ ), 37.5 (s,  $\text{CH}_2\text{CMe}_3$ ), 34.6 (q,  $\text{CH}_2\text{CMe}_3$ ), 27.7 and 26.8 (d's,  $\text{CHMe}_2$ ), 24.9 and 23.6 (q's,  $\text{CHMe}_2$ ). The compound did not analyze well.

**$[\text{Ta}(\text{O})(\text{DIPP})_3]_x$  (13).**  $\text{Ta}(\text{CHCMe}_3)(\text{DIPP})_3(\text{THF})$  (0.200 g, 0.23 mmol) was dissolved in ether (5 mL), and mesitylene (32  $\mu\text{L}$ , 0.23 mmol) was added to this solution as an internal standard. Acetone (17  $\mu\text{L}$ , 0.23 mmol) was then added to this solution, while stirring, via a syringe, and immediately a white powder precipitated. After the solution was allowed to stir for a total of 10 m, the solution was filtered through Celite, and the filtrate was shaken vigorously with alumina to remove any remaining tantalum species. Analysis of the filtrate by GLC indicated 94% formation of 2,4,4-trimethyl-2-pentene (the expected organic Wittig product-taken as evidence for formation of the expected tantalum Wittig product, 13). In a separate experiment, the white precipitate was collected for analysis. Due to the complete insolubility of 13, recrystallization for analysis could not be employed as a purification technique. Anal. Calcd for  $\text{TaC}_{36}\text{H}_{51}\text{O}_4$ : C, 59.32; H, 7.07. Found: C, 60.02; H, 7.22.

**$\text{Ta}[\text{CH}(\text{Ph})\text{CH}(\text{CMe}_3)\text{CH}_2](\text{DIPP})_3$  (15).** A solution of styrene (200  $\mu\text{L}$ , 1.74 mmol) in ether (20 mL) was cooled to  $-30^{\circ}$  and added dropwise to a stirring solution of  $\text{Ta}(\text{CHCMe}_3)(\text{DIPP})_3(\text{THF})$  (1.50 g, 1.75 mmol) in ether (40 mL) at  $-30^{\circ}$ . The solution was warmed to  $25^{\circ}$  and stirred for 30 m. The deep orange solution was then filtered through Celite and the solvent removed *in vacuo* to give an orange oil. The oil was dissolved in minimal pentane, and the solution was cooled to  $-30^{\circ}$  to yield orange crystals (0.87 g, 57%):  $^1\text{H}$  NMR (270 MHz)  $\delta$  7.05 (d, 6,  $\text{H}_m$ ) 7.0–6.6 (m, 8,  $\text{H}_p$  and phenyl protons), 3.47 (septet, 6,

$\text{CHMe}_2$ ), 3.10-2.85 (m, 2,  $\alpha$   $\text{CH}_2$ ), 2.17 (d, 1,  $J_{\text{HH}} = 12$ ,  $\alpha$   $\text{CHPh}$ ), 1.57 (m, 1,  $\beta$   $\text{CHCMe}_3$ ), 1.19 (d, 18,  $\text{CHMe}_2$ ), 1.18 (d, 18,  $\text{CHMe}_2$ ), 0.94 (s, 9,  $\text{CHCMe}_3$ );  $^{13}\text{C}$  NMR (67.9 MHz)  $\delta$  157.5 (s,  $\text{C}_{\text{ipso}}$ ), 147.9 (s,  $\text{C}_{\text{ipso}}$  phenyl), 138.1 (s,  $\text{C}_0$ ), 128.2, 127.8, and 123.2 (d's, phenyl carbons), 123.9 (d,  $\text{C}_p$ ), 123.7 (d,  $\text{C}_m$ ), 81.9 (d,  $J_{\text{CH}} = 133$ ,  $\text{CHPh}$ ), 63.8 (t,  $J_{\text{CH}} = 129$ ,  $\text{CH}_2$ ), 42.9 (d,  $J_{\text{CH}} = 125$ ,  $\text{CHCMe}_3$ ), 39.3 (s,  $\text{CHCMe}_3$ ), 28.1 (d,  $\text{CHMe}_2$ ), 27.7 (q,  $\text{CHCMe}_3$ ), 24.0 (q,  $\text{CHMe}_2$ ). Anal. Calcd for  $\text{TaC}_{49}\text{H}_{69}\text{O}_3$ : C, 66.34; H, 7.86. Found: C, 66.61; H, 7.63.

**Ta(CHPh)(DIPP)<sub>3</sub>(THF) (16).** A solution of styrene (110  $\mu\text{L}$ , 0.96 mmol) in ether (3 mL) was cooled to  $-30^\circ$  and added dropwise to a solution of  $\text{Ta}(\text{CHCMe}_3)(\text{DIPP})_3(\text{THF})$  (0.80 g, 0.94 mmol) in a mixture of ether (12 mL) and THF (5 mL) at  $-30^\circ$ . The solution was warmed to  $25^\circ$  and stirred for 1 h, during which time the color changed from orange-yellow to dark orange. The mixture was filtered through Celite and the solvent was removed *in vacuo* to yield a dark orange oil. The oil was dissolved in pentane and the solution was cooled to  $-30^\circ$  to give dark orange crystals (0.37 g, 45%):  $^1\text{H}$  NMR (270 MHz)  $\delta$  8.49 (s, 1,  $\text{CHPh}$ ), 7.23 (t, 2, phenyl  $\text{H}_m$ ), 7.10 (d, 6,  $\text{H}_m$ ), 6.95-6.90 (m, 5,  $\text{H}_p$  and phenyl  $\text{H}_o$ ), 6.62 (t, 1, phenyl  $\text{H}_p$ ), 3.74 (m, 10,  $\text{CHMe}_2$  and THF), 1.23 (d, 36,  $\text{CHMe}_2$ ), 1.00 (m, 4, THF);  $^{13}\text{C}$  NMR (67.9 MHz)  $\delta$  221.1 (d,  $J_{\text{CH}} = 114$ ,  $\text{CHPh}$ ), 157.9 (s,  $\text{C}_{\text{ipso}}$ ), 145.7 (s, phenyl  $\text{C}_{\text{ipso}}$ ), 137.7 (s,  $\text{C}_0$ ), 129.0, 127.3, and 124.1 (unresolved, phenyl carbons), 123.6 (d,  $\text{C}_m$ ), 122.0 (d,  $\text{C}_p$ ), 74.9 (t, THF), 27.3 (d,  $\text{CHMe}_2$ ), 25.4 (unresolved, THF), 24.3 (q,  $\text{CHMe}_2$ ). Decomposition of **16** upon recrystallization thwarted all attempts at elemental analysis.

**Ta(CH<sub>2</sub>CH<sub>2</sub>CH<sub>2</sub>)(DIPP)<sub>3</sub> (17).** A solution of  $\text{Ta}(\text{CHCMe}_3)(\text{DIPP})_3(\text{THF})$  (1.50 g, 1.75 mmol) in ether (20 mL) was placed in a pressure bottle. The bottle was then pressurized at 30 psi of ethylene for 10 m, during which time the solution became nearly colorless. The solution was filtered through Celite and the solvent removed from the filtrate *in vacuo* to give a colorless oil. This oil was dissolved in pentane and the solution cooled to  $-30^\circ$  to yield colorless crystals (0.95 g, 72%):  $^1\text{H}$  NMR (250 MHz)  $\delta$  6.99 (d, 6,  $\text{H}_m$ ), 6.84 (t, 3,  $\text{H}_p$ ), 3.86 (m, 4,  $\alpha$   $\text{CH}_2$ ), 3.52 (septet, 6,  $\text{CHMe}_2$ ), 1.12 (d, 36,  $\text{CHMe}_2$ ), 0.48 (m, 2,  $\beta$   $\text{CH}_2$ );

$^{13}\text{C}$  NMR (67.9 MHz)  $\delta$  156.6 (s,  $\text{C}_{\text{ipso}}$ ), 137.6 (s,  $\text{C}_\text{O}$ ), 123.4 (d,  $\text{C}_\text{m}$ ), 122.2 (d,  $\text{C}_\text{p}$ ), 96.1 (t,  $J_{\text{CH}} = 147$ ,  $\alpha$   $\text{CH}_2$ ), 27.7 (d,  $\text{CHMe}_2$ ), 23.8 (q,  $\text{CHMe}_2$ ), -0.68 (t,  $J_{\text{CH}} = 150$ ,  $\beta$   $\text{CH}_2$ ). Anal. Calcd for  $\text{TaC}_{39}\text{H}_{57}\text{O}_3$ : C, 62.05; H, 7.63. Found: C, 62.21; H, 7.58.

**Ta(CH<sub>2</sub>CH<sub>2</sub>CH<sub>2</sub>)(DIPP)<sub>3</sub>(py) (18).** Ta(CHCMe<sub>3</sub>)(DIPP)<sub>3</sub>(THF) (7.00 g, 8.19 mmol) was dissolved in ether (150 mL) and placed in a Schlenk flask sealed with a septum. The flask was attached to a Schlenk line, and ethylene was vigorously bubbled through the solution via a needle for ~60 seconds. During this time the color changed from yellow-orange to very pale yellow. The solution was then filtered through Celite, and the solvent removed from the filtrate *in vacuo*. The resulting oil was dissolved in pentane and the solution was cooled to -30°. Pyridine (1.98 mL, 24.6 mmol) was added dropwise while stirring the solution. A white precipitate formed quickly. After stirring the mixture for 10 m at room temperature this precipitate was collected and washed with cold pentane. Additional product was obtained by reducing the volume of the filtrate and cooling to -30° (total 4.90 g, 72%):  $^1\text{H}$  NMR (270 MHz)  $\delta$  8.58 (d, 2, py H<sub>O</sub>), 7.06 (d, 6, H<sub>m</sub>), 6.90 (t, 3, H<sub>p</sub>), 6.80 (t, 1, py H<sub>p</sub>), 6.45 (t, 2, py H<sub>m</sub>), 3.57 (septet, 6, CHMe<sub>2</sub>), 2.95 (m, 4,  $\alpha$  CH<sub>2</sub>), 2.00 (m, 2,  $\beta$  CH<sub>2</sub>), 1.15 (d, 36, CHMe<sub>2</sub>);  $^{13}\text{C}$  NMR (67.9 MHz)  $\delta$  156.6 (s,  $\text{C}_{\text{ipso}}$ ), 150.1 (d, py C<sub>O</sub>), 138.0 (s, C<sub>O</sub>), 136.0 (unresolved, py C<sub>p</sub>), 123.8 (d, py C<sub>m</sub>), 123.6 (d, C<sub>m</sub>), 122.3 (d, C<sub>p</sub>), 78.0 (t,  $J_{\text{CH}} = 120$ ,  $\alpha$  CH<sub>2</sub>), 36.3 (t,  $J_{\text{CH}} = 129$ ,  $\beta$  CH<sub>2</sub>), 27.6 (d, CHMe<sub>2</sub>), 24.0 (q, CHMe<sub>2</sub>). Anal. Calcd for TaC<sub>44</sub>H<sub>62</sub>NO<sub>3</sub>: C, 63.37; H, 7.49. Found: C, 63.85; H, 8.05.

**Ta(CHSiMe<sub>3</sub>)(DIPP)<sub>3</sub>(THF) (20).** A solution of trimethylsilylethylene (56  $\mu\text{L}$ , 0.39 mmol) in ether (4 mL) was cooled to -30° and added dropwise to a solution of Ta(CHCMe<sub>3</sub>)(DIPP)<sub>3</sub>(THF) (0.30 g, 0.35 mmol) in a mixture of ether (8 mL) and THF (2 mL) at -30°. The solution was warmed to room temperature and stirred for 40 m, during which time the color changed from orange-yellow to yellow. The solution was filtered through Celite, and the solvent was removed *in vacuo* from the filtrate to give a yellow oil. The yield is virtually quantitative by  $^1\text{H}$  NMR. Yellow crystals were obtained by crystallization from pentane at -30°:  $^1\text{H}$  NMR (300 MHz)  $\delta$  7.73 (s, 1, CHSiMe<sub>3</sub>), 7.11 (d, 6, H<sub>m</sub>), 6.94 (t, 3,

H<sub>p</sub>), 3.85-3.65 (m, 10, CHMe<sub>2</sub> and THF), 1.27 (d, 36, CHMe<sub>2</sub>), 1.12 (m, 4, THF), 0.17 (s, 9, CHSiMe<sub>3</sub>); <sup>13</sup>C NMR (67.9 MHz) δ 210.6 (d, J<sub>CH</sub> = 102, CHSiMe<sub>3</sub>), 158.3 (s, C<sub>ipso</sub>), 137.6 (s, C<sub>O</sub>), 123.7 (d, C<sub>m</sub>), 122.2 (d, C<sub>p</sub>), 73.2 (t, THF), 27.2 (d, CHMe<sub>2</sub>), 25.4 (unresolved, THF), 24.4 (q, CHMe<sub>2</sub>), 4.08 (q, CHSiMe<sub>3</sub>). Anal. Calcd for TaC<sub>44</sub>H<sub>69</sub>O<sub>4</sub>Si: C, 60.66; H, 8.00. Found: C, 60.76; H, 8.01.

**Ta[CH(SiMe<sub>3</sub>)CH(SiMe<sub>3</sub>)CH<sub>2</sub>](DIPP)<sub>3</sub> (21).** A solution of trimethylsilylethylene (134 μL, 0.92 mmol) in ether (4 mL) was cooled to -30° and added dropwise to a solution of Ta(CHSiMe<sub>3</sub>)(DIPP)<sub>3</sub>(THF) (0.40 g, 0.46 mmol) in ether (6 mL) at -30°. The solution was warmed to room temperature and stirred for 15 m, during which time the solution became colorless. Filtration through Celite followed by removal of the solvent *in vacuo* from the filtrate yielded a colorless oil. A white precipitate formed upon cooling a pentane solution to -30° (0.29 g, 71%): <sup>1</sup>H NMR (300 MHz) δ 6.96 (d, 6, H<sub>m</sub>), 6.82 (m, 3, H<sub>p</sub>), 4.98 (t, 1, J<sub>HH</sub> = 10.1, α CH<sub>2</sub>), 3.64 (t, 1, J<sub>HH</sub> = 10.7, α CH<sub>2</sub>), 3.6-3.2 (broad, 6, CHMe<sub>2</sub>), 2.95 (d, 1, J<sub>HH</sub> = 14.5, α CHSiMe<sub>3</sub>), 1.5-0.5 (broad multiplet, 36, CHMe<sub>2</sub>), 0.24 (s, 9, SiMe<sub>3</sub>), 0.14 (s, 9, SiMe<sub>3</sub>), -0.33 (m, 1, β CHSiMe<sub>3</sub>); <sup>13</sup>C NMR (75.4 MHz) δ 160-120 (ring carbons), 108.1 (t, J<sub>CH</sub> = 145, α CH<sub>2</sub>), 99.3 (d, J<sub>CH</sub> = 128, α CHSiMe<sub>3</sub>), 28-22 (m, CHMe<sub>2</sub> and CHMe<sub>2</sub>), 6.41 (d, J<sub>CH</sub> = 131, β CHSiMe<sub>3</sub>), 2.31 (q, SiMe<sub>3</sub>), 0.82 (q, SiMe<sub>3</sub>). Anal. Calcd for TaC<sub>45</sub>H<sub>73</sub>O<sub>3</sub>Si<sub>2</sub>: C, 60.11; H, 8.18. Found: C, 60.43; H, 8.24. A small amount of another isomer (~15%), thought to be Ta[CH(SiMe<sub>3</sub>)CH<sub>2</sub>CH(SiMe<sub>3</sub>)](DIPP)<sub>3</sub>, is present according to <sup>1</sup>H and <sup>13</sup>C NMR spectra; <sup>1</sup>H NMR: δ 3.93 (m, α CHSiMe<sub>3</sub>); <sup>13</sup>C NMR: δ 106.2 (d, J<sub>CH</sub> = 122 Hz, α CHSiMe<sub>3</sub>).

**Ta[CH<sub>2</sub>CH<sub>2</sub>CH<sub>2</sub>CH<sub>2</sub>O](DIPP)<sub>3</sub>(py) (22).** Paraformaldehyde (0.018 g, 0.60 mmol) was added as a solid to a stirring solution of Ta(CH<sub>2</sub>CH<sub>2</sub>CH<sub>2</sub>)(DIPP)<sub>3</sub>(py) (0.070 g, 0.08 mmol) in ether (5 mL) at -30°. The paraformaldehyde did not completely dissolve, and the solution remained cloudy throughout the reaction. After 12 hours the solution was filtered through Celite, followed by removal of the solvent *in vacuo*. A <sup>1</sup>H NMR spectrum (C<sub>6</sub>D<sub>6</sub>) of the resulting white solid showed the product to be ~75% **22**. Complex **22** can be isolated as a

white precipitate from ether/pentane (~1:1) solutions at  $-30^{\circ}$ :  $^1\text{H}$  NMR (300 MHz)  $\delta$  8.48 (broad, 2, py  $\text{H}_\text{O}$ ), 7.11 (d, 6,  $\text{C}_\text{m}$ ), 6.95 (t, 3,  $\text{C}_\text{p}$ ), 6.86 (broad, 1, py  $\text{H}_\text{p}$ ), 6.54 (broad, 2, py  $\text{H}_\text{m}$ ), 4.29 (t,  $J_{\text{HH}} = 5.5$ , 2,  $\text{OCH}_2$ ), 3.63 (septet, 6,  $\text{CHMe}_2$ ), 2.13 (broad, 2,  $\alpha$   $\text{CH}_2$ ), 1.92 (t, 2,  $J_{\text{HH}} = 6.6$ ,  $\beta$   $\text{CH}_2$ ), 1.56 (m, 2,  $\gamma$   $\text{CH}_2$ ), 1.20 (d, 36,  $\text{CHMe}_2$ );  $^{13}\text{C}$  NMR (75.4 MHz)  $\delta$  156.8 (s,  $\text{C}_{\text{ipso}}$ ), 150.1 (d, py  $\text{C}_\text{O}$ ), 138.1 (s,  $\text{C}_\text{O}$ ), 135.9 (unresolved, py  $\text{C}_\text{p}$ ), 123.7 (d,  $\text{C}_\text{m}$ ), 122.6 (d,  $\text{C}_\text{p}$ ), 121.0 (unresolved, py  $\text{C}_\text{m}$ ), 72.6 (unresolved,  $\text{OCH}_2$ ), 67.3 (unresolved,  $\alpha$   $\text{CH}_2$ ), 33.9 (unresolved,  $\beta$   $\text{CH}_2$ ), 27.4 (d,  $\text{CHMe}_2$ ), 25.9 (unresolved,  $\gamma$   $\text{CH}_2$ ), 24.2 (q,  $\text{CHMe}_2$ ). The complex readily loses pyridine under vacuum. Anal. Calcd for  $\text{TaC}_{40}\text{H}_{59}\text{O}_4$  (base-free): C, 61.21; H, 7.58. Found: C, 61.62; H, 7.64.

**Ta[CH<sub>2</sub>CH<sub>2</sub>CH<sub>2</sub>C(Me)<sub>2</sub>O](DIPP)<sub>3</sub> (23).** A solution of acetone (7.3  $\mu\text{L}$ , 0.10 mmol) in ether (5 mL) was cooled to  $-30^{\circ}$  and added to a solution of  $\text{Ta}(\text{CH}_2\text{CH}_2\text{CH}_2)(\text{DIPP})_3$  (0.075 g, 0.10 mmol) in ether (5 mL) at  $-30^{\circ}$ . The solution was held at  $-30^{\circ}$  overnight, during which time the color did not change and no precipitate was observed. Filtration of the solution followed by removal of the solvent *in vacuo* yielded a colorless oil in essentially quantitative yield by  $^1\text{H}$  NMR; the compound can be obtained as a white precipitate when the reaction is performed on a larger scale:  $^1\text{H}$  NMR (250 MHz)  $\delta$  7.06 (d, 6,  $\text{H}_\text{m}$ ), 6.91 (t, 3,  $\text{H}_\text{p}$ ), 3.59 (septet, 6,  $\text{CHMe}_2$ ), 2.40 (broad, 2,  $\alpha$   $\text{CH}_2$ ), 2.23 (broad, 2,  $\beta$   $\text{CH}_2$ ), 1.52 (broad, 2,  $\gamma$   $\text{CH}_2$ ), 1.22 (d, 36,  $\text{CHMe}_2$ ), 0.97 (s, 6,  $\text{CMe}_2$ );  $^{13}\text{C}$  NMR (67.9 MHz)  $\delta$  157.5 (s,  $\text{C}_{\text{ipso}}$ ), 137.5 (s,  $\text{C}_\text{O}$ ), 123.6 (d,  $\text{C}_\text{m}$ ), 122.5 (d,  $\text{C}_\text{p}$ ), 82.1 (s,  $\text{CMe}_2$ ), 66.9 (t,  $J_{\text{CH}} = 122$ ,  $\alpha$   $\text{CH}_2$ ), 45.4 (t,  $J_{\text{CH}} = 123$ ,  $\beta$   $\text{CH}_2$ ), 37.5 (q,  $\text{CMe}_2$ ), 29.5 (q,  $\text{CHMe}_2$ ), 27.4 (d,  $\text{CHMe}_2$ ), 23.9 (t,  $J_{\text{CH}} = 127$ ,  $\gamma$   $\text{CH}_2$ ). Anal. Calcd for  $\text{TaC}_{42}\text{H}_{63}\text{O}_4$ : C, 62.06; H, 7.81. Found: C, 61.99; H, 7.95.

**Ta[CH<sub>2</sub>CH<sub>2</sub>CH<sub>2</sub>CH(Ph)O](DIPP)<sub>3</sub>(py) (24).** A solution of benzaldehyde (61  $\mu\text{L}$ , 0.60 mmol) in ether (5 mL) was cooled to  $-30^{\circ}$  and added to a solution of  $\text{Ta}(\text{CH}_2\text{CH}_2\text{CH}_2)(\text{DIPP})_3(\text{py})$  (0.50 g, 0.60 mmol) in ether (15 mL) at  $-30^{\circ}$ . The solution was held at  $-30^{\circ}$  for 15 m and then  $25^{\circ}$  for an additional 60 m. A white solid precipitated from the solution but redissolved when the solution reached room temperature. The solution was

filtered through Celite and the solvent removed *in vacuo* to give a white solid that was reprecipitated from pentane at  $-30^{\circ}$  (yield 0.45 g, 80%):  $^1\text{H}$  NMR (270 MHz)  $\delta$  8.64 (broad s, 2), 7.15-6.85 (m, 6), 7.08 (d, 6), 6.93 (t, 3), and 6.61 (t, 2, all pyridine, phenyl, or DIPP ring resonances), 5.56 (d of d, 1,  $J_{\text{HH}} = 2.6$  and 10.4,  $\text{CHPh}$ ), 3.66 (septet, 6,  $\text{CHMe}_2$ ), 3.2-1.6 (m, 6,  $\alpha$   $\text{CH}_2$ ,  $\beta$   $\text{CH}_2$ , and  $\gamma$   $\text{CH}_2$ ), 1.16 (d, 18,  $\text{CHMe}_2$ ), 1.14 (d, 18,  $\text{CHMe}_2$ );  $^{13}\text{C}$  NMR (67.9 MHz)  $\delta$  157.0 (s), 150.2 (d), 144.8 (s), 138.0 (s), 135.6 (d), 129–126 (unresolved), 123.7 (d), and 122.7 (d, all pyridine, phenyl, or DIPP ring carbons), 85.1 (d,  $J_{\text{CH}} = 144$ ,  $\text{CHPh}$ ), 66.2 (t,  $J_{\text{CH}} = 120$ ,  $\alpha$   $\text{CH}_2$ ), 42.0 (t,  $J_{\text{CH}} = 126$ ,  $\beta$   $\text{CH}_2$ ), 27.6 (t,  $J_{\text{CH}} = 127$ ,  $\gamma$   $\text{CH}_2$ ), 27.4 (d,  $\text{CHMe}_2$ ), 24.3 (q,  $\text{CHMe}_2$ ), 24.0 (q,  $\text{CHMe}_2$ ). Anal. Calcd for  $\text{TaC}_{51}\text{H}_{68}\text{NO}_4$ : C, 65.15; H, 7.31. Found: C, 64.74; H, 6.87.

$\text{Ta}[\text{CH}_2\text{CH}_2\text{CH}_2\text{CH}(\text{CMe}_3)\text{O}](\text{DIPP})_3$  (**25**). Pivaldehyde (29  $\mu\text{L}$ , 0.27 mmol) was added to a stirred solution of  $\text{Ta}(\text{CH}_2\text{CH}_2\text{CH}_2)(\text{DIPP})_3$  (0.20 g, 0.26 mmol) in ether (5 mL) at  $-30^{\circ}$ . After standing the reaction mixture overnight at room temperature, the solvent was removed *in vacuo*, leaving behind a colorless oil in essentially quantitative yield by NMR. The product could not be obtained in crystalline form, even when the reaction was performed on a large scale:  $^1\text{H}$  NMR (300 MHz)  $\delta$  7.07 (d, 6,  $\text{H}_m$ ), 6.92 (t, 3,  $\text{H}_p$ ), 4.09 (d of d, 1,  $J_{\text{HH}} = 1.9$  and 11.4,  $\text{CHCMe}_3$ ), 3.58 (septet, 6,  $\text{CHMe}_2$ ), 3.11 (m, 1,  $\alpha$   $\text{CH}_2$ ), 2.63 (d of t, 1,  $J_{\text{HH}}$  unresolved,  $\alpha$   $\text{CH}_2$ ), 1.9–1.5 (multiplet, 4,  $\beta$   $\text{CH}_2$  and  $\gamma$   $\text{CH}_2$ ), 1.23 (d, 18,  $\text{CHMe}_2$ ), 1.19 (d, 18,  $\text{CHMe}_2$ ), 0.71 (s,  $\text{CHCMe}_3$ );  $^{13}\text{C}$  NMR (67.9 MHz)  $\delta$  157.1 (s,  $\text{C}_{\text{ipso}}$ ), 137.7 (s,  $\text{C}_o$ ), 123.6 (d,  $\text{C}_m$ ), 122.7 (d,  $\text{C}_p$ ), 91.8 (d,  $J_{\text{CH}} = 140$ ,  $\text{CHCMe}_3$ ), 66.8 (t,  $J_{\text{CH}} = 123$ ,  $\alpha$   $\text{CH}_2$ ), 35.1 (s,  $\text{CHCMe}_3$ ), 33.3 (t,  $J_{\text{CH}} = 123$ ,  $\beta$   $\text{CH}_2$ ), 27.6 (t,  $J_{\text{CH}} = 129$ ,  $\gamma$   $\text{CH}_2$ ), 27.4 (d,  $\text{CHMe}_2$ ), 26.0 (q,  $\text{CHCMe}_3$ ), 24.3 (q,  $\text{CHMe}_2$ ), 24.1 (q,  $\text{CHMe}_2$ ).

**X-Ray structure of  $\text{Ta}[\text{CH}(\text{Ph})\text{CH}(\text{CMe}_3)\text{CH}_2](\text{DIPP})_3$  (**15**).** Data were collected at  $-65^{\circ}$  on an Enraf-Nonius CAD4F-11 diffractometer equipped with a liquid-nitrogen low-temperature device and using Mo  $\text{K}\alpha$  radiation. Axial photographs were taken on the diffractometer about each of the reciprocal axes to check that the unit cell lengths were correct. The program TRACER run on the unit cell (which was calculated with 25 high angle

reflections ( $2\theta > 30^\circ$ ) revealed no higher symmetry. Data collection, reduction, and refinement procedures can be found elsewhere.<sup>83</sup> A total of 11816 reflections were collected in the range  $3^\circ < 2\theta < 45^\circ$  with the 7831 having  $F_o > 4\sigma(F_o)$  being used in the structure refinement which was carried out in two blocks (224 variables each) using SHELX-76. Final  $R_1 = 0.084$  and  $R_2 = 0.115$ . A semiempirical absorption correction was applied ( $\mu = 5.8 \text{ cm}^{-1}$ ). Two crystallographically independent but closely analogous molecules are present in the asymmetric unit. Only the Ta atoms were refined anisotropically. Most hydrogen atoms could be placed in calculated positions (C-H = 0.95 Å) and constrained to ride on their respective carbon atoms. Hydrogen atoms on the TaC<sub>3</sub> ring carbon atoms could not be located and were ignored. A final difference Fourier map showed no significant features. The crystal data are the following: space group  $P2_1/n$  with  $a = 21.338(11) \text{ \AA}$ ,  $b = 11.699(5) \text{ \AA}$ ,  $c = 37.198(23) \text{ \AA}$ ,  $\beta = 102.66(5)^\circ$ ,  $Z = 8$ ,  $M_r = 887.03 \text{ g}$ ,  $V = 9060.1 \text{ \AA}^3$ ,  $\rho(\text{calcd}) = 1.301 \text{ g cm}^{-3}$ .

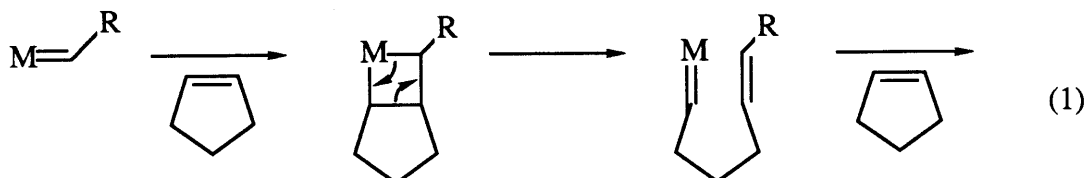
## CHAPTER 2

### Ring-Opening Polymerization of Norbornene and Related Cyclic Olefins with Tantalum Alkylidene and Metallacyclobutane Complexes



## INTRODUCTION

Ring-opening polymerization of cyclic olefins by olefin metathesis catalysts is well-known.<sup>2,3</sup> This polymerization is an olefin metathesis, with polymer formation a result of the cyclic nature of the olefin metathesized (equation 1; shown for cyclopentene). The reaction



is thermodynamically favorable for strained cyclic olefins such as  $C_3$ ,  $C_4$ ,  $C_8$  (*cis*), and higher cyclic olefins, and for some bicyclic olefins (e.g. norbornene) and tricyclic olefins. With cyclic olefins that contain less ring strain, the reaction may occur to give an equilibrium between polymer and monomer or not at all (see later).

While many examples can be found in the literature,<sup>2,3</sup> the first documented example of a *living* cyclic olefin polymerization in which monodisperse polymers were obtained was reported by Grubbs in 1986.<sup>84</sup> (A tungsten catalyst used for polymerizing NBE was shown to involve propagating carbene complexes, but the resulting polymers were not analyzed for their molecular weight distributions.<sup>85</sup>) Generally a living polymerization system is defined by efficient initiation, lack of termination and chain transfer in propagation, and the ability to obtain monodisperse polymers if the reaction is irreversible; monodisperse polymers are those which display a low polydispersity,  $d$ , defined by  $M_w/M_n$ . Knowledge of the mechanism and characterization of catalyst intermediates are also desirable. In Grubbs' system, a titanacyclobutane complex ( $Ti[CH(C_5H_8)CHCH(R)]Cp_2$ ) was shown to efficiently polymerize norbornene (NBE), yielding monodisperse polynorbornene on capping with benzophenone. The only limiting factor in this system was that polymer degradation occurred rapidly at the reaction temperature after complete consumption of NBE.

Some other catalysts (of tungsten,<sup>76,86</sup> molybdenum,<sup>78,86</sup> and other metals<sup>87</sup>) have also now been shown to polymerize NBE and other cyclic olefins in a controlled fashion, yielding monodisperse polymers. In a related tungsten system ( $\text{W}(\text{CHCMe}_3)(\text{OCH}_2\text{CMe}_3)_2\text{Br}_2/\text{GaBr}_3$  and NBE), although polymer molecular weight distributions have not been reported, significant progress has been made in understanding the mode of reactivity with NBE.<sup>62,85,88</sup>

In chapter 1 the preparation of several new tantalum alkylidene and metallacyclobutane complexes was discussed, and here the reactivity of these complexes with cyclic olefins is reported. Polymerization of the monomer NBE has been investigated most extensively, since this strained monomer reacts readily with a variety of classical metathesis catalysts and the polymers are well-characterized.<sup>2-4</sup> Some of this work has been published.<sup>17,89</sup>

## RESULTS

### Preparation and Crystal Structure of $\text{Ta}[\text{CH}(\text{C}_5\text{H}_8)\text{CHCH}(\text{CMe}_3)](\text{DIPP})_3$ (**26**).

$\text{Ta}(\text{CHCMe}_3)(\text{DIPP})_3(\text{THF})$  (**2**) polymerizes NBE very rapidly in toluene at room temperature, but the reaction is not well-defined. Examination of the organometallic species generated and analysis of the resulting polymers by gel permeation chromatography (GPC) suggest that the presence of THF is a major complication in the reaction. (The details of this reaction are described later.) Since base-free tantalacyclobutane complexes had been isolated by treating  $\text{Ta}(\text{CHCMe}_3)(\text{DIPP})_3(\text{THF})$  with certain olefins, a similar reaction between complex **2** with one equivalent of NBE in ether was attempted. Removal of the solvent *in vacuo* from the resulting colorless solution gave a white precipitate, identified as the base-free tantalacyclobutane complex  $\text{Ta}[\text{CH}(\text{C}_5\text{H}_8)\text{CHCH}(\text{CMe}_3)](\text{DIPP})_3$  (**26**; equation 2); colorless crystals of **26** can be obtained from cooled solutions of pentane in 64% yield. NMR data for **26** and other tantalacyclobutane complexes discussed here are given in Table I. The  $^1\text{H}$  NMR spectrum ( $\text{C}_6\text{D}_6$ ,  $25^\circ$ ) of complex **26** displays ring resonances at 5.32 (d,  $J_{\text{HH}} = 9.6$  Hz,  $\text{H}_1$ ), 3.88 (d,  $J_{\text{HH}} = 10.1$  Hz,  $\text{H}_2$ ), and 0.88 ppm (broad t,  $\text{H}_3$ ) (Figure 1a; cf. in

**Table I.** Proton and Carbon NMR Data for the TaC<sub>3</sub> Ring in Tantalacycles.<sup>a</sup>

Compound	H <sub>α</sub>	H <sub>β</sub>	C <sub>α</sub> (J <sub>CH</sub> )	C <sub>β</sub> (J <sub>CH</sub> )
<b>26</b>	5.32 (H <sub>1</sub> ) 3.88 (H <sub>2</sub> )	0.88 (H <sub>3</sub> )		
<b>27</b>	5.22 (H <sub>1</sub> ) 3.85 (H <sub>2</sub> )	obscured		
<b>28</b>	5.23 (H <sub>1</sub> ) 3.85 (H <sub>2</sub> )	obscured		
<b>30</b>	5.21 (H <sub>1</sub> ) 3.72 (H <sub>2</sub> )	0.84 (H <sub>3</sub> )	132.5 (132) 135.0 (142)	30.2 or 29.0 (149 <sup>c</sup> )
<b>31</b>	5.1 (H <sub>1</sub> ) 3.7 (H <sub>2</sub> )	obscured		

<sup>a</sup> Solvent = C<sub>6</sub>D<sub>6</sub> and T = 25°.

<sup>b</sup> Compounds: Ta[CH(C<sub>5</sub>H<sub>8</sub>)CHCH(CMe<sub>3</sub>)](DIPP)<sub>3</sub> (**26**); Ta[CH(C<sub>5</sub>H<sub>8</sub>)CHCH(P)](DIPP)<sub>3</sub> (**27**); Ta[CH(C<sub>5</sub>H<sub>8</sub>)CHCH(CHC<sub>5</sub>H<sub>8</sub>CHCHCMe<sub>3</sub>)](DIPP)<sub>3</sub> (**28**); Ta[CH(C<sub>5</sub>H<sub>8</sub>)CHCH(CMe<sub>3</sub>)](DMP)<sub>3</sub> (**30**); Ta[CH(C<sub>5</sub>H<sub>8</sub>)CHCH(P)](DMP)<sub>3</sub> (**31**).

<sup>c</sup> For 29.0 ppm resonance.

**Figure 1a.** The  $^1\text{H}$  NMR spectrum of  $\text{Ta}[\text{CH}(\text{C}_5\text{H}_8)\text{CHCH}(\text{CMe}_3)](\text{DIPP})_3$  (**26**) in  $\text{C}_6\text{D}_6$ .

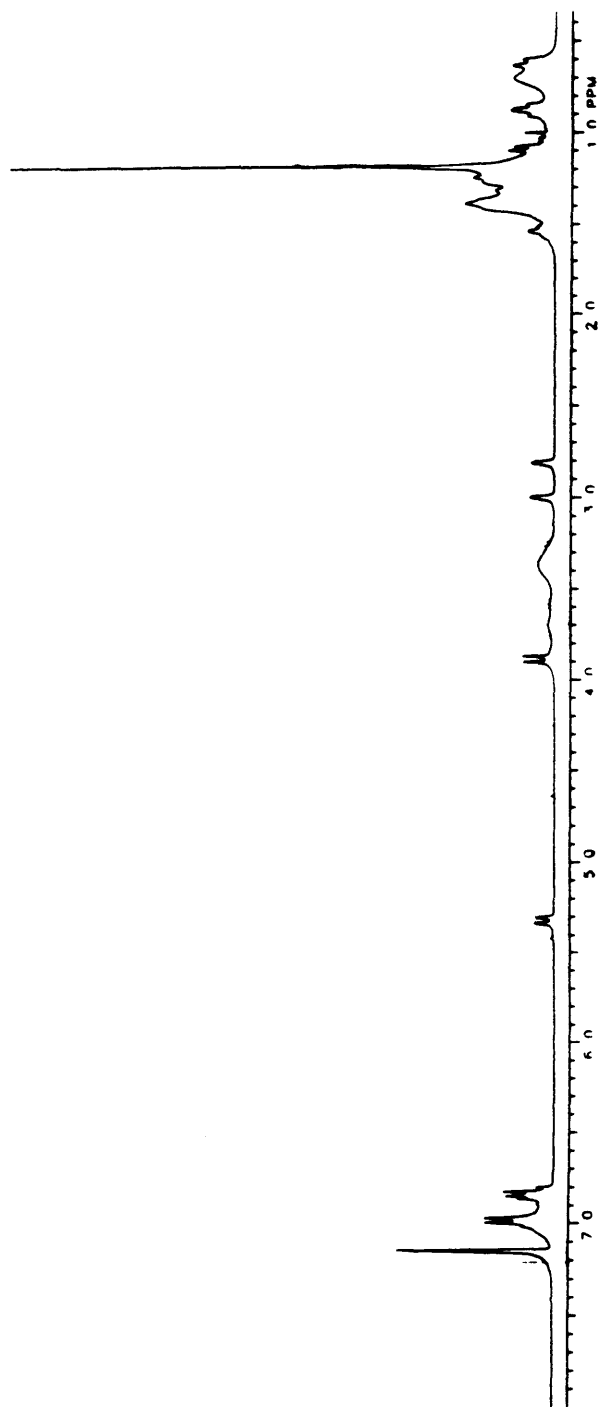
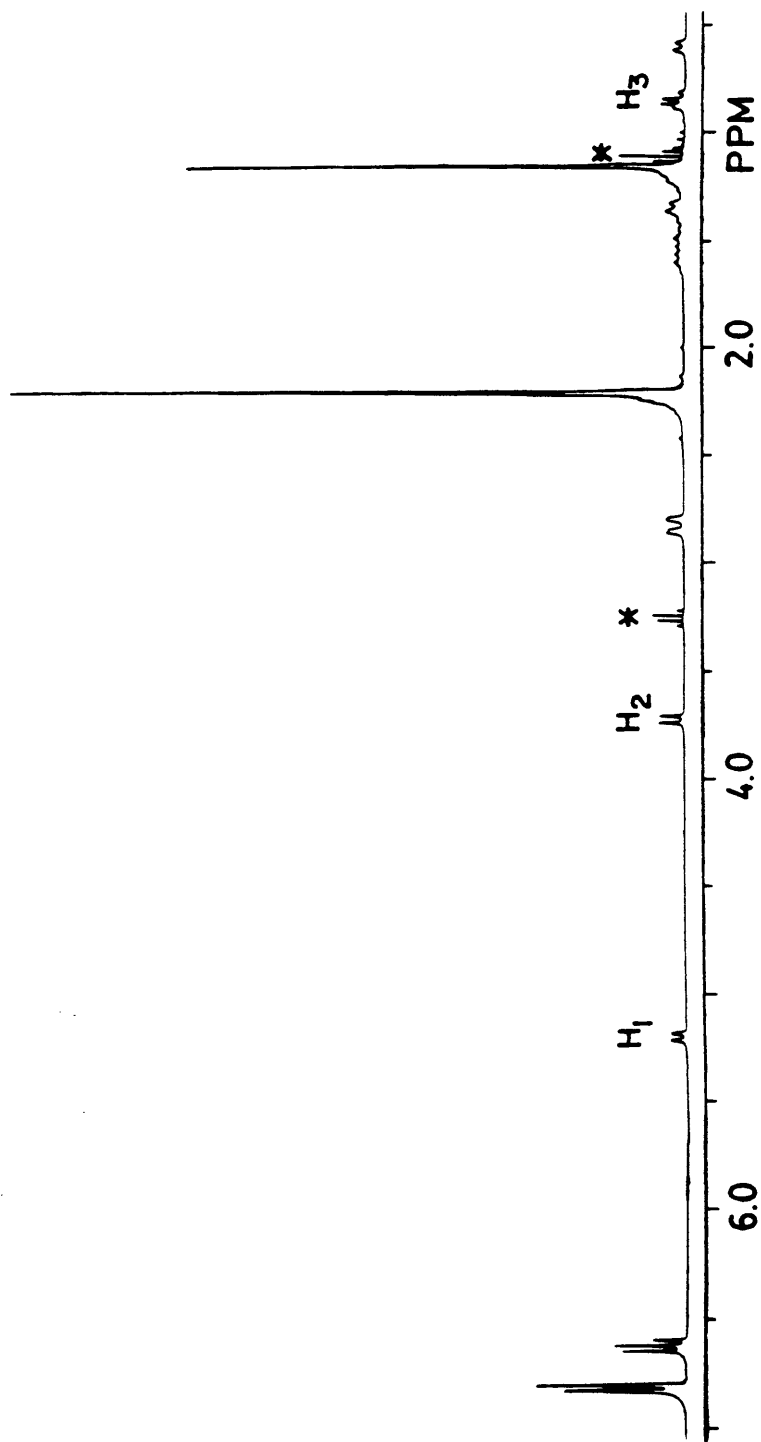
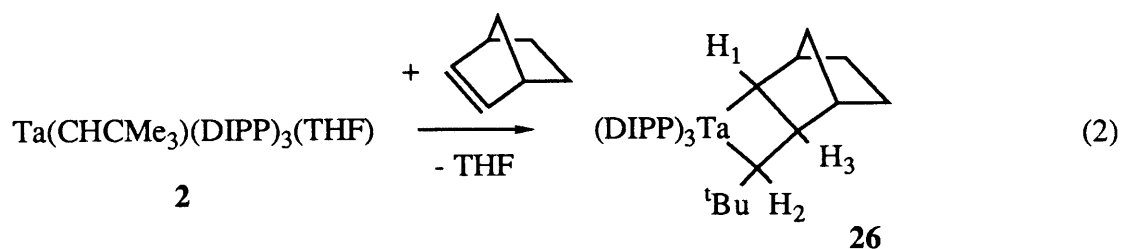


**Figure 1b.** The  $^1\text{H}$  NMR spectrum of  $\text{Ta}[\text{CH}(\text{C}_5\text{H}_8)\text{CHCH}(\text{CMe}_3)](\text{DMP})_3$  (**30**) in  $\text{C}_6\text{D}_6$  (\* = diethyl ether).



Ti[CH(C<sub>5</sub>H<sub>8</sub>)CHCH(R)]Cp<sub>2</sub>: 3.72, 2.63, and 0.08 ppm). Resonances for the DIPP ligands



are broad, as might be expected in a crowded trisubstituted metallacycle in which the inequivalent DIPP ligands cannot readily interconvert. Consequently, a <sup>13</sup>C NMR spectrum of **26** at 25° was not informative, and attempts to obtain a spectrum at ~50° resulted in some decomposition of the complex. At 25°, complex **26** decomposes 10-20% after one day in solution (C<sub>6</sub>D<sub>6</sub>), but is stable as a solid.

An X-ray study of complex **26** confirmed the metallacyclobutane assignment and showed H<sub>2</sub> and H<sub>3</sub> to be *trans* to one another (i.e. the α t-butyl and norbornane ring substituents are *trans*). A drawing of the molecule is shown in Figure 2, and relevant bond distances and angles are given in Table II. The overall geometry of this complex is approximately trigonal bipyramidal, allowing for constraints imposed within the complex by the metallacyclobutane ring. The ring resides in the equatorial plane, with ∠C<sub>α</sub>-M-C<sub>α</sub> = 78.7(7)° and M...C<sub>β</sub> = 2.382(16) Å being similar to those values observed in related trigonal bipyramidal tungstenacyclobutane complexes and contrasting with those values observed in related approximately square pyramidal metallacyclobutane complexes (as discussed in chapter 1); the axial phenoxide ligands display an interligand angle of 175.5(3)°. The Ta-C single bond distances (2.138(14) and 2.144(14) Å) are quite normal for early transition metal phenoxide complexes,<sup>1</sup> as are the Ta-O bond distances (~1.91 Å).<sup>21,90</sup> Additionally, as is usually the case, the relatively large Ta-O-C angles of 161.0(8)°, 159.3(8)°, and 163.7(7)° reveal a significant amount of π donation from these ligands. Finally, the ring in **26** is only slightly

Figure 2. A view of Ta[CH(C<sub>5</sub>H<sub>8</sub>)CHCH(CMe<sub>3</sub>)](DIPP)<sub>3</sub> (26).

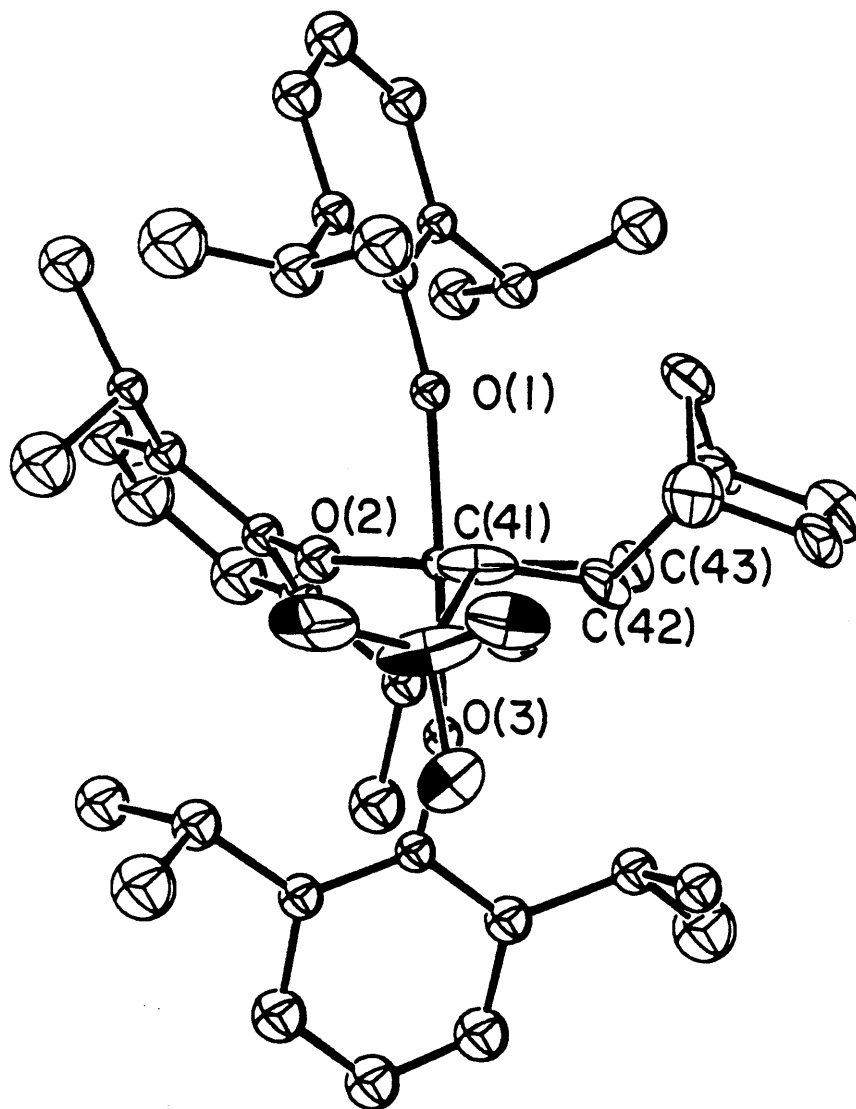


**Table II.** Selected Bond distances (Å) and Angles (°) in Complex **26**.<sup>a</sup>

Ta-O(1)	1.917(8)	O(2)-Ta-O(3)	87.5(3)
Ta-O(2)	1.904(9)	C(41)-Ta-O(1)	89.2(5)
Ta-O(3)	1.909(8)	C(41)-Ta-O(2)	136.1(5)
Ta-C(41)	2.138(14)	C(41)-Ta-O(3)	93.1(5)
Ta...C(42)	2.382(16)	C(43)-Ta-O(1)	95.3(4)
Ta-C(43)	2.144(13)	C(43)-Ta-O(2)	145.1(6)
C(41)-C(42)	1.546(22)	C(43)-Ta-O(3)	88.9(4)
C(42)-C(43)	1.553(21)	C(43)-Ta-C(41)	78.7(7)
Ta-C(41)-C(42)	78.8(9)	C(41)-C(42)-C(43)	122.4(13)
Ta-C(43)-C(42)	78.4(8)	Ta-O(1)-C(11)	161.0(8)
O(1)-Ta-O(2)	88.1(3)	Ta-O(2)-C(21)	159.3(8)
O(1)-Ta-O(3)	175.5(3)	Ta-O(3)-C(31)	163.7(7)

<sup>a</sup> Complex **26**: Ta[CH(C<sub>5</sub>H<sub>8</sub>)CHCH(CMe<sub>3</sub>)](DIPP)<sub>3</sub>.



puckered according to the dihedral angle of  $15.5^\circ$  (cf.  $25.2^\circ$  in the disubstituted tantalacycle  $\text{Ta}[\text{CH}(\text{Ph})\text{CH}(\text{CMe}_3)\text{CH}_2](\text{DIPP})_3$  (**15**).

**Polymerization of NBE with  $\text{Ta}[\text{CH}(\text{C}_5\text{H}_8)\text{CHCH}(\text{CMe}_3)](\text{DIPP})_3$  (**26**): General Considerations, Kinetic Experiments, and Isolation of Intermediate Complexes.**

Unlike the alkylidene complex **2**, base-free **26** will polymerize NBE in a controlled fashion. The reaction is very slow at  $25^\circ$ , but when solutions of complex **26** and excess NBE are heated to elevated temperatures (generally  $45$ - $65^\circ$ ) polymerization occurs readily. For example, when **26** was combined with excess NBE in  $\text{C}_6\text{D}_6$  at  $25^\circ$ , subsequent heating of the solution resulted in a complete consumption of NBE and the starting complex **26**, and new resonances characteristic of polynorbornene ( $\sim 55\%$  *trans*) and the propagating tantalacycle  $\text{Ta}[\text{CH}(\text{C}_5\text{H}_8)\text{CHCH}(\text{P})](\text{DIPP})_3$  (**27**; P = polymer) were observed (equation 3; Figure 3). (Isolation of the intermediate complexes **28** and **29**, shown in equation 3, is discussed later in the text.) The propagating catalyst **27** displays resonances for  $\text{H}_1$  and  $\text{H}_2$  at  $5.22$  (d) and  $3.85$

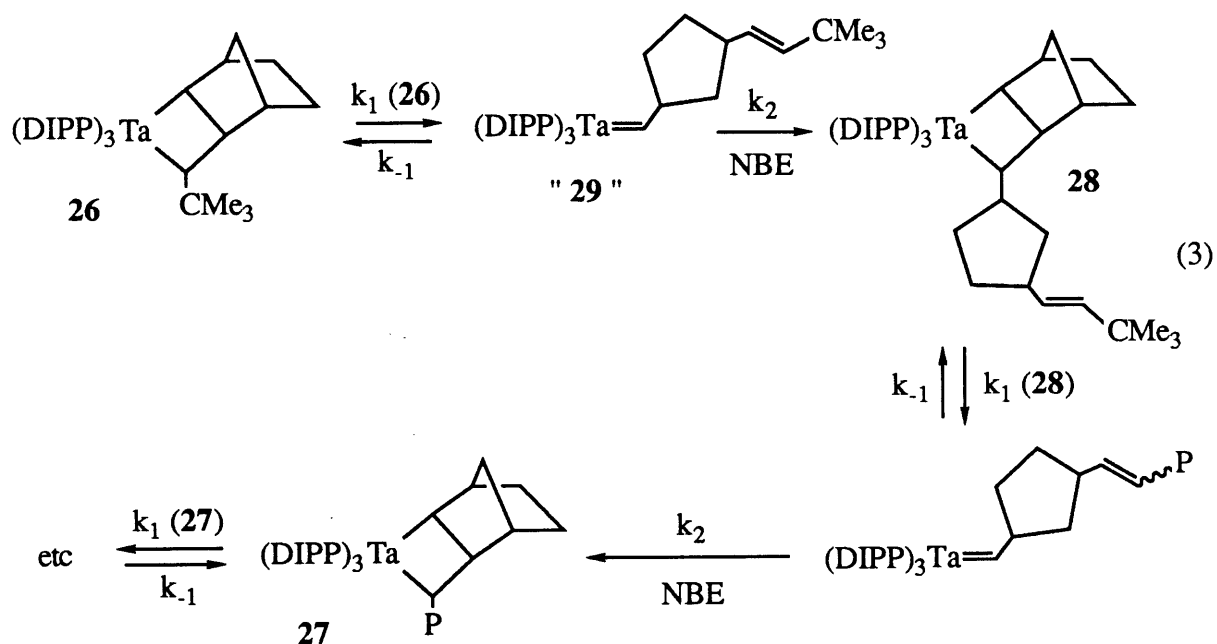
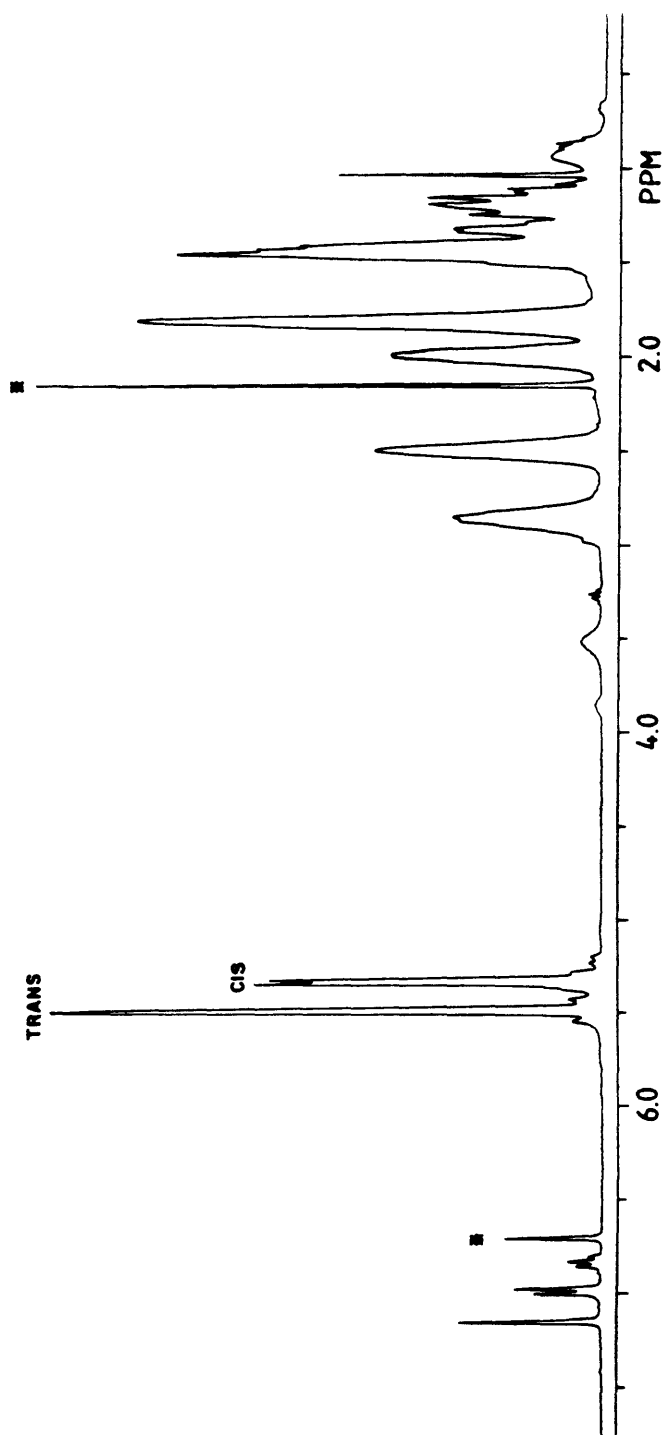


**Figure 3.** The  $^1\text{H}$  NMR spectrum of  $\text{Ta}[\text{CH}(\text{C}_5\text{H}_8)\text{CHCH}(\text{P})](\text{DIPP})_3$  (**27**) in  $\text{C}_6\text{D}_6$  at  $50^\circ$  (\* = mesitylene).



ppm (broad), while the upfield H<sub>3</sub> resonance is obstructed by other catalyst and polymer resonances in this region (Table I); no resonances indicative of an alkylidene complex were observed.

The polymerization reaction can be essentially stopped by cooling the reaction mixture (from 50° to 25°), and on reheating to 50° the polymerization resumes with the same rate as before (kinetics are described below). Furthermore, the reaction can be taken to completion with no sign of degradation of the catalyst. At 25°, in the absence of NBE complex **27** decomposes 5-10% after 24 hours, but in the presence of NBE the system shows no signs of decomposition in the same time period. The polymer in **27** (initially ~55% *trans*) slowly increases in the *trans* content over a period of days at 25° (~65% *trans* content was observed after 5 days at 25° in C<sub>6</sub>D<sub>6</sub>), indicating that secondary metathesis of the double bonds in the chain occurs to some extent. The isomerization to *trans* polymer is consistent with this isomer being the thermodynamically favored one (an equilibrium mixture is expected to give ~5% *cis* and ~95% *trans* polynorbornene at 25°<sup>84</sup>).

The rate of reaction of NBE with **27** was studied by <sup>1</sup>H NMR spectroscopy (samples in C<sub>6</sub>D<sub>6</sub>), by monitoring the consumption of NBE with time. From these studies, the reaction was found to be first order in catalyst and zero order in NBE throughout most of the reaction, consistent with rate limiting ring-opening of tantalacyclobutane complexes, to give intermediate alkylidene complexes that are rapidly trapped by NBE (as shown in equation 3). Loss of NBE from a metallacycle (k<sub>2</sub>) is considered highly unlikely relative to productive metathesis (k<sub>1</sub>), since the former generates a strained NBE monomer while the latter relieves the strain from a bicyclic system.<sup>84</sup> By applying the steady-state approximation to the intermediate alkylidene species of this reaction, the rate of consumption of NBE with time (or the formation of polymer with time, assuming no other NBE consuming processes present) can be described as is given in equation 4.

If k<sub>2</sub>[NBE] is much greater than k<sub>1</sub>, the reaction should be first order only in catalyst complex. Since the catalyst concentration is constant, a plot of [NBE] versus time would then

give a line with  $k_1[\text{Ta}]$  as the slope. A typical kinetic plot of this type is shown in Figure 4 (all

$$\begin{aligned} \frac{-d[\text{NBE}]}{dt} &= \frac{k_1 k_2 [\text{Ta}] [\text{NBE}]}{k_{-1} + k_2 [\text{NBE}]} \\ &= k_1 [\text{Ta}] && k_2 [\text{NBE}] \gg k_{-1} \\ &= (k_1 k_2 / k_{-1}) [\text{Ta}] [\text{NBE}] && k_2 [\text{NBE}] \ll k_{-1} \end{aligned} \quad (4)$$

kinetic data are given in Table III). As can be seen, once all of the starting complex **26** has been consumed, a linear consumption of NBE is observed except at the very end of the run. In this final region since the NBE concentration is very low,  $k_2[\text{NBE}] \gg k_{-1}$  is no longer valid, and the reaction becomes dependent on both the catalyst and NBE concentrations. If the point is reached where  $k_{-1} \gg k_2[\text{NBE}]$ , then a plot of  $\ln[\text{NBE}]$  versus time should give  $K[\text{Ta}]$  ( $K = k_1 k_2 / k_{-1}$ ) as the slope of the line. At  $57^\circ$  such a plot for the reaction of **27** with low concentrations of NBE did give a straight line. From this plot (which yielded  $k_1 k_2 / k_{-1}$ ) and the related first order plot at  $57^\circ$  (which yielded  $k_1$ ), the  $k_2 / k_{-1}$  ratio at this temperature was determined to be  $\sim 150 \text{ M}^{-1}$ . Activation parameters were determined for the reaction of **27** with NBE between  $35.2$  and  $64.6^\circ$ , for the region in which  $k_2[\text{NBE}] \gg k_{-1}$  was valid. An Arrhenius plot of  $\ln(k_1(\mathbf{27}))$  versus  $1/T$  ( $R = .997$ ) gave  $\Delta H^\ddagger = 24.0$  (0.9) kcal/mole,  $\Delta S^\ddagger = 4.8$  (2.8) e.u., and  $\Delta G^\ddagger_{338} = 22.4$  (1.3) kcal/mole. These values are similar to those obtained by Grubbs for the polymerization of NBE by  $\text{Ti}[\text{CH}(\text{C}_5\text{H}_8)\text{CHCH}(\text{R})]\text{Cp}_2$  ( $\Delta H^\ddagger = 27.1$  (0.5) kcal/mole,  $\Delta S^\ddagger = 9$  (4) e.u., and  $\Delta G^\ddagger_{338} = 24$  (1) kcal/mole); in that system the rate limiting step of NBE polymerization was also ring-opening of metallacycles. (Note:  $k_1$  is actually the average of two rate constants, one for ring-opening of *cis* metallacycles and one for ring-opening of *trans* metallacycles).

As mentioned above, plots of  $[\text{NBE}]$  versus time yield straight lines *after* all of the starting complex **26** has been consumed. Before all of **26** is consumed the slope is slightly less (Figure 4), suggesting that **26** ring-opens at a slower rate than does **27**. By monitoring the

Figure 4. A plot of the consumption of 20 equivalents of NBE by 26 (and 27) at 50° in C<sub>6</sub>D<sub>6</sub>.

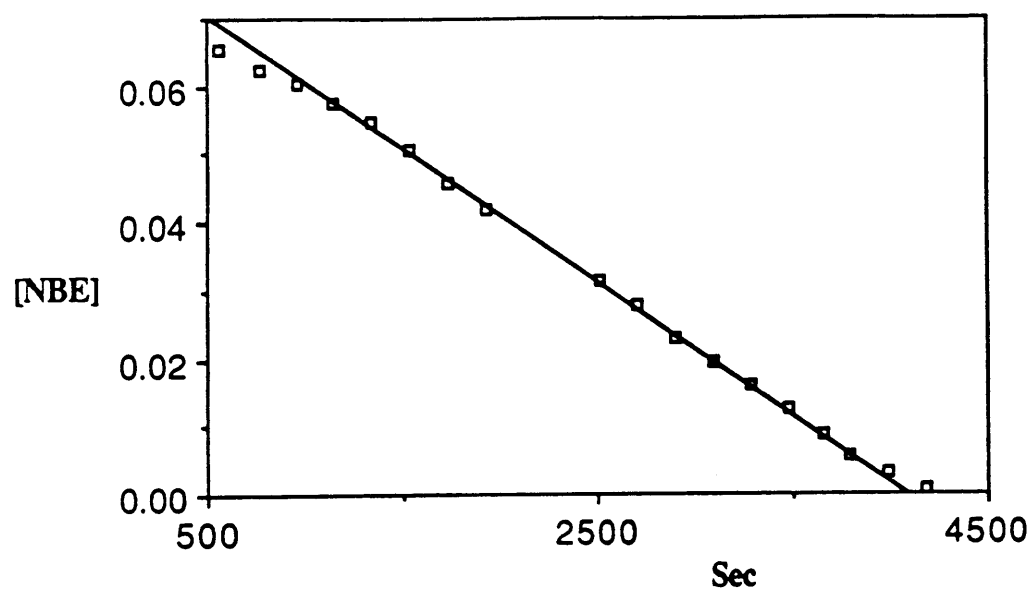


**Table III.** Kinetic Data for the Polymerization of NBE by **26** and **7**.

Catalyst	[Ta] (mM)	[NBE] <sub>0</sub> (mM)	T (K)	k x 10 <sup>3</sup>
<b>26</b>	10.9	111	308.4	0.64 s <sup>-1</sup>
<b>26</b>	5.59	80	317.9	2.0 s <sup>-1</sup>
<b>26</b>	5.59	55	323.3	3.5 s <sup>-1</sup>
<b>26</b>	6.84	183	323.3	3.9 s <sup>-1</sup>
<b>26</b>	7.98	189	323.3	3.9 s <sup>-1</sup>
<b>26</b>	2.91	46	323.3	3.8 s <sup>-1</sup>
<b>26</b>	5.59	45	330.0	7.1 s <sup>-1</sup>
<b>26</b>	5.70	177	330.0	7.6 s <sup>-1</sup>
<b>26</b>	9.32	87	333.1	12 s <sup>-1</sup>
<b>26</b>	5.59	200	337.8	23 s <sup>-1</sup>
<b>7</b>	9.08	166	313.0	48 M <sup>-1</sup> s <sup>-1</sup>
<b>7</b>	9.08	134	322.2	80 M <sup>-1</sup> s <sup>-1</sup>
<b>7</b>	17.8	199	322.4	94 M <sup>-1</sup> s <sup>-1</sup>
<b>7</b>	18.1	122	323.1	79 M <sup>-1</sup> s <sup>-1</sup>
<b>7a</b>	19.3	272	323.0	0.2 M <sup>-1</sup> s <sup>-1</sup>

<sup>a</sup> Polymerization carried out in the presence of 3 eq of pyridine and monitored over ~1 half life.

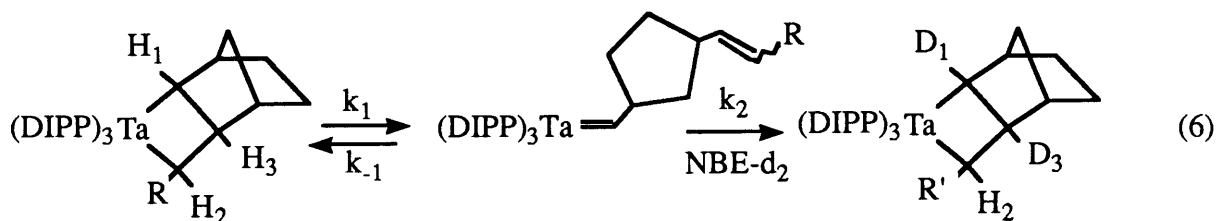
disappearance of the  $\alpha$  proton of **26** at 3.88 ppm ( $H_2$ ) in reaction with excess NBE, the rate of ring-opening of this initial metallacycle at 35.0° was obtained (equation 5). A plot of

$$\frac{-d[\mathbf{26}]}{dt} = k_1[\mathbf{26}] \quad (5)$$

$\ln[\mathbf{26}]$  versus time gave  $k_1(\mathbf{26}) = 3.9 \times 10^{-4} \text{ s}^{-1}$ . This compares with  $k_1 = 6.34 \times 10^{-4} \text{ s}^{-1}$  at 35.2° for the propagating tantalacycle **27**. The slightly slower rate of ring-opening observed for **26** might be due to the (on average) less crowded environment around the metal center in this complex, since the ring substituents are *trans* in **26** but ~45% *cis* in **27**.<sup>91</sup> Fortunately the effect of this difference, between initiation and propagation, is negligible on the polydispersities of polymers prepared from **26** (monodisperse polymers can be obtained, as described later).

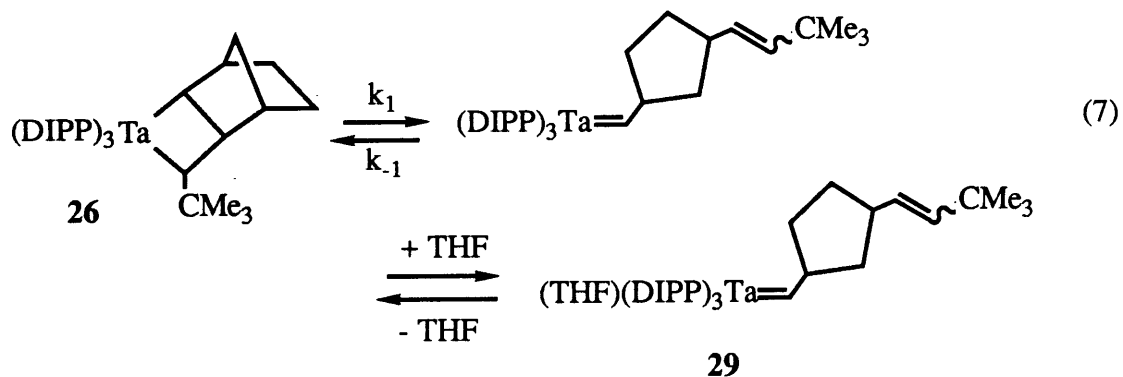
Providing further evidence for the polymerization mechanism shown in equation 3, the "intermediate" second insertion metallacycle **28**,  $\text{Ta}[\text{CH}(\text{C}_5\text{H}_8)\text{CHCH}(\text{CHC}_5\text{H}_8\text{CHCHCMe}_3)](\text{DIPP})_3$ , was prepared by reaction of complex **26** with one equivalent of NBE in toluene at 60°. Complex **28**, *extremely* soluble in common organic solvents, can be isolated as a white precipitate from concentrated solutions in pentane. The  $^1\text{H}$  NMR spectrum of **28** in  $\text{C}_6\text{D}_6$  at 25° displays broad resonances for the DIPP ligands but relatively sharp signals for the  $\alpha$  protons of the ring ( $H_1$ : 5.23 ppm, d,  $J_{\text{HH}} = 9.1 \text{ Hz}$ ;  $H_2$ : 3.85 ppm, ~t,  $J_{\text{HH}} = 8.6 \text{ Hz}$ ; Table I); the  $\beta$  proton resonance is obstructed by other upfield resonances. The rate of ring-opening of **28** can be determined by monitoring the disappearance of the  $\alpha$  proton of **28** at 5.23 ppm ( $H_1$ ) when **28** is reacted with NBE-2,3- $\text{d}_2$ . With regular NBE, the disappearance of  $H_1$  or  $H_2$  cannot be monitored as **27** grows in, since **27** also displays resonances in these areas. The deuteration of the ring site at  $H_1$  was chosen because this site is deuterated completely by reaction of **28** with one equivalent of NBE-2,3- $\text{d}_2$  (equation 6), and therefore the rate of this deuteration is representative of the rate of

ring-opening for **28**; the site at H<sub>2</sub> requires two equivalents of NBE-2,3-d<sub>2</sub> for deuteration.



A plot of  $\ln[\mathbf{28}]$  versus time gave  $k_1(\mathbf{28}) = 9.8 \times 10^{-4} \text{ s}^{-1}$  at 35.0° (cf.  $k_1$  for **26** at 35.0° =  $3.9 \times 10^{-4} \text{ s}^{-1}$  and  $k_1$  for **27** at 35.2° =  $6.34 \times 10^{-4} \text{ s}^{-1}$ ). Why **28** reacts faster with NBE than does the propagating metallacycle **27** is not altogether clear. The stereochemistry of the ring substituents may be an important factor, but unfortunately little information can be obtained by examination of the <sup>1</sup>H NMR spectrum, and crystals suitable for X-ray crystallography could not be obtained.

Although alkylidene complexes are not observed during polymerization of NBE by **27**, the alkylidene compound Ta(CHC<sub>5</sub>H<sub>8</sub>CHCHCMe<sub>3</sub>)(DIPP)<sub>3</sub>(THF) (**29**) does form when Ta[CH(C<sub>5</sub>H<sub>8</sub>)CHCH(CMe<sub>3</sub>)](DIPP)<sub>3</sub> (**26**) is heated in THF-d<sub>8</sub> (<sup>1</sup>H NMR  $\delta$  7.69 (d,  $J_{\text{HH}} = 8.6 \text{ Hz}$ , H <sub>$\alpha$</sub> ), 4.54 (multiplet, H <sub>$\beta$</sub> )). Complex **29** forms *slowly* from **26** in THF-d<sub>8</sub> (65°), with the rate limiting step qualitatively appearing to involve ring-opening of **26**, followed by trapping of the alkylidene intermediate with THF (equation 7). Recall earlier examples in

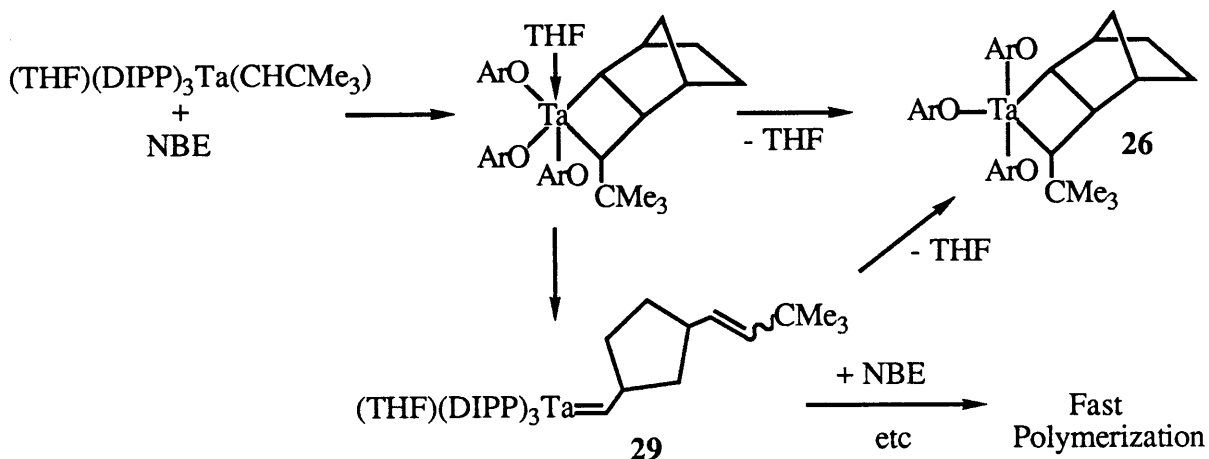




chapter 1 with less substituted metallacycles for which reaction with THF appeared to occur *before* ring-opening of the metallacyclobutane complexes. The highly soluble alkylidene **29** can be isolated in small amounts from pentane as a yellow precipitate. However, complex **29** is only stable in THF, and in other solvents such as ether, pentane, or C<sub>6</sub>D<sub>6</sub> **29** loses THF and reforms the metallacycle **26**. That the substrate olefin in this reverse reaction is attached to the alkylidene ligand probably facilitates reformation of the tantalacyclobutane **26**.

Interestingly, when Ta[CH(C<sub>5</sub>H<sub>8</sub>)CHCH(CMe<sub>3</sub>)](DIPP)<sub>3</sub> (**26**) is reacted with NBE at elevated temperatures in the presence of excess THF, the rate is not affected. Neither is formation of **29** observed, consistent with NBE serving as a better trap than THF for the base-free intermediate alkylidene (i.e.  $k_2[\text{NBE}] > k_2[\text{THF}]$ ). Earlier, however, THF was mentioned as a complicating factor in the polymerization of NBE by Ta(CHCMe<sub>3</sub>)(DIPP)<sub>3</sub>(THF) (**2**). Complex **2** reacts very rapidly with NBE in room temperature solution, and the polynorbornene obtained from this reaction displays a high molecular weight and very broad dispersity: 200 equivalents consumed yields a polymer with  $M_n = 146,000$  and  $d = 4.41$ ; a low molecular weight tail was also evident (GPC analysis of polynorbornene prepared from complex **27** is described in the next section).

Formation of an initial THF adduct metallacycle on reaction of **2** with one equivalent of NBE, *without* dissociation of THF from complex **2**, is thought to lead to the high polymer observed (Scheme I). Once this complex has formed, ring-opening to the subsequent alkylidene **29** should occur very rapidly (recall that the only example of a stable base adduct tantalacyclobutane complex, Ta(CH<sub>2</sub>CH<sub>2</sub>CH<sub>2</sub>)(DIPP)<sub>3</sub>(py), contains an unsubstituted ring). The generated alkylidene complex **29** could then further react with NBE to give another base adduct metallacycle, which again is expected to rapidly ring-open. The final result from all this would be high polymer formation. Summarized, the presence of bound THF is thought to accelerate the polymerization reaction by aiding in ring-opening of metallacycles and not seriously hindering reaction of THF bound alkylidenes with NBE (in chapter 1 Ta(CHCMe<sub>3</sub>)(DIPP)<sub>3</sub>(THF) (**2**) was shown to react rapidly with a variety of olefins).

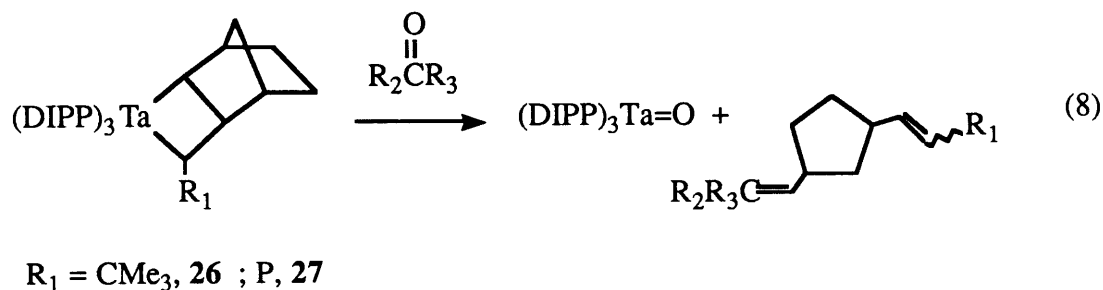
Scheme I: Possible Reaction Pathways in the Polymerization of NBE by **2**.

During this polymerization reaction, loss of THF from THF adduct alkylidenes or metallacycles would give the base-free tantalacyclobutane complex **27** or **26** (recall that THF loss from the alkylidene **29** occurred readily in solvents other than THF). Such a base loss should be considered a deactivation reaction, since **27** does not readily polymerize NBE in room temperature solution. Besides, if any reaction *did* occur, **27** should react with NBE preferentially, as noted earlier for NBE polymerization by **27** in the presence of THF. The tremendous polydispersity (4.41) and long low molecular weight tail of the polymer formed from **2** are consistent with such deactivation reactions, which should occur increasingly as the NBE concentration is lowered by polymerization.

#### Wittig Reactivity of Complexes **26** and **27**, and GPC analysis of the resulting Polynorbornene (from **27**).

The behavior of  $\text{Ta}[\text{CH}(\text{C}_5\text{H}_8)\text{CHCH}(\text{CMe}_3)](\text{DIPP})_3$  (**26**) when reacted with organic carbonyls is analogous to that seen for the disubstituted tantalacyclobutane complex **15** (i.e. only Wittig products are observed; equation 8). Reaction of **26** with 3 equivalents of

benzaldehyde in  $C_6D_6$  at  $50^\circ$  is essentially complete in 30 minutes, and the resulting organic



Wittig product is a mixture of *trans* and *cis* isomers (about the phenyl capped olefin group, *trans/cis* ratio = 2.7/1.0 based on spin simulation experiments performed with complex  $\mathbf{27}$ ). The geometry at the t-butyl end is thought to be all *trans*,<sup>91</sup> but could not be confirmed by NMR experiments. As with the starting complex  $\mathbf{26}$ , the propagating complex  $\mathbf{27}$  reacts with benzaldehyde to give all Wittig products (equation 8). When  $\mathbf{27}$  was reacted with three equivalents of benzaldehyde in  $C_6D_6$  at  $65^\circ$ , cleavage of the polymer chain yielding the capped polynorbornene  $PhCH(CHC_5H_8CH)_xCHCMe_3$  was complete in  $\sim 20$  minutes. The phenyl capped olefin group generated in this reaction is obtained as a mixture of isomers (2.1:1.0 *trans:cis* ratio), as evidenced by spin simulation experiments performed with the resulting capped polymers (details are given in the Experimental Section). The polymer chain in  $\mathbf{27}$  can also be cleaved with benzophenone or acetone. When complex  $\mathbf{27}$  is heated with benzophenone, a  $^1H$  NMR spectrum ( $C_6D_6$ ,  $25^\circ$ ) of the products reveals no resonances from the uncapped complex  $\mathbf{27}$  but does show a new doublet at  $\sim 6.0$  ppm, assigned to the new olefinic proton of the expected cleavage product,  $(Ph)_2C=CHC_5H_8CH=CH(P)$  (P = polymer). In the related titanacyclobutane system, this resonance was observed as a doublet at 5.95 ppm in  $CD_2Cl_2$ .<sup>92</sup>

Thus polynorbornene samples can be prepared straightforwardly by polymerization of a given number of NBE equivalents (with addition of NBE at  $-30^\circ$  and reaction at elevated temperature) and subsequent capping with an organic carbonyl such as benzaldehyde or

benzophenone (after all NBE has been consumed); toluene is generally employed as the solvent. The polynorbornene is obtained, after precipitation with methanol, as a white solid. The results of GPC analysis of polynorbornenes prepared from **26** are summarized in Table IV (as are all GPC results). The molecular weights reported are relative to polystyrene standards. At the present time absolute correction factors for polynorbornene relative to polystyrene have not been documented, although in previous reports division by two has been suggested for approximate correction.<sup>93,94</sup> As can be seen in Table IV, the results are somewhat consistent with this correction guideline (a representative GPC trace is shown in Figure 5a). Most importantly, however, the molecular weights of the polymer samples are seen to increase proportionally with the number of monomer equivalents employed, indicative of a system in which chain termination is absent (polymer samples from 100, 200, and 500 equivalents of NBE gave  $M_n = 22,000$ ,  $48,000$ , and  $127,000$ , respectively).

Secondary metathesis of olefins in the polymer chain is thought to occur in  $\text{Ta}[\text{CH}(\text{C}_5\text{H}_8)\text{CHCH}(\text{P})](\text{DIPP})_3$  (**27**), and this is evidenced in the GPC chromatograms by the larger than expected polydispersities observed ( $d = 1.63$ - $1.73$ ; cf. polynorbornene from Grubbs catalyst:  $d = 1.08$ - $1.25$ ). If a sample is heated for several hours after all of the monomer has been consumed, a very large polydispersity is observed ( $d = 1.95$ ). Actually, secondary metathesis should be *expected* in this system, since an active base-free four coordinate alkylidene intermediate is accessible at the reaction temperature (by ring-opening of the metallacyclobutane). Such a complex should show a high degree of reactivity with the ordinary olefins of the polymer chain, just as related phenoxide alkylidenes were shown to react readily with ordinary olefins in chapter 1. At lower temperatures, where such an intermediate is not as accessible and significant polymerization is not observed, secondary metathesis reactions should be much slower, consistent with the slow *cis* to *trans* isomerization observed at  $25^\circ$ . The secondary metathesis observed in these reactions occurs only *after* all of the NBE monomer has been consumed. When the polymerization of 200 equivalents of NBE

**Table IV.** The Results of GPC Analysis of Polynorbornenes.

Run	Catalyst	Equiv. NBE	$M_n$ (uncorr) <sup>e</sup>	$M_w/M_n$
1	26	100	22,000	1.63
2	26	200	48,000	1.66
3	26	500	127,000	1.73
4a,b	26	200	32,100	1.04
5 <sup>d</sup>	26	150	31,500	1.95
6	6	50	13,200	1.08
7	6	100	26,200	1.09
8	6	200	58,800	1.10
9	7	95	18,800	1.07
10	30	100	10,700	2.71
11	2	200	146,000	4.41
12 <sup>c</sup>	6	200	59,100	1.05
13 <sup>c</sup>	6	200	57,600	1.07

a The reaction was taken to ~75% completion.

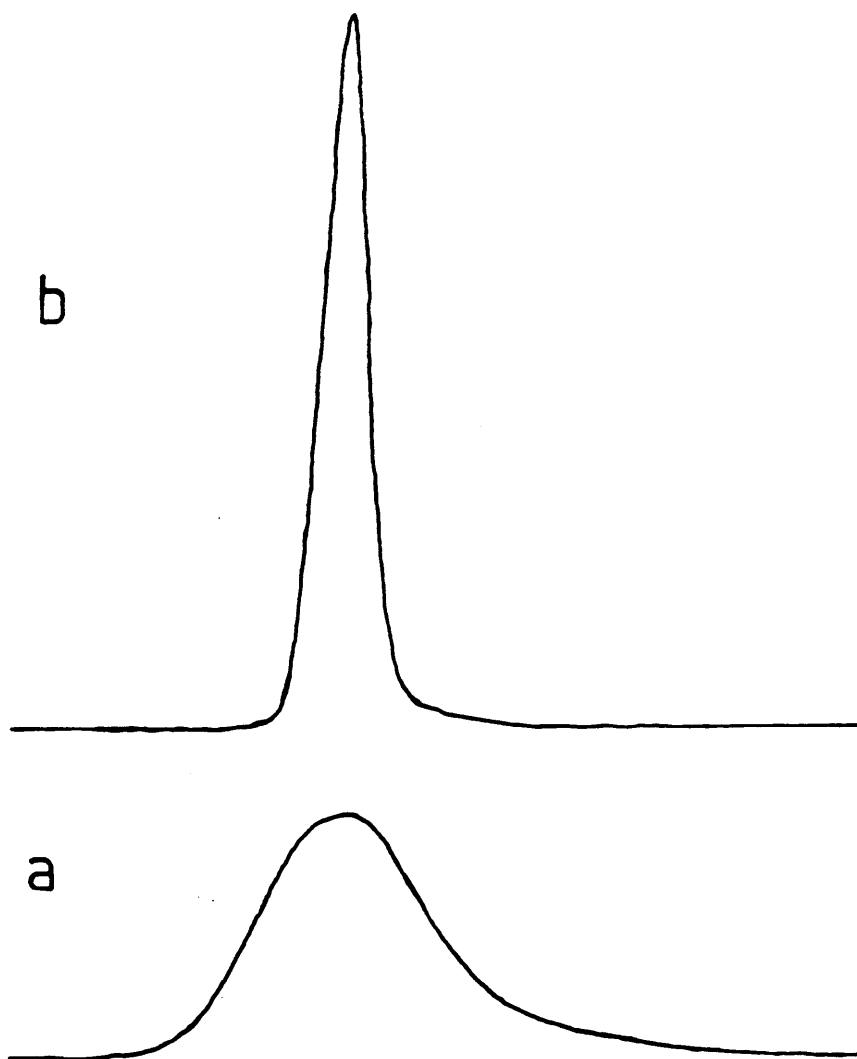
b A small fraction with a relatively high molecular weight could be resolved as a separate peak in this GPC trace (~6%).

c A sample for run 12 was taken after 20 minutes, at which time the polymerization was complete; a sample for run 13 was taken from the same reaction after 55 minutes.

d The reaction was heated at the polymerization temperature for several extra hours after all of the NBE had been consumed.

e Refractive index detection.

**Figure 5.** GPC traces for the benzylidene-capped polynorbornene produced by adding 100 eq of NBE to (a) **26** ( $d = 1.63$ ) and (b) **6** ( $d = 1.09$ ).



was stopped at ~75% completion, the dispersity of the resulting polymer (1.04) was that expected from a living polymerization, with no secondary metathesis.

Although the presence of THF severely limits control over polymerization of NBE by the DIPP complex **2**, the isolation of a base-free tantalacyclobutane complex, **26**, circumvents this problem. All of the results presented here strongly suggest that the reaction of complex **26** with NBE constitutes a living polymerization. Most notably, the molecular weights of the polymers are observed to increase linearly with the number of monomer equivalents employed, and monodisperse polymers can be isolated when the reaction is not taken beyond completion. The mode of reactivity has also been examined and shown to involve propagating metallacyclobutanes, based on X-ray characterization of the initiating complex **26**, isolation of the intermediate metallacyclobutane and alkylidene complexes **28** and **29**, respectively, and kinetic studies performed with the metallacyclobutane complexes **26**, **27**, and **28**. Complexes supported with DMP ligation were found to display some interesting differences in polymerization activity.

#### **Polymerization of NBE with Ta[CH(C<sub>5</sub>H<sub>8</sub>)CHCH(CMe<sub>3</sub>)](DMP)<sub>3</sub> (**30**).**

Ta(CH<sup>t</sup>Bu)(DMP)<sub>3</sub>(THF), **4**, reacts with one equivalent of NBE at -30° to give the trisubstituted tantalacyclobutane complex Ta[CH(C<sub>5</sub>H<sub>8</sub>)CH(CMe<sub>3</sub>)](DMP)<sub>3</sub>, **30**. The reaction is most successful when the reactants are present in low concentration. Complex **30**, *extremely* soluble in common organic solvents, can be isolated as a light yellow microcrystalline precipitate from pentane at -30° after several days (highest yields are obtained by allowing precipitation over a period of weeks). Unlike its DIPP counterpart, the <sup>1</sup>H NMR spectrum of **30** (Table I, Figure 1b) displays resonances for one averaged DMP ligand, suggesting facile exchange of the DMP ligands in this less crowded complex. The ring proton resonances, distinguished through decoupling experiments, were seen at 5.21 (H<sub>1</sub>), 3.72 (H<sub>2</sub>), and 0.84 ppm (H<sub>3</sub>) (H's as shown in equation 2 for the DIPP complex **26**). The stereochemistry about the MC<sub>3</sub> ring is not apparent from J<sub>HH</sub> values, but is thought to be *trans* based on

spectroscopic similarities with complex **26**. A  $^{13}\text{C}$  NMR spectrum was also obtained, displaying clear resonances for all carbon atoms of the molecule (Table I).

The formation of complex **30** from **4** and NBE contrasts sharply with the result obtained when **4** was combined with ethylene (no products were isolated; see chapter 1). Apparently the DMP ligands are not large enough to stabilize an unsubstituted tantalacyclobutane, but can stabilize a trisubstituted tantalacycle in which the ring substituents impose additional steric saturation. In general, DMP tantalacyclobutane and alkylidene complexes are thought to be more sensitive to intra- and intermolecular decomposition reactions (chapter 1). The concentration effect observed in the preparation of complex **30** is consistent with an increase in sensitivity to intermolecular decomposition (in the preparation of the DIPP tantalacycle **26** such a concentration dependence was not obvious).

Upon heating complex **30** with excess NBE in  $\text{C}_6\text{D}_6$ , polynorbornene is formed ( $\sim 53\%$  *trans* at  $45^\circ$ ), and new resonances indicative of the propagating metallacyclobutane  $\text{Ta}[\text{CH}(\text{C}_5\text{H}_8)\text{CHCH}(\text{P})](\text{DMP})_3$  (**31**) can be observed in the  $^1\text{H}$  NMR spectrum (Table I); the initial catalyst **30** is consumed within 5 equivalents of NBE, and no resonances indicative of an alkylidene complex are observed. When the polymerization of NBE by **31** (in  $\text{C}_6\text{D}_6$ ) was taken to completion and the solution left at the reaction temperature, no signs of catalyst degradation were seen in the  $^1\text{H}$  NMR spectrum when checked after 40 minutes. At  $25^\circ$ , solutions of **31** in  $\text{C}_6\text{D}_6$  showed no *obvious* signs of decomposition of the catalyst in the absence of NBE after several days (although the polymer isomerizes to  $\sim 70\%$  *trans*).

The rate of reaction of **31** with excess NBE was found to be, under certain conditions, comparable to that seen for **27**.<sup>95</sup> However, least squares analysis of kinetic plots ( $[\text{NBE}]$  versus time) did not always give acceptable R values, and over a period of several half lives a significant deviation from linearity was seen (i.e. as NBE was consumed the rate slowed), suggesting the reaction was not completely zero order in  $[\text{NBE}]$ . Plots of  $\ln[\text{NBE}]$  versus time, though, also did not consistently result in reasonable lines. Additionally, the values for  $k_1$  (obtained from  $[\text{NBE}]$  versus time, with the slope =  $k_1[\text{Ta}]$ ) increased as the catalyst

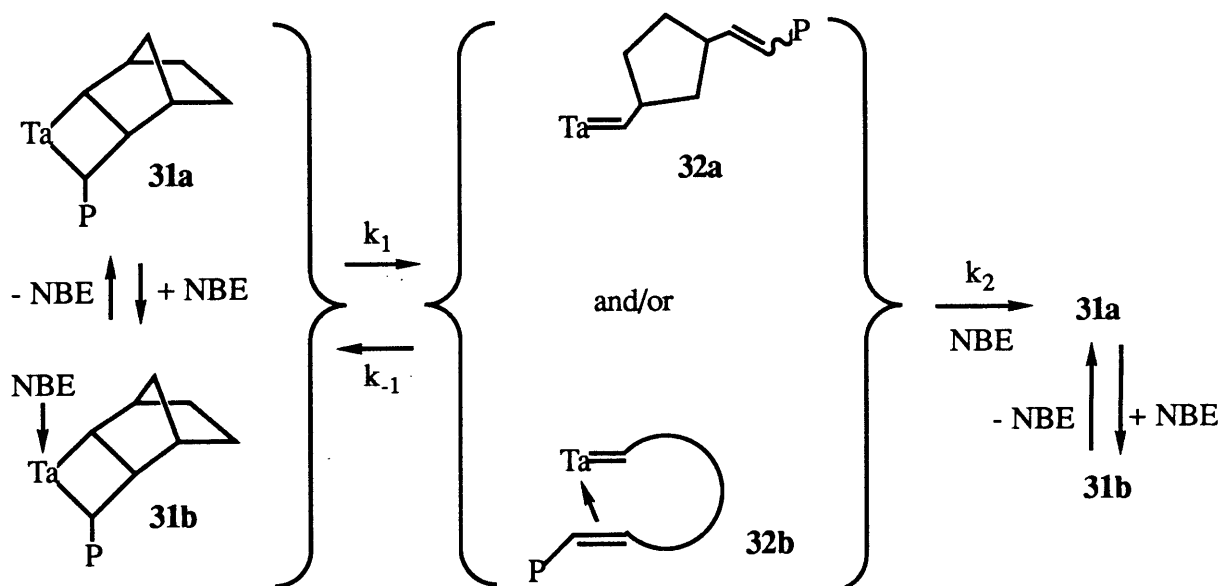


concentration was raised (at a set temperature), again indicating some kind of bimolecular interaction involved in the reaction. GPC analysis of polymers obtained from this system displayed very broad polydispersities (e.g. 100 equivalents polymerized gave a polymer with  $M_n = 10,700$  and  $d = 2.71$ ; Table IV). The kinetic data and GPC results together suggest that more than one type of polymerization mechanism is operative; secondary metathesis is also likely considering the noted isomerization at  $25^\circ$ .

Considering the less sterically demanding DMP ligands present in this system, coordination of NBE or olefins of the polymer chain to intermediate metallacyclobutane and alkylidene complexes might give rise to additional catalytic species during NBE polymerization. Some possible participating species are shown in Scheme II. Evidence for coordination related to that shown in **32b** has been documented in the literature,

Scheme II: Possible Catalyst Species Present in the Polymerization of NBE initiated by **30**.

(DMP ligands are omitted for clarity)



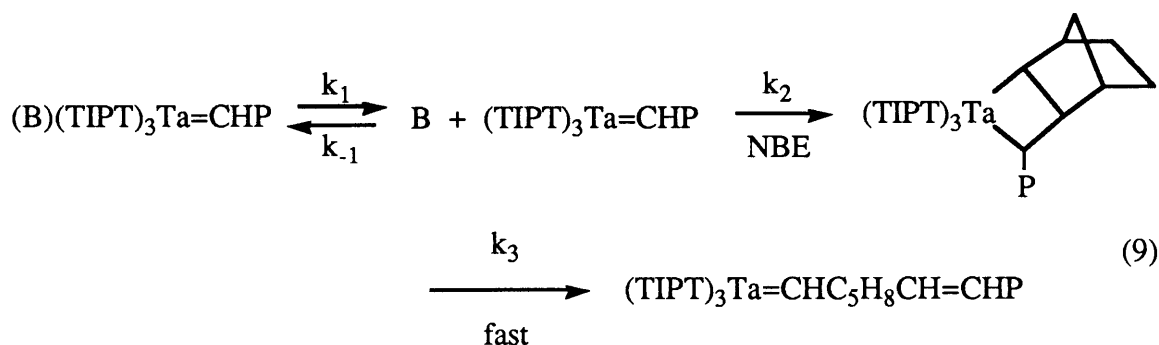
with the previously formed double bond in the polymer chain coordinated back to the metal.<sup>96-99</sup> Additionally, Osborn has recently suggested that related tungstenacyclobutane complexes might react with NBE *before* cleavage to subsequent carbene complexes,<sup>62</sup> thus implying formation of complexes analogous to **31b**. Coordination by NBE or the polymer chain could affect the rate in an ill-defined manner, since the amount of coordinated complex should vary with the concentration of the reactants.

The activity of complex **30** with NBE demonstrates that the differing steric properties of DMP and DIPP ligands affect the course of reactivity with both ordinary olefins (chapter 1) and strained cyclic olefins (NBE) in a consequential manner. Switching from a phenoxide (DIPP, DMP) to a thiolate (TIPT) donor ligand also changes the course of polymerization activity - in TIPT complexes metallacycles are destabilized, and alkylidene complexes are observed exclusively as the propagating species in NBE polymerization.

#### **Polymerization of NBE with Ta(CHCMe<sub>3</sub>)(TIPT)<sub>3</sub>(B) Complexes.**

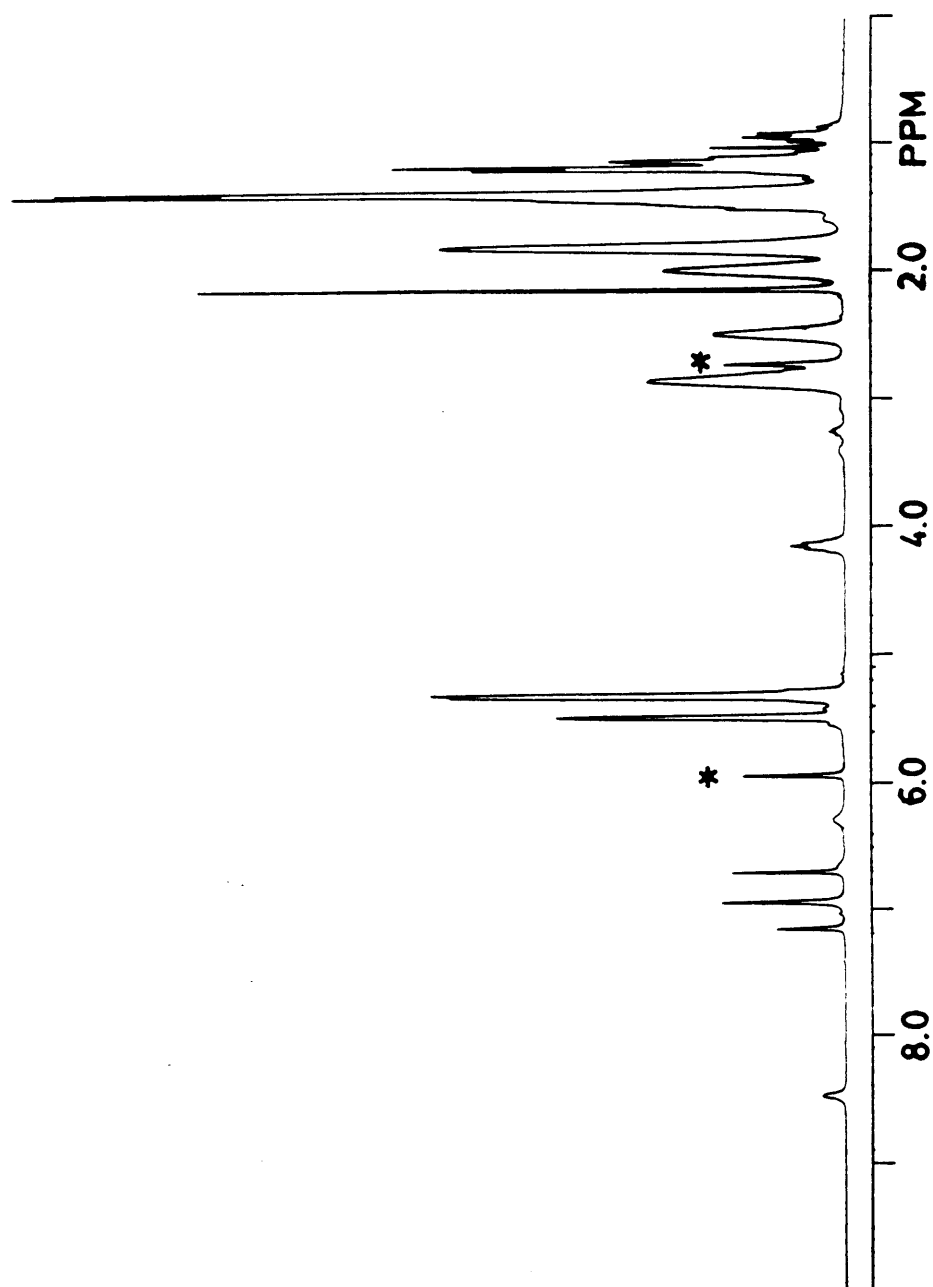
As discussed in chapter 1, the arylthiolate alkylidene complex Ta(CHCMe<sub>3</sub>)(TIPT)<sub>3</sub>(THF) (**6**) does not react with ordinary unstrained olefins such as *cis*-3-hexene or 2-pentenes. Complex **6**, however, does react rapidly with NBE at 25° in ether or toluene to give polynorbornene (~70% *cis*). When **6** was reacted with 10 equivalents of NBE in ether, after removal of the solvent *in vacuo* and redissolution in C<sub>6</sub>D<sub>6</sub>, the resulting <sup>1</sup>H NMR spectrum showed, in addition to signals indicative of polynorbornene, all of the initiating complex **6** consumed and signals for the new THF bound alkylidene complex Ta(CHC<sub>5</sub>H<sub>8</sub>CHCHP)(TIPT)<sub>3</sub>(THF) (**33**) (no resonances indicative of a metallacyclobutane complex were observed). The α proton resonance was not observed in the spectrum of **33**, just as the case was in spectra of the parent complex **6** and the related base adducts **8** (quinuclidine) and **9** (Et<sub>2</sub>S); in chapter 1 this was ascribed to an equilibrium between the base adduct complexes and a base-free complex (as evidenced by the rapid exchange of bound THF with free THF in solutions of complex **6**).

Interestingly, **6** does not react with NBE at 25° in THF (it does react slowly at elevated temperatures). This suggests that the activity of **6** and **33** depends on the accessibility of a reactive base-free intermediate (i.e. Ta(CHCMe<sub>3</sub>)(TIPT)<sub>3</sub>), which is not readily accessible from **6** in neat THF) (equation 9). Consistent with the proposed mechanism



shown in equation 9 is the lack of reactivity of the pyridine adduct Ta(CHCMe<sub>3</sub>)(TIPT)<sub>3</sub>(py) (**7**) with NBE at 25° in noncoordinating solvents (the <sup>1</sup>H NMR spectrum of **7** at 25° was described in chapter 1 as displaying broad resonances, indicative of a strongly bound pyridine ligand). At elevated temperatures a base-free intermediate is more accessible, and consequently **7** does react with excess NBE to produce polymer (~65 *cis*). In a typical spectrum (C<sub>6</sub>D<sub>6</sub>), as the α proton resonance of **7** disappears, new resonances for Ta(CHC<sub>5</sub>H<sub>8</sub>CHCHP)(TIPT)<sub>3</sub>(py), **34**, are seen to grow in, with complete consumption of **7** by 6 equivalents of NBE (Figure 6). Although a resonance for the α proton of **34** is not seen in the <sup>1</sup>H NMR spectrum, the α carbon resonance from **34** can be seen in the <sup>13</sup>C NMR spectrum in C<sub>6</sub>D<sub>6</sub> at 25° (249.3 ppm). Again no resonances indicative of a metallacyclobutane complex were observed, contrasting the previously described polymerization of NBE by Ta[CH(C<sub>5</sub>H<sub>8</sub>)CHCH(CMe<sub>3</sub>)](DIPP)<sub>3</sub> (**26**), in which tantalacyclobutane complexes served as the propagating species.

Figure 6. The  $^1\text{H}$  NMR spectrum of  $\text{Ta}(\text{CHC}_5\text{H}_8\text{CHCHP})(\text{TIPT})_3(\text{py})$  (**34**) in  $\text{C}_6\text{D}_6$  at  $50^\circ$  (\* = NBE; some mesitylene also present).



Considering the reaction mechanism given in equation 9, the rate of polymerization of NBE by **6** or **7** can be described as shown in equation 10. Of the three scenarios given, which

$$\frac{-d[\text{NBE}]}{dt} = \frac{k_1 k_2 [\text{Ta}][\text{NBE}]}{k_1 + k_{-1}[\text{B}]} = k_{\text{obs}}[\text{Ta}][\text{NBE}] \quad (10)$$

$$\begin{aligned} k_{\text{obs}} &= k_1 k_2 / (k_1 + k_{-1}[\text{B}]) & k_{-1}[\text{B}] &\approx k_1 \\ &= k_2 & k_{-1}[\text{B}] &\ll k_1 \\ &= k_1 k_2 / k_{-1}[\text{B}] & k_{-1}[\text{B}] &\gg k_1 \end{aligned}$$

[Ta] = Starting Catalyst Concentration (**6** or **7**)

[B] = Free Base (a constant at any given temperature)

applies is not known, since only averaged resonances are observed in the spectra of these complexes. When complexes **6**, **7**, **33**, and **34** are isolated from solution, a full equivalent of base is generally found to be present (by <sup>1</sup>H NMR resonance integrations from subsequently redissolved samples and/or elemental analysis), suggesting that  $k_1 \ll k_{-1}[\text{B}]$  might be most appropriate. In any case shown, however, the reaction should be first order in both catalyst and NBE.

Because the pyridine adduct **7** does not react readily with NBE in room temperature solution but does show reactivity at elevated temperatures, this complex was chosen for kinetic studies (these conditions make efficient mixing easy, as opposed to very low temperature mixing that would be required with the THF adduct **6**). When the rate of reaction of **34** with excess NBE was measured in C<sub>6</sub>D<sub>6</sub>, the reaction was found to be first order in both catalyst and monomer. From reactions at 39.8° and 49.0° (Table III), a plot of ln[NBE] versus time gave values of  $k_{\text{obs}} = 4.76 \times 10^{-2}$  and  $7.96 \times 10^{-2} \text{ M}^{-1}\text{s}^{-1}$ , respectively, from the slope of the lines ( $k_{\text{obs}}[\text{Ta}]$ ). Additionally, just as the THF adduct **6** displayed little reactivity with NBE in THF, the presence of 3 equivalents of pyridine was found to reduce the reaction rate of **34** with

NBE by a factor of  $\sim 400$  at  $50.0^\circ$  in  $C_6D_6$ . Since in these reactions the free base concentration ([B]) should remain constant only at a *given* temperature, no attempts were made to obtain activation parameters.

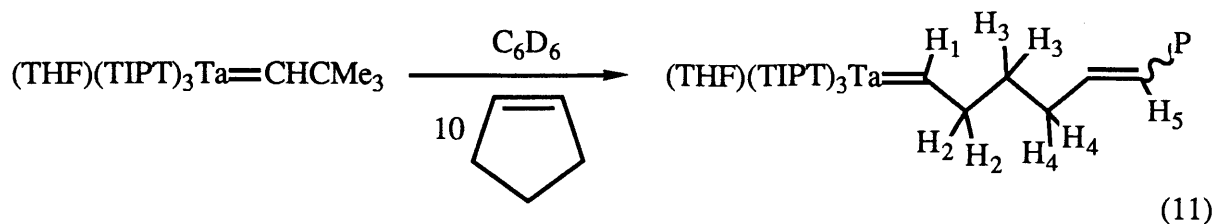
As in the DIPP and DMP systems, polynorbornene samples are readily obtained by reaction of the catalysts complexes (**6** and **7**) with a given number of NBE equivalents in toluene, followed by capping with benzaldehyde. Reaction of  $Ta(CHC_5H_8CH_2CH_2)(TIPT)_3(THF)$  **33** with 3 equivalents of benzaldehyde in  $C_6D_6$  at  $25^\circ$  resulted in a 90% yield of the cleaved polymer chain within 30 minutes. The capped polymer chains display new resonances in the  $^1H$  NMR spectrum between 6.0 and 6.5 ppm; the pattern seen is slightly different than that observed in the DIPP system, and based on spin simulation experiments (outlined in the Experimental Section), the stereochemistry at the site of cleavage is 64% *cis*. The results of GPC analysis for polynorbornene samples prepared using **6** and **7** are shown in Table IV (a representative GPC trace is shown in Figure 5b). Consistent with a living polymerization, the molecular weights of the polynorbornene samples increase linearly with the number of monomer equivalents employed (for 50, 100, and 200 equivalents), and in all cases the polydispersities are representative of monodisperse samples ( $d = 1.05 - 1.10$ ). Additional reaction time does not significantly affect the molecular weight distributions or the polydispersities of the polymers: 200 equivalents of NBE completely polymerized by **6** gave  $M_n = 59,100$  ( $d = 1.05$ ) after 20 minutes and  $M_n = 57,600$  ( $d = 1.07$ ) after 55 minutes.

Besides the absence of secondary metathesis of the polymer chain in complexes **33** and **34**, the most notable feature of the TIPT system is the large degree of base influence over reaction rates. Because the reactivity in the TIPT system depends on the accessibility of a reactive base-free intermediate, catalyst activity can be easily manipulated by adjusting the solvent, base, or reaction temperature employed. Thus a wide range of reactivity is available from one basic catalyst complex,  $Ta(CHCMe_3)(TIPT)_3(B)$ .

**Reactions of Other Cyclic Olefins with DIPP and TIPT Catalysts.**

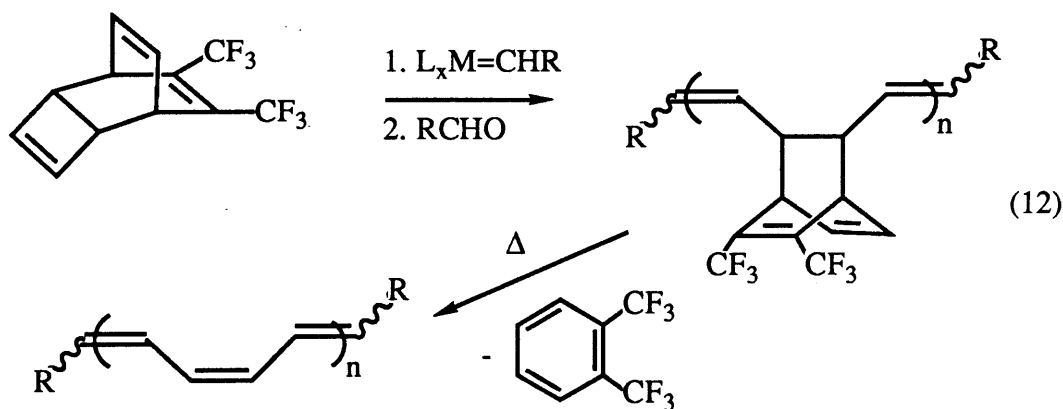
While the polymerization of NBE is highly favored thermodynamically due to ring strain within the monomer, the polymerization of less strained cyclic olefins such as cyclohexene and cyclopentene is less favored (at 25°,  $\Delta G^\circ$  of polymer formation = 6.8 kJ/mol for cyclohexene and -4.3 kJ/mol for cyclopentene;  $\Delta G^\circ$  given as average for *cis* and *trans* polymer formation).<sup>2</sup> In the case of cyclohexene, polymerization is generally not observed at all (the copolymerization of cyclohexene in the presence of NBE has been reported<sup>100</sup>). For other monomers, a "ceiling temperature" is oftentimes observed above which no polymerization activity will occur at a given monomer concentration, since  $\Delta S^\circ$  for these reactions is usually negative.<sup>2</sup> For example, the reaction of cyclopentene (3.11 M) with a tungsten alkylidene catalyst (0.04 M) in toluene-*d*<sub>8</sub> was found to give an equilibrium mixture of polymer and monomer with more than 90% polymer present at ~-50° but less than 10% polymer present at ~80°. <sup>101</sup> In these cases, even if the polymerization is living, monodisperse polymers may not be obtained, since equilibration of the polymer with monomer leads to the most probable distribution for the polymer (*d* ≈ 2.0).

For reactions with cyclopentene, the TIPT complex Ta(CHCMe<sub>3</sub>)(TIPT)<sub>3</sub>(THF) (**6**) was employed, since this complex reacts readily with the strained cyclic olefin NBE in room temperature solution, while DIPP metallacycles react only at elevated temperatures; an additional advantage with the TIPT system is the lack of reactivity with ordinary olefins (i.e. secondary metathesis). When complex **6** was reacted with 10 equivalents of cyclopentene (~0.6 M) in C<sub>6</sub>D<sub>6</sub> at 25°, the color of the solution turned deep red over 5-10 minutes. The resulting <sup>1</sup>H NMR spectrum showed all of complex **6** consumed and a mixture of cyclopentenamer and cyclopentene (~70% polymer); cyclopentenamer resonances occurred at 5.45 (H<sub>5</sub>), 2.05 (H<sub>4</sub>), and ~1.4 ppm (H<sub>3</sub>) (equation 11). A broad triplet resonance at 4.51 ppm (H<sub>1</sub>) and a multiplet resonance at ~4.8 ppm (H<sub>2</sub>), indicative of the alkylidene complex shown in equation 11, were also noted.



After 24 hours at 25° the monomer to polymer ratio in this sample was essentially the same, but the resonance for H<sub>1</sub> had *completely* disappeared. Thus the alkylidene complex formed from reaction of **6** with excess cyclopentene shows no extended stability, consistent with the presence of β hydrogens on the alkylidene ligand. (The TIPT alkylidene complexes **33** and **34**, which also contain β hydrogens, are stable throughout the duration of NBE polymerization. An increased stability of complexes with branched alkylidene ligands (with β hydrogens) has been documented elsewhere and attributed to the steric effect within these alkylidene ligands.<sup>102</sup>) No further attempts were made to characterize this cyclopentene system, after considering the limitations revealed by the NMR experiments.

In other reactions, complex **6** was found to display no significant activity with cyclooctene or cyclooctatetraene (up to ~65° in C<sub>6</sub>D<sub>6</sub>), but **6** does react with the unusual cyclic olefin 7,8-bis(trifluoromethyl)tricyclo[4.2.2.0<sup>2,5</sup>]deca-3,5,9-triene (HFF; a "Feast monomer") slowly in solution at 25°. Ring-opening of this monomer has been reported to produce a polymer which, after heating to induce a retro Diels-Alder reaction, yields polyacetylene.<sup>103</sup>





Block copolymers of NBE and acetylene have also been prepared employing HFF.<sup>86,104</sup> Furthermore, certain well-defined tungsten and molybdenum alkylidene catalysts ring-open oligomerize HFF to yield discrete polyenes not previously accessible (equation 12),<sup>86,105</sup> and this was the primary interest in reacting complex **6** with HFF.

When 5 equivalents of HFF were added to complex **6** in C<sub>6</sub>D<sub>6</sub> at 25°, the monomer was slowly consumed over a period of ~1 hour, as seen by <sup>1</sup>H NMR spectroscopy; little information could be obtained concerning the nature of the organometallic product due to the multiple broad resonances of the formed polymer (the solution was deep red in color). After capping with excess pivaldehyde and subsequent heating to affect the retro Diels-Alder reaction, the formation of polyenes was qualitatively confirmed by GPC analysis.<sup>106</sup> The reaction can also be performed on a larger scale (i.e. with 600 mg of **6**; see Experimental Section for details), allowing isolation of several polyenes (n = 3, 4, 5, 6, 7; equation 12) after low temperature column chromatography.

The alternative method of polyacetylene and/or polyene synthesis by ring-opening polymerization of cyclooctatetraene (COT) can also be envisioned, and this was briefly investigated using the DIPP complexes **2** and **26**. The alkylidene complex **2** reacts very rapidly with COT in common organic solvents - in a low temperature study initial reactivity was observed at -20° in ether. The initiation step in this reaction is apparently slow compared with propagation, as in all cases (including those in which only a few equivalents of COT were employed) only an insoluble black precipitate was obtained, presumed to be high molecular weight polyacetylene.

The tantalacycle **26** does not react readily with COT in solution at 25° (consistent with limited ring-opening of **26** at this temperature), but when solutions were heated a rapid reaction ensued. When 20 equivalents of NBE and 5 equivalents of COT were copolymerized by **26** in C<sub>6</sub>D<sub>6</sub> at an elevated temperature, and the reaction was monitored by <sup>1</sup>H NMR spectroscopy, the NBE monomer was completely consumed prior to reaction of any COT. However, upon complete consumption of NBE the COT was rapidly polymerized, causing a quick precipitation

of the catalyst species from solution (presumably due to the formation of high polymer, as was seen with **2**). When the copolymerization was performed on a preparative scale (with 100 equivalents of NBE and 5 equivalents of COT), the resulting solution (in toluene) turned a deep red color, but precipitation of the product polymer did *not* occur. Subsequent isolation of the polymer yielded a dark purple material, similar in form to polynorbornene but more brittle. Unfortunately, once isolated this polymer sample would not redissolve in hot toluene, impeding further analysis. Thus although COT is polymerized by complexes **2** and **26**, the ill-defined nature of these reactions prevents isolation of useful materials, thereby affirming the importance of well-defined processes which have been used to obtain unique materials such as polyenes.<sup>86,105</sup>

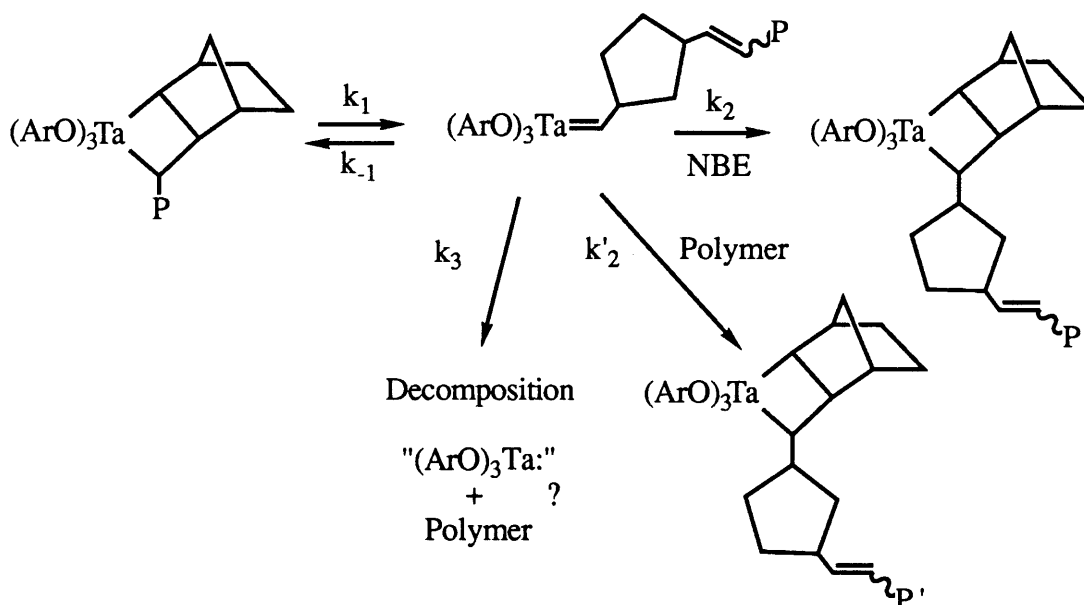
## DISCUSSION

Both the DIPP metallacycle **26** and the TIPT alkylidenes **6** and **7** polymerize NBE in a well-defined manner, while polymerization by the DMP metallacycle **30** is less impressive, but somewhat consistent with earlier complications noted for reactions between Ta(CHCMe<sub>3</sub>)(DMP)<sub>3</sub>(THF) (**4**) and ordinary olefins (chapter 1). The preparations of these catalysts are not complex (one or two steps from Ta(CHCMe<sub>3</sub>)(THF)<sub>2</sub>Cl<sub>3</sub>) and generally give good yields. Overall, Ta(CHCMe<sub>3</sub>)(TIPT)<sub>3</sub>(B) complexes are considered most useful for cyclic olefin polymerization, since reactions can be performed at lower temperatures, secondary metathesis is absent, and polymerization rates are easily controlled by manipulation of base (B). Additionally, the TIPT complex **6** can be used to prepare polyenes efficiently through the special ring-opening metathesis of HFF.

While tantalum alkylidene and metallacyclobutane complexes are fairly easily prepared and can display well-behaved metathesis and polymerization activity, their utility should also be considered with regard to inherent limitations, such as a high degree of oxophilicity. Thus polymerization of cyclic olefins containing functional groups, like *endo,endo*-5,6-dicarbomethoxynorbornene, results in deactivation before any significant monomer is consumed. (Less oxophilic molybdenum alkylidene complexes have been shown

to efficiently polymerize this monomer.<sup>78,86</sup>). Decomposition of propagating or intermediate alkylidene complexes that contain  $\beta$  hydrogens on the alkylidene ligand also must be taken into consideration. Decomposition of the tantalacyclobutane complex **27** in solution at 25° in the *absence* of NBE, although slow (5-10% in 24 hours), is thought to arise from such reactions (Scheme III). Since both decomposition and isomerization are observed, the rates of these

Scheme III: The Activity of Complexes **27** and **31** in Solution at 25°.



processes ( $k_3$  and  $k'_2[P]$ , respectively) must be competitive. In the presence of NBE, decomposition and isomerization are not observed, consistent with the ring-opening metathesis reaction being most favored ( $k_2[\text{NBE}] \gg k'_2[P]$  or  $k_3$ ). The DMP complex **31** shows no obvious signs of decomposition at 25° even in the absence of NBE. This is consistent with the earlier proposed hypothesis that DMP metallacycle and alkylidene complexes possess a more open coordination sphere, allowing increased interaction with the olefinic units of the polymer chain (i.e.  $k'_2[P] > k_3$ ).

Contrasting the behavior of phenoxide complexes,  $\text{Ta}(\text{CHCMe}_3)(\text{TIPT})_3(\text{B})$  complexes ( $\text{B} = \text{THF}$ , **6**;  $\text{py}$ , **7**) do not form stable metallacyclobutanes when reacted with cyclic olefins.

This probably is related to a preferential *trans* bonding orientation of the alkylidene and base (B) ligands in these five-coordinate complexes, as is observed in Ta(CHCMe<sub>3</sub>)(TIPT)<sub>3</sub>(Et<sub>2</sub>S) (9) (Appendix 1). The formation of a metallacyclobutane ring in a five-coordinate complex requires a *cis* orientation of the reactive groups (i.e. the alkylidene and olefin ligands). While intermediate tantalacyclobutanes must form during the polymerization of NBE by complexes 6 and 7, apparently rearrangement to the preferred geometry, characterized by equatorial TIPT bonding and a *trans* orientation for the other two ligands, occurs quickly, thus breaking up the metallacyclobutane rings.

Ta(CHCMe<sub>3</sub>)(TIPT)<sub>3</sub>(B) complexes do not react with ordinary unstrained olefins (chapter 1) but do react with strained cyclic olefins, such as NBE. The metathesis of a strained cyclic olefin is thermodynamically more favorable than the metathesis of an ordinary olefin, but in differentiating between these two reactions, kinetic considerations should also be addressed. If a cyclic olefin's ground state energy is relatively high due to strain within the molecule, the transition state required in a metathesis reaction (by an alkylidene complex) should be more readily attainable with a strained cyclic olefin than with an ordinary olefin, since the transition state for each involves a weakening of the C-C double bond, which is already strained in the cyclic olefin. (The transition states for the two cases are assumed to be of similar energy in this rationalization.) This argument, which is consistent with the trends of reactivity observed here, is considered only as a guideline.<sup>107</sup>

## Experimental Section

General experimental details are given in chapter 1. NBE-2,3-d<sub>2</sub><sup>108</sup> and HFF<sup>103</sup> can be prepared as reported in the literature; in this study they were provided by S. A. Krouse and K. Knoll (HFF) and J. K. Stille via R. H. Grubbs (NBE-2,3-d<sub>2</sub>).

All polymer samples were analyzed in toluene (after passage through a 0.5 μm disposable filter unit; ~0.3% by weight polynorbornene in solution) at 25° versus polystyrene standards (1260 - 1.030 x 10<sup>6</sup> MW) on one of two GPC systems: (1) a Waters 150C instrument equipped with three Styragel columns (10<sup>3</sup>, 10<sup>4</sup>, and 10<sup>5</sup> Å), a refractive index detector, and a Waters Data Module for data analysis (2) a GPC system employing a Rheodyne Model 7125 sample injector, a Kratos Spectroflow 400 pump, five Shodex GPC columns (KF-802, 802.5, 803, 804, and 805), a Kratos Spectrflow 757 UV/VIS absorbance detector, a Knauer Model R981 refractive index detector, and a MacAdios Model 411 and Macintosh Plus computer for data analysis.

**Preparation of Compounds. Ta[CH(C<sub>5</sub>H<sub>8</sub>)CHCH(CMe<sub>3</sub>)](DIPP)<sub>3</sub> (26).** A solution of norbornene (0.077 g, 0.82 mmol) in ether (10 mL) was added to a stirring solution of Ta(CHCMe<sub>3</sub>)(DIPP)<sub>3</sub>(THF) (0.70 g, 0.82 mmol) in ether (30 mL) at -30°. The color of the solution rapidly disappeared. After stirring the solution at room temperature for 30 m, the solvent was removed *in vacuo* to yield a white powder. Crystallization from ether yielded a microcrystalline white precipitate (0.46 g, 64%): <sup>1</sup>H NMR (300 MHz) δ 7.1–6.8 (m, 9, H<sub>m</sub> and H<sub>p</sub>), 5.32 (d, 1, J<sub>HH</sub> = 9.6, α CHC<sub>5</sub>H<sub>8</sub>), 3.88 (d, 1, J<sub>HH</sub> = 10.1, α CHCMe<sub>3</sub>), 3.8–3.2 (broad, 6, CHMe<sub>2</sub>), 3.00 and 2.82 (each a broad s, 1 each, CH's of C<sub>5</sub>H<sub>8</sub>), 0.88 (broad t, 1, J<sub>HH</sub> unresolved, β C<sub>5</sub>H<sub>8</sub>CH), 1.6–0.5 (broad; no other specific assignments could be made); a <sup>13</sup>C NMR spectrum at room temperature displayed broad resonances. Anal. Calcd for TaC<sub>48</sub>H<sub>71</sub>O<sub>3</sub>: C, 65.72; H, 8.18. Found: C, 65.90; H, 8.36.

**Ta[CH(C<sub>5</sub>H<sub>8</sub>)CHCH(CHC<sub>5</sub>H<sub>8</sub>CHCHCMe<sub>3</sub>)](DIPP)<sub>3</sub> (28).** A solution of norbornene (0.083 g, 0.88 mmol) in ether (20 mL), cooled to -30°, was added to a solution of Ta(CHCMe<sub>3</sub>)(DIPP)<sub>3</sub>(THF) (0.750 g, 0.88 mmol) in ether (30 mL) at -30°. After stirring the

solution at room temperature for 20 m, the solvent was removed *in vacuo*. The off-white solid left behind was dissolved in toluene (10 mL), and a solution of norbornene (0.083 g, 0.88 mmol) in toluene (10 mL) was added at room temperature. This solution was then heated to 60°. After 25 m the solution was filtered through Celite, and the solvent was removed *in vacuo*. Dissolution of the resulting colorless oil in pentane (the compound is *extremely* soluble), followed by cooling to -30°, yielded after several days a white precipitate (0.34 g, 40%): <sup>1</sup>H NMR (300 MHz) δ 6.99 (br d, 6, H<sub>m</sub>), 6.84 (br t, 3, H<sub>p</sub>), 5.6–5.3 (m, 2, olefinic H's), 5.23 (d, 1, J<sub>HH</sub> = 9.1, α CHC<sub>5</sub>H<sub>8</sub>), 3.85 (t, 1, J<sub>HH</sub> = 8.6, α CH(C<sub>5</sub>H<sub>8</sub>CHCH<sup>t</sup>Bu)), 3.8–3.1 (broad, CHMe<sub>2</sub>), 1.12 (s, CMe<sub>3</sub>). All other resonances were broad and complex. Isolation of pure product is very difficult, due to the complex's high solubility and the presence of some Ta[CH(C<sub>5</sub>H<sub>8</sub>)CHCH(CMe<sub>3</sub>)](DIPP)<sub>3</sub> impurity. Analysis attempts were not successful.

**Ta[CH(C<sub>5</sub>H<sub>8</sub>)CHCH(CMe<sub>3</sub>)](DMP)<sub>3</sub> (30).** A solution of norbornene (0.055 g, 0.58 mmol) in ether (20 mL), cooled to -30°, was added to a solution of Ta(CHCMe<sub>3</sub>)(DMP)<sub>3</sub>(THF) (0.40 g, 0.58 mmol) in ether (40 mL) at -30°. The color of the solution rapidly turned yellow, and after 15 m at -30° the solvent was removed *in vacuo* to give a yellow oil. This oil was dissolved in pentane, and the solution was cooled to -30°, yielding a pale yellow precipitate (0.13 g, 31%). A <sup>1</sup>H NMR spectrum of the crude oil showed clean formation of the product; the low isolated yield is thought to arise from the high solubility of the compound: <sup>1</sup>H NMR (300 MHz) δ 6.82 (d, 6, H<sub>m</sub>), 6.62 (t, 3, H<sub>p</sub>), 5.21 (d, 1, J<sub>HH</sub> = 9.6, α CHC<sub>5</sub>H<sub>8</sub>), 3.72 (d, 1, J<sub>HH</sub> = 10.0, α CHCMe<sub>3</sub>), 2.86 and 2.80 (each a broad d, 1 each, CH's of C<sub>5</sub>H<sub>8</sub>), 2.21 (s, 18, DMP Me), 1.7–1.4 (m, 4, CH<sub>2</sub>'s of C<sub>5</sub>H<sub>8</sub>), 1.35 and 0.60 (each a broad d, 1 each, bridgehead H's of C<sub>5</sub>H<sub>8</sub>), 1.16 (s, 9, CMe<sub>3</sub>), 0.84 (t, J<sub>HH</sub> = 9.1, β C<sub>5</sub>H<sub>8</sub>CH); <sup>13</sup>C NMR (67.9 MHz) δ 159.6 (s, C<sub>ipso</sub>), 135.0 and 132.5 (each a d, J<sub>CH</sub> = 142 and 132, α C's), 128.5 (d, C<sub>m</sub>), 127.1 (s, C<sub>o</sub>), 121.2 (d, C<sub>p</sub>), 45.7 and 45.0 (each a d, CH's of C<sub>5</sub>H<sub>8</sub>), 38.6 (s, CMe<sub>3</sub>), 34.5 and 34.6 (each a t, CH<sub>2</sub>'s of C<sub>5</sub>H<sub>8</sub>), 33.1 (q, CMe<sub>3</sub>), 30.2 (t, bridgehead C of C<sub>5</sub>H<sub>8</sub>), 29.0 (d, J<sub>CH</sub> = 149, β C<sub>5</sub>H<sub>8</sub>CH), 18.0 (q, DMP Me). A solid sample

left under vacuum at 25° showed significant decomposition after 1 day. The compound did not analyze well.

**X-Ray structure of Ta[CH(C<sub>5</sub>H<sub>8</sub>)CHCH(<sup>t</sup>Bu)](DIPP)<sub>3</sub> (26).** Data were collected at -65° on an Enraf-Nonius CAD4F-11 diffractometer equipped with a liquid nitrogen low temperature device and using Mo K $\alpha$  radiation. Data collection, reduction, and refinement procedures have been detailed elsewhere.<sup>83</sup> A total of 7749 reflections (+*h*, +*k*,  $\pm$ *l*) were collected in the range  $3^\circ \leq 2\theta \leq 50^\circ$  with the 4679 having  $F_o > 4\sigma(F_o)$  being used in the structure refinement which was by full-matrix least-squares techniques (278 variables) using SHELX-76 with final  $R_1 = 0.068$  and  $R_2 = 0.061$ . The tantalum and all the non-hydrogen atoms of the metalacyclobutane ring were refined anisotropically. All remaining non-hydrogen atoms in the complex were refined isotropically. The three hydrogen atoms on the metalacyclobutane ring were omitted, but all remaining hydrogen atoms were placed in calculated positions and were constrained to ride on their respective carbon atoms. A final difference-Fourier map showed no chemically significant features. The crystal data are the following: space group  $P2_1/n$ ,  $a = 11.587(4)$  Å,  $b = 20.795(4)$  Å,  $c = 18.388(4)$  Å,  $Z = 4$ ,  $M_r = 877.03$  g,  $V = 4416.6$  Å<sup>3</sup>,  $\rho(\text{calcd}) = 1.319$  g cm<sup>-3</sup>,  $\mu = 24.0$  cm<sup>-1</sup>. A semi-empirical absorption correction was applied.

**Preparation of Polynorbornene with 6, 7, 26, and 30 for GPC Analysis.** In a typical reaction, a solution of norbornene in toluene (10 mL) was added to a stirring solution of 26 (20 mg) in toluene (10 mL) at 25°. The resulting solution was heated in an oil bath to 65°, and the reaction monitored by GLC. After all norbornene was consumed, excess benzaldehyde, benzophenone, or acetone (~50  $\mu$ L) was added, and the mixture was heated at 65° for another 15 minutes. The solvent was then removed *in vacuo*, and the resulting polymer sample was rinsed with 20-30 mL methanol (containing a small amount of BHT, 2,6-di-*t*-butyl-4-methylphenol). The polymer was thoroughly dried *in vacuo* before redissolution for GPC analysis. Polymer preparations with complexes 30 and 7 were performed in an analogous

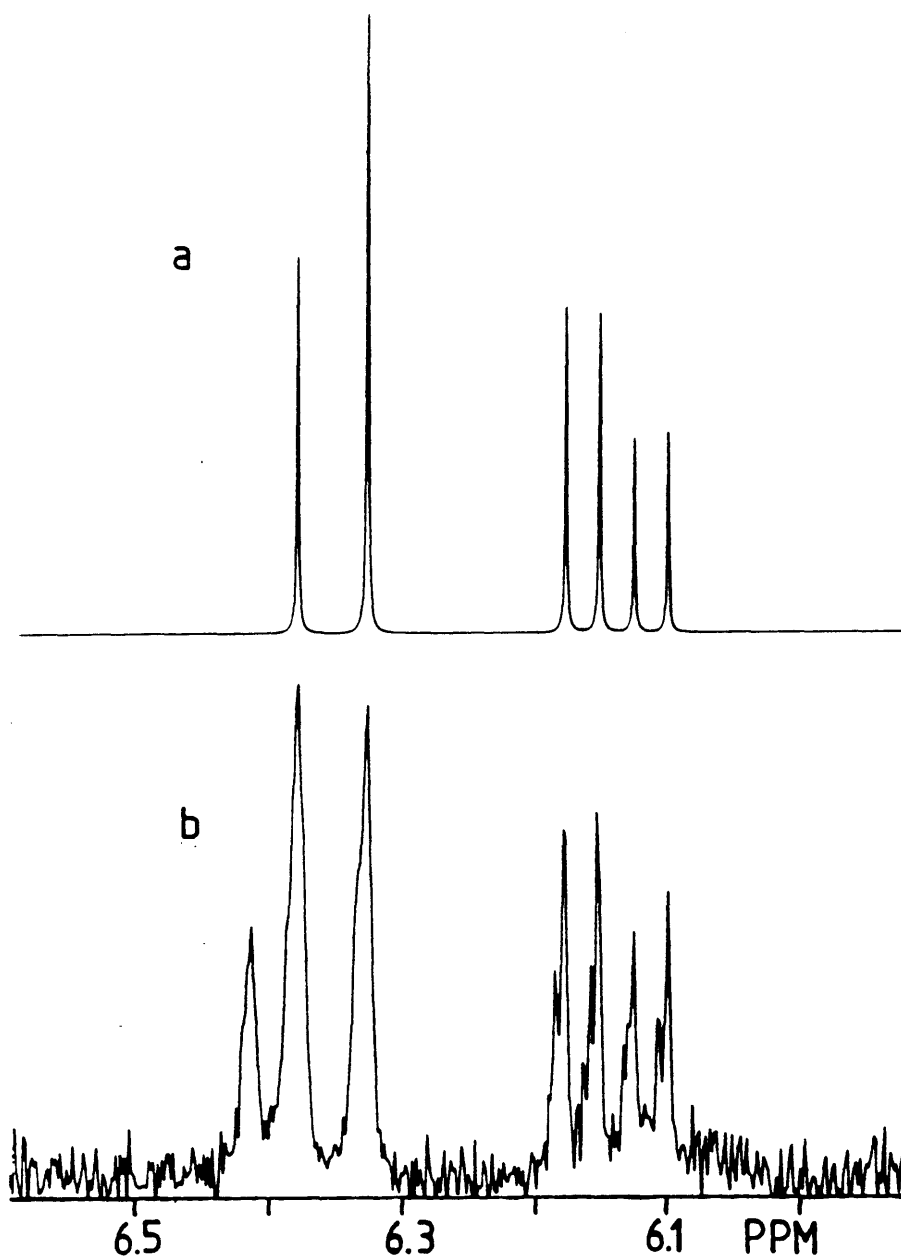
fashion. When **6** was employed as the catalyst, the polymerization and capping reactions were done at 25°.

**Kinetics of Polymerization of Norbornene.** Stock solutions of NBE in C<sub>6</sub>D<sub>6</sub> and of the catalyst **26** in C<sub>6</sub>D<sub>6</sub> (with a few equivalents of mesitylene as internal standard) were utilized for accurate measurements. In a typical reaction, measured portions of each solution were added to an NMR tube, and additional C<sub>6</sub>D<sub>6</sub> was added to create a total volume of 1 mL. The NMR tube was sealed while the solution inside was kept frozen in liquid nitrogen; after sealing, the sample was kept frozen until use. For the experiment, the sample was placed in the probe of a Varian XL-300 NMR spectrometer maintained at the reaction temperature (determined before and after the run with ethylene glycol). After allowing 10 m for equilibration of the sample, and after all the initiating catalyst had been consumed, the disappearance of the olefinic protons of NBE was monitored relative to the internal standard. All runs were monitored for at least 3 half lives, and in all cases acceptable R values were obtained from the subsequent kinetic plots (unless otherwise noted in the text). An analogous procedure was employed for the reactions of **30** and **7** with norbornene, except that the signal from C<sub>6</sub>D<sub>5</sub>H was utilized as the internal standard. For reaction of **28** with NBE-2,3-d<sub>2</sub>, samples were prepared as described above employing stock solutions of NBE-2,3-d<sub>2</sub> in toluene-d<sub>8</sub> and **28** in C<sub>6</sub>D<sub>6</sub>. The rate of ring opening of **28** was determined by monitoring the disappearance of the α proton at 5.23 ppm.

**Capping Living Polymers; Spin Simulation Experiments.** A sample of **27** was treated with three equivalents of benzaldehyde in C<sub>6</sub>D<sub>6</sub> at 65°. A <sup>1</sup>H NMR spectrum of the resulting capped polymer, PhH<sub>A</sub>C=CH<sub>B</sub>[C<sub>5</sub>H<sub>8</sub>CH=CH]<sub>x</sub>CMe<sub>3</sub>, displayed olefinic resonances in the region 6.0-6.5 ppm for H<sub>A</sub> and H<sub>B</sub> (Figure 7b). Based on related studies<sup>106</sup> in which only the *trans* isomer (of the phenyl capped olefin group) was observed, the resonances at 6.38 and 6.33 were assigned to H<sub>A</sub> of the *trans* isomer, and those at 6.18-6.10 ppm were assigned to H<sub>B</sub> of the *trans* isomer. Using the values δ H<sub>A</sub> = 1905 Hz and δ H<sub>B</sub> = 1841 Hz at 300 MHz, and J<sub>AB</sub> = 16 Hz and J<sub>BX</sub> = 8 Hz (H<sub>X</sub> is the first cyclopentyl tertiary proton), a theoretical spectrum for the *trans* isomer was calculated (Figure 7a) utilizing a software program based on



**Figure 7.** (a) Calculated spectrum for the protons of the *trans* phenyl-substituted olefin cap in the Wittig product produced on treating Ta[CH(C<sub>5</sub>H<sub>8</sub>)CHCH(P)](DIPP)<sub>3</sub> (**27**) with benzaldehyde. (b) Observed spectrum for the protons of the phenyl-substituted olefin cap in the Wittig product produced on treating **27** with benzaldehyde.





Celite being the top layer), followed by removal of the solvent *in vacuo* and redissolution of the resulting oil in a minimal volume of methylene chloride, gave an intense orange solution.

This solution was then applied to a column of silica gel maintained at  $-40^{\circ}$ . The product polyenes were chromatographed through the column employing a pentane/methylene chloride solvent system, starting with 100% pentane, followed by solutions of pentane/methylene chloride with a systematically increasing fraction of methylene chloride. After removal of the solvent *in vacuo* from the polyene fractions, each was identified by its distinct UV/VIS absorbance spectrum.<sup>86,105</sup> For  ${}^t\text{Bu}(\text{CH}=\text{CH})_n{}^t\text{Bu}$ :  $n = 7$  (47 mg; 0.16 mmol), 9 (43 mg; 0.12 mmol), 11 (33 mg; 0.08 mmol), 13 (14 mg; 0.03 mmol), and 15 (8 mg; 0.02 mmol); total yield = 0.41 mmol (71%).

## CHAPTER 3

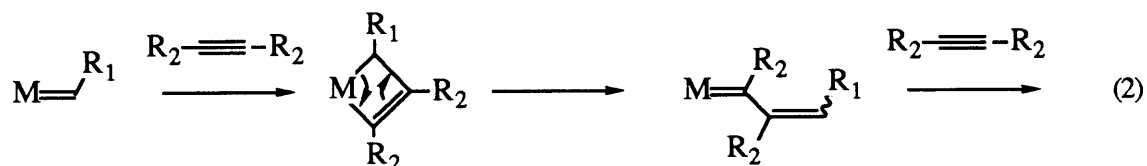
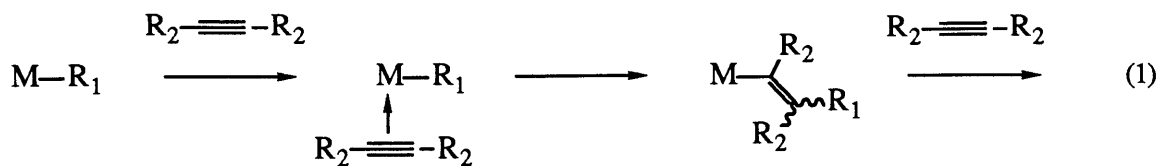
### The Living Polymerization of 2-Butyne by a Tantalum Alkylidene Catalyst and Related Reactions

## INTRODUCTION

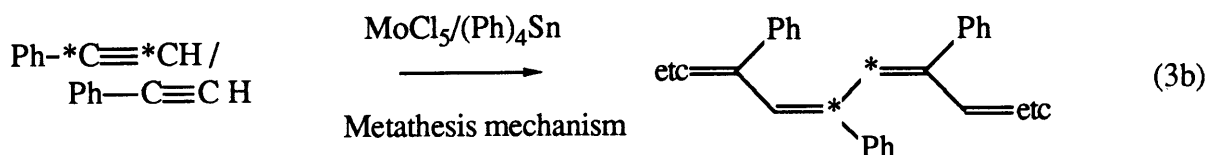
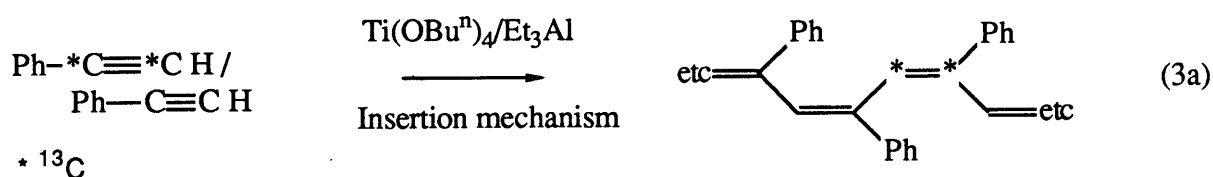
The polymerization of acetylenes has received much attention in recent years, since both parent polyacetylene and substituted polyacetylenes display interesting properties of theoretical and practical importance.<sup>110-112</sup> The interest in parent polyacetylene has largely been centered on its conducting properties when doped, and in order to understand more fully the source of this conductance, well-defined models of polyacetylene such as discrete polyenes<sup>105</sup> and block copolymers of polyacetylene<sup>104</sup> are also under investigation. Substituted polyacetylenes do not display the conductive properties of parent polyacetylene, but properties such as radiation degradation, selective gas and liquid permeability, and electrical insulation make these polymers attractive for study.<sup>112,113</sup>

Transition metal catalysts are generally used in the preparation of these polymers. For the synthesis of parent polyacetylene, a  $\text{Ti}(\text{OR}')_4/\text{AlR}_3$  catalyst system is oftentimes employed.<sup>114,115</sup> For substituted acetylene polymerization many different catalysts have been utilized, although most recently the very effective combination of a group V or VI based transition metal halide catalyst and main group alkyl cocatalyst (such as an aluminum alkyl) has attracted the most investigation.<sup>112,116</sup> In a few cases well-defined organometallic carbene<sup>117,118</sup> and carbyne<sup>119</sup> complexes have been employed, although the exact nature of the propagating species in these cases is still of some question.<sup>120</sup>

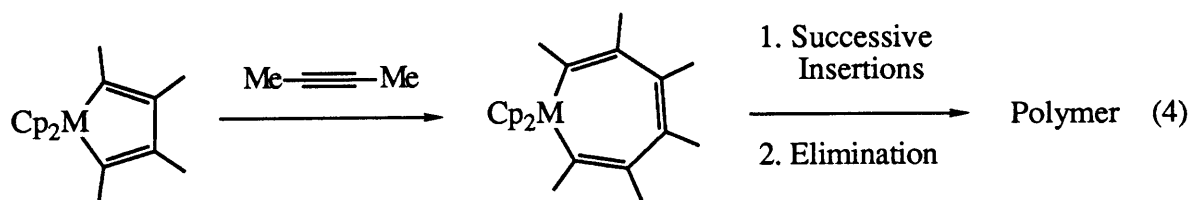
Two general mechanisms have been proposed to explain the polymerization of acetylenes by transition metal catalysts: insertion of an acetylene into a metal carbon single bond (equation 1; insertion mechanism)<sup>114,121-123</sup> and the addition of an acetylene across a metal carbon double bond to give a metallacyclobutene complex, which then ring-opens to give a complex with a new metal carbon double bond (equation 2; "metathesis-like" mechanism).<sup>2,3,112,117,118,120,124</sup> (Other less general mechanisms have also been postulated.<sup>125,126</sup>) Evidence for both mechanisms has been documented, and it appears that the exact mechanism of polymerization depends on the catalyst system employed and the type of acetylene polymerized.



Evidence for the insertion mechanism is derived largely from acetylene polymerization by Ziegler-type catalysts (e.g.  $\text{Ti}(\text{OR}')_4/\text{AlR}_3$ <sup>114,115</sup> and  $\text{Cp}_2\text{MCl}_2/\text{EtAlCl}_2$ ,  $\text{M} = \text{Ti}, \text{Zr}$ <sup>127</sup>) and by late transition metal catalysts,<sup>128,129</sup> many of which are known to polymerize acyclic olefins by successive insertions of an olefin into a metal carbon single bond. Nutation NMR experiments carried out by Katz, Yannoni, and coworkers offer some of the most conclusive evidence for this mechanism.<sup>120,121</sup> In these experiments, polymerization of doubly labelled  $^{13}\text{C}$  parent acetylene ( $\text{H}^{13}\text{C}^{13}\text{CH}$ ) or phenylacetylene ( $\text{Ph}^{13}\text{C}^{13}\text{CH}$ ) using a  $\text{Ti}(\text{OR}')_4/\text{AlR}_3$  catalyst gave polymers in which the labelled carbon atoms were separated by a double bond, the result expected from insertion of an acetylene into a metal carbon single bond (equation 3a; shown for phenylacetylene). Further support comes from polymerization experiments



performed by Farona with a  $\text{Cp}_2\text{MCl}_2/\text{EtAlCl}_2$  ( $\text{M} = \text{Ti}, \text{Zr}$ ) catalyst system.<sup>127</sup> These catalysts affected the oligomerization of terminal and internal acetylenes, and in one case ( $\text{Cp}_2\text{ZrCl}_2/\text{EtAlCl}_2$  with 2-butyne) a metallacyclopentadiene complex ( $\text{Cp}_2\text{ZrC}(\text{Me})\text{C}(\text{Me})\text{C}(\text{Me})\text{C}(\text{Me})$ ) was observed in the reaction. When several metallacyclopentadiene complexes, prepared separately, were then used as the starting catalysts, oligomers of a molecular weight similar to those obtained from the  $\text{Cp}_2\text{MCl}_2/\text{EtAlCl}_2$  catalysts were isolated. Additionally, the reaction of metallacyclopentadiene complexes with acetylenes led to the formation of larger expanded metallacycles. The authors explained these results by proposing stepwise insertions of the acetylenes into the metallacycles, leading to large rings that eventually eliminated oligomers (equation 4).



The polymerization of acetylenes via a metathesis-like reaction (equation 2) was first proposed by Masuda<sup>130</sup> for the polymerization of phenylacetylene by  $\text{WCl}_6$  and  $\text{MoCl}_5$ , and several observations now support this mechanism for high oxidation state group V and VI based catalysts. The reaction of a tantalum alkylidene complex with diphenylacetylene which lead to formation of a vinylalkylidene complex, was reported by Schrock;<sup>35</sup> similar reactions have been seen with carbene complexes.<sup>131-134</sup> Katz has noted polymerization reactions of this type for well known metathesis catalysts (e.g.  $\text{WCl}_6$ ),<sup>118</sup> for lower oxidation state carbene complexes,<sup>117</sup> and for metal carbyne complexes.<sup>119</sup> A related reaction of an acetylene with a carbene complex gave products derived from the formation of an intermediate metallacyclobutene complex.<sup>124</sup> Interestingly, though, the results of nutation NMR spectroscopy<sup>120</sup> demonstrated that representative metal carbene and carbyne catalysts

polymerized acetylenes by the insertion reaction; the results for  $WCl_6$  were inconclusive. However, the results with  $MoCl_5/SnPh_4$  were those expected for a metathesis-like mechanism (equation 3b), thus lending support to this mechanism for at least some group V and VI based catalysts. In other experiments, reaction between  $W(CO)_6$  and olefins in chloroform was shown as a source of carbene species.<sup>135</sup>

The varying results obtained in acetylene polymerization for these and other<sup>112</sup> catalyst systems demonstrate the need for well-defined catalysts in order to more fully understand the mechanisms involved in acetylene polymerization. Only one example of a living polymerization of acetylenes (using  $MoCl_5$  or  $MoOCl_4/Bu_4^nSn/EtOH$ ) has been reported.<sup>136</sup> In that case the nature of the propagating species was not identified, and the catalyst efficiencies ranged from 2-16%. There are no reported examples (in acetylene polymerization) of a well-defined catalyst system in which the active complex has been isolated and clearly shown to be representative of the propagating species.

Tantalum alkylidene complexes of the general formula  $Ta(CHCMe_3)X_3(B)$  ( $X = DIPP$ ,  $TIPT$ ;  $B = THF$ ,  $py$ ) serve as catalysts for the living polymerization of norbornene (NBE; chapter 2). Here the reactivity of these tantalum alkylidene complexes towards substituted acetylenes is described. In some cases tantalum alkylidenes polymerize substituted acetylenes, and in one case, with 2-butyne and a phenoxide based alkylidene complex, a living polymerization reaction is evident. Deactivation processes are also considered on the basis of compounds isolated.

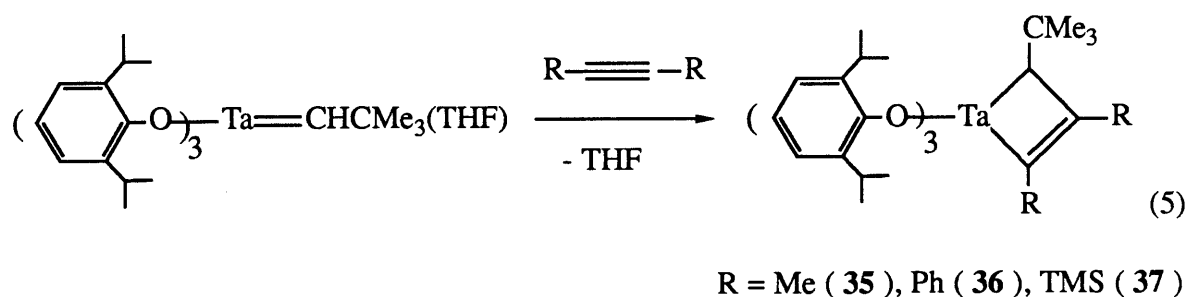
## RESULTS

### Formation of Metallacyclobutene Complexes and their Reactivity with Bases.

$Ta(CHCMe_3)(DIPP)_3(THF)$  (**2**) reacts with one equivalent of the substituted acetylenes 2-butyne, diphenylacetylene, and bistrimethylsilylacetylene to give the base-free metallacyclobutene complexes **35** (~quantitative), **36** (79%), and **37** (43%), respectively (equation 5). These metallacyclobutenes can be isolated in crystalline form from pentane; the



complexes are orange (35, 36) or yellow (37) in color.  $^1\text{H}$  and  $^{13}\text{C}$  NMR



data are listed in Table I for all metallacyclobutene complexes; the  $^1\text{H}$  NMR spectrum of  $\text{Ta}[\text{C}(\text{Me})\text{C}(\text{Me})\text{CH}_2](\text{DIPP})_3$  (35) is displayed in Figure 1. Of particular importance in distinguishing these metallacyclobutene complexes from the corresponding vinyl alkylidene complexes are the resonances observed for the saturated  $\alpha$   $\text{CH}(\text{CMe}_3)$  group of the ring; the absence of olefinic H resonances is also consistent with metallacyclobutene formation. In the NMR spectra at  $25^\circ$  in  $\text{C}_6\text{D}_6$ ,  $\text{H}_\alpha$  resonances were seen as singlets at 2.71 (35), 3.32 (36), and 3.99 (37), while  $\text{C}_\alpha\text{H}(\text{CMe}_3)$  resonances occurred as doublets ( $J_{\text{CH}} = 116\text{-}132$  Hz) at 84.1 (35), 87.7 (36), and 59.9 (37). Signals for only one type of DIPP ligand were observed in the spectra at  $25^\circ$  for all these complexes, indicating that the phenoxide ligands must be rapidly exchanging (similar behavior was observed for DIPP complexes of unsymmetrically substituted tantalacyclobutanes; chapter 1). The geometrical configuration of the ligands around the metal center is not known; in related tantalacyclobutane complexes the geometry ranged from trigonal bipyramidal to distorted square pyramidal (by X-ray crystallography; chapters 1 and 2) The formation of stable metallacyclobutene complexes observed here contrasts with the behavior previously reported for the related alkylidene complex  $\text{Ta}(\text{CHCMe}_3)\text{CpCl}_2$  when reacted with diphenylacetylene. In that case the initially formed metallacycle was not stable but ring-opened to yield a vinyl alkylidene complex.<sup>35</sup> Metallacyclobutene complexes have been reported for other metals, such as those formed from reaction of Tebbe's reagent or titanacyclobutane complexes with acetylenes.<sup>137-139</sup> A

**Table I.** NMR Data for the MC<sub>3</sub> Ring in Metallacyclobutene Complexes.<sup>a</sup>

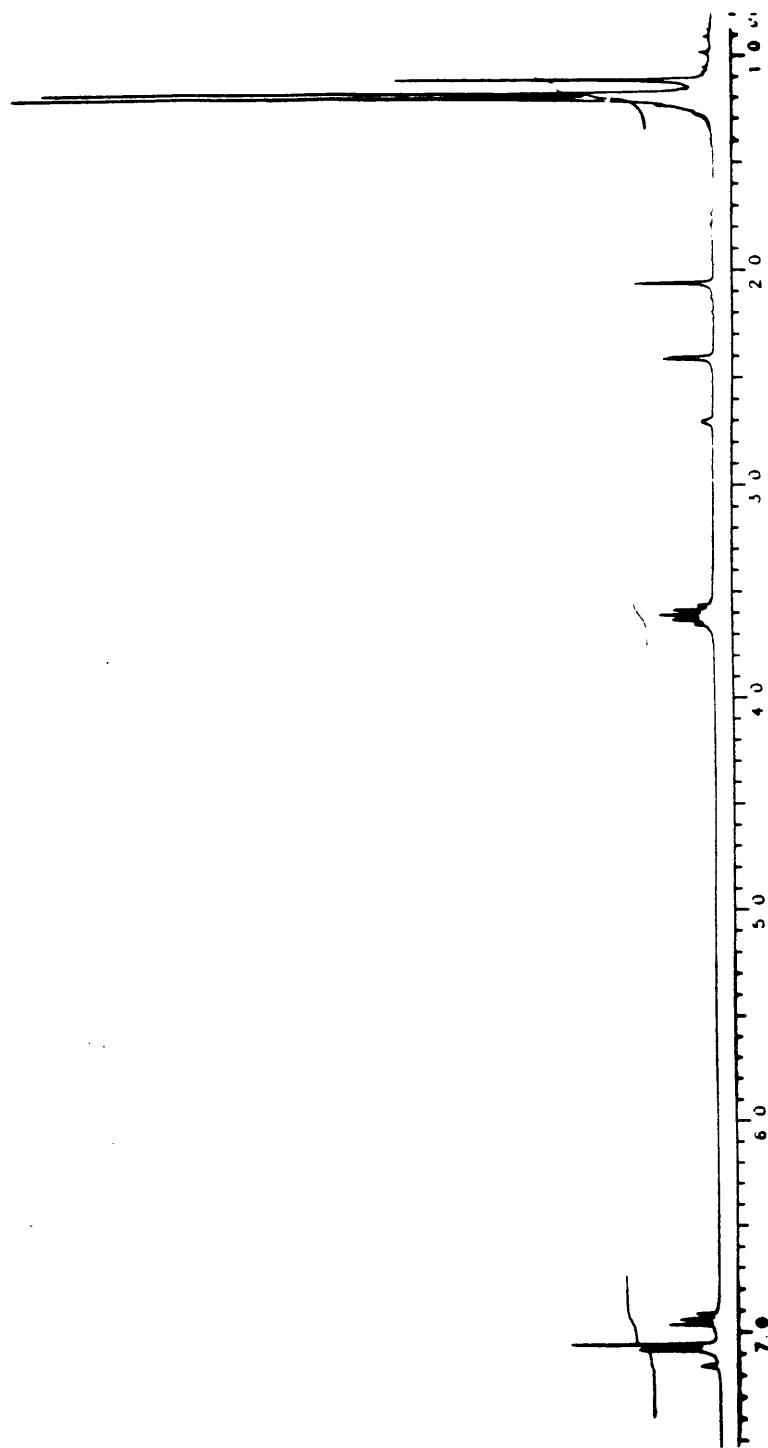
Compound	H <sub>α</sub>	C <sub>α</sub> (J <sub>CH</sub> )	C <sub>β</sub> (J <sub>CH</sub> )
Ta[C(Me)C(Me)CH(CMe <sub>3</sub> )](DIPP) <sub>3</sub> ( <b>35</b> )	2.71 (s)	84.1 (d, 134) 217.9 (s)	156.2 (s)
Ta[C(Ph)C(Ph)CH(CMe <sub>3</sub> )](DIPP) <sub>3</sub> ( <b>36</b> )	3.32 (s)	87.7 (d, 132) 224.0 (s)	151.6 (s)
Ta[C(SiMe <sub>3</sub> )C(SiMe <sub>3</sub> )CH(CMe <sub>3</sub> )](DIPP) <sub>3</sub> ( <b>37</b> )	3.99 (s)	59.9 (d, 116) 254.8 (s)	232.2 (s)
Ta[CH <sub>2</sub> C(Me)C(CHCHCMe <sub>3</sub> )](DIPP) <sub>3</sub> ( <b>38</b> )	2.15 (s)	57.3 (t, 141) 216.9 (s)	150.5 (s)
Ta[CH <sub>2</sub> C(Me)C(CHCHCMe <sub>3</sub> )](DIPP) <sub>3</sub> (py) ( <b>39</b> )	1.76 (s)	56.7 (t, 140) 212.8 (s)	148.2 (s)
Ta[C(SiMe <sub>3</sub> )C(SiMe <sub>3</sub> )CH(CMe <sub>3</sub> )](DIPP) <sub>3</sub> (py) ( <b>40</b> )	3.99 (s)		
Ta[CH <sub>2</sub> C(Me)C(CHCHCMe <sub>3</sub> )](DIPP) <sub>3</sub> (quin) ( <b>41</b> )	2.12 (s)		
W[C(SiMe <sub>3</sub> )C(SiMe <sub>3</sub> )CH <sub>2</sub> ](NAr)(OR) <sub>2</sub> <sup>b</sup>	4.89 (q) 4.85 (q)	121.5 (t, 159) 247.3 (s)	144.5 (s)
Ti[C(SiMe <sub>3</sub> )C(SiMe <sub>3</sub> )CH <sub>2</sub> ]Cp <sub>2</sub> <sup>c</sup>	4.64 (s)	108.3	
Ti[C(Ph)C(Ph)CH <sub>2</sub> ]Cp <sub>2</sub> <sup>c</sup>	3.37 (s)		

<sup>a</sup> Listed in ppm; solvent = C<sub>6</sub>D<sub>6</sub> and temperature = 25° unless otherwise noted.

<sup>b</sup> Reference 140. NAr = N-2,6-C<sub>6</sub>H<sub>3</sub><sup>i</sup>Pr<sub>2</sub>; OR = OC(Me)(CF<sub>3</sub>)<sub>2</sub>. (The possibility of a vinyl alkylidene assignment was also mentioned for this complex.)

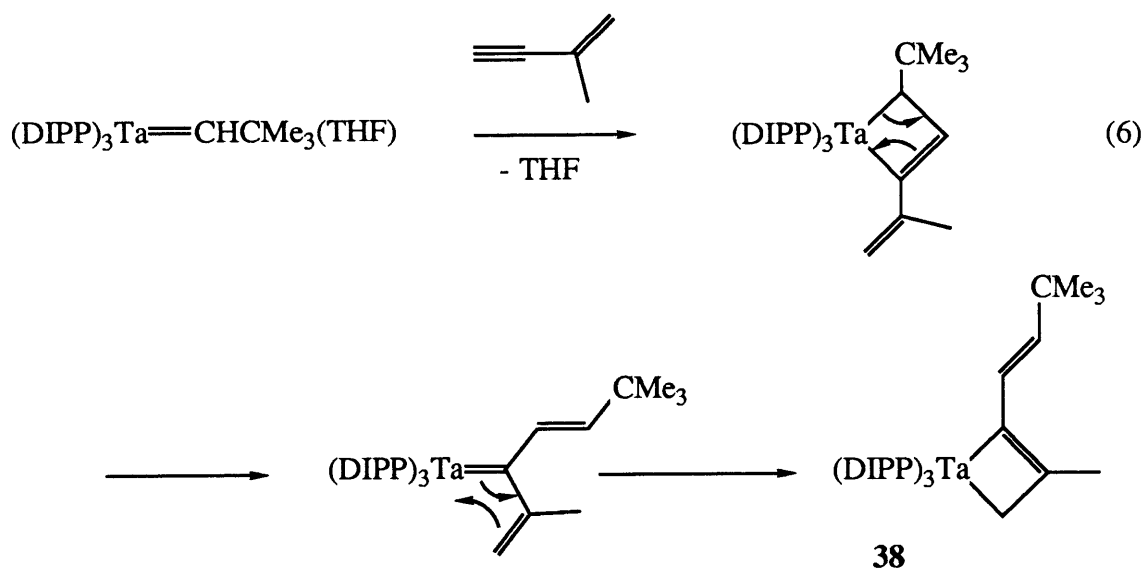
<sup>c</sup> Reference 137. Solvent = toluene-d<sub>8</sub>.

Figure 1. The  $^1\text{H}$  NMR spectrum of  $\text{Ta}[\text{C}(\text{Me})\text{C}(\text{Me})\text{CH}(\text{CMe}_3)](\text{DIPP})_3$  (**35**) in  $\text{C}_6\text{D}_6$ .



tungstenacyclobutane complex also has been shown to form a stable metallacyclobutene, from reaction with bistrimethylsilylacetylene.<sup>140</sup>

$\text{Ta}(\text{CHCMe}_3)(\text{DIPP})_3(\text{THF})$  (**2**) also reacts with the terminal acetylene 2-methylbut-1-ene-3-yne to give a metallacyclobutene complex, but not the one expected from a simple addition reaction. The  $^1\text{H}$  and  $^{13}\text{C}$  NMR spectra (Table I) displayed resonances indicative of a metallacyclobutene complex containing an alpha methylene group in the ring and an attached olefin group containing two inequivalent H's ( $J_{\text{HH}} = 16$  Hz), consistent with the formation of  $\text{Ta}[\text{CH}_2\text{C}(\text{Me})\text{C}(\text{CHCHCMe}_3)](\text{DIPP})_3$  (**38**) as shown in equation 6.

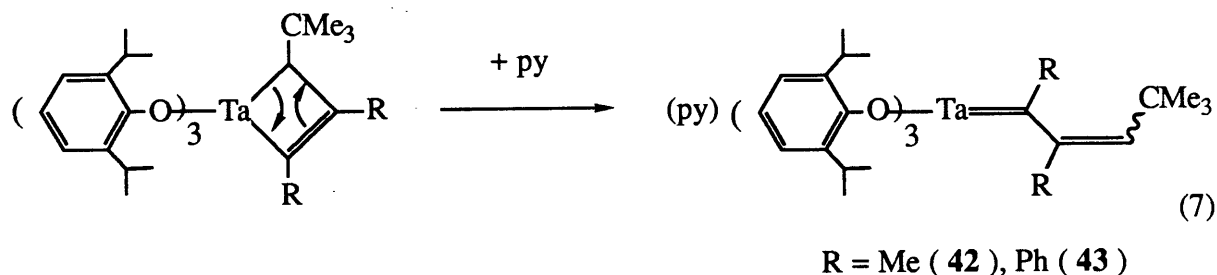


Apparently the initially formed metallacyclobutene complex, containing an  $\alpha$  t-butyl group, rearranges to give the more stable complex **38**, a less sterically congested species. A related rearrangement in which an  $\alpha$  t-butyl group isomerized to the  $\beta$  position of a tantalacyclobutane ring was observed for  $\text{Ta}[\text{CH}(\text{Ph})\text{CH}(\text{CMe}_3)\text{CH}_2](\text{DIPP})_3$  (**15**) (chapter 1).

The metallacyclobutene complexes **35-38** are quite stable and do not react with more acetylene to give subsequent alkylidenes, metallacyclobutenes, or polymer formation, except in the case of 2-butyne with **35** for which some intractible polymer is formed (this behavior will be discussed later). Similar behavior is observed when  $\text{Ta}(\text{CHCMe}_3)(\text{DIPP})_3(\text{THF})$  (**2**) is

reacted with an excess of the acetylenes - only the initial metallacyclobutenes form and no polymer formation is observed, except again in the case of 2-butyne an intractable polymer is seen. The synthesis of these metallacyclobutene complexes clearly demonstrates that the alkylidene complex  $\text{Ta}(\text{CHCMe}_3)(\text{DIPP})_3(\text{THF})$  (**2**) will react with acetylenes in a metathesis-like reaction, the first step of the polymerization reaction shown in equation 2. However, in order for alkylidene or metallacyclobutene complexes to function as effective polymerization catalysts, these complexes must display controlled reactivity towards additional equivalents of acetylene.

The metallacyclobutenes **35-38** were reacted with base in an attempt to ring-open the compounds to subsequent vinyl alkylidene complexes, which might be more reactive with acetylenes. While  $\text{Ta}[\text{C}(\text{SiMe}_3)\text{C}(\text{SiMe}_3)\text{CH}(\text{CMe}_3)](\text{DIPP})_3$  (**37**) and  $\text{Ta}[\text{CH}_2\text{C}(\text{Me})\text{C}(\text{CHCHCMe}_3)](\text{DIPP})_3$  (**38**) only react with pyridine and/or quinuclidine to give base adducts (Complexes **39-41**; listed in Experimental Section and Table I),  $\text{Ta}[\text{C}(\text{Me})\text{C}(\text{Me})\text{CH}(\text{CMe}_3)](\text{DIPP})_3$  (**35**) and  $\text{Ta}[\text{C}(\text{Ph})\text{C}(\text{Ph})\text{CH}(\text{CMe}_3)](\text{DIPP})_3$  (**36**) react with pyridine to give the new vinyl alkylidene complexes  $\text{Ta}(\text{CMeCMeCHCMe}_3)(\text{DIPP})_3(\text{py})$  (**42**) and  $\text{Ta}(\text{CPhCPhCHCMe}_3)(\text{DIPP})_3(\text{py})$  (**43**), respectively (equation 7). The vinyl alkylidene complexes, which are much darker in color than the analogous metallacyclobutene complexes, can be isolated as dark purple crystals from cooled pentane solutions.



The NMR data for these alkylidenes (Table II) are consistent with those observed for the previously reported  $\text{Ta}[(\text{Ph})\text{C}(\text{Ph})\text{CHCMe}_3]\text{CpCl}_2$ .<sup>35</sup> In the  $^{13}\text{C}$  NMR spectra ( $\text{C}_6\text{D}_6$ ), the  $\alpha$

**Table II.** NMR Data for the Alkylidene Ligand in Tantalum Vinyl Alkylidene Complexes.<sup>a</sup>

Cmpd	CHCMe <sub>3</sub>	C <sub>α</sub>
Ta(CMeCMeCHCMe <sub>3</sub> )(DIPP) <sub>3</sub> (py) ( <b>42</b> ) <sup>b</sup>	c	256.4
	6.57 (s)	232.1
Ta(CPhCPhCHCMe <sub>3</sub> )(DIPP) <sub>3</sub> (py) ( <b>43</b> )	d	243.1
Ta(CMeCMeCMeP)(DIPP) <sub>3</sub> ( <b>44</b> )	5.2-5.4 (br s's)	258.3
Ta(CPhCPhCHCMe <sub>3</sub> )CpCl <sub>2</sub> <sup>e</sup>	f	259

<sup>a</sup> Listed in ppm; solvent = C<sub>6</sub>D<sub>6</sub> and temperature = 25° unless otherwise noted.

<sup>b</sup> In toluene-d<sub>8</sub> at -60°.

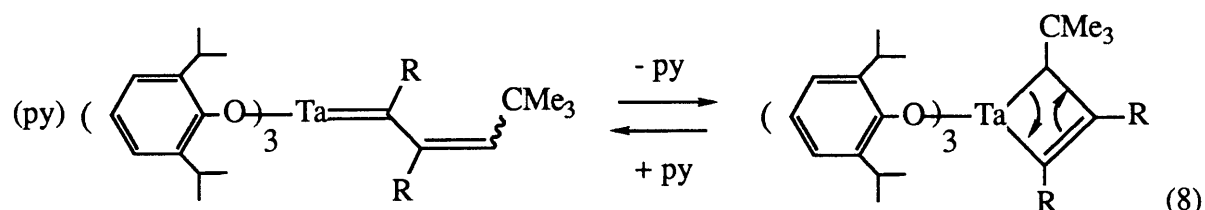
<sup>c</sup> Another resonance for this group is thought to occur in the multiplet region of 6.7-7.2 ppm.

<sup>d</sup> Obstructed in multiplet region of 6.7-7.5 ppm.

<sup>e</sup> Reference 35.

<sup>f</sup> Obstructed in multiplet region 6.3-7.3 ppm.

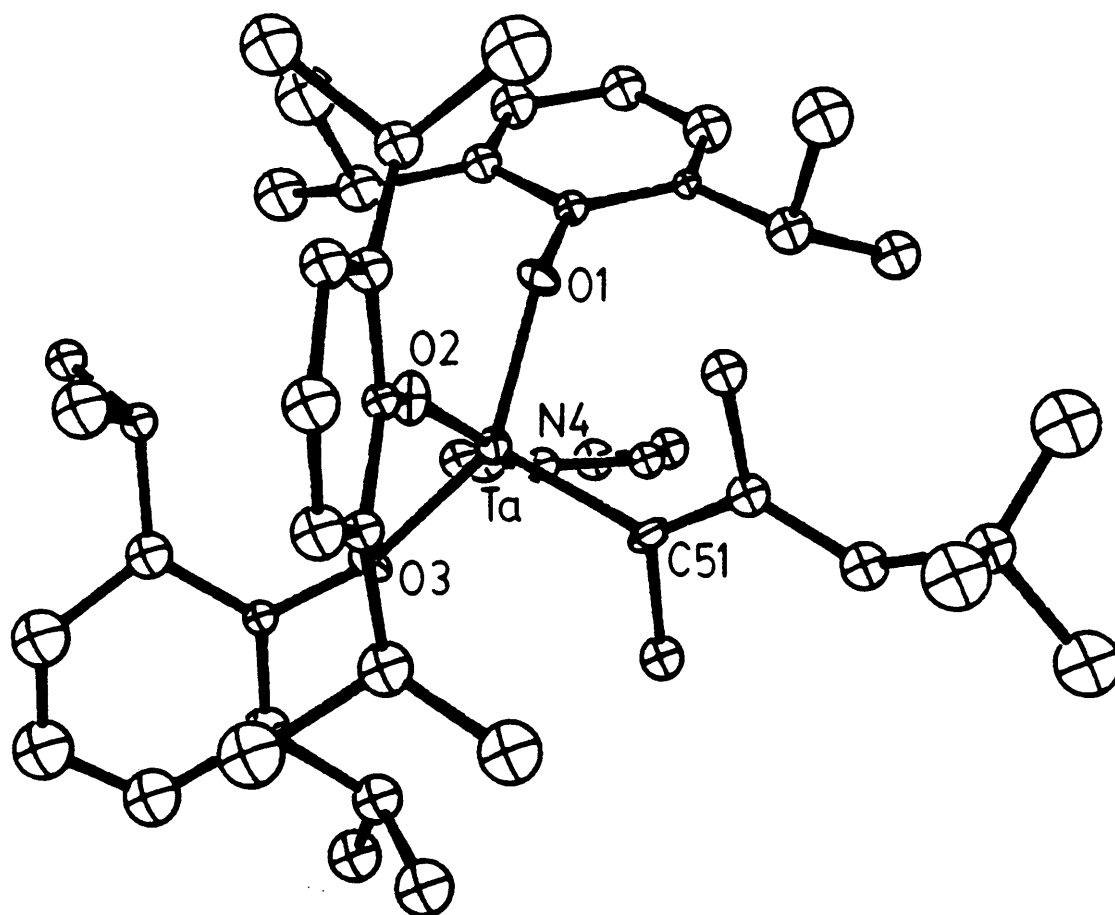
carbon resonances were observed downfield at 256.4 and 232.1 ppm (**42**, two isomers;  $-60^\circ$ ) and at 243.1 ppm (**43**), and no resonances indicative of metallacyclobutenes were observed. In solution, at ambient and elevated temperatures, especially when in low concentration, these vinyl alkylidenes appear to be in equilibrium with the corresponding metallacyclobutenes (equation 8). This equilibrium is most evident for  $\text{Ta}(\text{CMeCMeCHCMe}_3)(\text{DIPP})_3(\text{py})$  (**42**) - the  $^1\text{H}$  and  $^{13}\text{C}$  NMR spectra ( $\text{C}_6\text{D}_6$ ) at  $25^\circ$  display no clear resonances



for atoms involved in this equilibrium (see Experimental Section for details), and at elevated temperatures only the metallacyclobutene complex is observed (with free pyridine). Low temperature spectra, though, support the alkylidene assignment (Table II; also discussed later in this section). Again in these complexes resonances are observed for only one type of DIPP ligand; the same has been observed for other phenoxide tantalum alkylidene complexes (chapter 1).

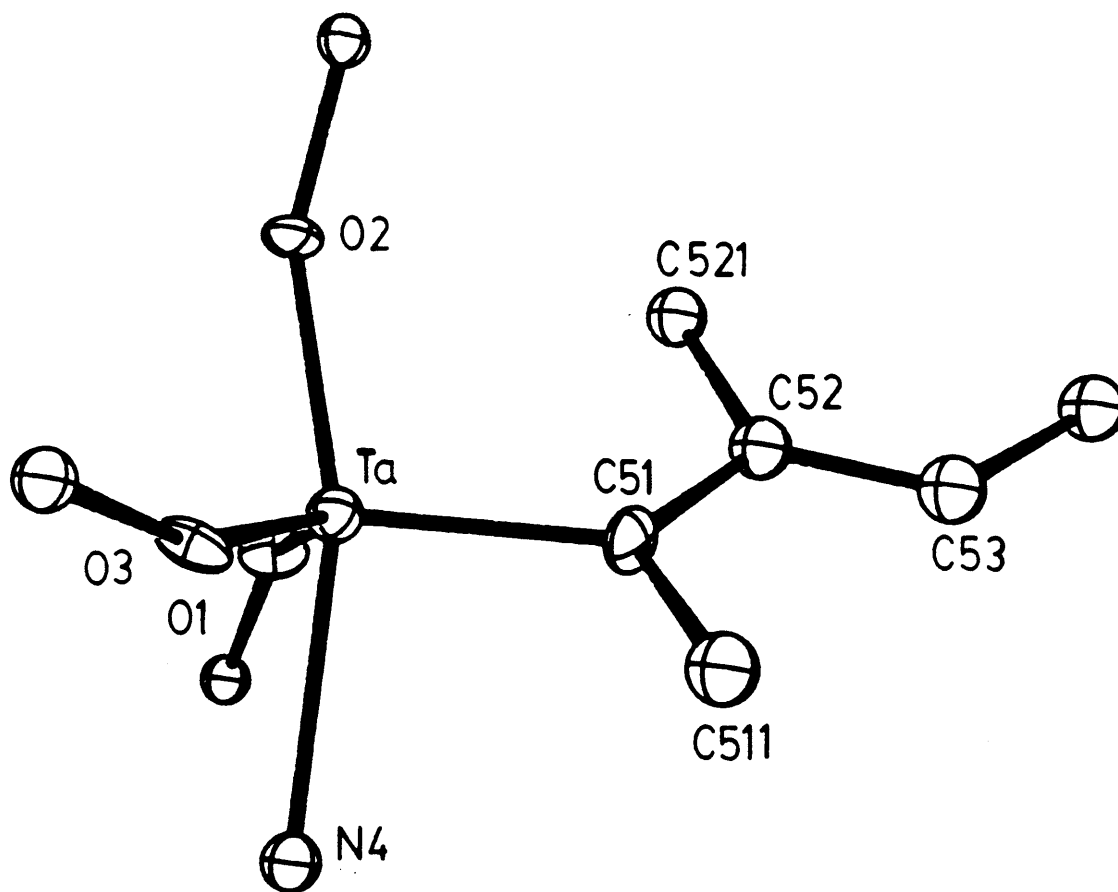
An X-ray study confirmed the alkylidene assignment for complex **42** and serves as the only example of such a study for the  $\text{Ta}(\text{CHR})(\text{DIPP})_3(\text{B})$  ( $\text{B} = \text{base}$ ) class of compounds. An ORTEP drawing of complex **42** is shown in Figure 2a, and the core geometry is displayed in Figure 2b. Relevant bond distances and angles are given in Table III. The overall geometry of this complex is thought best described as a distorted trigonal bipyramid, with the alkylidene ligand occupying an equatorial site and the pyridine ligand occupying an axial site. The angles between the various substituents reflect the bulky nature of the phenoxide ligands. In the equatorial plane the angle between the two DIPP ligands (containing O(1) and O(3)) is  $139.0(7)^\circ$ , while the angles between the alkylidene ligand (containing C(51)) and the DIPP

Figure 2a. A view of  $\text{Ta}(\text{CMeCMeCHCMe}_3)(\text{DIPP})_3(\text{py})$  (**42**).





**Figure 2b.** The core geometry of Ta(CMeCMeCHCMe<sub>3</sub>)(DIPP)<sub>3</sub>(py) (**42**).



**Table III.** Selected Bond Distances (Å) and Angles (°) in **42**.<sup>a</sup>

Ta-O(1)	1.93(1)	O(2)-Ta-C(51)	103.8(8)
Ta-O(2)	1.90(1)	O(1)-Ta-C(51)	106.9(8)
Ta-O(3)	1.95(1)	O(3)-Ta-C(51)	110.3(8)
Ta-C(51)	1.99(2)	O(1)-Ta-N(4)	82.2(7)
Ta-N(4)	2.31(2)	O(2)-Ta-N(4)	164.0(7)
C(51)-C(52)	1.47(3)	O(3)-Ta-N(4)	79.9(6)
C(52)-C(53)	1.38(3)	C(51)-Ta-N(4)	92.0(8)
O(1)-Ta-O(3)	139.0(7)	C(11)-O(1)-Ta	141(1)
O(2)-Ta-O(1)	90.8(7)	C(21)-O(2)-Ta	155(1)
O(2)-Ta-O(3)	96.5(6)	C(31)-O(3)-Ta	156(1)

<sup>a</sup> Ta(CMeCMeCHCMe<sub>3</sub>)(DIPP)<sub>3</sub>(py) (**42**).

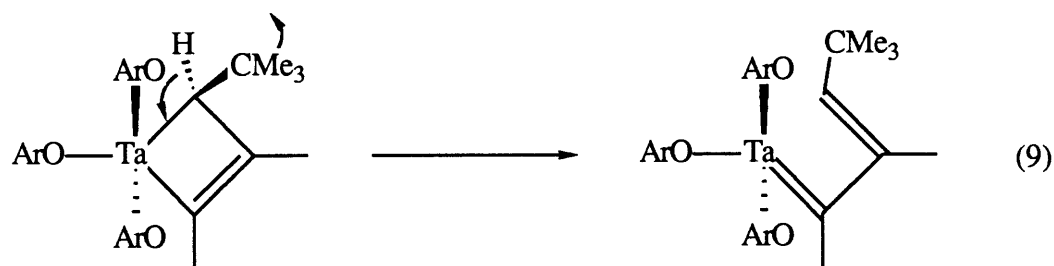
ligands are smaller ( $110.3(8)^\circ$  and  $106.9(8)^\circ$ ). Additionally, the equatorial groups are slightly bent towards the axial pyridine ligand (containing N(4);  $\angle$  O(1)-Ta-N(4) =  $82.2(7)^\circ$ ,  $\angle$  O(3)-Ta-N(4) =  $79.9(6)^\circ$ , and  $\angle$  C(51)-Ta-N(4) =  $92.0(8)^\circ$ ) and away from the axial DIPP ligand (containing O(2);  $\angle$  O(1)-Ta-O(2) =  $90.8(7)^\circ$ ,  $\angle$  O(3)-Ta-O(2) =  $96.5(6)^\circ$ , and  $\angle$  C(51)-Ta-O(2) =  $103.8(8)^\circ$ ). The angle between the two axial substituents is  $164.0(7)^\circ$ .

A related dinitrogen compound,  $(\text{THF})(\text{DIPP})_3\text{Ta}=\text{N}=\text{N}=\text{Ta}(\text{DIPP})_3(\text{THF})$ , displayed a somewhat analogous geometrical configuration,<sup>19</sup> suggesting that DIPP ligands do display certain geometrical preferences (as discussed in chapter 1). In complex **42**, the observed equatorial binding of the alkylidene ligand and axial binding of the pyridine ligand (making these two groups *cis* to one another) is an especially important feature, since this represents a fundamental difference between the structure of a five-coordinate phenoxide alkylidene complex and an analogous thiolate alkylidene complex (in which the base is *trans* to the alkylidene ligand, as is seen in  $\text{Ta}(\text{CHCMe}_3)(\text{TIPT})_3(\text{Et}_2\text{S})$  (**9**); chapter 1 and appendix 1).

The Ta-O bond lengths (average length  $\approx 1.93 \text{ \AA}$ ) are similar to those observed in other tantalum DIPP complexes (chapters 1 and 2), and the Ta-C(51) bond distance of  $1.99(2) \text{ \AA}$  is consistent with a tantalum carbon double bond.<sup>1</sup> Other bond lengths of the alkylidene chain suggest, as anticipated, a vinyl alkylidene assignment, with carbon atoms C(51) and C(52) (originally from 2-butyne) separated by  $1.47(3) \text{ \AA}$  and carbon atoms C(52) and C(53) separated by  $1.38(3) \text{ \AA}$ . The dihedral angle between the planes defined by Ta-C(51)-C(511) and C(521)-C(52)-C(53) of  $\sim 10^\circ$  reveals that the vinyl alkylidene chain is not planar as would be expected in a highly conjugated chain but instead slightly twisted about the C(51)-C(52) bond, perhaps thereby relieving some steric strain in the complex. The alkylidene ligand is also twisted out of the "equatorial plane" (i.e. about Ta-C(51)).

Another interesting feature in the structure of complex **42** is the *cis* configuration of the *t*-butyl and methyl groups on the end olefin group of the alkylidene ligand. This *cis* configuration is not surprising, when considering the ring-opening reaction that leads to the

formation of **42** (equation 9). As can be seen in equation 9, rotation of the  $\alpha$  hydrogen

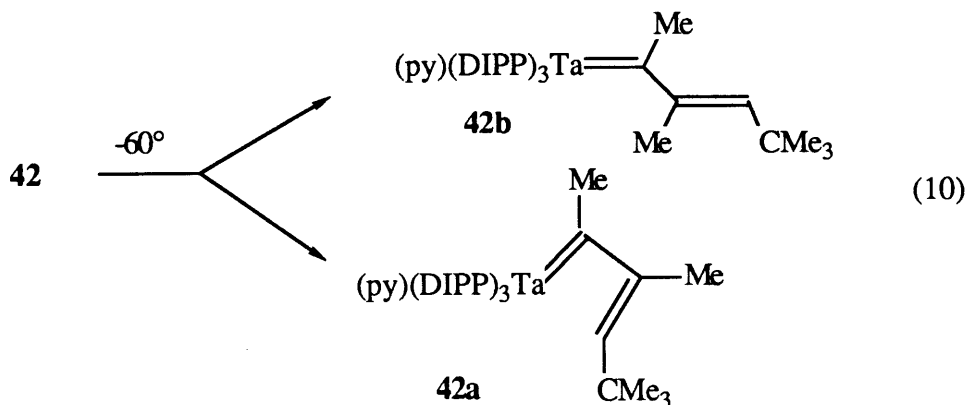


towards the metal and concomitant rotation of the  $\alpha$  t-butyl group away from the metal leads to the observed *cis* configuration about the end olefin group of the alkyldiene chain. The opposite rotations would be required to give a *trans* configuration, and this would involve an unfavorable steric interaction between the t-butyl group and phenoxide ligands.

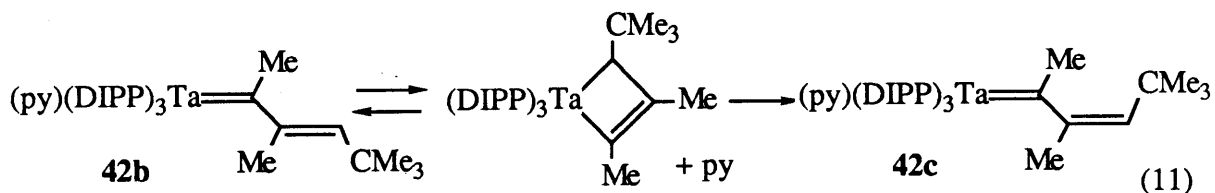
In solution complex **42** is in equilibrium with the metallacyclobutene **35**, and ring-opening as shown in equation 9 is thought to be predominant, although low temperature NMR experiments (performed in an attempt to freeze out the alkyldiene complex) did show evidence for two distinct alkyldiene species. A low temperature ( $\sim -60^\circ$ )  $^1\text{H}$  NMR spectrum of **42** in *dg*-toluene displayed resonances for two distinct types of pyridine ( $\text{py}_{\text{ortho}}$ : 8.64 and 8.22 ppm, both broad,  $\sim 1:3$  ratio), and dual signals were also seen for other substituents (such as the  $\alpha$  *CMe* group of the alkyldiene chain). A low temperature  $^{13}\text{C}$  NMR spectrum ( $\sim -60^\circ$ , *dg*-toluene) displayed similar resonances, with two resonances observed for the alkyldiene carbon at 246.4 (major) and 232.0 ppm (minor).

The resonances noted in these NMR spectra are thought to arise from two geometric isomers of complex **42**. One possible pair of isomers is shown below in equation 10. In complex **42a** the end olefin group is rotated towards the metal (possibly allowing interaction with the metal), while in complex **42b** (the observed solid-state structure), the end olefin group is rotated away from the metal (in both isomers the methyl and t-butyl substituents of the end olefin group are *cis* to one another). If **42a** and **42b** give rise to the NMR resonances described

above, the  $C_{\alpha}$  resonance at 232.0 ppm should be ascribed to **42a**, since this complex is most closely related to the metallacyclobutene complex **35** ( $C_{\alpha}$ : 217.9 ppm).

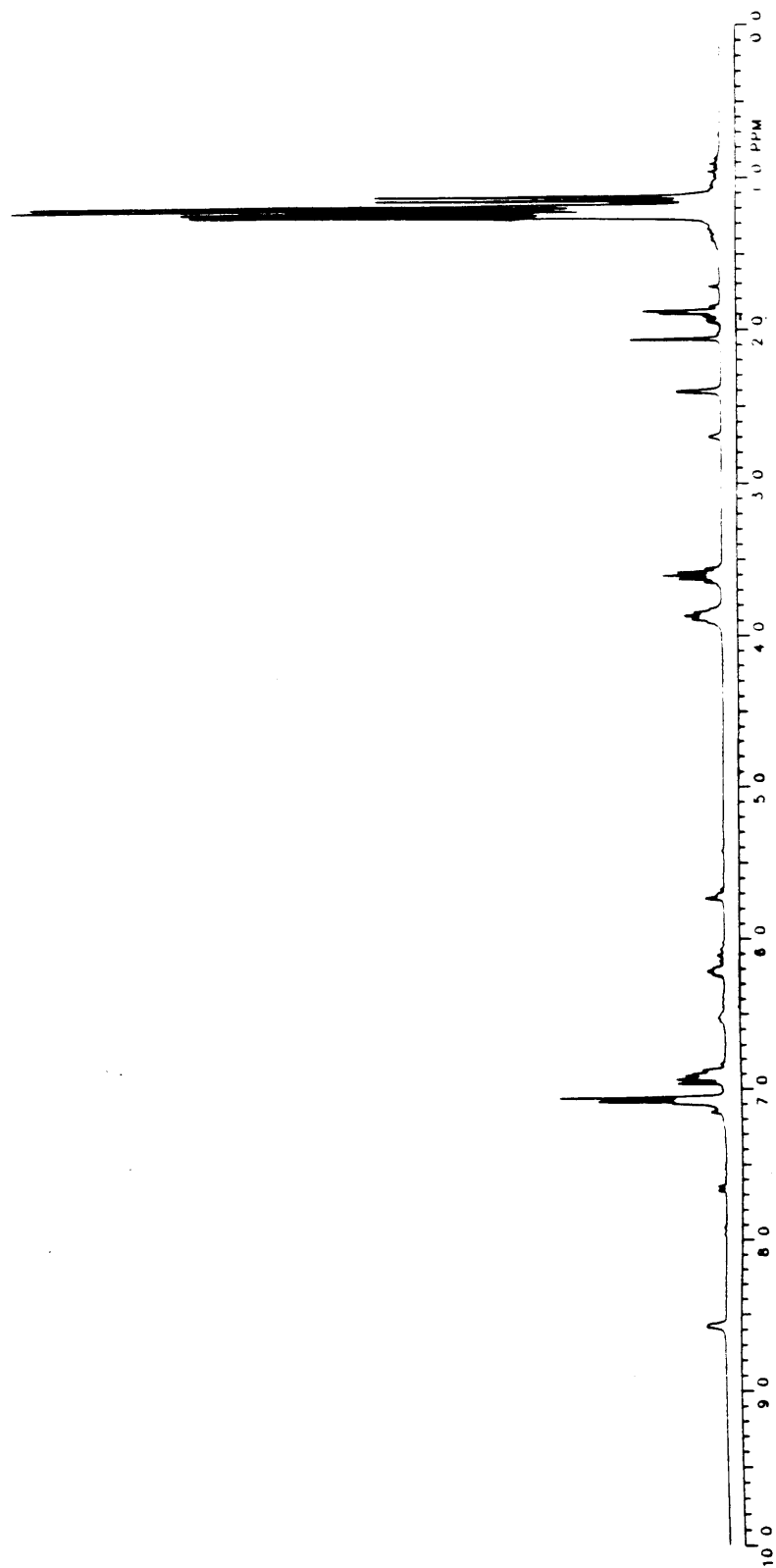


One might also consider the two isomers of complex **42** shown below in equation 11 (**42b** and **42c**) as possibly giving rise to the low temperature dual resonances. However, based on decomposition studies with complex **42** (see below), formation of the *trans* isomer **42c** (i.e. substituents are *trans* about the end olefin group) is thought to be largely irreversible. In the low temperature studies described above, upon warming samples back to 25° only one set of resonances was observed, so formation of **42c** in the low temperature experiments is thought unlikely.



When complex **42** is left in  $C_6D_6$  at 25°, over one day new resonances are seen to grow in as those for **42** decrease in intensity. When this solution is then left at a slightly elevated temperature (~40°) for an additional 2 days, the resulting  $^1H$  NMR spectrum shows all of complex **42** consumed. Furthermore, resonances indicative of a new complex (thought to be

Figure 3. The  $^1\text{H}$  NMR spectrum of **42** in  $\text{C}_6\text{D}_6$  after standing at  $40^\circ$  for 2 days.

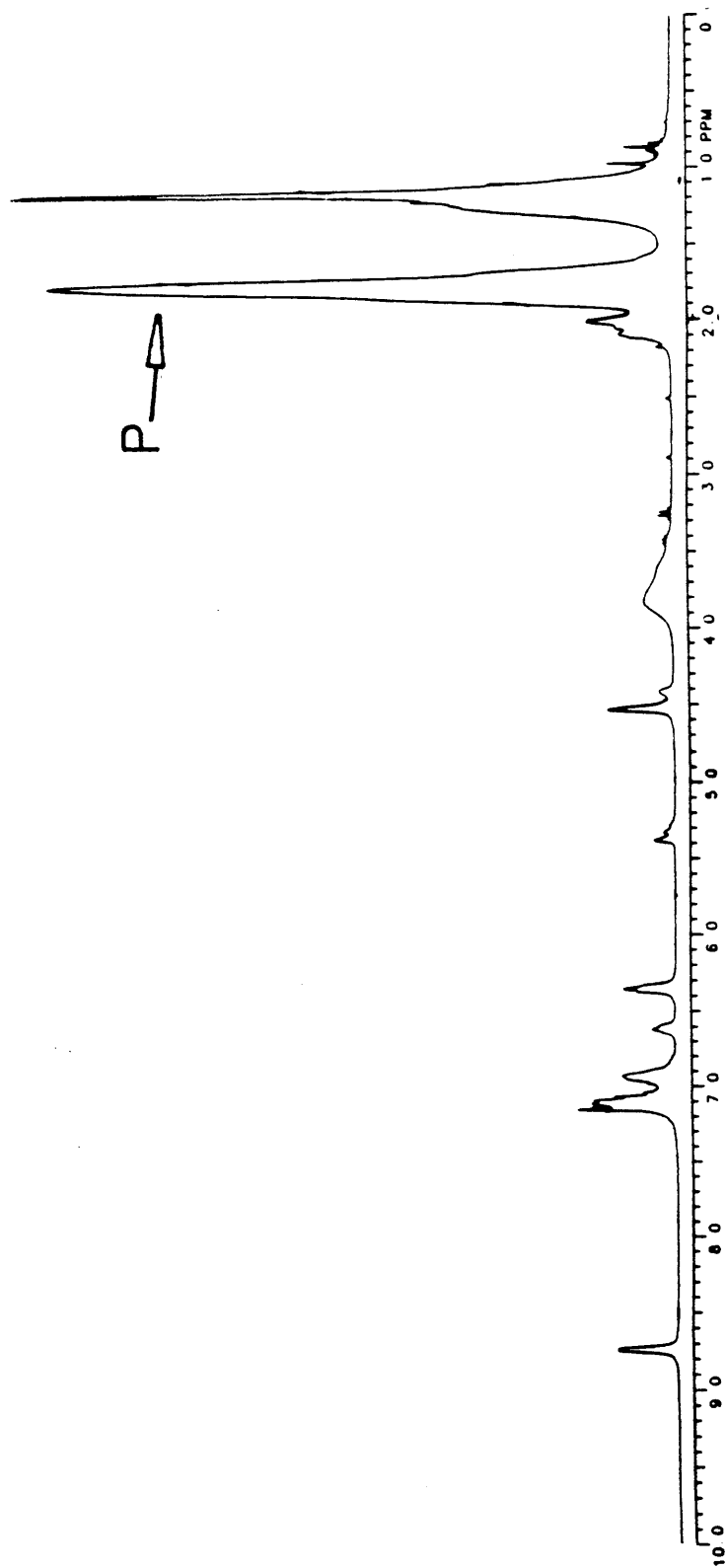


**42c**;<sup>141</sup> equation 11) and of the metallacyclobutene complex **35** are observed (~1:1 mixture), along with other resonances attributed to unidentified decomposition (this <sup>1</sup>H NMR spectrum is shown in Figure 3). The formation of **42c** appears to be irreversible (i.e. complex **42c** is not in equilibrium with the metallacyclobutene complex **35**). The irreversibility is not surprising, since the *trans* configuration of the olefin group in **42c** should hinder addition of this group to the tantalum carbon double bond. Unfortunately, the isomerization is accompanied by other complicating decomposition reactions, and all attempts to isolate complex **42c** failed, making a positive identification impossible. The significant amount of base-free metallacyclobutene complex **35** formed is thought to result from the consumption of all free pyridine by other decomposition reactions (in addition to the formation of **42c**), thereby stabilizing the metallacycle.

#### **Polymerization of 2-Butyne by Ta(CMeCMeCHCMe<sub>3</sub>)(DIPP)<sub>3</sub>(py) (**42**).**

While the trisubstituted metallacyclobutene complex Ta[C(Ph)C(Ph)CH(CMe<sub>3</sub>)](DIPP)<sub>3</sub> (**36**) reacts with pyridine to form the disubstituted alkylidene Ta(CPhCPhCHCMe<sub>3</sub>)(DIPP)<sub>3</sub>(py) (**43**), complex **43** does not polymerize acetylenes in a controlled manner. With diphenylacetylene no reactivity is observed, and with 2-butyne, although some polymer formation is evident, only the starting complex **43** is seen in subsequent spectra (suggesting a poor initiation step in this reaction). This lack of reactivity is thought to arise from steric constraints that would be associated with a polymerization reaction involving **43** and a disubstituted acetylene (a very crowded metallacyclobutene complex would have to form at least as a transient intermediate). However, the less hindered alkylidene Ta(CMeCMeCHCMe<sub>3</sub>)(DIPP)<sub>3</sub>(py) (**42**) does show further reactivity and will polymerize 2-butyne in a controlled fashion. When complex **42** was reacted with 10 equivalents of 2-butyne in C<sub>6</sub>D<sub>6</sub> at 25°, the color of the solution rapidly changed from dark purple to deep red, and a <sup>1</sup>H NMR spectrum of the resulting solution showed all 2-butyne consumed and resonances indicative of poly-2-butyne<sup>119</sup> (Figure 4). All of the starting alkylidene was also consumed, and resonances indicative of the new alkylidene complex

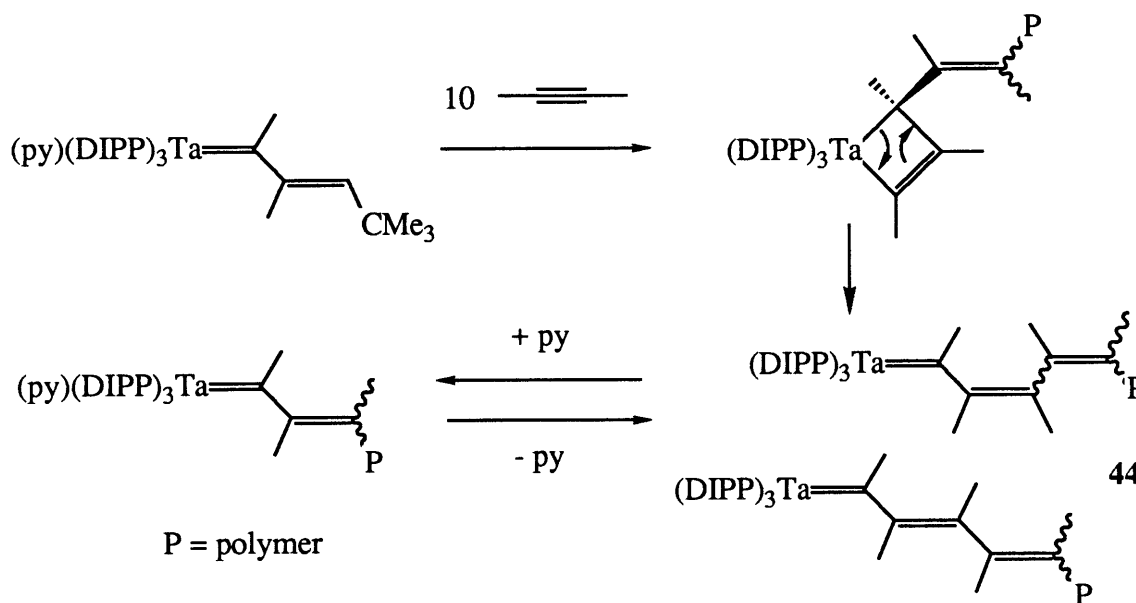
**Figure 4.** The  $^1\text{H}$  NMR spectrum of **42** after reaction with 10 equivalents of 2-butyne in  $\text{C}_6\text{D}_6$  (i.e. complex **44**); P = poly-2-butyne.





Ta(CMeCMeCMeP)(DIPP)<sub>3</sub>(py) (P = poly-2-butyne) (**44**) were observed (Scheme I); no resonances for tetrasubstituted metallacyclobutene species involved in this reaction were noted. In the spectrum of this propagating complex, several broad resonances for the end olefinic H

Scheme I: Reaction of Complex **42** with excess 2-Butyne

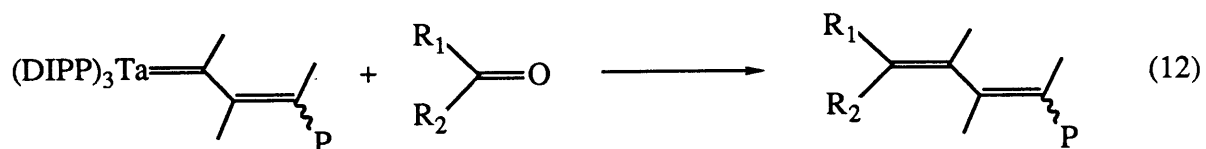


were observed between 5.2 and 5.4 ppm, consistent with a distribution of lengths for the polymer chain in **44**. Two broad overlapping singlets were also observed for the  $\alpha$  CMe group of **44** ( $\sim 4.55$  and  $\sim 4.45$ ,  $\sim 4:1$  ratio), indicative of the two possible orientations for this group relative to the polymer chain (shown in Scheme I; poly-2-butyne does not show extensive conjugation, so both *trans* and *cis* isomers are sterically accessible with a twisting of the polymer chain). A <sup>13</sup>C NMR spectrum (C<sub>6</sub>D<sub>6</sub>, 25°) displayed the C<sub>α</sub> resonance at 258.3 ppm (Table II).

When the solvent was removed *in vacuo* from this sample of **44** in C<sub>6</sub>D<sub>6</sub> and the resulting solid redissolved in C<sub>6</sub>D<sub>6</sub>, a <sup>1</sup>H NMR spectrum indicated that less than one equivalent of pyridine was present, and the resonances for pyridine were very broad. Thus, pyridine is not

thought to be bound strongly to the metal in the alkylidene **44** or to be important in the stabilization of **44** from metallacyclobutene formation (although the presence of *some* pyridine does indicate an equilibrium between base-free and base bound alkylidene species). This contrasts the behavior of Ta(CMeCMeCHCMe<sub>3</sub>)(DIPP)<sub>3</sub>(py) (**42**) in solution: the trisubstituted metallacyclobutene **35** reforms upon dissociation of pyridine from complex **42** (these two complexes are in ready equilibrium in room temperature solution). The decreased stability of a tetrasubstituted metallacyclobutene complex (such as the one shown in Scheme I) versus a trisubstituted complex is consistent with the greater steric demands in a tetrasubstituted complex. In fact, this decreased stability is an important aspect of the catalyst's activity, since less substituted metallacycles might be more stable and consequently less reactive. This also could explain why reaction of 2-butyne with the trisubstituted metallacyclobutene **35** results only in formation of an intractable polymer and recovery of most of the starting complex **35**. Only a small amount of the initiator **35** reacts further *in the absence of a base* to give subsequent alkylidenes and tetrasubstituted metallacyclobutenes, which are much more reactive than **35** and rapidly consume all of the 2-butyne, resulting in high polymer formation.

Complex **42** polymerizes large amounts of 2-butyne rapidly in room temperature solution (100 equivalents within 30 minutes), and the resulting polymers can be cleaved from the metal by reaction with an organic carbonyl such as acetone or benzaldehyde (equation 12). The poly-2-butyne is obtained as a white solid, consistent with the unconjugated nature of this polymer (substituted polyacetylenes often display a lack of extended conjugation in the polymer



chain<sup>2,112</sup>). Polymers prepared from **42** are rubbery in nature and show a limited solubility in common organic solvents. Samples are most soluble in benzene or toluene, somewhat less

soluble in methylene chloride, and only sparingly soluble in pentane. Limited solubilities for polymers of symmetrically substituted acetylenes (relative to other polymers of substituted acetylenes) have been documented,<sup>112,117,119</sup> and for this reason no attempts were made to prepare polymers from more than 200 equivalents of 2-butyne. The assignment as poly-2-butyne was confirmed by <sup>1</sup>H NMR spectroscopy (C<sub>6</sub>D<sub>6</sub>, 300 MHz: δ 1.8 (broad s, [=C(*Me*)-C(*Me*)=]<sub>n</sub>). The *trans* versus *cis* content of the polymers is not known, but is thought to be some combination of both, considering the two resonances observed for the α methyl group of **44**; data have not been reported in the literature that differentiate between these two configurations<sup>119,142</sup> (the polymer chain is shown as all *trans* in most equations only for convenience).

Samples of poly-2-butyne prepared from complex **42** (in toluene) were found to be monodisperse by GPC analysis (in toluene or methylene chloride;  $M_w/M_n$  (d) < 1.05; all GPC results are listed in Table IV), even when the polymerization reaction was quenched a significant amount of time after all of the acetylene had been consumed. While the alkylidene ligand of the living polymer **44** should be highly reactive (and in fact does show reactivity with norbornene; see later), secondary metathesis reactions with the tetrasubstituted olefins of the polymer chain are nevertheless inhibited by steric constraints. As was suggested earlier, pyridine was not found to be a significant factor in this polymerization system. When 50 equivalents of 2-butyne were polymerized by **42** in toluene, followed by removal of the solvent *in vacuo* and then redissolution in toluene, subsequent reactions with 50 additional equivalents of 2-butyne in the presence of 0, 1, and 10 added equivalents of pyridine displayed no significant differences (as evidenced by GPC analysis, Table IV), nor was the reaction rate qualitatively observed to change. (Note: in these reactions removal of the solvent *in vacuo* followed by redissolution in toluene causes deactivation<sup>143</sup> of ~5-10% of the catalyst complex before reaction with the second aliquot of 2-butyne, probably due to a reaction of this highly air/moisture sensitive catalyst with trace amounts of water in the solvent. When 50 equivalents of 2-butyne were polymerized followed by a subsequent addition of 50 more equivalents of

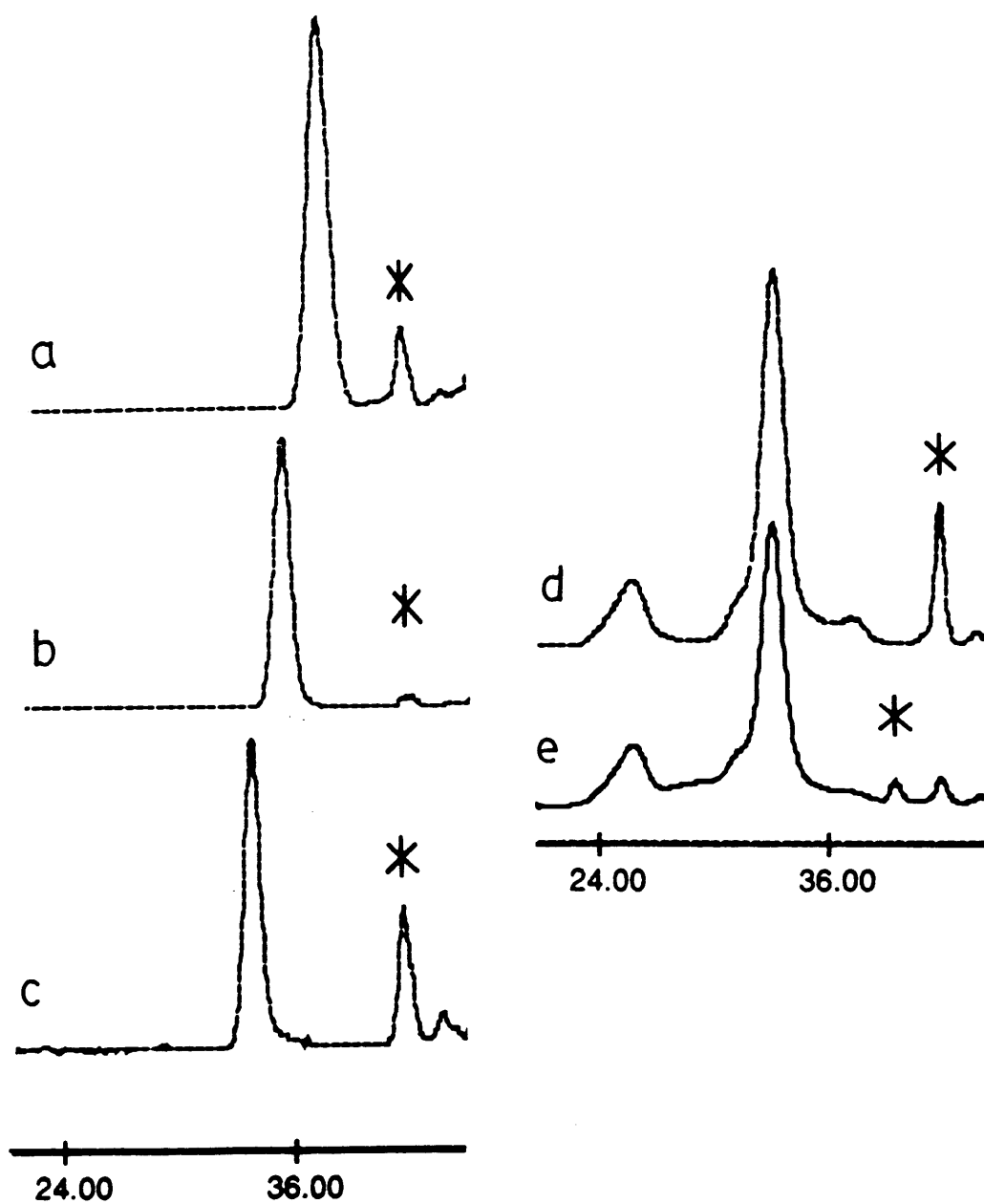
**Table IV.** The Results of GPC Analysis of Polyacetylenes.<sup>a,e</sup>

Run	Cat	2-Butyne	Other	Solvent	M <sub>n</sub> (uncorr)	M <sub>w</sub> /M <sub>n</sub>
1	42	50	0	M.C.	3,900 (UV)	1.04
2	42	100	0	M.C.	7,400 (UV)	1.03
3	42	150	0	M.C.	11,200 (UV)	1.03
4	42	100	0	Tol	9,900 (R.I.)	1.05
5	42	200	0	Tol	17,900 (R.I.)	1.03
6 <sup>h,i</sup>	42	100	0	M.C.	7,400 (UV)	1.03
7 <sup>h,i</sup>	42	100	0	M.C.	7,300 (UV)	1.03
8 <sup>h,i</sup>	42	100	0	M.C.	7,400 (UV)	1.03
9 <sup>i</sup>	42	50	50 (NBE) <sup>c</sup>	M.C.	15,100 (UV)	1.12
					332,800 (UV)	1.39
10 <sup>i</sup>	42	100	100 (NBE) <sup>c</sup>	Tol	46,200 (R.I.)	1.07
					~400,000 (R.I.)	>1.50
11 <sup>i</sup>	d	50	50 (NBE)	M.C.	18,400 (UV)	1.23
					219,500 (UV)	1.41
12 <sup>f</sup>	47	100	0	M.C.	16,900 (UV)	~1.03
					66,800 (UV)	1.20
13 <sup>b</sup>	42	0	100 (1-pentyne)	M.C.	13,000 (R.I.)	1.30
14 <sup>b</sup>	42	0	100 (1-pentyne)	M.C.	13,700 (R.I.)	1.21
15	42	0	200 (1-pentyne)	M.C.	15,900 (R.I.)	2.60
16	g	100	0	M.C.	6,900 (UV)	1.47

**Table IV (continued)**

- a M.C. = methylene chloride; Tol = toluene; UV = UV/VIS detection; R.I. = refractive index detection; Cat = catalyst complex employed. Solvent = solvent employed in GPC system and solvent in which the polymer sample was dissolved for analysis (i.e. these solvents are identical, unless otherwise noted). In all block copolymer experiments, after polymerization of the first monomer a sample confirmed clean formation of the expected polymer from the first monomer.
- b Run 13 reaction time = 60 minutes; run 14 reaction time = 15 minutes (runs 13 and 14 from same experiment, with samples taken at two different times).
- c NBE added after polymerization of 2-butyne.
- d Catalyst = Ta[CH(C<sub>5</sub>H<sub>8</sub>)CHCH(CMe<sub>3</sub>)](DIPP)<sub>3</sub> (**26**); 2-butyne was added after polymerization of NBE and subsequent addition of 3 equivalents of pyridine. The higher molecular weight fraction was the largest.
- e Some higher molecular weight samples of poly-2-butyne did not completely dissolve in solution for analysis (for further information see Experimental Section).
- f In presence of 2 equivalents of pyridine; sample dissolved in 1/1 M.C./Tol for analysis.
- g Catalyst = Ta(CHCMe<sub>3</sub>)(TIPT)<sub>3</sub>(THF) (**6**); sample dissolved in 4/1 M.C./Tol for analysis.
- h In these runs, after polymerization of 50 equivalents of 2-butyne, the solvent was removed *in vacuo*, and the sample was redissolved in toluene with 0 (run 6), 1 (run 7), or 10 (run 8) equivalents of pyridine. 50 additional equivalents of 2-butyne was then polymerized.
- i A small amount of deactivation after polymerization of the first monomer was also evidenced by GPC (as discussed in the text).

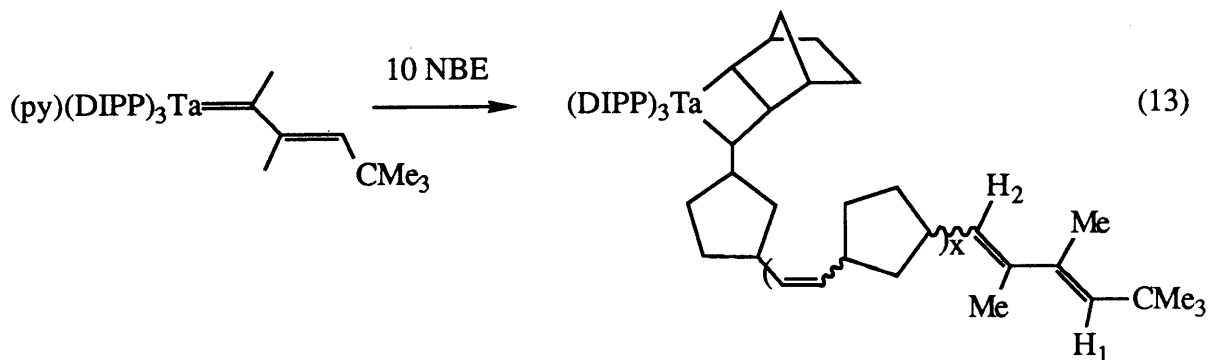
**Figure 5.** GPC traces for the benzylidene-capped poly-2-butyne formed by reaction of **42** with (a) 50 equivalents, (b) 100 equivalents, and (c) 150 equivalents of 2-butyne, and GPC traces for a benzylidene capped block copolymer formed by reaction of **42** with 50 equivalents of 2-butyne and 50 equivalents of NBE ((d) UV/VIS detection (e) refractive index detection). x axis = minutes; \* = highest molecular weight solvent peak (i.e. all peaks of a lower molecular weight, or a higher retention time, are also solvent peaks).



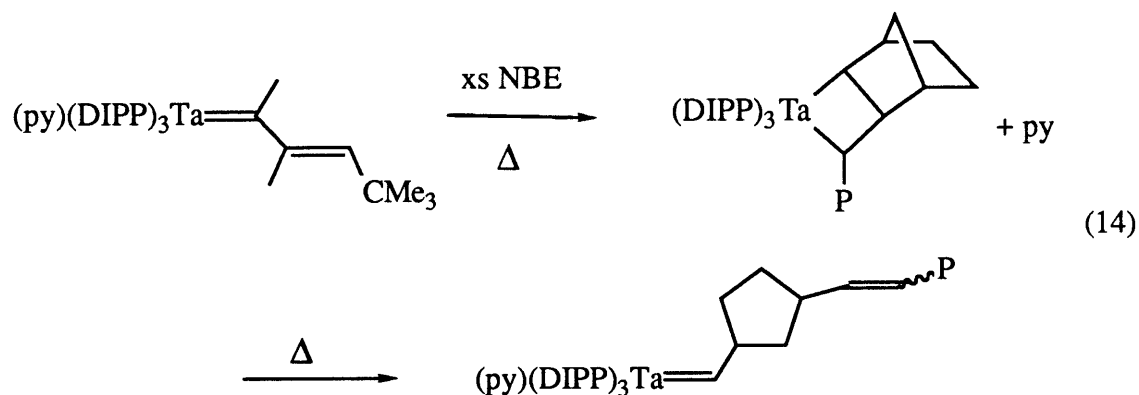
2-butyne, *without* removal of the solvent and redissolution in toluene between additions, no catalyst deactivation was observed.) In addition to the formation of monodisperse polymers, the molecular weights of the polymers also increase proportionally with the number of equivalents employed (Table IV, Figure 5), confirming the absence of chain termination in this system (for 50, 100, and 150 equivalents of monomer consumed,  $M_n = 3,900, 7,400,$  and  $11,200,$  respectively). All of these results are indicative of a living polymerization and represent a rare example of such a reaction for the polymerization of an acetylene.<sup>136</sup>

#### Preparation of 2-Butyne/NBE Block Copolymers.

The successful synthesis of monodisperse poly-2-butyne using  $\text{Ta}(\text{CMeCMeCHCMe}_3)(\text{DIPP})_3(\text{py})$  (**42**) and the related synthesis of monodisperse polynorbornene using  $\text{Ta}[\text{CH}(\text{C}_5\text{H}_8)\text{CHCH}(\text{CMe}_3)](\text{DIPP})_3$  (**26**) (chapter 2) presented an attractive situation for the investigation of block copolymer synthesis. To test the utility of complex **42** as a catalyst for the ring-opening polymerization of NBE, an initial NMR experiment was performed. Complex **42** was reacted with 10 equivalents of NBE in  $\text{C}_6\text{D}_6$ , with addition of NBE at room temperature followed by heating, to give a colorless solution. The resulting  $^1\text{H}$  NMR spectrum revealed polynorbornene formation and all starting material consumed, and showed resonances characteristic of a propagating tantalacyclobutane species (analogous to that seen for  $\text{Ta}[\text{CH}(\text{C}_5\text{H}_8)\text{CHCH}(\text{P})](\text{DIPP})_3$ ,  $\text{P} = \text{polynorbornene}$ ). Resonances for  $\text{H}_1$  (s,  $\sim 5.7$  ppm) and  $\text{H}_2$  (d,  $\sim 5.1$  ppm), as shown in equation 13, were also



noted. When **42** was reacted with 100 equivalents of NBE (with addition at room temperature followed by reaction at elevated temperature; see Experimental Section for details), analysis of the resulting polymer by GPC gave  $M_n = 18,700$  (a trace amount of a higher molecular weight polymer was also observed), consistent with results obtained earlier with  $\text{Ta}[\text{CH}(\text{C}_5\text{H}_8)\text{CHCHCMe}_3](\text{DIPP})_3$ , except for the trace amount of high molecular weight polymer observed. Additionally, the dispersity of this polymer (1.04) was much lower than those obtained with  $\text{Ta}[\text{CH}(\text{C}_5\text{H}_8)\text{CHCH}(\text{CMe}_3)](\text{DIPP})_3$ , indicating the presence of pyridine actually inhibited a secondary metathesis reaction. In fact, towards the end of the polymerization reaction of NBE by **42**, the solution changed from colorless to light yellow (not observed for NBE polymerization by  $\text{Ta}[\text{CH}(\text{C}_5\text{H}_8)\text{CHCH}(\text{CMe}_3)](\text{DIPP})_3$ ), suggesting the formation of an alkylidene species (equation 14; tantalum alkylidene complexes generally show



more color than related tantalacyclobutane complexes; chapter 1). The formation of a pyridine bound alkylidene complex as shown in equation 14 would be expected to decrease the rate of secondary metathesis reactions, since pyridine occupies a potential coordination site on the metal.

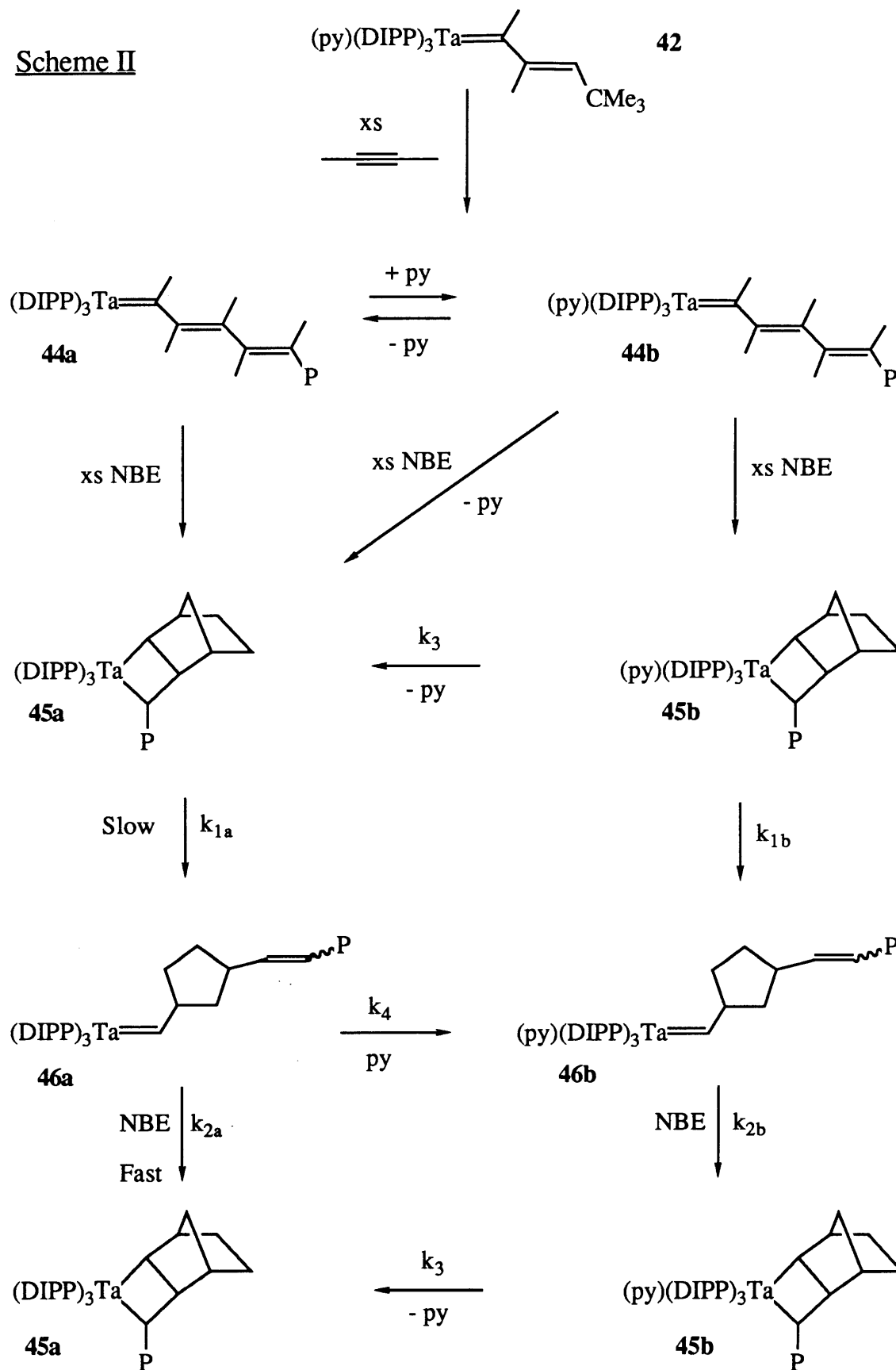
Related reactions involving the polymerization of both 2-butyne and norbornene by  $\text{Ta}(\text{CMeCMeCHCMe}_3)(\text{DIPP})_3(\text{py})$  (**42**) do result in the formation of block copolymers, as evidenced by GPC analysis and  $^1\text{H}$  NMR spectroscopy (resonances indicative of both



polynorbornene and poly-2-butyne were seen), although certain complications are apparent. The polymerization of 50 equivalents of 2-butyne followed by the polymerization of 50 equivalents of NBE yielded, by GPC analysis (Table IV, Figure 5), both the expected block copolymer ( $M_n = 15,100$ ,  $d = 1.12$ ; 75% by UV/VIS detection) and a higher molecular weight polymer ( $M_n = 332,800$ ,  $d = 1.39$ ; 19% by UV/VIS detection). A small amount of poly-2-butyne ( $M_n = 4,200$ ,  $d = 1.04$ ; 6%) was also observed. Refractive index detection of this polymer sample showed a similar distribution of molecular weights (also shown in Figure 5), although the molecular weight distributions appeared to be broader, as evidenced by a less defined baseline in the chromatogram. Changing the temperature of addition for NBE ( $-30^\circ$ , r.t.,  $60^\circ$ ) did not alter the results significantly.

The problems noted above for block copolymer synthesis using complex **42** as the catalyst in some ways appear to mimic the problems noted earlier (in chapter 2) for the polymerization of NBE by  $\text{Ta}(\text{CHCMe}_3)(\text{DIPP})_3(\text{THF})$  (**2**) (i.e. the presence of a base might allow formation of highly reactive base adduct metallacycles). Considering this, one possible explanation for the formation of both the expected block copolymer and a higher molecular weight polymer (also thought to be a block copolymer) is shown in Scheme II. Complex **42** reacts with 2-butyne to give an equilibrium mixture of **44a** and the pyridine adduct **44b** (as discussed earlier). Complex **44a** should react with NBE to give the base-free metallacyclobutane complex **45a**, while **44b** could react with NBE to give either the base-free metallacyclobutane **45a** or the pyridine adduct metallacyclobutane **45b**. Assuming that the metallacyclobutane complexes **45a** and **45b** ring-open to the alkylidene complexes **46a** and **46b**, respectively, *before* reaction with NBE or base (as was demonstrated for related base-free tantalacyclobutane complexes in chapter 2), complex **45b** should react to form **46b** much faster than complex **45a** reacts to form **46a**, since ring-opening of **45b** to the alkylidene complex (**46b**) is base assisted ( $k_{1b} \gg k_{1a}$ ). Knowing  $k_{2a}[\text{NBE}] \gg k_{1a}$  (from chapter 2) and assuming  $k_{2b}[\text{NBE}] \gg k_{1a}$  (related base bound alkylidenes have been reported to react readily

## Scheme II

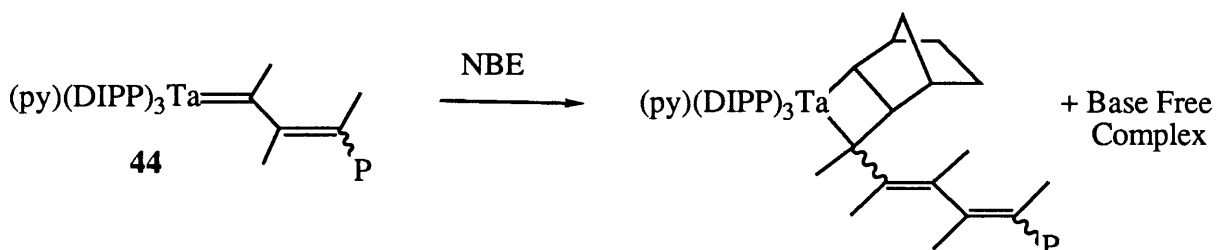
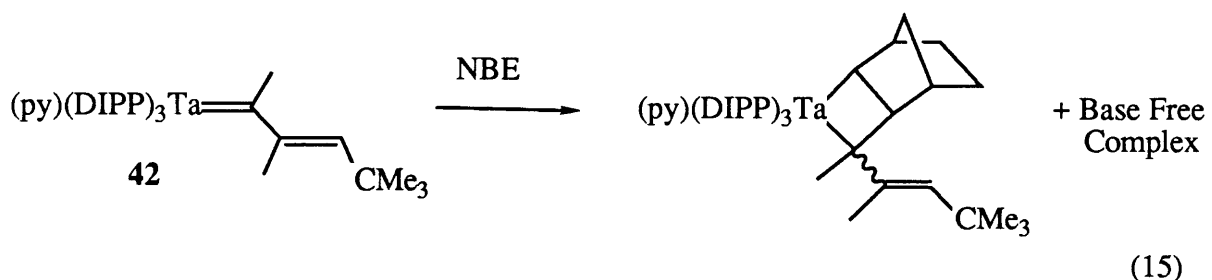


with olefins in room temperature solution, while metallacycles like **45a** do not; chapter 2), then regardless of whether  $k_{1b}$  is greater than  $k_{2b}[\text{NBE}]$  or vice versa, NBE reaction with **45b/46b** should be faster than NBE reaction with **45a/46a**. Consequently, the polymer formed from NBE reaction with **45b/46b** should be of a higher molecular weight (i.e. the high molecular weight polymer observed in the GPC chromatogram).

The formation of **45a** from **45b** may also occur to some degree ( $k_3$ ) and would help to explain the larger polydispersity observed for the high molecular weight polymer, since the formation of **45a** from **45b** can be viewed as a deactivation reaction for the "base on" mechanism if  $k_{1b} \gg k_{1a}$  and  $k_{2b}[\text{NBE}] \gg k_{1a}$  (as is thought). Finally, it is also possible that the base free alkylidene **46a** could react with pyridine to give the pyridine adduct alkylidene **46b** (i.e.  $k_4[\text{py}] > k_{2a}[\text{NBE}]$ ), although this is thought to be unlikely since the expected block copolymer displays a somewhat narrow molecular weight distribution ( $d = 1.12$ ) and related complexes (chapter 2) react faster with NBE than with the base THF; additionally, polymerization of NBE by  $\text{Ta}(\text{CMe}_2\text{CHCMe}_3)(\text{DIPP})_3(\text{py})$  (**42**) appeared to result in formation of a pyridine adduct alkylidene only *after* NBE was consumed (see earlier). Clearly the presence of a base (pyridine) in this reaction is a limiting factor, although the "base on" polymerization does produce only the minor product (~19%).

Why complex **42** functions as an efficient catalyst for the polymerization of NBE (with only a trace of high polymer formed) while **44** does not is unclear. The only obvious difference between these reactions is the structure of the initial tantalacyclobutanes formed from reaction of the pyridine bound complexes with one equivalent of NBE (equation 15). If the initial pyridine adduct metallacycle formed from **42** loses pyridine at a rate much greater than that for the one formed from **44b** (i.e.  $k_3$  of Scheme II), then conceivably the "base on" mechanism could be effectively eliminated for the reaction initiated by **42**. The "all *cis*" configuration of the  $\alpha$   $\text{C}(\text{Me})=\text{CH}(\text{CMe}_3)$  group on the metallacycle derived from **42** should allow rotation of this group towards the metal (as is shown for **42a** in equation 10), possibly

aiding in pyridine loss from this complex during reaction with NBE. Other attempts to prepare

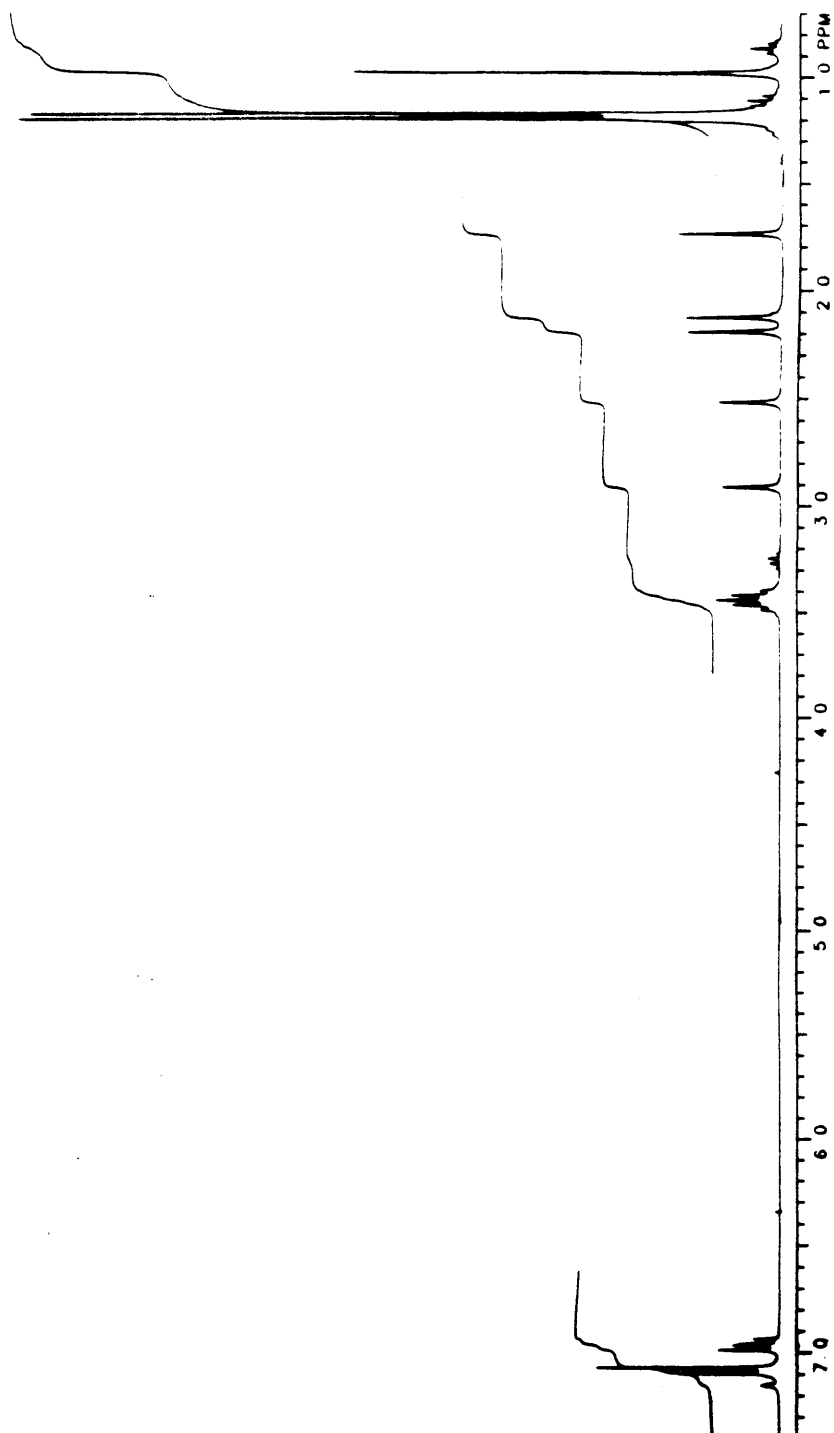


monodisperse block copolymers, such as employing  $\text{Ta}[\text{CH}(\text{C}_5\text{H}_8)\text{CHCH}(\text{CMe}_3)](\text{DIPP})_3$  (**26**) as the catalyst (adding NBE first, followed by addition of pyridine and then 2-butyne), were somewhat less successful.

#### Reaction of $\text{Ta}(\text{CMeCMechCMe}_3)(\text{DIPP})_3(\text{py})$ (**42**) with One Equivalent of 2-Butyne.

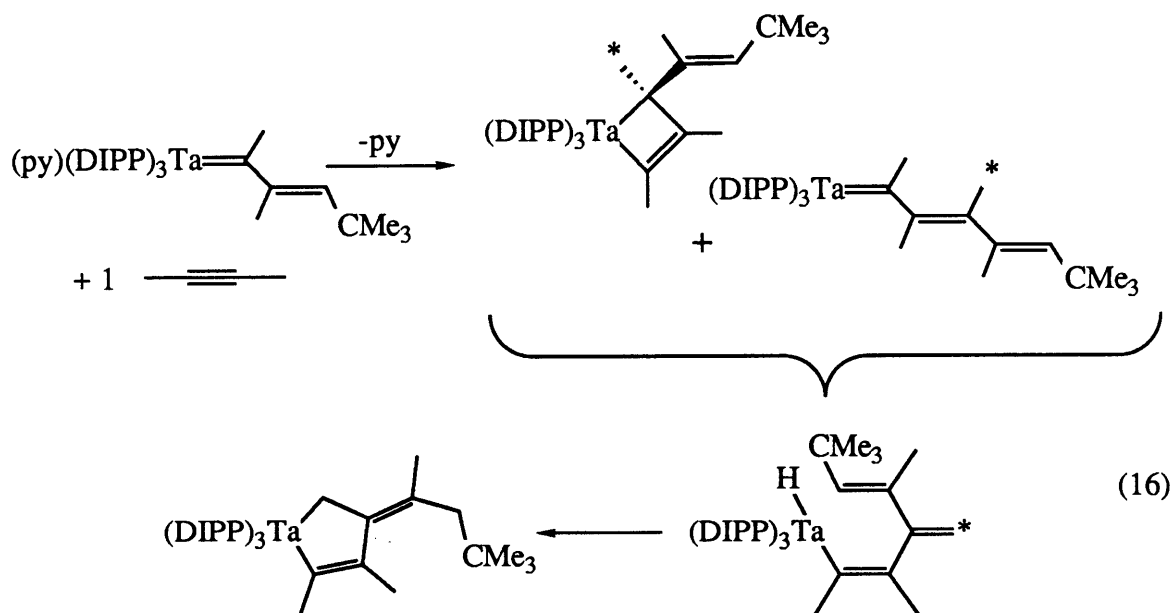
In an attempt to isolate intermediate species involved in the polymerization of 2-butyne by  $\text{Ta}(\text{CMeCMechCMe}_3)(\text{DIPP})_3(\text{py})$  (**42**), complex **42** was reacted with one equivalent of 2-butyne. From this reaction (in ether), after removal of the solvent *in vacuo*, a deep red oil was obtained. This oil is extremely soluble in common organic solvents such as ether and pentane, but a red precipitate can be isolated from pentane at  $-30^\circ$  after several days; light orange crystals of this product can be obtained on recrystallization of the precipitate. A  $^1\text{H}$  NMR spectrum of the precipitate (or crystals) ( $\text{C}_6\text{D}_6$ ,  $25^\circ$ ) showed a single product (**47**) that does not contain pyridine (Figure 6). In addition to resonances for the DIPP ligands and a *t*-butyl group, five singlets were observed at 2.91 (2H), 2.51 (2H), 2.19 (3H), 2.12 (3H), and 1.74 (3H), and no resonances were observed in the region for olefinic H's. The spectrum at elevated temperatures revealed no significant differences. A  $^{13}\text{C}$  NMR spectrum of this

Figure 6. The  $^1\text{H}$  NMR spectrum of **47** in  $\text{C}_6\text{D}_6$ .



precipitate ( $C_6D_6$ ,  $25^\circ$ ) displayed the expected resonances for the DIPP ligands and the *t*-butyl group, and additional resonances were observed at 214.0 (s), 158.7 (s), 148.9 (s), 129.2 (s), 82.3 (t,  $J_{CH} = 119$  Hz), and 47.5 (t,  $J_{CH} = 124$  Hz); three Me resonances were also noted. Although an additional equivalent of 2-butyne apparently had been incorporated into the initial complex **42**, the NMR data were not consistent with the formation of either a simple metallacyclobutene or alkylidene complex, the two compounds thought most likely to be formed from this reaction.

Because the above mentioned reaction is closely related to the polymerization of 2-butyne by complex **42**, the structure of **47** was determined by X-ray crystallography and found to be an unusual metallacyclopentene complex (shown in equation 16). An ORTEP



drawing of the molecule is shown in Figure 7, and relevant bond distances and angles are given in Table V. As with other DIPP complexes, the geometry of **47** is neither clearly a trigonal bipyramid or a square pyramid, but most interligand angles are more characteristic of the former (considering C(1) and O(3) in pseudo axial positions). Bond distances and angles for the DIPP ligands are normal (average Ta-O bond length  $\approx 1.88$  Å; average  $\angle$  Ta-O-C  $\approx$

Figure 7. A view of Ta[C(Me)C(Me)C(CMeCH<sub>2</sub>CMe<sub>3</sub>)CH<sub>2</sub>](DIPP)<sub>3</sub> (47).

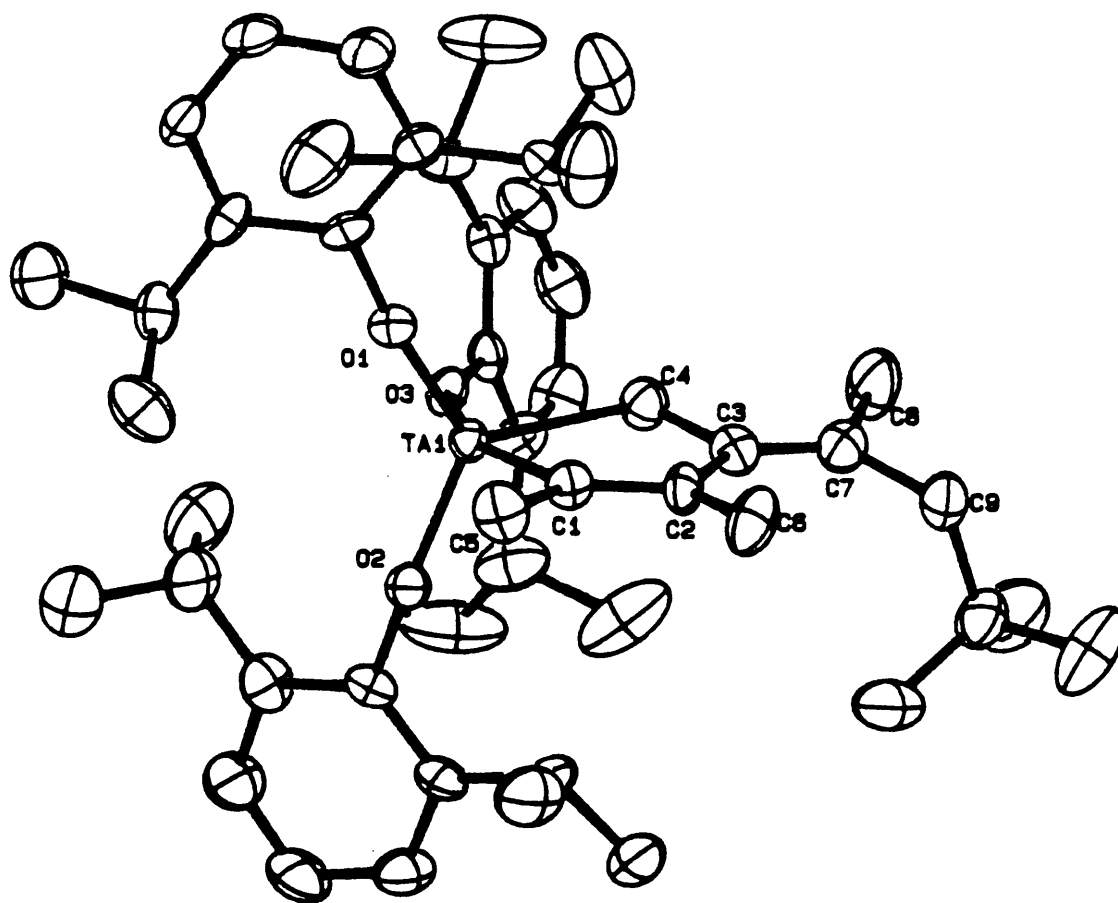


**Table V.** Selected Bond Distances (Å) and Angles (°) in **47**.

Ta-O(1)	1.857(7)	O(1)-Ta-C(4)	115.9(3)
Ta-O(2)	1.860(7)	O(2)-Ta-C(1)	93.9(3)
Ta-O(3)	1.917(7)	O(2)-Ta-C(4)	122.1(4)
Ta-C(1)	2.12(1)	O(3)-Ta-C(1)	154.1(3)
Ta-C(4)	2.18(1)	O(3)-Ta-C(4)	80.8(4)
C(1)-C(2)	1.35(1)	C(1)-Ta-C(4)	73.3(4)
C(2)-C(3)	1.46(1)	C(11)-O(1)-Ta	171.7(6)
C(3)-C(7)	1.35(1)	C(21)-O(2)-Ta	158.6(7)
C(3)-C(4)	1.52(1)	C(31)-O(3)-Ta	151.8(6)
O(1)-Ta-O(2)	121.4(3)	C(2)-C(1)-Ta	122.8(8)
O(1)-Ta-O(3)	98.9(3)	C(3)-C(4)-Ta	116.7(7)
O(2)-Ta-O(3)	97.8(3)	C(1)-C(2)-C(3)	115(1)
O(1)-Ta-C(1)	94.4(3)	C(2)-C(3)-C(4)	110(1)

<sup>a</sup> Ta[C(Me)C(Me)C(CMeCH<sub>2</sub>CMe<sub>3</sub>)CH<sub>2</sub>](DIPP)<sub>3</sub> (**47**)



161°) and suggest a significant amount of  $\pi$  donation. The Ta-C bond distances also are in the expected range for tantalum carbon single bonds (2.12(1) Å and 2.18(1) Å),<sup>1</sup> and the data clearly show a double bond for C(1)-C(2) (1.35(1) Å) and C(3)-C(7) (1.35(1) Å).

While the exact mechanism of formation for Ta[C(Me)C(Me)C(CMeCH<sub>2</sub>CMe<sub>3</sub>)CH<sub>2</sub>](DIPP)<sub>3</sub> (**47**) is not known, the activation of a methyl group in an intermediate complex does appear to have occurred. Since initial formation of a metallacyclobutene or vinyl alkylidene complex seems most likely, these complexes are shown as probable intermediates in equation 16. Activation of a methyl group in one of these complexes (indicated in equation 16 with asterisks), possibly leading to the formation of an intermediate metal hydride complex, eventually results in the formation of **47**. The formation of complex **47** is in some ways reminiscent of previously noted reactions for alkylidene complexes in which a  $\beta$  hydrogen was activated by the metal, resulting in the reductive elimination of an olefin.<sup>29</sup> In the reaction observed here, however, instead of a reductive elimination occurring the hydrogen is transferred to the end olefin group (onto the t-butyl substituted carbon) resulting in the formation of a tantalum carbon single bond and a metallacyclopentene complex.

Complex **47** does not react in a controlled fashion with additional equivalents of 2-butyne - only starting material (i.e. **47**, by <sup>1</sup>H NMR spectroscopy) and intractible polymer are observed. Thus the formation of complex **47** appears to be largely irreversible (in the absence of a base) and can be considered a potential deactivation reaction in 2-butyne polymerization (deactivation processes are discussed in the next section); the intractible polymer is thought to arise from a small amount of some highly activated species. When pyridine (15-20 equivalents) was added to a sample of **47** in C<sub>6</sub>D<sub>6</sub> the only noticeable difference in the spectrum (from a spectrum of **47** in C<sub>6</sub>D<sub>6</sub> with no added pyridine) was that all resonances were slightly broadened. Addition of a lesser amount of pyridine (~1 equivalent) resulted in even less changes. However, when this sample of **47** with one equivalent of pyridine was heated to 65°, in addition to the normal resonances observed for complex **47**, a

very broad resonance centered around 3.7 ppm was noted. This resonance occurs at approximately the same shift as do resonances for the DIPP methyne H's of  $\text{Ta}(\text{CMeCMeCMeP})(\text{DIPP})_3$  (**44**), and accounts for ~10% of the sample (at 65°) if the resonances are assumed to occur from the DIPP methyne H's of a related species. Upon cooling the sample back to room temperature, only resonances for **47** are observed.

Complex **47** will react with 100 equivalents of 2-butyne in the presence of pyridine to give soluble poly-2-butyne. GPC analysis (Table IV) revealed a monodisperse polymer (of a higher than expected molecular weight;  $M_n = 16,900$ ,  $d = 1.03$ ) along with a small but significant amount (19%) of another polymer ( $M_n = 66,800$ ,  $d = 1.20$ ). These results demonstrate that the catalyst **44** is not efficiently reformed from addition of pyridine to **47** (since subsequent reaction with 2-butyne yields a polymer that displays a bimodal distribution), although **44** might be involved at least in part in this polymerization reaction. Apparently more than one mechanism is operative.

#### **Deactivation Reactions of Tantalum Catalysts in Acetylene Polymerization.**

Although  $\text{Ta}[\text{C}(\text{Me})\text{C}(\text{Me})\text{C}(\text{CMeCH}_2\text{CMe}_3)\text{CH}_2](\text{DIPP})_3$  (**47**) forms from the reaction of  $\text{Ta}(\text{CMeCMeCHCMe}_3)(\text{DIPP})_3(\text{py})$  (**42**) with one equivalent of 2-butyne, reaction of excess 2-butyne with **42** does not result in any significant formation of **47** or related species, even after all 2-butyne has been consumed (a  $^1\text{H}$  NMR spectrum of complex **42** reacted with ~10 equivalents of 2-butyne showed only trace formation of **47**; Figure 4). Thus the deactivation reaction is not competitive with 2-butyne consumption and does not occur after several equivalents of 2-butyne have been consumed. The absence of such deactivations for the propagating alkylidene  $\text{Ta}(\text{CMeCMeCMeP})(\text{DIPP})_3$  (**44**) is probably related to the substitution on the polymer chain in this complex. In **44**, the polymer chain is tetrasubstituted in the proximity of the metal (the terminal trisubstituted olefin group is far removed from the metal center). However, the intermediate complex involved in the formation of complex **47** from **42** contains a terminal trisubstituted olefin group which should be accessible for reaction with the metal center (since only 2 equivalents of 2-butyne have been incorporated into the

alkylidene chain). In the formation of **47** from this intermediate complex, accessibility of the terminal trisubstituted olefin group to the metal is critical, as the activated hydrogen is transferred to this part of the chain, forming an alkyl group from an alkene group. Once a group such as this is no longer available for reaction with the metal, no deactivation is seen - this apparently is the case for all intermediates (i.e. **44**) except the first one formed from reaction of **42** with one equivalent of 2-butyne. (Reversible CH activation may occur but is not apparent, and if present it does not affect the polymerization reaction.)

The obvious question arising from the above discussion is: could a similar deactivation process hinder the polymerization of terminal acetylenes, the polymers from which contain only trisubstituted olefin groups? Reaction of complex **42** with 100 equivalents of the terminal acetylene 1-pentyne in toluene gives a deep orange solution, which upon quenching with benzaldehyde remains deep orange. Removal of the solvent *in vacuo* yields an orange oily polymer, with  $M_n = 13,700$  and  $d = 1.21$  (by GPC analysis; Table IV). When the same reaction is performed with 200 equivalents of 1-pentyne, the resulting polymer shows a very broad polydispersity, suggesting that significant deactivation does occur. The deactivation may be the result of reactions similar to the one discussed above for formation of **47**. Additionally, or alternatively, certain di- and trisubstituted metallacyclobutenes may form in this reaction that are stable from further reaction with 1-pentyne (as was noted earlier for the metallacyclobutene complexes **35-38**). Other deactivation reactions are also probable, such as metathesis of the growing polymer chain, which would lead to a more disperse polymer and possibly cyclic organic products (cyclic products were thought to form in a related polymerization study involving an alkylidyne catalyst<sup>144</sup>). In fact, the polydispersity of poly-1-pentyne formed from reaction of **42** with 1-pentyne does increase with reaction time (Table IV), consistent with secondary metathesis reactions. In any case, the polymerization of terminal acetylenes with **42** involves complications not seen for the polymerization of the disubstituted acetylene 2-butyne. <sup>1</sup>H NMR spectra of **42** reacted with 1-pentyne in C<sub>6</sub>D<sub>6</sub> (25°) display broad resonances and

multiple peaks, hindering analysis. The polymerization of 1-pentyne using a tungsten alkylidene catalyst has been explored,<sup>145</sup> and this system exhibited similar complications.

#### **Polymerization of Acetylenes with Ta(CHCMe<sub>3</sub>)(TIPT)<sub>3</sub>(THF).**

The thiolate alkylidene complex Ta(CHCMe<sub>3</sub>)(TIPT)<sub>3</sub>(THF) (**6**) was also investigated for its utility as an acetylene polymerization catalyst. This complex serves as an effective catalyst for the polymerization of NBE (chapter 2), and it was hoped that a similar well-behaved reactivity would be observed in acetylene polymerization. When complex **6** was reacted with 10 equivalents of 2-butyne, followed by removal of the solvent *in vacuo*, the resulting <sup>1</sup>H NMR spectrum (C<sub>6</sub>D<sub>6</sub>, 25°) did show all the starting catalyst consumed and resonances indicative of poly-2-butyne. Additionally, no resonances were observed for THF, indicating that THF is not coordinated strongly to the metal center of the active species. However, multiple resonances were observed (most being broad) for the catalyst species, likely arising from more than a single type of complex. Resonances of significant intensity similar to those seen for **47** were also noted.

When 100 equivalents of 2-butyne were polymerized by Ta(CHCMe<sub>3</sub>)(TIPT)<sub>3</sub>(THF) (**6**), GPC analysis (Table IV) of the resulting polymer confirmed that this reaction is not well-behaved. The polymer displayed M<sub>n</sub> = 6900, a reasonable number based on observations in the phenoxide system, but the polydispersity was large (d = 1.47), and a low molecular weight tail persisted into the oligomeric region. Secondary metathesis can be ruled out as a contributing problem in this system, since arylthiolate alkylidenes have been shown to lack reactivity with ordinary olefins (chapter 1); deactivation reactions similar to the one resulting in the formation of **47** may be more predominant in this system, based on the NMR information described above. Polymerization of the monosubstituted acetylene 1-pentyne employing Ta(CHCMe<sub>3</sub>)(TIPT)<sub>3</sub>(THF) (**6**) as the catalyst was even less impressive, suggesting again that deactivation pathways are more pronounced in terminal acetylene polymerization, where the growing polymer chain is less substituted. Attempts to isolate intermediates from the reactions of complex **6** with acetylenes, in order to better understand the mechanisms of reaction and

possibly obtain more effective catalysts, were not successful. Thiolate complexes tend to be much more soluble than analogous phenoxide complexes, making the isolation of polymerization intermediates containing an organic polymer chain very difficult.

## DISCUSSION

For several years now the controlled polymerization of cyclic olefins by well-defined transition metal catalysts has been a popular and productive area of research.<sup>2,3,62,76,78,84-87</sup> The results reported here demonstrate the feasibility of controlled acetylene polymerization using well-defined transition metal catalysts, as shown for 2-butyne polymerization by Ta(CMeCMeCHCMe<sub>3</sub>)(DIPP)<sub>3</sub>(py) (**42**), which gave monodisperse polymers of controllable molecular weights. Based on characterization of the initiating complex **42** and other intermediates involved in the reaction, a metathesis-like mechanism (equation 2) has been shown to be operative, and this represents *direct* evidence in support of the metathesis-like polymerization mechanism for Ta(V) alkylidenes. Of course all catalyst systems are unique, and the metathesis-like mechanism noted here should not be generalized to other systems where another mechanism, such as the insertion reaction shown in equation 1, might be operative.

The recognition of an operative metathesis-like mechanism in acetylene polymerization by tantalum alkylidenes, however, has been vital for the design of a catalyst that will polymerize 2-butyne effectively. Since Ta(CHCMe<sub>3</sub>)(DIPP)<sub>3</sub>(THF) (**2**) reacts with 2-butyne to give a stable trisubstituted metallacyclobutene complex that does not polymerize 2-butyne controllably, a compound that would react with 2-butyne to give less stable metallacyclobutene complexes was required (i.e. a disubstituted alkylidene). In addition to controlled initiation and propagation, because alkylidenes are known to undergo Wittig-like reactions with organic carbonyls, the poly-2-butyne formed with complex **42** can be capped selectively through a Wittig-like reaction. Selective capping of polyacetylenes is rare, since in most polymerization systems reported to date the exact nature of the propagating species is not known. In a recent review article by Masuda,<sup>112</sup> the need for research in this area was discussed in terms of obtaining polymers with well-defined end groups.

Complex **42** does *not* polymerize other disubstituted acetylenes such as diphenylacetylene, 3-hexyne, methylphenylacetylene, or methyltrimethylsilylacetylene. When excess 3-hexyne is reacted with **42**, ~one equivalent of 3-hexyne does appear to be incorporated into the complex by  $^1\text{H}$  NMR spectroscopy. However, no further reaction is observed at  $25^\circ$  or elevated temperatures (at  $65^\circ$  the solution turns cloudy, but no polymerization is evident by  $^1\text{H}$  NMR spectroscopy or GPC analysis). This lack of reactivity is unfortunate but does demonstrate a sometimes inherent feature of a carefully designed, well-behaved catalyst: the versatility of the system is sometimes sacrificed for control over a specific application. In this system, bulky phenoxide ligands are employed to prevent deleterious intra- and intermolecular decomposition reactions. Additionally, a disubstituted alkylidene ligand is present in the initiator **42** in order that subsequently formed metallacyclobutene intermediates will be tetrasubstituted and consequently less stable (than trisubstituted metallacyclobutenes from a monosubstituted alkylidene such as  $\text{Ta}(\text{CHCMe}_3(\text{DIPP})_3(\text{THF}))$  (**2**)). These same features that contribute to a well-behaved polymerization of 2-butyne, however, prevent any significant reaction with other bulkier acetylenes. In other more traditional systems, such as the use of a metal halide and a cocatalyst main group alkyl, a wide range of acetylenes might be polymerized, but usually the resulting polymers are not monodisperse (with one previously noted exception<sup>136</sup>), control over molecular weight can be quite difficult, and catalyst efficiencies tend to be low.

When a living polymerization system is developed, the potential to form block copolymers is increased significantly, since after the polymerization of one monomer the catalyst is still active and can be further reacted with a second monomer. There is much interest in synthesizing block copolymers, as evidenced in today's literature,<sup>78,104,136,146</sup> because these materials display certain properties otherwise not accessible. In some cases, by synthesizing a block copolymer of two monomers with different properties, the properties of both monomers can be obtained in the resulting polymer. Another application is the solubilization of an otherwise insoluble polymer. For example the formation of block

copolymers of NBE and parent acetylene (from a Feast monomer) has been shown as a means of solubilizing segments of parent polyacetylene.<sup>104</sup>

In this report the preparation of block copolymers of 2-butyne and NBE was investigated, in part to increase the solubility of poly-2-butyne. The results demonstrate the subtle problems that can be associated with block copolymer synthesis. The successful synthesis of a block copolymer requires a catalyst that will not only initiate the polymerization of one monomer effectively but also give rise to a propagating species that will initiate the polymerization of a second monomer effectively. Although the catalyst **42** polymerizes either NBE or 2-butyne effectively in separate experiments, the reaction of **42** with 2-butyne followed by reaction with NBE resulted in a polymer displaying a bimodal distribution of molecular weights (~4:1 ratio). This bimodal distribution is thought to result from the presence of two independent propagating species during the NBE polymerization, a highly reactive base assisted metallacyclobutane complex and a less reactive base-free metallacyclobutane complex (Scheme II). These two types of complexes form upon reaction of Ta(CMeCMeCMeP)(DIPP)<sub>3</sub> (**44**) with NBE, and their dual formation represents an uncontrolled initiation reaction for the second part of the polymerization (NBE). Apparently the difference between **42** and **44** is great enough such that one (**42**) will polymerize NBE effectively while the other (**44**) will not. That the monomers 2-butyne and NBE are polymerized by two separate mechanisms (propagating alkylidenes for 2-butyne and propagating metallacyclobutanes for NBE) surely contributes to the difficulty in preparing block copolymers here. The polymerization of two monomers that involves a single type of mechanism (e.g. two acetylenes with different substituents) might invoke less complications.

Useful information regarding the development of well-defined polymerization catalysts can be obtained through the study of both efficient and inefficient polymerization systems. By recognizing significant deactivation pathways present in an inefficient polymerization system, the pursuit of a more robust catalyst becomes a systematic, as opposed to a random, process. One example of such a study, related to both acetylene metathesis and acetylene

polymerization, investigated the aborted polymerization of t-butylacetylene by a molybdenum alkylidyne complex.<sup>147</sup> In that report insertions of the acetylene into the metal carbon double bonds of a molybdenacyclic complex were shown to lead to formation of a substituted benzene group in the complex, thus demonstrating the potential for cyclization deactivation reactions in acetylene polymerization reactions involving successive insertions of the acetylene into growing metallacycles. The reaction pathway most favored in those reactions, and related ones referred to in the report, was largely dependent upon the nature of the acetylene employed and the ligation about the metal complex.

In this chapter, two potentially deactivating reactions have been identified. The formation of the inactive metallacyclopentene **47**, by activation of a methyl substituent in the "polymer" chain of a preceding intermediate, demonstrates the extreme electrophilicity of the Ta(V) metal center in these complexes. Fortunately, this deactivation reaction was not observed for catalyst species derived from **42** (i.e. **44**) after reaction with one equivalent of 2-butyne. The lack of deactivation observed for **44** is associated with the lack of available reaction sites in the growing polymer chain (since the olefin groups are tetrasubstituted, reaction with the metal center is sterically hindered). In polymerization reactions involving less substituted acetylenes and/or less sterically congested complexes, such as reaction of **42** with 1-pentyne, deactivation processes become a limiting problem.

Another more subtle deactivation-like reaction observed in this study was the formation of the disubstituted metallacyclobutene Ta[CH<sub>2</sub>C(Me)C(CHCHCMe<sub>3</sub>)](DIPP)<sub>3</sub> (**38**) from reaction of Ta(CHCMe<sub>3</sub>)(DIPP)<sub>3</sub>(THF) (**2**) with 2-methylbut-1-ene-3-yne (equation 6). In the formation of complex **38**, after initial addition of the alkyne portion of the ene-yne to the alkylidene ligand, the intermediate alkylidene complex rearranged by addition of the attached olefin group (originally from the ene portion of the ene-yne) to the alkylidene ligand. This rearrangement led to the formation of the stable unreactive disubstituted metallacyclobutene complex **38**. Thus in the polymerization of acetylenes containing potentially reactive functionalities such as an alkene group, this type of reaction (at least for tantalum alkylidene



complexes) should be considered. The synthesis of soluble, conjugated polymers has attracted recent attention, since films and other solid forms of these polymers can be systematically prepared (for doping and subsequent conductance studies).<sup>146</sup> The polymerization of an ene-yne could also potentially result in a soluble polymer with enhanced conjugation, due to the presence of olefin substituents (if the alkyne fragment is polymerized). For future investigations in this area, an emphasis should be placed on choosing a monomer that will yield a polymer in which the alkene substituents are highly substituted, thereby decreasing the chances for reactions of the type leading to complex **38**.

The successful use of alkylidenes for acetylene polymerization is not surprising when one considers the similarity to cyclic olefin polymerization - both types of polymerization involve a metathesis (or metathesis-like) reaction, and many desirable features for the catalyst complex are mutual (such as the presence of bulky substituents to stabilize the complex from deactivation processes). In all likelihood, other alkylidene or metallacyclobutane complexes that are known to effectively polymerize cyclic olefins could also serve as efficient acetylene polymerization catalysts. Well-defined metal alkyl systems for acetylene polymerization might also prove to be an interesting area of future investigation (equation 1). In any approach taken, careful consideration must be given to the requirements for the polymerization of a specific substrate, if monodisperse polymers of a controlled molecular weight are desired.

## Experimental Section

General Details are listed in chapter 1. All polymer samples were analyzed in toluene or methylene chloride, as described for polynorbornene samples in chapter 2.

**Preparation of Compounds. Ta[C(Me)C(Me)CH(CMe<sub>3</sub>)](DIPP)<sub>3</sub> (35).** A solution of 2-butyne (9.2  $\mu$ L, 0.12 mmol) in ether (5 mL), cooled to -30°, was added to a stirring solution of Ta(CHCMe<sub>3</sub>)(DIPP)<sub>3</sub>(THF) (0.100 g, 0.12 mmol) in ether (5 mL) at -30°. The solution was stirred at room temperature, and the color of the solution turned orange. After 10 minutes, following filtration of the solution through Celite, the solvent was removed *in vacuo* to give an orange oil. A <sup>1</sup>H NMR spectrum of this oil in C<sub>6</sub>D<sub>6</sub> showed clean formation of the product. Orange crystals can be isolated by crystallization of the oil from pentane: <sup>1</sup>H NMR (C<sub>6</sub>D<sub>6</sub>, 300 MHz)  $\delta$  7.07 (d, 6, H<sub>m</sub>), 6.93 (t, 3, H<sub>p</sub>), 3.61 (septet, 6, CHMe<sub>2</sub>), 2.71 (broad s, 1,  $\alpha$  CHCMe<sub>3</sub>), 2.40 (d, 3, J<sub>HH</sub> = 2.6,  $\beta$  CMe), 2.06 (s, 3,  $\alpha$  CMe), 1.20 (d, 36, CHMe<sub>2</sub>), 1.12 (s, 9, CMe<sub>3</sub>). <sup>13</sup>C NMR (C<sub>6</sub>D<sub>6</sub>, 67.9 MHz)  $\delta$  217.9 (s,  $\alpha$  CMe), 157.0 (s, C<sub>ipso</sub>), 156.2 (s,  $\beta$  CMe), 138.5 (s, C<sub>o</sub>), 123.7 (d, C<sub>m</sub>), 123.6 (d, C<sub>p</sub>), 84.1 (d, J<sub>CH</sub> = 134,  $\alpha$  CHCMe<sub>3</sub>), 36.7 (s, CMe<sub>3</sub>), 33.5 (q, CMe<sub>3</sub>), 27.3 (d, CHMe<sub>2</sub>), 24.3 (q, CHMe<sub>2</sub>), 20.4 and 16.9 (q's, Me's). Anal. Calcd for TaC<sub>45</sub>H<sub>67</sub>O<sub>3</sub>: C, 64.56; H, 8.08. Found: C, 64.75; H, 8.12.

**Ta[C(Ph)C(Ph)CH(CMe<sub>3</sub>)](DIPP)<sub>3</sub> (36).** A solution of diphenylacetylene (0.063 g, 0.35 mmol) in ether (5 mL), cooled to -30°, was added to a stirring solution of Ta(CHCMe<sub>3</sub>)(DIPP)<sub>3</sub>(THF) (0.300 g, 0.35 mmol) in ether (10 mL) at -30°. The solution was stirred at room temperature for 60 minutes, during which time the color changed to orange. The solution was then filtered through Celite, followed by removal of the solvent *in vacuo*. An orange precipitate was obtained by crystallization of the resulting solid from pentane at -30° (0.266 g, 79%): <sup>1</sup>H NMR (C<sub>6</sub>D<sub>6</sub>, 250 MHz)  $\delta$  7.48 - 6.76 (m, 10, phenyl H resonances), 7.04 (d, 6, H<sub>m</sub>), 6.95 (t, 3, H<sub>p</sub>), 3.67 (septet, 6, CHMe<sub>2</sub>), 3.32 (s, 1,  $\alpha$  CHCMe<sub>3</sub>), 1.14 (d, 36, CHMe<sub>2</sub>), 1.12 (unresolved, 9, CMe<sub>3</sub>). <sup>13</sup>C NMR (C<sub>6</sub>D<sub>6</sub>, 67.9 MHz)  $\delta$  224.0 (s,  $\alpha$  CPh), 157.0 (s, C<sub>ipso</sub>), 151.6 (s,  $\beta$  CPh), 143.6 (s, phenyl<sub>ipso</sub> C's), 138.6 (s, C<sub>o</sub>), 130.1 - 125.9 (unresolved, phenyl<sub>o,m,and p</sub> C's), 123.8 (d, C<sub>m</sub> and p), 87.7 (d, J<sub>CH</sub> = 132,  $\alpha$  CHCMe<sub>3</sub>), 39.4

(s,  $CMe_3$ ), 34.1 (q,  $CMe_3$ ), 27.4 (d,  $CHMe_2$ ), 24.5 (q,  $CHMe_2$ ). Anal. Calcd for  $TaC_{55}H_{71}O_3$ : C, 68.72; H, 7.46. Found: C, 68.71; H, 7.44.

**Ta[C(SiMe<sub>3</sub>)C(SiMe<sub>3</sub>)CH(CMe<sub>3</sub>)](DIPP)<sub>3</sub> (37).** A solution of bistrimethylsilylacetylene (133  $\mu$ L, 0.59 mmol) in ether (10 mL) was added to a stirring solution of Ta(CHCMe<sub>3</sub>)(DIPP)<sub>3</sub>(THF) (0.500 g, 0.58 mmol) in ether (20 mL) at room temperature. After 4.5 hours the solution was filtered through Celite, and the solvent was removed *in vacuo*. The resulting yellow oil was dissolved in pentane and the solution cooled to -30°, yielding yellow crystals (0.242 g, 43%): <sup>1</sup>H NMR (C<sub>6</sub>D<sub>6</sub>, 250 MHz)  $\delta$  7.04 (d, 6, H<sub>m</sub>), 6.91 (t, 3, H<sub>p</sub>), 3.99 (s, 1,  $\alpha$  CHCMe<sub>3</sub>), 3.64 (septet, 6, CHMe<sub>2</sub>), 1.24 and 1.23 (d's, 36, CHMe<sub>2</sub>), 0.97 (s, 9, CMe<sub>3</sub>), 0.39 and -0.09 (s's, 18, SiMe<sub>3</sub>'s). <sup>13</sup>C NMR (C<sub>6</sub>D<sub>6</sub>, 67.9 MHz)  $\delta$  254.8 (s,  $\alpha$  CSiMe<sub>3</sub>), 232.2 (s,  $\beta$  CSiMe<sub>3</sub>), 157.4 (s, C<sub>ipso</sub>), 137.9 (s, C<sub>o</sub>), 123.7 (d, C<sub>m</sub>), 123.2 (d, C<sub>p</sub>), 59.9 (d, J<sub>CH</sub> = 116,  $\alpha$  CHCMe<sub>3</sub>), 35.1 (s, CMe<sub>3</sub>), 31.5 (q, CMe<sub>3</sub>), 27.6 (d, CHMe<sub>2</sub>), 25.5 (q, CHMe<sub>2</sub>), 2.27 and 1.95 (q's, SiMe<sub>3</sub>'s). Anal. Calcd for TaC<sub>49</sub>H<sub>79</sub>O<sub>3</sub>Si<sub>2</sub>: C, 61.74; H, 8.35. Found: C, 61.85; H, 8.25.

**Ta[CH<sub>2</sub>C(Me)C(CHCHCMe<sub>3</sub>)](DIPP)<sub>3</sub> (38).** 2-methylbut-1-ene-3-yne (32  $\mu$ L, 0.33 mmol) was added via syringe to a stirring solution of Ta(CHCMe<sub>3</sub>)(DIPP)<sub>3</sub>(THF) (0.280 g, 0.33 mmol) in ether (10 mL) at -30°. The solution was stirred at room temperature for 20 minutes, during which time the color changed to orange. Filtration of the solution through Celite followed by removal of the solvent *in vacuo* yielded an orange oil (extremely soluble in pentane). Repeated attempts to obtain the compound in solid form failed. The yield is ~quantitative by <sup>1</sup>H NMR: <sup>1</sup>H NMR (C<sub>6</sub>D<sub>6</sub>, 250 MHz)  $\delta$  7.07 (d, 6, H<sub>m</sub>), 6.94 (t, 3, H<sub>p</sub>), 6.77 (d, 1, J<sub>HH</sub> = 16, CHCHCMe<sub>3</sub>), 5.43 (d, 1, J<sub>HH</sub> = 16, CHCHCMe<sub>3</sub>), 3.57 (septet, 6, CHMe<sub>2</sub>), 2.20 (s, 3,  $\beta$  CMe), 2.15 (s, 2,  $\alpha$  CH<sub>2</sub>), 1.21 (d, 36, CHMe<sub>2</sub>), 0.83 (s, 9, CMe<sub>3</sub>). <sup>13</sup>C NMR (C<sub>6</sub>D<sub>6</sub>, 67.9 MHz)  $\delta$  216.9 (s,  $\alpha$  CR), 156.8 (s, C<sub>ipso</sub>), 150.5 (s,  $\beta$  CMe), 145.6 (d, J<sub>CH</sub> = 150, CHCHCMe<sub>3</sub>), 138.4 (s, C<sub>o</sub>), 124.9 (d, J<sub>CH</sub> = 149, CHCHCMe<sub>3</sub>), 123.6 (d, C<sub>m</sub> and p), 57.3 (t, J<sub>CH</sub> = 141,  $\alpha$  CH<sub>2</sub>), 33.1 (s, CMe<sub>3</sub>), 29.7 (q, CMe<sub>3</sub>), 27.5 (d, CHMe<sub>2</sub>), 24.0 (q, CHMe<sub>2</sub>), 20.1 (q,  $\beta$  CMe).

**Ta[CH<sub>2</sub>C(Me)C(CHCHCMe<sub>3</sub>)](DIPP)<sub>3</sub>(py) (39).** A solution of 2-methylbut-1-ene-3-yne (46  $\mu$ L, 0.47 mmol) in ether (5 mL), cooled to -30°, was added to a stirring solution of Ta(CHCMe<sub>3</sub>)(DIPP)<sub>3</sub>(THF) (0.400 g, 0.47 mmol) in ether (10 mL) at -30°. The solution was stirred at room temperature, during which time the color turned orange. After 75 minutes pyridine (140  $\mu$ L, 1.74 mmol) was added via syringe, and the solution was stirred for another 75 minutes at room temperature. Subsequent filtration of the solvent *in vacuo* yielded a light orange oil. Light orange crystals were obtained by crystallization from pentane at -30° (0.227 g, 52%): <sup>1</sup>H NMR (C<sub>6</sub>D<sub>6</sub>, 250 MHz)  $\delta$  8.64 (br d, 2, py<sub>ortho</sub>), 7.09 (d, 6, H<sub>m</sub>), 6.92 (t, 3, H<sub>p</sub>), 6.78 (t, 1, py<sub>p</sub>), 6.27 (br, 3, CHCHCMe<sub>3</sub> and py<sub>m</sub>), 5.18 (d, 1, J<sub>HH</sub> = 16, CHCHCMe<sub>3</sub>), 3.55 (septet, 6, CHMe<sub>2</sub>), 2.26 (s, 3,  $\beta$  CMe), 1.76 (s, 2,  $\alpha$  CH<sub>2</sub>), 1.10 (d, 36, CHMe<sub>2</sub>), 0.89 (s, 9, CMe<sub>3</sub>). <sup>13</sup>C NMR (C<sub>6</sub>D<sub>6</sub>, 67.9 MHz)  $\delta$  212.8 (s,  $\alpha$  CR), 157.1 (s, C<sub>ipso</sub>), 149.8 (d, py<sub>o</sub>), 148.2 (s,  $\beta$  CMe), 139.8 (unresolved, CHCHCMe<sub>3</sub>), 138.5 (s, C<sub>o</sub>), 137.7 (unresolved, py<sub>p</sub>), 127.1 (unresolved, CHCHCMe<sub>3</sub>), 124.7 (unresolved, py<sub>m</sub>), 123.9 (d, C<sub>m</sub>), 122.2 (d, C<sub>p</sub>), 56.7 (t, J<sub>CH</sub> = 140,  $\alpha$  CH<sub>2</sub>), 33.0 (s, CMe<sub>3</sub>), 30.1 (q, CMe<sub>3</sub>), 27.0 (d, CHMe<sub>2</sub>), 24.5 (q, CHMe<sub>2</sub>), 20.3 (q,  $\beta$  CMe). Anal. Calcd for TaC<sub>51</sub>H<sub>72</sub>NO<sub>3</sub>: C, 66.00; H, 7.82; N, 1.51. Found: C, 65.81; H, 7.99; N, 1.29.

**Ta[C(SiMe<sub>3</sub>)C(SiMe<sub>3</sub>)CH(CMe<sub>3</sub>)](DIPP)<sub>3</sub>(py) (40).** Pyridine (17  $\mu$ L, 0.21 mmol) was added via syringe to a stirring solution of Ta[C(SiMe<sub>3</sub>)C(SiMe<sub>3</sub>)CH(CMe<sub>3</sub>)](DIPP)<sub>3</sub> (0.050 g, 0.05 mmol) in ether (5 mL) at room temperature. The solution was stirred for 75 minutes, during which time no color change was observed. Filtration of the solution through Celite, followed by removal of the solvent *in vacuo*, yielded a yellow oil (yield ~ quantitative by <sup>1</sup>H NMR): <sup>1</sup>H NMR (C<sub>6</sub>D<sub>6</sub>, 250 MHz)  $\delta$  8.53 (d, 2, py<sub>o</sub>), 7.05 (d, 6, H<sub>m</sub>), 6.96 (unresolved, 2, py<sub>m</sub>), 6.91 (t, 3, H<sub>p</sub>), 6.63 (t, 1, py<sub>p</sub>), 3.99 (s, 1,  $\alpha$  CHCMe<sub>3</sub>), 3.64 (septet, 6, CHMe<sub>2</sub>), 1.24 and 1.23 (d's, 36, CHMe<sub>2</sub>), 0.97 (s, 9, CMe<sub>3</sub>), 0.39 and -0.09 (s's, 18, SiMe<sub>3</sub>'s).

**Ta[CH<sub>2</sub>C(Me)C(CHCHCMe<sub>3</sub>)](DIPP)<sub>3</sub>(quin) (41).** A solution of quinuclidine (quin; 0.100 g, 0.90 mmol) in ether (5 mL) was added to a solution of

Ta[CH<sub>2</sub>C(Me)C(CHCHCMe<sub>3</sub>)](DIPP)<sub>3</sub> (0.150 g, 0.18 mmol) in ether (5 mL) at room temperature. The solution was stirred at room temperature for 100 minutes, during which time the color remained orange. Filtration of the solution through Celite, followed by removal of the solvent *in vacuo*, yielded an orange oil (a <sup>1</sup>H NMR spectrum of this oil in C<sub>6</sub>D<sub>6</sub> showed clean formation of a quinuclidine adduct): <sup>1</sup>H NMR (C<sub>6</sub>D<sub>6</sub>, 250 MHz) δ 7.06 (d, 6, H<sub>m</sub>), 6.93 (t, 3, H<sub>p</sub>), 6.75 (d, 1, J<sub>HH</sub> = 16, CHCHCMe<sub>3</sub>), 5.41 (d, 1, J<sub>HH</sub> = 16, CHCHCMe<sub>3</sub>), 3.55 (septet, 6, CHMe<sub>2</sub>), 2.74 (t, 6, N(CH<sub>2</sub>CH<sub>2</sub>)<sub>3</sub>CH), 2.19 (s, 3, β CMe), 2.12 (s, 2, α CH<sub>2</sub>), 1.50 (m, 1, N(CH<sub>2</sub>CH<sub>2</sub>)<sub>3</sub>CH), 1.28 (m, 6, N(CH<sub>2</sub>CH<sub>2</sub>)<sub>3</sub>CH), 1.19 (d, 36, CHMe<sub>2</sub>), 0.81 (s, 9, CMe<sub>3</sub>).

**Ta(CMeCMeCHCMe<sub>3</sub>)(DIPP)<sub>3</sub>(py) (42).** A solution of 2-butyne (37 μL, 0.47 mmol) in ether (10 mL), cooled to -30°, was added to a stirring solution of Ta(CHCMe<sub>3</sub>)(DIPP)<sub>3</sub>(THF) (0.400 g, 0.47 mmol) in ether (10 mL) at -30°. The color of the solution rapidly changed to orange. After stirring at room temperature for 30 minutes, the solution was recooled to -30°, and pyridine (113 μL, 1.40 mmol) was added via a syringe. The color immediately turned very dark, and after stirring at room temperature for 20 minutes, the solution was filtered through Celite. The solvent was removed *in vacuo*, and the resulting black residue was dissolved in pentane. Cooling this solution to -30° resulted in the formation of deep purple crystals (0.330 g, 77%): <sup>1</sup>H NMR (C<sub>6</sub>D<sub>6</sub>, 300 MHz) δ 8.49 (br d, 2, py<sub>o</sub>), 7.06 (d, 6, H<sub>m</sub>), 6.92 (t, 3, H<sub>p</sub>), 6.9 - 6.7 (br, 1, py<sub>p</sub>), 6.55 (br, 2, py<sub>m</sub>), 3.64 (septet, 6, CHMe<sub>2</sub>), 2.08 (s, 3, β CMe), 1.21 (d, 36, CHMe<sub>2</sub>), 1.15 (s, 9, CMe<sub>3</sub>). The α CMe group and olefinic H resonances were not observed in room temperature spectra, due to a fluxional process that interconverts the alkylidene and the corresponding metallacyclobutene. <sup>1</sup>H NMR (toluene-d<sub>8</sub>, -60°, 300 MHz) δ 8.64 and 8.22 (d's, 2, py<sub>o</sub>), 7.2-6.7 (m, H<sub>m</sub> and p and CHCMe<sub>3</sub>), 6.57 (s, ~0.33, CHCMe<sub>3</sub>), 6.26 (t, 1, py<sub>p</sub>), 5.98 (t, 2, py<sub>m</sub>), 4.34 and 4.18 (s's, 3, α CMe), 4.05 and 3.57 (broad, 6, CHMe<sub>2</sub>), 2.24 (s, 3, β CMe), 1.4-1.1 (broad, CHMe<sub>2</sub> and CMe<sub>3</sub>). <sup>13</sup>C NMR (C<sub>6</sub>D<sub>6</sub>, 67.9 MHz) δ 157.4 (s, C<sub>ipso</sub>), 150.3 (d, py<sub>o</sub>), 138.3 (s, C<sub>o</sub>), 136.4 (d, py<sub>p</sub>), 124.0 and 123.7 (d's, C<sub>p</sub> and m), 122.9 (d, py<sub>m</sub>), 33.4 (q, CMe<sub>3</sub>), 27.2 (d,

CHMe<sub>2</sub>), 24.5 (q, CHMe<sub>2</sub>), 23.9 and 20.4 (q's, α CMe and β CMe). The C<sub>α</sub>, C<sub>β</sub>, and C<sub>γ</sub> resonances were not observed in room temperature spectra, due to a fluxional process that interconverts the alkylidene and the corresponding metallacyclobutene. The CMe<sub>3</sub> resonance was also not observed. <sup>13</sup>C NMR (toluene-d<sub>8</sub>, -60°, 75.4 MHz) δ 256.4 and 232.1 (α CMe). Anal. Calcd for TaC<sub>50</sub>H<sub>72</sub>O<sub>3</sub>N: C, 65.54; H, 7.94. Found: C, 65.38; H, 7.97.

**Ta(CPhCPhCHCMe<sub>3</sub>)(DIPP)<sub>3</sub>(py) (43).** Pyridine (75 μL, 0.93 mmol) was added via syringe to a stirring solution of Ta[C(Ph)C(Ph)CH(CMe<sub>3</sub>)](DIPP)<sub>3</sub> (0.165 g, 0.17 mmol) in ether (10 mL) at room temperature. The color of the solution quickly turned dark purple. After 30 minutes the solution was filtered through Celite, and the solvent was removed *in vacuo*. Dissolution of the resulting dark oil in pentane followed by cooling the solution to -30° yielded dark purple crystals (0.085 g, 47%): <sup>1</sup>H NMR (C<sub>6</sub>D<sub>6</sub>, 250 MHz) δ <sup>1</sup>H NMR (C<sub>6</sub>D<sub>6</sub>, 250 MHz) 8.54 (br, 2, py<sub>o</sub>), 7.47 - 6.73 (m, 12, phenyl H resonances, py<sub>p</sub>, and CHCMe<sub>3</sub>), 7.05 (d, 6, H<sub>m</sub>), 6.93 (t, 3, H<sub>p</sub>), 6.58 (br, 2, py<sub>m</sub>), 3.67 (br septet, 6, CHMe<sub>2</sub>), 1.14 (d, 36, CHMe<sub>2</sub>), 1.10 (s, 9, CMe<sub>3</sub>). <sup>13</sup>C NMR (C<sub>6</sub>D<sub>6</sub>, 67.9 MHz; decoupled only) δ 243.1 (α CPh), 157.2 (C<sub>ipso</sub>), 150.3 (py<sub>o</sub>), 143.9 (phenyl<sub>ipso</sub> C's), 138.7 (C<sub>o</sub>), 135.8 (py<sub>p</sub>), 130.2 - 122.0 (unresolved, β CPh, γCHCMe<sub>3</sub>, phenyl<sub>o,m</sub>, and p C's, and py<sub>m</sub>), 124.0 (C<sub>m</sub> and p), 39.0 (CMe<sub>3</sub>), 34.1 (CMe<sub>3</sub>), 27.5 (CHMe<sub>2</sub>), 24.6 (CHMe<sub>2</sub>). Also a broad resonance at ~88 ppm was observed after several hours; this resonance occurs in the region expected for a β C in a metallacyclobutene complex, and is thought to arise from an equilibrium of the alkylidene with the corresponding metallacyclobutene. Anal. Calcd for TaC<sub>60</sub>H<sub>76</sub>NO<sub>3</sub>: C, 69.27; H, 7.38. Found: C, 69.23; H, 7.56.

**Ta[C(Me)C(Me)C(CMeCH<sub>2</sub>CMe<sub>3</sub>)CH<sub>2</sub>](DIPP)<sub>3</sub> (47).** A solution of 2-butyne (69 μL, 0.88 mmol) in ether (5 mL), cooled to -30°, was added to a stirring solution of Ta(CMeCMeCHCMe<sub>3</sub>)(DIPP)<sub>3</sub>(py) (0.800 g, 0.87 mmol) in ether (15 mL) at -30°. The solution was stirred at room temperature, and the color of the solution turned orange-red. After 20 minutes, following filtration of the solution through Celite, the solvent was removed *in vacuo* to give a deep red oil. The yield is ~ quantitative by <sup>1</sup>H NMR. A red precipitate can be

isolated from pentane at  $-30^{\circ}$  after several days (0.365 g, 47%); when obtained in crystalline form the compound appears as light orange crystals:  $^1\text{H}$  NMR ( $\text{C}_6\text{D}_6$ , 300 MHz)  $\delta$  7.08 (d, 6,  $\text{H}_m$ ), 6.96 (t, 3,  $\text{H}_p$ ), 3.44 (septet, 6,  $\text{CHMe}_2$ ), 2.91 (s, 2,  $\alpha$   $\text{CH}_2$ ), 2.51 (s, 2,  $\text{CH}_2\text{CMe}_3$ ), 2.19 (s, 3,  $\alpha$   $\text{CMe}$ ), 2.12 and 1.74 (s's, 6,  $\beta$   $\text{CMe}$  and  $\text{CMeCH}_2\text{CMe}_3$ ), 1.18 (d, 36,  $\text{CHMe}_2$ ), 0.98 (s, 9,  $\text{CMe}_3$ ).  $^{13}\text{C}$  NMR ( $\text{C}_6\text{D}_6$ , 75.4 MHz)  $\delta$  214.0 (s,  $\alpha$   $\text{CMe}$ ), 158.7, 148.9, and 129.2 (s's,  $\beta$  C's and  $\text{CMeCH}_2\text{CMe}_3$ ), 156.9 (s,  $\text{C}_{\text{ipso}}$ ), 138.4 (s,  $\text{C}_o$ ), 123.6 (d's,  $\text{C}_m$  and p), 82.3 (t,  $J_{\text{CH}} = 119$ ,  $\alpha$   $\text{CH}_2$ ), 47.5 (t,  $J_{\text{CH}} = 124$ ,  $\text{CH}_2\text{CMe}_3$ ), 33.1 (s,  $\text{CMe}_3$ ), 32.2 (q,  $\text{CMe}_3$ ), 27.6 (d,  $\text{CHMe}_2$ ), 25.2, 20.0, and 18.5 (q's, Me's), 24.0 (q,  $\text{CHMe}_2$ ). Anal. Calcd for  $\text{TaC}_{49}\text{H}_{73}\text{O}_3$ : C, 66.05; H, 8.26. Found: C, 65.79; H, 8.12.

**X-Ray Structure of  $\text{Ta}(\text{CMeCMeCHCMe}_3)(\text{DIPP})_3(\text{py})$  (42).** Single crystals suitable for X-ray analysis were obtained with difficulty, and the high electron density in the final difference-Fourier map may be related to this problem. The spurious peaks did not appear to be chemically significant regarding the structure.

A dark purple prism crystal (grown in pentane at  $-30^{\circ}$ ) of  $\text{TaC}_{50}\text{H}_{72}\text{O}_3\text{N}$  having approximate dimensions of 0.500 x 0.300 x 0.400 mm was mounted on a glass fiber. All measurements were made on a Rigaku AFC6R diffractometer with graphite monochromated Mo  $\text{K}\alpha$  radiation and a 12KW rotating anode generator. Cell constants and an orientation matrix for data collection, obtained from a least-squares refinement using the setting angles of 24 carefully centered reflections in the range  $30.00 < 2\theta < 35.01^{\circ}$  corresponded to a monoclinic cell with dimensions:  $a = 14.791(4)$  Å,  $b = 19.716(4)$  Å,  $c = 16.115(5)$  Å,  $V = 4668(4)$  Å<sup>3</sup>, and  $\beta = 96.60(3)^{\circ}$ . For  $Z = 4$  and F.W. = 916.07, the calculated density is 1.30 g/cm<sup>3</sup>. Based on the systematic absences of  $h0l$ :  $h+1 \neq 2n$  and  $0k0$ :  $k \neq 2n$  and the successful solution and refinement of the structure, the space group was determined to be  $\text{P}2_1/n$  (#14).

The data were collected at a temperature of  $-65^{\circ} \pm 1^{\circ}$  using the  $\omega$ - $2\theta$  scan technique to a maximum  $2\theta$  value of  $55.1^{\circ}$ . Of the 11510 reflections which were collected, 11096 were unique ( $R_{\text{int}} = .037$ ). The intensities of three representative reflections which were measured after every 100 reflections remained constant throughout data collection indicating crystal and

electronic stability (no decay correction was applied). The linear absorption coefficient for Mo  $K\alpha$  is  $25.2 \text{ cm}^{-1}$ . An empirical absorption correction, using the program DIFABS,<sup>148</sup> was applied which resulted in transmission factors ranging from 0.66 to 1.15. The data were corrected for Lorentz and polarization effects.

The structure was solved by the Patterson method. The non-hydrogen atoms were refined either anisotropically or isotropically. Hydrogen atoms were included in the structure factor calculation in idealized positions ( $d_{\text{C-H}} = 0.95 \text{ \AA}$ ), and were assigned isotropic thermal parameters which were 20% greater than the  $B_{\text{eq}}$  value of the atom to which they were bonded. The final cycle of full-matrix least-squares refinement<sup>149</sup> was based on 5993 observed reflections ( $I > 3.00\sigma(I)$ ) and 246 variable parameters and converged (largest parameter shift was 0.03 times its esd) with unweighted and weighted agreement factors of  $R = 0.096$  and  $R_w = 0.167$ .

The standard deviation of an observation of unit weight<sup>150</sup> was 3.63. The weighting scheme was based on counting statistics and included a factor ( $p = 0.05$ ) to downweight the intense reflections. Plots of  $\sum w (|F_o| - |F_c|)^2$  versus  $|F_o|$ , reflection order in data collection,  $\sin \theta/\lambda$ , and various classes of indices showed no unusual trends. The maximum and minimum peaks on the final difference Fourier map corresponded to 3.04 and  $-3.89 \text{ e}/\text{\AA}^3$ , respectively.

Neutral atom scattering factors were taken from Cromer and Waber.<sup>151a</sup> Anomalous dispersion effects were included in  $F_{\text{calc}}$ <sup>152</sup>; the value for  $\Delta f'$  and  $\Delta f''$  were those of Cromer.<sup>151b</sup> All calculations were performed using the TEXSAN<sup>153</sup> crystallographic software package of Molecular Structure Corporation (College Station, Texas).

**X-Ray Structure of Ta[C(Me)C(Me)C(CMeCH<sub>2</sub>CMe<sub>3</sub>)CH<sub>2</sub>](DIPP)<sub>3</sub> (47).** A light orange pyramid crystal (grown in pentane at  $-30^\circ$ ) of  $\text{TaC}_{49}\text{H}_{73}\text{O}_3$  having approximate dimensions of  $0.250 \times 0.300 \times 0.300 \text{ mm}$  was mounted on a glass fiber. All measurements were made on an Enraf-Nonius CAD-4 diffractometer with graphite monochromated Mo  $K\alpha$  radiation.



Cell constants and an orientation matrix for data collection, obtained from a least-squares refinement using the setting angles of 25 carefully centered reflections in the range  $20.00 < 2\theta < 26.00^\circ$  corresponded to a monoclinic cell with dimensions:  $a = 10.632(4)$  Å,  $b = 12.750(9)$  Å,  $c = 34.144(9)$  Å,  $V = 4627(6)$  Å<sup>3</sup>, and  $\beta = 91.42(3)^\circ$ . For  $Z = 4$  and F.W. = 891.06, the calculated density is 1.279 g/cm<sup>3</sup>. Based on the systematic absences of  $h0l: l \neq 2n$  and  $0k0: k \neq 2n$  and the successful solution and refinement of the structure, the space group was determined to be  $P2_1/c$  (#14).

The data were collected at a temperature of  $-65^\circ \pm 1^\circ$  using the  $\omega$  scan technique to a maximum  $2\theta$  value of  $55.0^\circ$ . Of the 11686 reflections which were collected, 11089 were unique ( $R_{\text{int}} = .056$ ); equivalent reflections were emerged. The intensities of three representative reflections which were measured after every 60 minutes of X-ray exposure time remained constant throughout data collection indicating crystal and electronic stability (no decay correction was applied). The linear absorption coefficient for Mo  $K\alpha$  is  $25.4 \text{ cm}^{-1}$ . An empirical absorption correction, using the program DIFABS,<sup>148</sup> was applied which resulted in transmission factors ranging from 0.79 to 1.24. The data were corrected for Lorentz and polarization effects.

The structure was solved by direct methods<sup>154</sup>. The non-hydrogen atoms were refined anisotropically. Hydrogen atoms were included in the structure factor calculation in idealized positions ( $d_{\text{C-H}} = 0.95$  Å), and were assigned isotropic thermal parameters which were 20% greater than the  $B_{\text{eq}}$  value of the atom to which they were bonded. The final cycle of full-matrix least-squares refinement<sup>149</sup> was based on 4417 observed reflections ( $I > 3.00\sigma(I)$ ) and 478 variable parameters and converged (largest parameter shift was 0.00 times its esd) with unweighted and weighted agreement factors of  $R = 0.048$  and  $R_w = 0.050$ .

The standard deviation of an observation of unit weight<sup>150</sup> was 1.09. The weighting scheme was based on counting statistics and included a factor ( $p = 0.05$ ) to downweight the intense reflections. Plots of  $\sum w (|F_o| - |F_c|)^2$  versus  $|F_o|$ , reflection order in data collection,  $\sin \theta/\lambda$ , and various classes of indices showed no unusual trends. The maximum

and minimum peaks on the final difference Fourier map corresponded to 0.67 and -1.34 e-/Å<sup>3</sup>, respectively.

Neutral atom scattering factors were taken from Cromer and Waber.<sup>151a</sup> Anomalous dispersion effects were included in  $F_{\text{calc}}$ <sup>152</sup>; the value for  $\Delta f'$  and  $\Delta f''$  were those of Cromer.<sup>151b</sup> All calculations were performed using the TEXSAN<sup>153</sup> crystallographic software.

**Preparation of Poly-2-butyne with 42, 47, and Ta(CHCMe<sub>3</sub>)(TIPT)<sub>3</sub>(THF), for GPC Analysis.** Standard solutions of 2-butyne in toluene (~2.5M) were utilized for the accurate measurement of smaller amounts of 2-butyne. Because 2-butyne is volatile, all solutions of 2-butyne were prepared at -30°. In a typical reaction, 100 equivalents of 2-butyne in toluene (5 mL), cooled to -30°, were added to a stirring solution of the catalyst complex 42 (25 mg) in toluene (10 mL), also cooled to -30°. The reaction solution was then stirred at room temperature. After allowing sufficient time for consumption of all the 2-butyne (these reactions are fast at room temperature, such that 100 equivalents of 2-butyne is consumed *within* 30 minutes), the polymer was cleaved from the metal by addition of excess benzaldehyde (~50 µL). Removal of the solvent *in vacuo* resulted in isolation of a rubbery colorless polymer. The poly-2-butyne can be dissolved in toluene or, with more difficulty, methylene chloride for GPC analysis (before GPC analysis the polymer solution is passed through alumina to remove any remaining metal complexes). Higher molecular weight samples (150-200 equivalents of 2-butyne polymerized) dissolve in methylene chloride only with heating, and even with heating not all of the polymer dissolves. However, the solubility of these samples in methylene chloride can be enhanced significantly by the addition of a small amount of toluene. The resulting GPC chromatograms (run in methylene chloride) are identical in form to those obtained by dissolving the polymers only in methylene chloride.

The decreased solubility of these higher molecular weight samples (especially in methylene chloride) is consistent with the general insolubility noted for symmetrically substituted polyacetylenes.<sup>112</sup> The synthesis of poly-2-butyne has been reported only in a few

cases,<sup>112,117,119,142</sup> and the molecular weight distributions have been analyzed only once.<sup>117</sup> In that report, ~15% of the isolated polymer was soluble in chloroform, and GPC analysis (50 equivalents polymerized) showed  $M_n = 5800$  and  $M_w = 24,000$  ( $d = 4.14$ ). Considering the small fraction of soluble polymer formed and the large dispersity observed, the insoluble fraction probably was characterized by higher molecular weight polymer. However, the incomplete dissolution of the higher molecular weight samples of this study is not thought to arise from the presence of other higher molecular weight fractions, since GPC analysis shows the dissolved fraction to be monodisperse ( $d < 1.05$ ). If the polymers were not monodisperse, but rather characterized by a wider range of molecular weights, then results similar to those described above might be expected. Additionally, in the current experiments, the molecular weights of the polymers increase systematically with the number of equivalents polymerized, and no "solubility cut-off" molecular weight is observed (recall studies are restricted to the polymerization of 200 equivalents or less, since solubility is limited).

The preparation of poly-2-butyne from complex **47** and  $\text{Ta}(\text{CHCMe}_3)(\text{TIPT})_3(\text{THF})$  was performed in a manner analogous to that described above for **42** (except in the case of **47** pyridine was added to the solution of **47** in toluene before the addition of 2-butyne); these reactions occur readily in room temperature solution (100 equivalents of 2-butyne consumed *within* 60 minutes).

**Preparation of NBE and 2-Butyne/NBE Block Copolymers with 42, for GPC Analysis.** For the polymerization of NBE by **42**, 100 equivalents of NBE in toluene (5 mL), cooled to  $-30^\circ$ , were added to a solution of **42** (20 mg) in toluene (10 mL), also cooled to  $-30^\circ$ , resulting in the formation of a colorless solution (indicating metallacyclobutane formation). The reaction solution was heated to  $65^\circ$  for 2 hours to allow polymerization of NBE, and after the NBE was consumed the reaction solution turned light yellow in color (indicating alkylidene formation by reaction with the pyridine). Benzaldehyde was then added ( $\sim 50\mu\text{L}$ , at  $65^\circ$ ; reaction time of  $\sim 15$  minutes) in order to cleave the polymer from the metal. Removal of the solvent *in vacuo* yielded colorless polynorbornene. The polymer sample was rinsed with

methanol, dissolved in methylene chloride, and filtered through alumina to remove any remaining metal complexes in preparation for GPC analysis.

The preparation of block copolymers was performed by addition of 2-butyne to complex **42** followed by addition of NBE, or addition of NBE to Ta[CH(C<sub>5</sub>H<sub>8</sub>)CHCH(CMe<sub>3</sub>)](DIPP)<sub>3</sub> (**26**) followed by addition of pyridine and then 2-butyne. When 2-butyne was added first, a solution of 2-butyne in toluene (5 mL), cooled to -30°, was added to a rapidly stirred solution of the catalyst complex **42** (~25 mg) in toluene (10 mL), also cooled to -30°. The reaction solution was then stirred at room temperature. After allowing sufficient time for consumption of all the 2-butyne, the reaction solution was recooled to -30°, and a fraction of the polymer solution was removed for GPC analysis. A solution of NBE in toluene (5 mL), also cooled to -30°, was then added to the reaction solution with rapid stirring. This solution was heated to 65°, and after allowing sufficient time for NBE polymerization, benzaldehyde (~50 µL) was added at 65° for cleavage of the polymer from the metal. After ~15 minutes, the solvent was removed *in vacuo*, resulting in a colorless polymer. This polymer was rinsed with methanol, dissolved in methylene chloride or toluene, and filtered through alumina in preparation for GPC analysis.

When NBE was polymerized first, a solution of NBE in toluene (5 mL), cooled to -30°, was added to a solution of Ta[CH(C<sub>5</sub>H<sub>8</sub>)CHCH(CMe<sub>3</sub>)](DIPP)<sub>3</sub> (**26**) (~25 mg) in toluene (10 mL), also cooled to -30°. The reaction solution was heated to 65° to allow polymerization of NBE. After allowing sufficient time for NBE polymerization, a fraction of the polymer solution was removed for GPC analysis, and pyridine (3 equivalents) was added to the remaining solution at 65°. A solution of 2-butyne in toluene (5 mL), at room temperature, was then added to the reaction solution (at 65°) in a closed system, so that 2-butyne would not be lost from the system. After allowing sufficient time for consumption of all the 2-butyne (~15 minutes for 50 equivalents), benzaldehyde was added to cleave the polymer from the metal, and the solvent was removed *in vacuo* to yield the colorless polymer. This polymer was rinsed

with methanol, dissolved in methylene chloride, and filtered through alumina in preparation for GPC analysis.

**Preparation of Poly-1-pentyne with 42 and Ta(CHCMe<sub>3</sub>)(TIPT)<sub>3</sub>(THF), for GPC Analysis.** These reactions were performed as described above for the polymerization of 2-butyne. Polymer samples of poly-1-pentyne are deep orange in color and oily in nature, and all samples dissolve readily in common organic solvents (polyacetylenes that are not symmetrically substituted are known to display enhanced solubility properties<sup>112</sup>).

**Appendix 1: X-Ray Analysis of Ta(CHCMe<sub>3</sub>)(TIPT)<sub>3</sub>(Et<sub>2</sub>S) (9).**

$\text{Ta}(\text{CHCMe}_3)(\text{TIPT})_3(\text{Et}_2\text{S})$  (**9**) is prepared by addition of  $\text{Et}_2\text{S}$  to  $\text{Ta}(\text{CHCMe}_3)(\text{TIPT})_3(\text{THF})$  (**6**) in ether; the complex can be obtained as orange crystals from cooled solutions of pentane (chapter 1). The solid state structure of complex **9** was determined through an X-ray study, and although the structure is still in the process of refinement, several aspects of the structure are described here. A view of the compound is shown in Figure 1, and relevant bond distances and angles are listed in Table I (these values may change slightly with further refinement; at present,  $R_1 = 4.8$  and  $R_2 = 7.0$ ).

The structure of this complex is neither an ideal trigonal bipyramid or square pyramid; as with other complexes described in this dissertation, the steric demands of the ligands in complex **9** are manifested in their arrangement about the metal center (see below). If the complex is described as a distorted square pyramid, the thiolate ligand defined by S(3) is bound at the apex, with interligand angles between this group and the basal groups ranging from  $96^\circ$  to  $114^\circ$ . If described as a distorted trigonal bipyramid, the axial sites are occupied by the alkylidene ligand, C(1), and the coordinated base ( $\text{Et}_2\text{S}$ ), S(4), with the angle between these groups being the largest interligand angle in the complex ( $\angle \text{S}(4)\text{-Ta-C}(1) = 162.2(2)^\circ$ ). These two ligands are effectively *trans* to one another, as opposed to the *cis* orientation observed for the analogous ligands in the phenoxide complex  $\text{Ta}(\text{CMeCMeCHCMe}_3)(\text{DIPP})_3(\text{py})$  (**42**) (chapter 3; the interligand angle in that case is  $92^\circ$ ). The core geometries for these two alkylidene complexes are compared in Figure 2. The *trans* orientation of the alkylidene and base ( $\text{Et}_2\text{S}$ ) ligands is the most important feature in the solid state structure of complex **9**, as it represents a basic structural difference between analogous phenoxide and thiolate complexes and carries implications regarding reactivity differences (as discussed fully in chapters 1 and 2). Thus, considering a hypothetical olefin adduct for each of these complexes in which the olefin occupies the position formally occupied by the base (considering the preferred phenoxide and arylthiolate orientations), a direct reaction between the alkylidene ligand and the olefin can be envisioned in the phenoxide complex (interligand angle  $\approx 90^\circ$ ) but not in the arylthiolate complex (interligand angle  $\approx 160^\circ$ ).

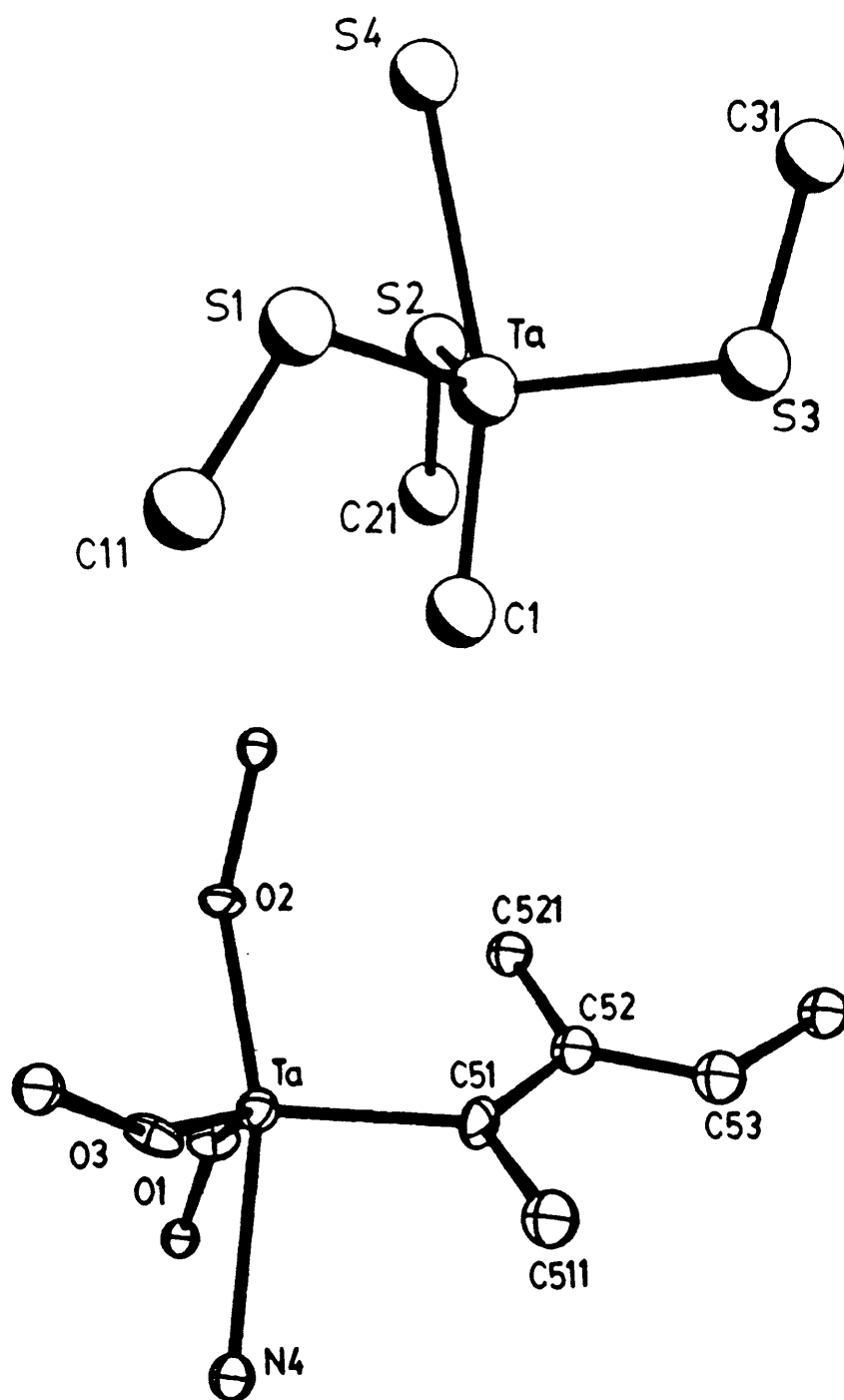




**Table 1.** Selected bond distances (Å) and angles (°) in Ta(CHCMe<sub>3</sub>)(TIPT)<sub>3</sub>(Et<sub>2</sub>S) (**9**).

Ta-C(1)	1.895(6)	S(2)-Ta-S(3)	113.98(6)
Ta-S(1)	2.394(2)	S(1)-Ta-S(4)	71.05(6)
Ta-S(2)	2.391(2)	S(1)-Ta-C(1)	98.7(2)
Ta-S(3)	2.391(2)	S(2)-Ta-C(1)	98.0(2)
Ta-S(4)	2.750(2)	S(2)-Ta-S(4)	77.23(6)
Ta-S(1)-C(11)	116.9(2)	S(3)-Ta-C(1)	101.3(2)
Ta-S(2)-C(21)	116.7(2)	S(3)-Ta-S(4)	96.22(6)
Ta-S(3)-C(31)	110.7(2)	S(4)-Ta-C(1)	162.2(2)
S(1)-Ta-S(2)	123.90(6)	Ta-C(1)-C(2)	172.8(5)
S(1)-Ta-S(3)	114.43(6)		

**Figure 2.** A comparison of the core geometries in Ta(CHCMe<sub>3</sub>)(TIPT)<sub>3</sub>(Et<sub>2</sub>S) (**9**) and Ta(CMeCMeCHCMe<sub>3</sub>)(DIPP)<sub>3</sub>(py) (**42**).



The description of Ta(CHCMe<sub>3</sub>)(TIPT)<sub>3</sub>(Et<sub>2</sub>S) (**9**) as a distorted trigonal bipyramid (versus a distorted square pyramid) is less important, as with any description the alkylidene and Et<sub>2</sub>S ligands can be considered effectively *trans* to one another. In all structurally characterized trigonal bipyramidal complexes of this type (i.e. containing at least three bulky arylthiolate ligands), the arylthiolate ligands occupy equatorial sites, with the arylthiolate ligands bent out of the equatorial plane ("two up and one down").<sup>19,22-26</sup> In a trigonal bipyramidal description of complex **9**, the three arylthiolate ligands are also bound at equatorial sites, with two pointed toward the alkylidene ligand and one pointed toward the Et<sub>2</sub>S base (Ta-S-C angles range from 111-117°). Considering the analogy, and considering the similar Ta-SAr bond lengths in **9** (each = 2.39 Å) which suggest bonding modes are not significantly different among the arylthiolate ligands, the remaining discussion will treat the structure of complex **9** as a distorted trigonal bipyramid, with the arylthiolate ligands in equatorial sites.

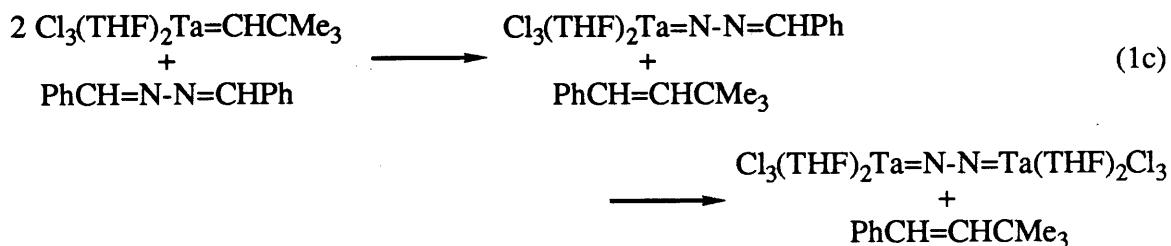
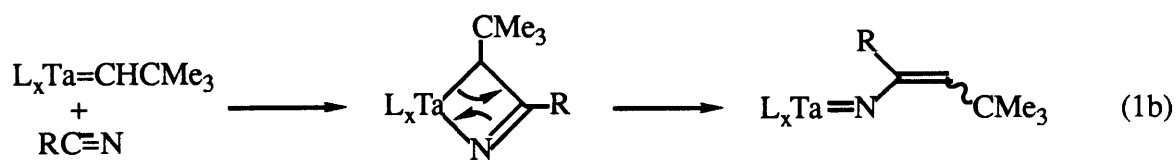
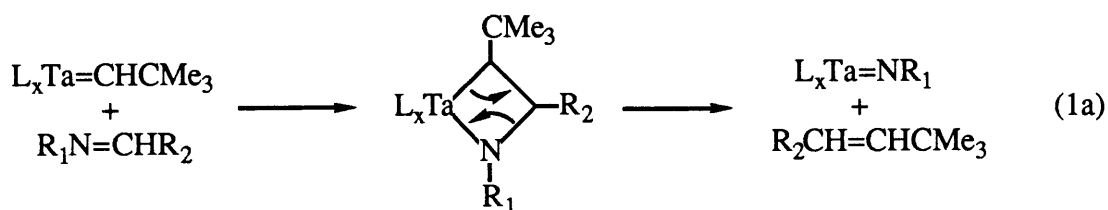
The interligand angle between the two arylthiolate ligands bent in the same direction ( $\angle$  S(1)-Ta-S(2) = 123.90(6)°) is greater than interligand angles between arylthiolate ligands bent in opposite directions ( $\angle$  S(1)-Ta-S(3) = 114.43(6)° and  $\angle$  S(2)-Ta-S(3) = 113.98(6)°), which is what one would expect considering the steric bulk of these groups (the same is seen in the thiolate dinitrogen complex (THF)(DIPT)<sub>3</sub>Ta=N-N-Ta(DIPT)<sub>3</sub>(THF), DIPT = 2,6-diisopropylbenzenethiolate<sup>19</sup>). The sulfur atoms of the three arylthiolate ligands are also displaced out of the "equatorial plane" in the direction of the axial Et<sub>2</sub>S, probably because the Et<sub>2</sub>S ligand is farther removed from the metal center than is the other axial ligand (Ta-S(4) = 2.750(2) Å versus Ta-C(1) = 1.895(6) Å). The Ta-SAr bond lengths mentioned above (each = 2.39 Å) are similar to those observed in (THF)(DIPT)<sub>3</sub>Ta=N-N-Ta(DIPT)<sub>3</sub>(THF) (average Ta-S ≈ 2.40 Å) and are thought to be indicative of Ta-S single bonds; a Ta(V) thiolato complex, Ta(S)Cl<sub>3</sub>(bpte) (bpte = PhSCH<sub>2</sub>CH<sub>2</sub>SPh), was described as containing a terminal tantalum sulfur double bond, and the bond length in that case was 2.204(5) Å.<sup>155</sup> The Ta-C bond distance of ~1.90 Å is consistent with the alkylidene assignment (i.e. a tantalum carbon double bond)<sup>1</sup> and is ~0.1 Å shorter than that bond in the related phenoxide alkylidene complex

Ta(CMeCMeCHCMe<sub>3</sub>)(DIPP)<sub>3</sub>(py) (**42**) (chapter 3). The Ta-C<sub>α</sub>-C<sub>β</sub> angle is also quite large (172.8(5)°) and indicative of a highly distorted alkylidene ligand, consistent with the low J<sub>CαH</sub> values observed for the related THF adduct **6** (J<sub>CαH</sub> = 76 Hz; THF-d<sub>8</sub>) and pyridine adduct **7** (J<sub>CαH</sub> = 94 Hz; C<sub>6</sub>D<sub>6</sub>). (the resonance for the α carbon of complex **9** was very broad in the <sup>13</sup>C NMR spectrum, and J<sub>CαH</sub> could not be determined; C<sub>6</sub>D<sub>6</sub>, 25°).

**Appendix 2: Preparation and Reactivity of Tantalum Imido and Dinitrogen Compounds.**

The preparation of several "(DIPP)<sub>3</sub>Ta" imido and dinitrogen complexes has been investigated, along with their reactivity versus related arylthiolate complexes (prepared separately by M. Wesolek<sup>82</sup>). The majority of these results has been reported in a full paper accepted for publication in *Inorganic Chemistry*,<sup>19</sup> an overview of this report and some aspects of the chemistry not included in the report are given here.

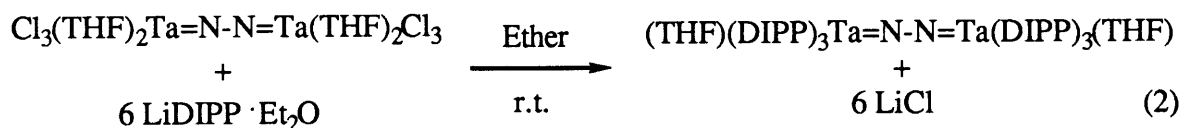
Tantalum imido complexes are conveniently prepared by reactions of alkylidene complexes with imines or nitriles (equations 1a and 1b, respectively).<sup>35,156-158</sup> In a related process, the tantalum dinitrogen complex (THF)<sub>2</sub>Cl<sub>3</sub>Ta=N-N=TaCl<sub>3</sub>(THF)<sub>2</sub> was prepared by reaction of Ta(CHCMe<sub>3</sub>)(THF)<sub>2</sub>Cl<sub>3</sub> with diphenylazine (equation 1c).<sup>159</sup>



The phenoxide complex Ta(CHCMe<sub>3</sub>)(DIPP)<sub>3</sub>(THF) (**2**) reacts with acetonitrile in a manner analogous to that shown in equation 1b, giving Ta(NCMeCHCMe<sub>3</sub>)(DIPP)<sub>3</sub>(THF) (**48**). However, when diphenylazine (0.5 equivalents) is added to complex **2**, only a partial reaction

is observed (after heating at elevated temperatures for several hours), resulting in the formation of the "metallazine" complex  $\text{Ta}(\text{N}=\text{N}=\text{CHPh})(\text{DIPP})_3(\text{THF})$  (**49**) and one equivalent of  $\text{PhCH}=\text{CHCMe}_3$ ; the pyridine adduct  $\text{Ta}(\text{N}=\text{N}=\text{CHPh})(\text{DIPP})_3(\text{py})$  (**50**) readily forms on addition of pyridine to complex **49**. A partial reaction is also observed between  $\text{Ta}(\text{CHCMe}_3)(\text{TIPT})_3(\text{THF})$  (**6**) and diphenylazine,<sup>82</sup> and steric constraints imposed by the DIPP and TIPT ligands are thought to prevent further reaction in both cases.

The DIPP dinitrogen complex  $(\text{THF})(\text{DIPP})_3\text{Ta}=\text{N}=\text{N}=\text{Ta}(\text{DIPP})_3(\text{THF})$  (**51**) can be prepared, however, by the alternative route shown in equation 2. Again, a pyridine adduct (**52**) can be prepared by addition of pyridine to complex **51**.



The solid state structure of complex **51** was determined through an X-ray study ( $\text{Ta}-\text{N} = 1.796(5) \text{ \AA}$ ), and the compound was found to display a distorted trigonal bipyramidal geometry with the "imido" ligand (equatorial position) and the base THF (axial position) *cis* to one another, just as the alkylidene and base ligands were found to be *cis* to one another in the structure of the alkylidene  $\text{Ta}(\text{CMeCMeCHCMe}_3)(\text{DIPP})_3(\text{py})$  (**42**) (chapter 3). Arylthiolate dinitrogen complexes can also be prepared, by addition of  $\text{NaSAr}$  ( $\text{SAr} = \text{DIPT}$  or  $\text{TIPT}$ ) to  $(\text{THF})_2\text{Cl}_3\text{Ta}=\text{N}=\text{N}=\text{TaCl}_3(\text{THF})_2$  in room temperature solution.<sup>82</sup> The solid state structure of the DIPT complex,  $(\text{THF})(\text{DIPT})_3\text{Ta}=\text{N}=\text{N}=\text{Ta}(\text{DIPT})_3(\text{THF})$ , displays a trigonal bipyramidal geometry with the "imido" ligand and the base THF *trans* to one another in axial sites ( $\text{Ta}-\text{N} = 1.90(6)$  and  $1.72(6) \text{ \AA}$ ); a similar arrangement is seen in  $\text{Ta}(\text{CHCMe}_3)(\text{TIPT})_3(\text{Et}_2\text{S})$  (**9**) for the alkylidene and base ligands (appendix 1). Both the DIPP and TIPT dinitrogen complexes react with benzaldehyde in a "Wittig-like" fashion to some degree; the reaction yields

PhCH=N-N=CHPh (and a metal oxo complex) in 83% yield from the phenoxide complex but only in ~25% yield from the arylthiolate complex.

Since tantalum dinitrogen complexes have also been prepared directly from reaction of Ta(III) complexes with nitrogen<sup>160</sup> or by reduction of Ta(V) complexes (such as Ta(CHCMe<sub>3</sub>)L<sub>2</sub>Cl<sub>3</sub><sup>159</sup>) in the presence of nitrogen, the phenoxide complex Ta(DIPP)<sub>3</sub>Cl<sub>2</sub> was prepared for related experiments. Ta(DIPP)<sub>3</sub>Cl<sub>2</sub>(Et<sub>2</sub>O) (**53**) forms slowly from reaction of LiDIPP·Et<sub>2</sub>O (3 equivalents) with TaCl<sub>5</sub> in ether. Rothwell has reported that TaCl<sub>5</sub> reacts with excess LiDIPP to give Ta(DIPP)<sub>2</sub>Cl<sub>3</sub>,<sup>161</sup> but recently Wigley has also shown Ta(DIPP)<sub>3</sub>Cl<sub>2</sub>(Et<sub>2</sub>O) forms from reaction of TaCl<sub>5</sub> with LiDIPP·Et<sub>2</sub>O.<sup>162</sup> Complex **53** reacts readily with excess THF to form a THF adduct, and when dissolved in neat THF the bis adduct forms cleanly; reaction of complex **53** with pyridine gives bis adduct formation exclusively.

When 2 equivalents of Na/Hg were added to solutions of **53** in pentane, ether, or THF, a reaction did occur (by <sup>1</sup>H NMR spectroscopy), but no new products were isolated, and no formation of the dinitrogen complex **51** was evident (THF was added in the workup or was present during the reactions). The reduction of complex **53** in toluene gave a light purple solution (from yellow), and on workup a small amount of a light purple precipitate was isolated; the NMR spectrum of this species in C<sub>6</sub>D<sub>6</sub> at 25° showed multiple and broad resonances. Interestingly, Wigley has reported that reduction of Ta(DIPP)<sub>2</sub>Cl<sub>3</sub> in the presence of certain acetylenes leads to the formation of substituted benzene adducts, Ta(DIPP)<sub>2</sub>Cl(η<sup>6</sup>-C<sub>6</sub>R<sub>6</sub>), which are blue in color (and thermally sensitive).<sup>162</sup> Thus the purple precipitate isolated from the reduction performed in toluene may be some kind of Ta(III) toluene adduct, but no attempts were made to further characterize this complex (the main interest of this study was to determine if a direct preparation of complex **51** from Ta(DIPP)<sub>3</sub>Cl<sub>2</sub> was possible). Reduction of Ta(TIPT)<sub>3</sub>Cl<sub>2</sub> in the presence of nitrogen was also found to give no dinitrogen complex formation.<sup>82</sup>



## Experimental Section

General details are given in chapter 1. The preparative details for complexes **49-52** are reported elsewhere.<sup>19</sup>

**Preparation of Compounds. Ta(NCMeCHCMe<sub>3</sub>)(DIPP)<sub>3</sub>(THF) (48).** A solution of acetonitrile (24  $\mu$ L, 0.45 mmol) in ether (10 mL), cooled to -30 $^{\circ}$ , was added to a stirring solution of Ta(CHCMe<sub>3</sub>)(DIPP)<sub>3</sub>(THF) (0.400 g, 0.47 mmol) in ether (10 mL) at -30 $^{\circ}$ . The solution turned colorless, and after 25 minutes the solution was filtered through Celite, and the solvent was removed *in vacuo*. Dissolution of the resulting white solid in pentane, followed by cooling the solution to -30 $^{\circ}$ , yielded a white precipitate (0.354 g, 85%): <sup>1</sup>H NMR (270 MHz)  $\delta$  7.14 (d, 6, H<sub>m</sub>), 6.94 (t, 3, H<sub>p</sub>), 4.78 (s, 1, NCMeCHCMe<sub>3</sub>), 3.9-3.8 (m, 10, CHMe<sub>2</sub> and THF), 1.66 (s, 3, NCMeCHCMe<sub>3</sub>), 1.30 (d, 36, CHMe<sub>2</sub>), 1.11 (s, 9, NCMeCHCMe<sub>3</sub>), 1.03 (broad, 4, THF); <sup>13</sup>C NMR (67.9 MHz)  $\delta$  157.4 (s, C<sub>ipso</sub>), 149.7 (s, NCMeCHCMe<sub>3</sub>), 137.6 (s, C<sub>O</sub>), 128.5 (unresolved, NCMeCHCMe<sub>3</sub>), 123.3 (d, C<sub>m</sub>), 121.7 (d, C<sub>p</sub>), 73.1 (t, THF), 32.0 (q, NCMeCHCMe<sub>3</sub>), 30.3 (s, NCMeCHCMe<sub>3</sub>), 26.9 (d, CHMe<sub>2</sub>), 25.3 (t, THF), 24.0 (q, CHMe<sub>2</sub>), 21.0 (q, NCMeCHCMe<sub>3</sub>). Anal. Calcd for TaC<sub>47</sub>H<sub>72</sub>NO<sub>4</sub>: C, 63.00; H, 8.01; N, 1.56. Found: C, 63.24; H, 8.09; N, 1.32.

**TaCl<sub>2</sub>(DIPP)<sub>3</sub>(Et<sub>2</sub>O) (53).** LiDIPP·Et<sub>2</sub>O (1.082 g, 4.19 mmol) was added as a solid to a mixture of TaCl<sub>5</sub> (0.500 g, 1.40 mmol) in ether (20 mL) at room temperature. After stirring the mixture for 22 hours, the solution was filtered through Celite to remove LiCl and any unreacted TaCl<sub>5</sub>. Dissolution of the resulting yellow oil in a mixture of pentane/Et<sub>2</sub>O (50/50), followed by cooling to -30 $^{\circ}$ , yielded a bright yellow microcrystalline precipitate (0.730 g). A second crop was obtained from pentane (0.220 g, total yield = 79%): <sup>1</sup>H NMR (300 MHz)  $\delta$  7.08 (broad d, 6, H<sub>m</sub>), 6.89 (t, 3, H<sub>p</sub>), 4.05 (broad septet, 10, CHMe<sub>2</sub> and Et<sub>2</sub>O), 1.24 (broad d, 36, CHMe<sub>2</sub>), 0.92 (t, 10, Et<sub>2</sub>O). All resonances and integrations sharpen at elevated temperature. Anal. Calcd for TaC<sub>40</sub>H<sub>61</sub>Cl<sub>2</sub>O<sub>4</sub>: C, 56.01; H, 7.17; Cl, 8.27. Found: C, 55.52; H, 7.26; Cl, 7.86.

Reaction of **53** with excess THF in ether at room temperature results in the mono THF adduct,  $\text{TaCl}_2(\text{DIPP})_3(\text{THF})$ :  $^1\text{H NMR}$  (300 MHz)  $\delta$  7.13 and 7.01 (d's, 6,  $\text{H}_m$ ), 6.92 and 6.85 (t's, 3,  $\text{H}_p$ ), 4.08 (multiplet, 10,  $\text{CHMe}_2$  and THF), 1.26 and 1.20 (d's, 36,  $\text{CHMe}_2$ ). The upfield THF resonance is obstructed by the  $\text{CHMe}_2$  resonances. Dissolution of **53** in neat THF yields the bis THF adduct,  $\text{TaCl}_2(\text{DIPP})_3(\text{THF})_2$ :  $^1\text{H NMR}$  (300 MHz)  $\delta$  7.12 and 7.01 (d's, 6,  $\text{H}_m$ ), 6.92 and 6.84 (t's, 3,  $\text{H}_p$ ), 4.08 (multiplet, 10,  $\text{CHMe}_2$  and THF), 3.57 (broad, 4, THF), 1.42 (broad, 4, THF), 1.26 and 1.20 (d's, 36,  $\text{CHMe}_2$ ). The upfield THF resonance is obstructed by the  $\text{CHMe}_2$  resonances. Addition of pyridine to complex **53** in ether gives the bis pyridine adduct,  $\text{TaCl}_2(\text{DIPP})_3(\text{py})_2$ :  $^1\text{H NMR}$  (300 MHz)  $\delta$  8.85 and 8.51 (d's, 4, py  $\text{H}_o$ ), 7.14 and 7.06 (d's, 6,  $\text{H}_m$ ), 7.0-6.8 (multiplet, 5,  $\text{H}_p$  and py  $\text{H}_m$ ), 6.68 and 6.25 (multiplets, 4, py  $\text{H}_m$ ), 4.23 and 3.89 (septets, 6,  $\text{CHMe}_2$ ), 1.27 and 1.15 (d's, 36,  $\text{CHMe}_2$ ).

### Appendix 3: Organization of Notebooks, Spectra, and Other Data.

Experimental data are contained in twelve research notebooks, KCW1-KCW12. Reaction mixtures, solutions, and crude products (i.e. oils or solids obtained on removal of solvent from a reaction solution) are identified by a notebook number, a page number, and a letter, while isolated products are identified by a notebook number, a page number, and another number. For example, in notebook 8 on page 59  $\text{Ta}(\text{CHCMe}_3)(\text{TIPT})_3(\text{THF})$  is combined with cyclopentene in  $\text{C}_6\text{D}_6$ . This reaction mixture is described as KCW8-59-A. In notebook 12 on page 4 the preparation of  $\text{Ta}(\text{CH}_2\text{CMe}_3)_2(\text{DIPP})_3$  is described. The first crop of isolated crystals is described as KCW12-4-1, and the second crop is described as KCW12-4-2. Spectral data are labelled in a similar fashion. From the preparation reaction on page 4 in notebook 12, an NMR spectrum of the crude product would be labelled as KCW12-4-A, while a spectrum of the isolated crystals (first crop) would be labelled as KCW12-4-1.

In addition to the labelling described above, each NMR spectrum is assigned a number. All spectra are contained in blue folders, and all  $^{13}\text{C}$  NMR spectra are contained in a single folder. (Due to the large number of spectra involved, NMR spectra associated with kinetic experiments are collected separately in yellow envelopes, according to the specific kinetic experiment.) Other spectral data, such as those associated with gel permeation chromatography, gas chromatography, or infrared spectroscopy, are arranged in envelopes according to the method of analysis.

**REFERENCES**

- (1) Schrock, R. R.. In *Reactions of Coordinated Ligands*; Braterman, P. S. Ed.; Plenum Press: New York, 1986.
- (2) Ivin, K. J. *Olefin Metathesis*; Academic Press: London, 1983.
- (3) Dragutan, V.; Balaban, A. T.; Dimonic, M. *Olefin Metathesis and Ring-Opening Polymerization of Cyclo-Olefins*; 2nd Ed.; Wiley-Interscience: New York, 1985.
- (4) Grubbs, R. H.. In *Comprehensive Organometallic Chemistry*; Wilkinson, G.; Stone, F. G. A.; Abel, E. W., Eds.; Pergamon: 1982, Volume 8, Chapter 54.
- (5) Schrock, R. R. *J. Am. Chem. Soc.* **1974**, *96*, 6796.
- (6) Schrock, R. R. *J. Am. Chem. Soc.* **1976**, *98*, 5399.
- (7) Rocklage, S. M., Fellmann, J. D., Rupprecht, G. A., Messerle, L. W., Schrock, R. R. *J. Am. Chem. Soc.* **1981**, *103*, 1440.
- (8) Schrock, R. R. *Acc. Chem. Res.* **1979**, *12*, 98.
- (9) McLain, S. J., Sancho, J., Schrock, R. R. *J. Am. Chem. Soc.* **1979**, *101*, 5451.
- (10) McLain, S. J., Sancho, J., Schrock, R. R. *J. Am. Chem. Soc.* **1980**, *102*, 5610.
- (11) Schrock, R. R. *Acc. Chem. Res.* **1986**, *19*, 342.
- (12) Churchill, M. R.; Ziller, J. W.; Freudenberger, J. H.; Schrock, R. R. *Organometallics*, **1984**, *3*, 1554.
- (13) Freudenberger, J. H.; Schrock, R. R.; Churchill, M. R.; Rheingold, A. L.; Ziller, J. W. *Organometallics* **1984**, *3*, 1563.
- (14) Listemann, M. L.; Schrock, R. R. *Organometallics* **1985**, *4*, 74.
- (15) McCullough, L. G.; Schrock, R. R.; Dewan, J. C.; Murdzek, J. S. *J. Am. Chem. Soc.* **1985**, *107*, 5987.
- (16) Wallace, K. C.; Dewan, J. C.; Schrock, R. R. *Organometallics* **1986**, *5*, 2162.
- (17) Wallace, K. C.; Liu, A. H.; Dewan, J. C.; Schrock, R. R. *J. Am. Chem. Soc.*, in press.

(18) Rupprecht, G. A.; Messerle, L. W.; Fellmann, J. D.; Schrock, R. R. *J. Am. Chem. Soc.* **1980**, *102*, 6236.

(19) Schrock, R. R.; Wesolek, M.; Liu, A. H.; Wallace, K. C.; Dewan, J. C. *Inorg. Chem.*, in press.

(20) This strategy was successfully employed for the isolation of base-free LuCp<sub>2</sub>(Me): Watson, P. L.; Parshall, G. W. *Acc. Chem. Res.* **1985**, *18*, 51.

(21) Chamberlain, L. R.; Rothwell, I. P.; Folting, K.; Huffman, J. C. *J. Chem. Soc. Dalton Trans.* **1987**, 155, and references contained therein.

(22) Koch, S. A.; Millar, M. *J. Am. Chem. Soc.* **1983**, *105*, 3362.

(23) Blower, P. J.; Dilworth, J. R.; Hutchinson, J. P.; Zubieta, J. A. *J. Chem. Soc. Dalton Trans.* **1985**, 1533.

(24) Bishop, P. T.; Dilworth, J. R.; Hutchinson, J.; Zubieta, J. A. *J. Chem. Soc. Dalton Trans.* **1986**, 967.

(25) Dilworth, J. R.; Hutchinson, J.; Zubieta, J. A. *J. Chem. Soc. Chem. Commun.* **1983**, 1034.

(26) Walborsky, E. C.; Wigley, D. E.; Roland, E.; Dewan, J. C.; Schrock, R. R. *Inorg. Chem.* **1987**, *26*, 1615.

(27) Murdzek, J. S.; Blum, L.; Schrock, R. R. *Organometallics* **1988**, *6*, 436.

(28) Cotton, F. A.; Wilkinson, G. *Advanced Inorganic Chemistry*, 4th Ed.; John Wiley and Sons: New York, 1980.

(29) Collman, J. P.; Hegedus, J. R.; Norton, J. R.; Finke, R. G. *Principles and Applications of Organotransition Metal Chemistry*; University Science Books: Mill Valley, CA, 1987.

(30) Schrock, R. R. *J. Organometal. Chem.* **1976**, *122*, 209.

(31) Edwards, D. S.; Blondi, L. V.; Ziller, J. W.; Churchill, M. R.; Schrock, R. R. *Organometallics*, **1983**, *2*, 1505.

- (32) Chamberlain, L. R.; Rothwell, A. P.; Rothwell, I. P. *J. Am. Chem. Soc.* **1984**, *106*, 1847.
- (33) Fryzuk, M. D.; MacNeil, P. A.; Rettig, S. J. *J. Am. Chem. Soc.* **1985**, *107*, 6708.
- (34) Chamberlain, L. R.; Rothwell, I. P. *J. Chem. Soc. Dalton Trans.* **1987**, 163.
- (35) Wood, C. D.; McLain, S. J.; Schrock, R. R. *J. Am. Chem. Soc.* **1979**, *101*, 3210.
- (36) Ivan, K. J.; Rooney, J. J.; Stewart, D.; Green, M. L. H.; Mahtab, R. J. *J. Chem. Soc., Chem. Commun.* **1978**, 604.
- (37) Turner, H. W.; Schrock, R. R. *J. Am. Chem. Soc.* **1982**, *104*, 2331.
- (38) Agüero, A.; Kress, J.; Osborn, J. A. *J. Chem. Soc. Chem. Commun.* **1986**, 531.
- (39) Clift, S. M.; Schwartz, J. *J. Am. Chem. Soc.* **1984**, *106*, 8300.
- (40) Hartner, F. W., Jr.; Schwartz, J.; Clift, S. M. *J. Am. Chem. Soc.* **1983**, *105*, 640.
- (41) Tebbe, F. N.; Parshall, G. W.; Reddy, G. S. *J. Am. Chem. Soc.* **1978**, *100*, 3611.
- (42) Pine, S. H.; Zahler, R.; Evans, D. A.; Grubbs, R. H. *J. Am. Chem. Soc.* **1980**, *102*, 3270.
- (43) Buchwald, S. L.; Grubbs, R. H. *J. Am. Chem. Soc.* **1983**, *105*, 5490.
- (44) Stille, J. R.; Grubbs, R. H. *J. Am. Chem. Soc.* **1986**, *108*, 855.
- (45) Ho, S. C.; Hentges, S.; Grubbs, R. H. *Organometallics*, **1988**, *7*, 780.
- (46) Chamberlain, L.; Keddington, J.; Rothwell, I. P. *Organometallics* **1982**, *1*, 1538.
- (47) Chamberlain, L.; Rothwell, I. P.; Huffman, J. C. *J. Am. Chem. Soc.* **1982**, *104*, 7338.
- (48) Listeman, M. L.; Dewan, J. C.; Schrock, R. R. *J. Am. Chem. Soc.* **1985**, *107*, 7207.

- (49) Listemann, M. L.; Schrock, R. R.; Dewan, J. C.; Kolodziej, R. M. *Inorg. Chem.* **1988**, *27*, 264.
- (50) Schrock, R.R.; DePue, R. T.; Feldman, J.; Schaverien, C. J.; Dewan, J. C.; Liu, A. H. *J. Am. Chem. Soc.* **1988**, *110*, 1423.
- (51) J. Feldman, unpublished results.
- (52) Straus, D.A.; Grubbs, R.H. *Organometallics* **1982**, *1*, 1658.
- (53) Gordon, A.J.; Ford, R.A. *The Chemist's Companion: A Handbook of Practical Data, Techniques, and References*; John Wiley and Sons, Inc.: New York, 1972.
- (54) Schrock, R. R.; Sharp, P. R. *J. Am. Chem. Soc.* **1978**, *100*, 2389.
- (55) Tikkanen, W.R.; Petersen, J.L. *Organometallics* **1984**, *3*, 1651.
- (56) Erker, G.; Czisch, P.; Kruger, C.; Wallis, J.M. *Organometallics* **1985**, *4*, 2059.
- (57) Seetz, J.W.F.L.; Schat, G.; Akkerman, O.S.; Bickelhaupt, F. *Angew. Chem. Int Ed. Engl.* **1983**, *22*, 248.
- (58) Seetz, J.W.F.L.; Van de Heistee, B. J. J.; Schat, G.; Akkerman, O.S.; Bickelhaupt, F. *J. Mol. Catal.* **1985**, *28*, 71.
- (59) Lee, J. B.; Gajda, G. J.; Schaefer, W. P.; Howard, T. R.; Ikariya, T.; Straus, D.A.; Grubbs, R.H. *J. Am. Chem. Soc.* **1981**, *103*, 7358.
- (60) Bruno, J. W.; Marks, T. J.; Day, V. W. *J. Am. Chem. Soc.* **1982**, *104*, 7357.
- (61) Schaverien, C. J.; Dewan, J. C.; Schrock, R. R. *J. Am. Chem. Soc.* **1986**, *108*, 2771.
- (62) Kress, J.; Osborn, J. A.; Greene, R. M. E.; Ivin, K. J.; Rooney, J. J. *J. Am. Chem. Soc.* **1987**, *109*, 899.
- (63) J. S. Murdzek, unpublished results.
- (64) Calculated for acids in aqueous solution: Perrin, D. D.; Dempsey, B.; Serjeant, E. P. *pK<sub>a</sub> Prediction for Organic Acids and Bases*; Chapman and Hall: New York, 1981.
- (65) Roland, E.; Walborsky, E. C.; Dewan, J. C.; Schrock, R. R. *J. Am. Chem. Soc.* **1985**, *107*, 5795.



- (66) Ashby, M. T.; Enemark, J. H. *J. Am. Chem. Soc.* **1986**, *108*, 730.
- (67) Chamberlain, L. R.; Rothwell, I. P. *J. Am. Chem. Soc.* **1983**, *105*, 1665.
- (68) Chamberlain, L. R.; Rothwell, I. P.; Huffman, J. C. *J. Am. Chem. Soc.* **1986**, *108*, 1502.
- (69) Chamberlain, L. R.; Kerschner, J. L.; Rothwell, A. P.; Rothwell, I. P.; Huffman, J. C. *J. Am. Chem. Soc.* **1987**, *109*, 6471.
- (70) Albright, T. A.; Burdett, J. K.; Whangbo, M.-H. *Orbital Interactions in Chemistry*; John Wiley and Sons: New York, 1985, p 95.
- (71) Jeske, G.; Lauke, H.; Mauermann, H.; Swepston, P. N.; Schumann, H.; Marks, T. J. *J. Am. Chem. Soc.* **1985**, *107*, 8091.
- (72) Jeske, G.; Schock, L. E.; Swepston, P. N.; Schumann, H.; Marks, T. J. *J. Am. Chem. Soc.* **1985**, *107*, 8103.
- (73) LaPointe, R. E.; Wolczanski, P. T.; Van Duyne, G. D. *Organometallics* **1985**, *4*, 1810.
- (74) Toreki, R.; LaPointe, R. E.; Wolczanski, P. T. *J. Am. Chem. Soc.* **1987**, *109*, 7558.
- (75) Fanwick, P. E.; Ogilvy, A. E.; Rothwell, I. P. *Organometallics* **1987**, *6*, 73.
- (76) Schrock, R. R.; Feldman, J.; Cannizzo, L. F.; Grubbs, R. H. *Macromolecules* **1987**, *20*, 1169.
- (77) Murdzek, J. S.; Schrock, R. R. *Organometallics* **1987**, *6*, 1373.
- (78) Murdzek, J. S.; Schrock, R. R. *Macromolecules* **1987**, *20*, 2640.
- (79) Horton, A. D.; Schrock, R. R.; Freudenberger, J. H. *Organometallics* **1987**, *6*, 893.
- (80) Pearson, D. E.; Caine, D.; Field, L. *J. Org. Chem.* **1960**, *25*, 867.
- (81) L. Blum, Ph.D. Thesis, 1985.
- (82) M. Wesolek final report, 1986 (postdoctoral study with R. R. Schrock).

(83) Silverman, L. D.; Dewan, J. C.; Giandomenico, C. M.; Lippard, S. J. *Inorg. Chem.* 1980, 19, 3379.

(84) Gilliom, L. R.; Grubbs, R. H. *J. Am. Chem. Soc.* 1986, 108, 855.

(85) Kress, J.; Osborn, J. A.; Greene, R. M. E.; Ivin, K. J.; Rooney, J. J. *J. Chem. Soc., Chem. Commun.* 1985, 874.

(86) Schrock, R. R.; Krouse, S. A.; Knoll, K.; Feldman, J.; Murdzek, J. S.; Yang, D. *C. J. Mol. Catal.*, submitted.

(87) Novak, B. M.; Grubbs, R. H. *J. Am. Chem. Soc.* 1988, 110, 960.

(88) Youinou, M. T.; Kress, J.; Fischer, J.; Aguero, A.; Osborn, J. A. *J. Am. Chem. Soc.* 1988, 110, 1488.

(89) Wallace, K. C.; Schrock, R. R. *Macromolecules* 1987, 20, 448.

(90) Chisholm, M. H.; Rothwell, L. P.. In *Comprehensive Coordination Chemistry*; Wilkinson, G.; Gillard, R.; McCleverty, J. A., Eds. ; Pergamon: 1987, Volume 2.

(91) Grubbs has postulated that the stereochemistry of polynorbornene produced on ring-opening of a titanacyclobutane complex is a result of the stereochemistry imposed within that complex;<sup>84</sup> a similar dependence is thought to be present in the tantalacyclobutane complexes described here.

(92) Cannizzo, L. F.; Grubbs, R. H. *Macromolecules* 1988, 20, 1488.

(93) Katz, T. J.; Lee, S. J.; Acton, N. *Tetrahedron Lett.* 1976, 4247.

(94) Katz, T. J.; Acton, N. *Tetrahedron Lett.* 1976, 4251.

(95) At 45.3°,  $k_{\text{obs}}(\mathbf{31}) = 2.74 \times 10^{-3} \text{ s}^{-1}$  when  $[\mathbf{31}] = 4.24 \text{ mM}$  and  $[\text{NBE}]_0 = 63 \text{ mM}$ , from  $[\text{NBE}]$  versus time;  $k_1(\mathbf{27}) = 2.02 \times 10^{-3} \text{ s}^{-1}$  at 44.8°.

(96) Patton, P. A.; McCarthy, T. J. *Macromolecules* 1987, 20, 778, and references contained therein.

(97) Quignard, F.; Leconte, M.; Basset, J. M. *J. Mol. Catal.* 1985, 28, 27.

(98) Hamilton, J. G.; Ivin, K. J.; Rooney, J. J. *J. Mol. Catal.* 1985, 28, 255.

- (99) Greene, R. M. E.; Hamilton, J. G.; Ivin, K. J.; Rooney, J. J. *Makromol. Chem.* **1986**, *187*, 619.
- (100) Patton, P. A.; Lillya, C. P.; McCarthy, T. J. *Macromolecules* **1986**, *19*, 1266.
- (101) H. Sitzmann final report, 1986 (postdoctoral study with R. R. Schrock).
- (102) J. H. Freudenberger, Ph.D. Thesis, 1986.
- (103) Feast, W. J.; Winter, J. N. *J. Chem. Soc., Chem. Commun.* **1985**, 202.
- (104) Krouse, S. A.; Schrock, R. R. *Macromolecules*, submitted, and references contained therein.
- (105) Knoll, K.; Krouse, S. A.; Schrock, R. R. *J. Am. Chem. Soc.*, in press.
- (106) S. A. Krouse, unpublished results.
- (107) These arguments are based on the Hammond Postulate; a description is given in: Lowry, T. H.; Richardson, K. S. *Mechanism and Theory in Organic Chemistry*, 2nd Ed.; Harper and Row: New York, 1981; p. 197.
- (108) Stille, J. K.; Hughes, R. D. *J. Org. Chem.* **1971**, *36*, 340.
- (109) Silverstein, R. M.; Bassler, G. C.; Morrill, T. C. *Spectrometric Identification of Organic Compounds*; 4th Ed.; John Wiley and Sons: New York, 1981; p 227.
- (110) For a comprehensive review of the synthesis and properties of parent polyacetylene see reference 111 and: Chien, J. C. W. *Polyacetylene Chemistry, Physics and Material Science*; Academic Press, New York, 1984.
- (111) Bredas, J. L.; Street, G. B. *Acc. Chem. Res.* **1985**, *18*, 309.
- (112) For a comprehensive review of the synthesis and properties of substituted polyacetylenes see: Masuda, T.; Higashimura, T. *Adv. Polym. Sci.* **1986**, *81*, 121.
- (113) Yoshimura, T.; Masuda, T.; Higashimura, T.; Ishihara, T. *J. Polym. Sci. Polym. Chem. Ed.* **1986**, *24*, 3569.
- (114) Shelburne, III, J. A.; Baker, G. L. *Macromolecules* **1987**, *20*, 1212, and references contained therein.

- (115) Ito, T.; Shirakawa, H.; Ikeda, S. *J. Polym. Sci. Polym. Chem. Ed.* **1974**, *12*, 11.
- (116) Gal, Y.-S.; Choi, S.-K. *J. Polym. Sci. Polym. Chem. Ed.* **1987**, *25*, 2323.
- (117) Katz, T. J.; Lee, S. J. *J. Am. Chem. Soc.* **1980**, *102*, 422.
- (118) Han, C.-C.; Katz, T. J. *Organometallics* **1985**, *4*, 2186.
- (119) Katz, T. J.; Ho, T. H.; Shih, N.-Y.; Ying, Y.-C.; Stuart, V. I. W. *J. Am. Chem. Soc.* **1984**, *106*, 2659.
- (120) Katz, T. J.; Hacker, S. M.; Kendrick, R. D.; Yannoni, C. S. *J. Am. Chem. Soc.* **1985**, *107*, 2182.
- (121) Clarke, T. C.; Yannoni, C. S.; Katz, T. J.; *J. Am. Chem. Soc.* **1983**, *105*, 7787.
- (122) Shirakawa, S.; Ikeda, S. *J. Polym. Sci. Polym. Chem. Ed.* **1974**, *12*, 929.
- (123) Wegner, G. *Angew. Chem., Int. Ed. Engl.* **1981**, *20*, 361.
- (124) Katz, T. J.; Sivavec, T. M. *J. Am. Chem. Soc.* **1985**, *107*, 737.
- (125) Faron, M. F.; Lofgren, P. A.; Woon, P. S. *J. Chem. Soc., Chem. Commun.* **1974**, 246.
- (126) Levisalles, J.; Rose-Munch, F.; Rudler, H.; Daran, J.-C.; Dromzee, Y.; Jeannin, Y. *J. Chem. Soc., Chem. Commun.* **1981**, 152.
- (127) Faron, M. F.; Thanedar, S.; Famili, A. *J. Polym. Sci. Chem. Ed.* **1986**, *24*, 3529.
- (128) Brown, C. K.; Georjgin, D.; Wilkinson, G. *J. Chem. Soc. A* **1971**, 3120.
- (129) Kern, R. J. *J. Poly. Sci., A-1* **1969**, *7*, 621.
- (130) Masuda, T.; Sasaki, N.; Higashimura, T. *Macromolecules* **1975**, *8*, 717.
- (131) Dotz, K. H.; Kreiter, C. G. *J. Organomet. Chem.* **1975**, *99*, 309.
- (132) Dotz, K. H.; Kreiter, C. G. *Chem. Ber.* **1976**, *109*, 2026.
- (133) Fisher, H.; Dotz, K. H. *Chem. Ber.* **1980**, *113*, 193.

- (134) Wulff, W. D.; Kaesler, R. W.; Peterson, G. A.; Tang, P.-C. *J. Am. Chem. Soc.* **1985**, *107*, 1060.
- (135) Garnier, F.; Krausz, P.; Rudler, H. *J. Organomet. Chem.* **1980**, *186*, 77.
- (136) Masuda, T.; Yoshimura, T.; Fujimori, J.; Higashimura, T. *J. Chem. Soc., Chem. Commun.* **1987**, 1805.
- (137) Tebbe, F. N.; Harlow, R. L. *J. Am. Chem. Soc.* **1980**, *102*, 6149.
- (138) McKinney, R. J.; Tulip, T. H.; Thorn, D. L.; Coolbaugh, T. S.; Tebbe, F. N. *J. Am. Chem. Soc.* **1981**, *103*, 5584.
- (139) Howard, T. R.; Lee, J. B.; Grubbs, R. H. *J. Am. Chem. Soc.* **1980**, *102*, 6876.
- (140) C. J. Schaverien final report, 1985 (postdoctoral study with R. R. Schrock).
- (141) **42c**:  $^1\text{H}$  NMR ( $\text{C}_6\text{D}_6$ , 300 MHz)  $\delta$  8.59 (broad d, 2, pyortho), 6.52 (broad t, 1, pypara), 6.21 (broad t, 2, pymeta), 5.73 (~s, 1, CHCMe<sub>3</sub>), 3.88 (septet, 6, CHMe<sub>2</sub>), 1.88 and 1.89 (s's, 6,  $\alpha$  CMe and  $\beta$  CMe), 1.24 (d, 36, CHMe<sub>2</sub>), 1.15 (s, 9, CHCMe<sub>3</sub>).
- (142) Green, M. L. H.; Knight, J.; Mitchard, L. C.; Roberts, G. G.; Silverthorn, W. E. *J. Chem. Soc., Chem. Commun.* **1972**, 987.
- (143) Deactivation was measured by the amount of cleaved polymer (from 50 equivalents of 2-butyne polymerized) observed in subsequent GPC chromatograms acquired after the second aliquot of 2-butyne (50 additional equivalents) was polymerized.
- (144) Krouse, S. A.; Schrock, R. R.; Cohen, R. E. *Macromolecules* **1987**, *20*, 903.
- (145) R. T. DePue final report, 1987 (postdoctoral study with R. R. Schrock).
- (146) Grubbs, R. H.; Swager, T. M. *J. Am. Chem. Soc.* **1987**, *109*, 894.
- (147) Strutz, H.; Dewan, J. C.; Schrock, R. R. *J. Am. Chem. Soc.* **1985**, *107*, 5999, and references contained therein.
- (148) DIFABS: Walker, N.; Stuart, D. *Acta Cryst.* **1983**, *A39*, 158.
- (149) Least Squares, function minimized:  $\sum w (|F_o| - |F_c|)^2$ , where:  $w = 4F_o^2/\sigma^2(F_o^2)$ ,  $s^2(F_o^2) = [S^2(C + R^2B) + (pF_o^2)^2]/Lp^2$ , S = scan rate, C = total integrated

peak count, R = ratio of scan time to background counting time, B = total background count, Lp = Lorentz-polarization factor, p = p-factor.

(150) Standard deviation of an observation of unit weight:  $[\sum w (|F_o| - |F_c|)^2 / (N_o - N_v)]^{1/2}$ , where  $N_o$  = number of observations,  $N_v$  = number of variables.

(151) (a) Cromer, D. T.; Waber, J. T. *International Tables for X-ray Crystallography*; Vol. IV; The Kynoch Press: Birmingham, England, 1974, Table 2.2 A. (b) Ibid, Table 2.3.1.

(152) Ibers, J. A.; Hamilton, W. C. *Acta Cryst.* **1964**, *17*, 781.

(153) TEXSAN - TEXRAY Structure Analysis Package, Molecular Structure Corporation (1985).

(154) Structure solution methods: PHASE: Calabrese, J. C.; PHASE - Patterson Heavy Atom Solution Extractor. Univ. of Wisconsin-Madison, Ph. D. Thesis (1972). DIRDIF: Beurskens, P. T. ; Direct Methods for Difference Structures - an automatic procedure for phase extension and refinement of difference structure factors. Technical Report 1984/1 Crystallography Laboratory, Toernooiveld, 6525 Ed Nijmegen, Netherlands.

(155) Drew, M. G. B.; Rice, D. A.; Williams, D. M. *J. Chem. Soc. Dalton Trans.* **1984**, 845.

(156) Schrock, R. R.; Fellman, J. D. *J. Am. Chem. Soc.* **1978**, *100*, 3359.

(157) Rocklage, S. M.; Schrock, R. R. *J. Am. Chem. Soc.* **1980**, *102*, 7808.

(158) Rocklage, S. M.; Schrock, R. R. *J. Am. Chem. Soc.* **1982**, *104*, 3077.

(159) Turner, H. W.; Fellman, J. D.; Rocklage, S. M.; Schrock, R. R. *J. Am. Chem. Soc.* **1980**, *102*, 7809.

(160) Rocklage, S. M.; Turner, H. W.; Fellman, J. D.; Schrock, R. R. *Organometallics* **1982**, *1*, 703.

(161) Chamberlain, L. R.; Rothwell, I. P.; Huffman, J. C. *Inorg. Chem.* **1984**, *23*, 2575.

(162) Bruck, M. A.; Copenhaver, A. S.; Wigley, D. E. *J. Am. Chem. Soc.* **1987**, *109*, 6525.

## Acknowledgements

I would like to thank Dick Schrock for support and guidance over the last four years, and for giving me the opportunity to explore a wide variety of tantalum chemistry.

I thank the Central Research Department of the Dow Chemical Company for a predoctoral fellowship, and I thank Andy Liu, John Dewan, and Bill Davis for their assistance in the area of X-ray crystallography.

I have had the good fortune of working with a fine group of people at MIT - thanks to all of you for your friendship and sound scientific advice. I especially want to thank Steve Krouse, John Buzinkai, Joe Payack, and Oliver Chyan, who together with me shared the challenges of course work, cumulative examinations, teaching, and proposition.

Thanks also to Lauren Blum for getting me started, and to John Freudenberger, Andy Liu, and John Murdzek for helping me along. And I thank Rick Kolodziej for joining the group and livening things up a bit! I wish you the best of luck in your research and your career beyond MIT.

I want to thank my Mom and Dad for their encouragement, and most of all for their unconditional love. I can only hope to be as good a parent. Thanks also to Mom Stevens for her love and support.

Finally, and most importantly, I want to thank Susie. Thanks for your love, your encouragement, and your patience. We have experienced many things during our stay in Boston, and we have grown stronger.

Billy Pilgrim travels in time, but we must be content with our memories.